We thank reviewer 1 for the thorough work and the positive and helpful feedback. We adjusted our manuscript accordingly.

> Page 1, line 19: processes instead of mechanisms.
> Page 5, line 1: Correct the sentence.
> Page 10, line 12/13: The compound is missing.… "the main degradation product of the OH initiated oxidation of" ? (2-oxo-3-hydroxy-succinaldehyde)
> Page 10, line 15: Figure 11c/d shows…(not show)
> Page 11, lines 29-41: Please, rewrite this section to make it clearer.
> Page 19, line 30: Check the unit for Henry's law coefficient.
> Page 20, line 1:…carboxyl functional groups and not "functions".
> Page 20, line 67/68: Correct the whole sentence: "Furthermore, uptake processes…"
> Page 22, line 27: …has been developed and tested.
> Page 23, line 12: Check the unit for Henry's law coefficient.
> Table 4: (c)…by switching of the UV-C
> Figure 9: ..5-dicarbonlys
> ESM:
> Page 19: First two lines?
> Page 20: line 10: …plotted as box model in ? (Where?)
> Page 24, line 6: Dashed lines in subfigure d (not c).

In particular we corrected all typos, rephrased unclear or misleading sentences, corrected wrong cross-references and units as pointed out in the specific comments listed above.

> Page 2, line 38: Use "auto-generation" throughout the manuscript. "Auto-construction" is not a good choice.
> In Table3 "automated mechanism self-generation" is used; in line 17 (page 15) "automated aqueous-phase mechanism generation", but mostly "auto-generation" is used. I would suggest using the same through the whole article.

Mechanism self-construction was consistently renamed to mechanism auto-generation in the main article and the ESM.

> The manuscript is very extensive with a lot of material including also ESM; I would suggest to shorten a bit if possible (especially the text/sentences, which are repeated can be deleted).
> I suggest also checking the English language.
> Page 3, lines 12-15 (Overall, a database…) can be deleted; the same is written below (lines 30-32).

To shorten the paper, the introductory part of section 2 was removed and partly moved to subsections 2.1 and 2.2. The article was carefully revised for the use of the English language. The analysis of the simple correlations in section 2.2 was shortened. This addresses the following comments:

> Page 3, lines 9-11: If aromatics are excluded here, then this sentence can be deleted.

However, we kept the sentence on p. 3, ll. 9-11 to make the reader aware of the additional aromatics data of the kinetics database, even though the data wasn't used for the CAPRAM/GECKO-A protocol at this stage.

> Further, I strongly suggest a separate list of abbreviation, which would be very helpful. The full name should be used at the beginning, and after abbreviation can be used throughout the manuscript.
> Page 1, line 33: Instead of mesitylene I would use 1,3,5-timethylbenzene or TMB later in the manuscript.

> The meaning of UPT, RNX, etc. sensitivity runs should be involved in the list of abbreviations.

Furthermore, we have introduced a list of abbreviations in a new appendix A, which is split into different topics/sections. In this context, we have removed Table 2 and moved the contents to appendix A.2. The appendix includes species abbreviations with 1,3,5-trimethylbenzene as TMB as suggest to address the following comments:

> Page 19, line 10: How OH radicals are formed from the photolysis of O_3 in the gas phase?
> During photolysis, O atom is formed, which with H_2O forms OH (RH 75%)?

We introduced two new reactions of

$O3 + hv \rightarrow O(^1D) + O2$

$O(^1D) + H_2O \rightarrow 2\ OH$

to clarify the formation of hydroxyl radicals from ozone photolysis in section 5.

> Page 13: Why do you use HLC abbreviation for the Henry's Law coefficient and not as it is usually used?

We have used HLC as abbreviation for Henry's law coefficient in the text of the article rather than the K_H or H as this is a it can be easily associated with Henry's Law coefficient and is a more spoken abbreviation and, hence, fits better with the text flow.

> Figure 19 & 20: TMB cannot not be seen.
> Page 20, line 41: From Fig. 19, the particle growth (red color) in the model run TMB cannot be seen.

In Figures 19 and 20, the concentrations in the model runs TMB and UPT were almost identical and graphs were on top of each other. Therefore, the concentrations in the run TMB were not visible. To overcome this issue, we introduced new dash-dotted line types for the scenarios UPT and RXN.

> Page 24, line 76: The grey dashed-dotted line is not visible.

As the overall carbonyl correlation is identical to the ketone correlation, both graphs are on top of each other. With the previous colour scheme, the grey dash-dotted line was hard to detect. Therefore, we have changed the colour to black and adjusted the figure caption accordingly.

> Page 30: Figure S9: Give the reference for the standard SAR.

In Fig. S9 in the ESM, reference to the construction method of the main SAR has been given citing all papers and cross-referencing Table 2 of the main article with the explanation of the construction method.

> Page 31: Correct the title for Figure S10.

As Figure 10 has no title, we are not quite sure, what the following comment meant. However, we detected a mistake in the unit of the organic mass and corrected the y axis label. Furthermore, we spelled out "organic" in the legend.

> Page 32: Figure S12: It is good to shortly explain alpha, beta and gamma scenarios also here.

The caption of Fig. S12 has been expanded to shortly explain the different subversions of the CAPRAM/GECKO-A protocol.

> Figure 13: Add conditions or at least mark cloud and non-cloud periods. This should be done also for other figures.

We have expanded on the conditions in all figures of the sensitivity runs and explained the shading of cloud and night-time periods in the plots in the figure captions.

> Page22, line 5: Do you have an idea how malic acid is formed?

As stated on page 21, ll. 18-21, the formation of malic acid from TMB cannot be explained with the current knowledge. Therefore, we attributed the formation to background chemistry, most likely from reactions with the chamber walls and possible residue of previous experiments.

We thank Andrea Chlebikova for the very thorough work and the positive and helpful feedback. We adjusted our manuscript accordingly. In particular we corrected all typos, rephrased unclear or misleading sentences, corrected wrong cross-references and units as pointed out in the technical corrections of section 3. In the following, general and specific comments are addressed.

> p6, line 4/5: mistakenly referring to **R**2 value as correlation coefficient
> ESM, p15, p18, p20, p21, p22, p23: throughout (including the labels of Tables S3, S5, S6, S7), **R**2 is mistakenly referred to as the correlation coefficient

We have corrected the mis-used term ‘correlation coefficient’ to ‘coefficient of determination’.

> p21, line 7: change “has also" to “also has" and add comma before “decreasing"
> Inconsistent use of hyphenation of gas-phase/aqueous-phase throughout this section – standardise

Concerning the seemingly inconsistent use of ‘gas-phase’ and ‘gas phase’, we have used the hyphenated form for the use as adjective as in `gas-phase compounds` and the unhyphenated form to address the gas phase as a noun. Therefore, we believe that the hyphenation is correct in this context. Mechanism self-construction was consistently renamed to mechanism auto-generation.

> While I have found the written text (despite the reservations above) for the most part easy to follow, I believe some of the figures used are quite difficult to read and interpret, and would benefit from replotting. This applies in particular to Figure 1, where I am struggling to see what the different boxplots represent. Figures 3, 4, 5, 7, S1, S3, S4, S5, S6 and S7 would benefit from using different symbols as markers rather than just different colours, as some of the colours are quite difficult to distinguish. Figure 8 could be made clearer by using more significantly different markers (rather than crosses with different orientations).

We have replotted Figures 1, 3-5, 7, S1-S7 with a revised colour and marker scheme. The marker scheme compromises between the distinctness of shapes and shapes that don’t cover other data points, when many data are close together in a graph. Moreover, we have expanded on the axis labels in Fig. 1 and introduced an additional legend. Moreover, alternate grey and white shading was used to mark boxplots of corresponding compound classes.

While replotting these figures, some mistakes were correct in the old graphs. This includes some mislabelled data as well as an update of some data from an earlier version of the kinetics database. Correlations in Table S3 and S7 were updated in this context and the tables slightly reformatted.

> I would try to move more of the detail into the ESM, as the main text is currently very long. For example, at present, sections discussed at length in the ESM are still discussed in a lot of detail in the main text (e.g page 2 and page 7), when referencing the ESM should be enough. The text also feels unnecessarily long when sections are introduced carefully, and then go on to repeat the context mentioned previously.

To shorten the paper, the introductory part of section 2 was removed and partly moved to subsections 2.1 and 2.2. The analysis of the simple correlations in section 2.2 was shortened. Furthermore, we have introduced a list of abbreviations in a new appendix A, which is split into different topics/sections. In this context, we have removed Table 2 and moved the contents to appendix A.2.

> ESM, p25, Table S9, p27, Table S10, p28 Tables S11 and S12: please check the units;
> I can understand those in Table S8, even though it would perhaps make more sense

> to say C itself is dimensionless (etc.) unless the division by its units is also added into the equation; for these other tables, the volume part of the units does not seem to add up correctly.

In Tables S8 to S12, correlations are used to derive a second order aqueous-phase rate constant in $M^{-1}\ s^{-1}$ from the BDE in $kJ\ mol^{-1}$. Therefore, constants in the regression have the same unit as k_{2nd} and are in in $M^{-1}\ s^{-1}$. For terms with the BDE, the units are $M^{-1}\ s^{-1}\ kJ^{-1}\ mol$ to yield the unit of k_{2nd}. With M = mol l^{-1}, the unit can be simplified to $l\ mol^{-1}\ s^{-1}\ kJ^{-1}\ mol$ = $l\ kJ^{-1}\ s^{-1}$. For terms with a quadratic BDE, $kJ\ mol^{-1}$ has to be squared, which yields $mol\ l\ kJ^{-2}\ s^{-1}$ after simplification. To unify all notations, units in Table S8 have been changed to the simplified form. In Tables S10 and S12, l^2 was correct to l in the units of the quadratic term.

> The figures showing simulation data can only be understood in conjunction with careful reading of the main text, and would benefit from more detailed descriptions in their labels.

We have expanded on the conditions in all figures of the sensitivity runs and explained the shading of cloud and night-time periods in the plots in the figure captions.

> The new “advanced" Evans-Polanyi correlation strikes me as unusual, in that it can no doubt usefully scale with molecular size – but it would intuitively seem to me that we are losing most of the useful information that the individual bond enthalpies provide by lumping them into one sum. There ought to be a “better" way of accounting for more than the weakest bond than using the sum of BDEs, and perhaps this will be something that can be further improved in the future.

We thank Andrea Chlebikova for the useful feedback provided. Clearly, there is potential for further improvement of chemical mechanism development on both the experimental and theoretical side. To illustrate this fact, we added the below sentences in section 4.1 about the CAPRAM/GECKO-A protocol on page 15, ll. 28–30:

„There is a need for further development of a prediction method for kinetic and mechanistic data of nitrate radical reactions with organic compounds. However, for more advanced predication methods such as SARs, a more comprehensive experimental database is needed.“

Moreover, we have re-phrased the following sentence

“A certain disadvantage of this method is that information about branching ratios and reaction products is lost.“

to „… cannot be provided.“ The previous description implied that the original Evans-Polanyi method was able to provide branching ratios, however, it can only suggest the major reaction products. This information is still available from the individual BDEs, but a quantitative analysis of the branching ratios is not straight-forward.

Development of a protocol for the auto-generation of explicit aqueous-phase oxidation schemes of organic compounds

Peter Bräuer[1, a], Camille Mouchel-Vallon[2, b], Andreas Tilgner[1], Anke Mutzel[1], Olaf Böge[1], Maria Rodigast[1, c], Laurent Poulain[1], Dominik van Pinxteren[1], Ralf Wolke[3], Bernard Aumont[2], and Hartmut Herrmann[1]

[1]Atmospheric Chemistry Department (ACD), Leibniz Institute for Tropospheric Research (TROPOS), Permoserstr. 15, 04318 Leipzig, Germany
[2]Laboratoire Interuniversitaire des Systèmes Atmosphériques, UMR CNRS/INSU 7583, Université Paris Est Créteil et Université Paris Diderot, Institut Pierre Simon Laplace, 94010, Créteil, France
[3]Modelling of Atmospheric Processes Department (MAPD), Leibniz Institute for Tropospheric Research (TROPOS), Permoserstr. 15, 04318 Leipzig, Germany
[a]Now at Wolfson Atmospheric Chemistry Laboratories and National Centre for Atmospheric Science, University of York, York, YO10 5DD, UK
[b]Now at National Center for Atmospheric Research, Boulder, Colorado, USA
[c]Now at Indulor Chemie GmbH & Co. KG Produktionsgesellschaft Bitterfeld, 06749 Bitterfeld-Wolfen, Germany

Correspondence to: Hartmut Herrmann (herrmann@tropos.de)

Abstract.

This paper presents a new CAPRAM/GECKO-A protocol for mechanism auto-generation of aqueous-phase organic processes. For the development, kinetic data in the literature were reviewed and a database with 464 aqueous-phase reactions of the hydroxyl radical with organic compounds and 130 nitrate radical reactions with organic compounds has been compiled and evaluated. Five different methods to predict aqueous-phase rate constants have been evaluated with the help of the kinetics database: gas aqueous phase correlations, homologous series of various compound classes, radical reactivity comparisons, Evans-Polanyi-type correlations, and structure-activity relationships (SARs). The quality of these prediction methods was tested as well as their suitability for automated mechanism construction. Based on this evaluation, SARs form the basis of the new CAPRAM/GECKO-A protocol. Evans-Polanyi-type correlations have been advanced to consider all available H-atoms in a molecule besides the H-atoms with only the weakest bond dissociation enthalpy (BDE). The improved Evans-Polanyi-type correlations are used to predict rate constants for aqueous-phase NO_3 + organic compounds reactions.

Deleted: mechanisms

Deleted: was

Deleted: -

Extensive tests have been performed on essential parameters and highly uncertain parameters with limited experimental data. These sensitivity studies led to further improvements in the new CAPRAM/GECKO-A protocol, but also showed current limitations. Biggest uncertainties were observed in uptake processes and the estimation of Henry's Law coefficients as well as radical chemistry, in particular the degradation of alkoxy radicals. Previous estimation methods showed several deficits, which impacted particle growth.

For further evaluation, a 1,3,5-timethylbenzene oxidation experiment has been performed at the aerosol chamber LEAK at high relative humidity conditions and compared to a multiphase mechanism using the MCMv3.2 in the gas phase and a methylglyoxal oxidation scheme of about 600 reactions generated with the new CAPRAM/GECKO-A protocol in the aqueous phase. While it was difficult to evaluate single particle constituents due to concentrations close to the detection limits of the instruments applied, the model studies showed the importance of aqueous-phase chemistry in respect to SOA formation and particle growth. The new protocol forms the basis for further CAPRAM mechanism development towards a new version 4.0. Moreover, it can be used as a supplementary tool for aerosol chambers to design and analyse experiments of chemical complexity and help understanding them on a molecular level.

Deleted: mesitylene

1 Introduction

The ubiquitous abundance of organic compounds in natural and anthropogenically influenced ecosystems impacts climate, air quality, human health, the oxidation capacity of the troposphere, crop yields, particle growth and composition. Their detrimental effects cause enormous economic cost (Boucher et al., 2013; Brasseur et al., 2003; Dunmore et al., 2015; Hallquist et al., 2009; Pereira et al., 2018). With large annual emissions of about 1300 Tg C/a (Goldstein and Galbally, 2007), non-methane volatile organic compounds have been a research interest for many decades. Despite intense research efforts, the system of organic compounds is still insufficiently understood because of its complexity. The large emissions do not only lead to a large mass of organic compounds in the atmosphere, but also to a large variety of organic compounds. Currently, 10^4 to 10^5 different organic compounds have been identified, but are assumed to be only a small fraction of the actual number (Goldstein and Galbally, 2007).

Deleted: effects

Formatted: Font color: Black

The multiphase nature of the oxidation of organic compounds further contributes to the complexity. Organic compounds are ubiquitously found in aerosol particles around the globe with contributions between 20% and 90% of the total aerosol mass (Jimenez et al., 2009). While primary organic aerosol (POA) is an additional source of organic compounds in the atmosphere to direct gas-phase emissions, gas-to-particle conversion, multiphase and heterogeneous processes form secondary organic aerosol (gasSOA) influence the composition in either phase (Ervens et al., 2011; Hallquist et al., 2009; Jimenez et al., 2009). With aerosol water being in excess of dry aerosol mass by a factor of 2 to 3 (Ervens et al., 2011), aqueous-phase chemistry plays an important role in the degradation of organic compounds. Organic aerosol oxidation state, size and product distribution as well as relative humidity dependence can only be explained by aqueous-phase chemistry forming secondary organic aerosol (aqSOA; Ervens et al., 2011).

Deleted: and

Numerical modelling provides a useful tool for the analysis of such comprehensive and complex processes. Comprehensive benchmark mechanisms exist for either the gas phase (e.g., the Master Chemical Mechanism, MCM, http://mcm.leeds.ac.uk/; Jenkin et al., 2003; Saunders et al., 2003) or the aqueous phase (e.g., the Chemical Aqueous Phase RAdical Mechanism, CAPRAM, http://projects.tropos.de/capram/ Herrmann et al., 2005, with latest updates by Bräuer et al., 2013). With a growing mechanism size in either phase of currently about 17,000 gas phase (MCM v3.3.1) and 777 aqueous-phase reactions (CAPRAM 3.0), mechanism auto-generation becomes increasingly important (see also Vereecken et al., 2018). This method has several advantages over manual mechanism construction. Among its key strong points are a reduced proneness to errors as any errors embedded in the generation routines produce systematic errors in the output chemical mechanisms, which are easier to detect than random errors in manual mechanisms. Most importantly, with suitable estimation methods for the prediction of the necessary kinetic and mechanistic data, it is possible to overcome the inevitable lack of experimental data for the large number of organic compounds measured in field and laboratory experiments or produced by mechanism auto-generation. The detailed explicit mechanism produced with an auto-generation method can help to interpret experimental data (e.g., La et al., 2016; Lee-Taylor et al., 2015; McVay et al., 2016). Modelling can suggest isomer information along with detailed information about the production and degradation processes.

Deleted: Mechanisms

Deleted: automated

Deleted: construction

Deleted: constructing

Deleted: (e.g., La et al., 2016; Lee-Taylor et al., 2015; Mcvay et al., 2016)

Currently, atmospheric organic chemistry is more widely studied and understood in the gas phase than in the aqueous phase, whether through experimental or modelling studies (Ervens, 2015). The current study aims to reduce this gap by providing a protocol for the auto-generation of comprehensive aqueous-phase mechanisms. While with the Generator for Explicit Chemistry and Kinetics of Organics in the Atmosphere (GECKO-A; Aumont et al., 2005), tools for mechanism auto-generation are already available for the gas phase, only first attempts have been presented for the aqueous phase with the study by Li and Crittenden (2009). Mouchel-Vallon et al. (2013) investigated a protocol for phase transfer processes between the gas and the aqueous phase and effects on the composition in either phase. The current study takes the study by Mouchel-Vallon et al. (2013) a step further with a new protocol for mechanism auto-generation of chemical processes in the aqueous phase. A new protocol has been developed and incorporated in the expert system GECKO-A. Test mechanisms were generated and validated against experiments performed at the aerosol chamber LEAK (Leipziger Aerosol Kammer; Mutzel et al., 2016). Beforehand,

Deleted: construction

Deleted: for such an approach

Deleted: construction

an extensive literature review of kinetic data and suitable estimation methods for the prediction of kinetic and mechanistic data for aqueous-phase reactions of organic compounds has been performed to ensure the generation of comprehensive, state-of-the-art aqueous-phase mechanisms.

2 Evaluation of kinetic data and prediction methods

2.1 Evaluation of experimental kinetic data

For the construction of a protocol for mechanism auto-generation, a large database with kinetic data is a prerequisite. Data are used directly to assign rate constants to reactions created by the mechanism generator and indirectly to evaluate or advance current prediction methods for missing rate constants based on the known experimental values. The present study focuses on aliphatic organic compounds; however, the kinetics database includes aromatic compounds of atmospheric interest for completeness. Overall, 464 aqueous-phase hydroxyl radical (OH) and 130 nitrate radical (NO_3) reactions with organic compounds have been reviewed and can be found in section S1 of the electronic supplementary material (ESM). The database includes compound classes of atmospheric interest, i.e. alkanes, alcohols (including di- and polyols), carbonyl compounds, carboxylic acids and diacids, esters, ethers, unsaturated, cyclic, aromatic compounds, and polyfunctional compounds composed of these functionalities.

The kinetics database is based on existing recommendations and compilations (Buxton et al., 1988; Ross et al., 1998; Herrmann, 2003; Herrmann et al., 2010) with additional data collected from recent literature. In exceptional cases, where no other data existed, data from unpublished TROPOS measurements have been used for the database as well. In cases, where no clear preference to a dataset could be given, averaging was used.

2.2 Simple correlations

Besides the review of kinetic data, it is equally important to review estimation methods for the prediction of missing kinetic data in auto-generated mechanisms. A number of prediction methods exist, which include straight-forward correlations that are easy to implement in automated tools for mechanism generation. These correlations include gas–aqueous phase correlations, extrapolations of homologous series of compound classes, and reactivity comparisons between different radical oxidants.

These methods were therefore evaluated for their use in mechanism generators. Correlations were derived for the various compound classes and absolute errors are analysed with box plots. Results from the analysis are shown in Figure 1, while a detailed analysis is given in section S2 of the ESM. For such simplistic approaches, good results are obtained from these methods and one can expect to at least predict the correct order of magnitude for a given rate constant (see Figure 1). In general, slightly negative absolute errors are observed in Figure 1, thus, the predictions tend to overpredict the rate constants somewhat. The largest deviations of the absolute errors of the logarithmised rate constants range from -2.1 to 0.9. Simple structures like pure hydrocarbons are predicted far more accurately than more complex structures. The largest deviations are observed for carbonyls and carboxylic acids. Moreover, often the smallest members of a compound class show large deviations from the general trend as in the case of carboxylic acids. For alkanes, methane is excluded in the evaluation of homologous series in Figure 1 as its absolute log error of 16.8 does not fit in the scale of the plot.

While the easy implementation of the above correlations in computer-assisted tools make their usage desirable, they are unsuitable for mechanism auto-generation for several reasons. Overall, their accuracy is satisfactory, but can be improved. More importantly, all of the above correlations have a very restricted applicability. For gas–aqueous-phase correlations, gas-phase kinetic data are needed. For complex systems such as CAPRAM/GECKO-A, many data had to be estimated, which would increase errors to unsatisfactory levels. For radical comparisons, the lack of the needed aqueous-phase data is even

Deleted: have

Moved (insertion) [1]

Deleted: In the

Deleted: , the aim of

Deleted: is to deliver a comprehensive set of reviewed rate constants in the aqueous phase for reactions of hydroxyl and nitrate radicals with a wide range of organic compounds. The recommendations of experimental data include

Deleted: , however, at the current state this compound class is excluded to evaluate prediction methods for mechanism auto-generation.¶
An extensive review and evaluation of available kinetic data from literature has been undertaken.

Deleted: a database with

Deleted: reactions of the

Deleted: and 130 reactions of the nitrate radical reactions with organic compounds has been created and is introduced in section 2.1. Tables with lists of the recommended values

Deleted: ¶
Secondly, the literature review was focused on already available prediction methods for radical reactions with organic compounds. Prediction methods investigated include gas–aqueous phase correlations, homologous series of various

Deleted: , reactivity comparisons between radicals, Evans-Polanyi-type correlations (including the BDE prediction method after Benson, 1976), and structure-activity relationships (SARs).¶
In the following sections, these prediction methods are discussed for the OH and the NO_3 radical with a focus on the applicability in mechanism auto-generation.¶

Moved up [1]: **2.1 Evaluation of experimental kinetic data**¶

Deleted: Several comprehensive compilations and recommendations exist for aqueous-phase kinetic data (e.g., Buxton et al., 1988; Ross et al., 1998; Herrmann, 2003; Herrmann et al., 2010). Experimental data relevant for tropospheric chemistry of organic compounds were collected from these compilations and assembled in a comprehensive kinetics database. Moreover, kinetic data from further laboratory experiments were collected from literature and, in exceptional cases where no other data existed, from unpublished TROPOS measurements. Rate constants were carefully reviewed. In general, already recommended values from compilations were taken over from literature. Further experimental data (including more recent data, where no recommendations existed) were selected by actuality, but also quality of the data. If no clear preference was ... [1]

Deleted: So far, only the reactions of aliphatic compounds (including 282 OH and 76 NO_3 reactions) have been used to design ... [2]

Deleted: -

Deleted:

Deleted: Largest

Moved (insertion) [2]

Deleted: disqualify

Deleted: application. To predict

Deleted: rate constants by correlating gas- and aqueous-phase kinetic data

Deleted: is

Deleted: Gas-phase kinetic measurements are not sufficient to support this method in

Deleted: mechanism generators

Deleted: . Gas-phase kinetic

Deleted: would have

Deleted: in order to apply this method for mechanism auto-generation…

Deleted: the errors significantly. Extrapolations of homologous series of compound classes

Deleted: limited

worse. The prediction with homologous series is restricted to very distinct molecule structures as detailed in the ESM. Therefore, the focus of this study is on more complex correlations and prediction methods.

2.3 Evans-Polanyi-type correlations

More advanced correlations for the prediction of rate constants of organic compounds are Evans-Polanyi correlations. Originally developed for the gas phase by Evans (1938), they have been successfully applied to the aqueous phase (see, e.g., Herrmann and Zellner, 1998; Hoffmann et al., 2009). In an Evans-Polanyi-type correlation, a linear relationship between the activation energy and the bond dissociation enthalpy (BDE) of a molecule is derived by:

$$E_A = a' + b' \cdot BDE(C-H) \qquad (1)$$

Using the Arrhenius expression in its logarithmised form ln k = ln(A) - E_A/RT and assuming a rupture of only the weakest C–H bonds in molecule leads to:

$$\log(k_H) = \log\left(\frac{k_{2nd}}{n_H}\right) = a - b \cdot BDE(C-H) \qquad (2)$$

where $a = \log(A/n_H) - a'/(RT\ln 10)$ and $b = b'/(RT\ln 10)$, n_H is the number of H-atoms bonded with the lowest BDE in a molecule, R is the universal gas constant, and T is the temperature. A is the pre-exponential factor of the Arrhenius equation, which has to be similar for all reactants correlated to fulfil equation 2. k_H is the second order rate constant of the reaction scaled by the number of weakest C–H bonds. The method relies on BDEs as input for the correlation, which can be estimated reliably with a precision of ±8 kJ mol^{-1} (Benson, 1976). The method by Benson (1976) estimates the strength of a bond as a function of the adjacent atoms/molecular groups.

2.3.1 OH rate constant prediction

The kinetics database was used to derive Evans-Polanyi-type correlations, which are plotted in Figure S5 in the ESM. Parameters for the regression equations and further statistical data are given in Table S8 in the ESM. Even for a large database as used in this assessment, a reliable correlation is hardly achieved (see Figure S5 in the ESM). Several outliers can be found in the dataset. A critical evaluation of the data is necessary and depending on this evaluation, several possible correlations can be found. Furthermore, there are several cases where data points have exactly the same BDE, but vary in their reaction rate constants by more than one order of magnitude. The reason for this behaviour is the correlation of the rate constants to only the weakest BDE, which corresponds to the main radical attack site in a molecule or the main reaction channel. When correlating a homologous series of compounds to the bond dissociation enthalpy, the lowest BDE in each molecule varies only slightly. On the other hand, rate constants increase significantly with the carbon number due to side attacks of the radical oxidants at the remaining carbon skeleton. With increasing chain length, side attacks become more likely even if the BDE is higher compared to the weakest bond. With the correlation of log(k_H) against only the smallest BDE of a molecule, this fact cannot be considered in the correlation.

Accordingly, the use of Evans-Polanyi correlations in this way results in large uncertainties. The evaluation of the absolute errors of the predicted versus experimental data with box plots confirms the discussion above. Relatively large errors are seen for carbonyl compounds and carboxylic acids while errors are somewhat smaller for alcohol compounds and alkanes (see Figure 2). The performance is not significantly better than the performance of the much simpler correlations described in the preceding section. However, a major advantage of Evans-Polanyi-type correlations is the much wider applicability.

For further details, the prediction method has been re-analysed with the help of scatter plots, where the predicted data derived from the correlations is plotted over the experimental data. In a perfect correlation, all data should line up on the 1:1 line in such a plot with a coefficient of determination R^2 of 1. Any deviations of the y-intercept of the regression line from 0 or of the slope from 1 indicate a general bias of the prediction method. Reductions of the coefficient of determination are due to deviations of the single predictions.

Deleted: defined

Moved up [2]: For alkanes, methane is excluded in the evaluation of homologous series in Figure 1 as its absolute log error of 16.8 does not fit in the scale of the plot.

Deleted: , such as terminal mono-alcohols or diols. The restrictions are best demonstrated by the simplest compound class of alkanes. While extrapolations are very accurate, one has to carefully revise the existing data to derive accurate predictions. Different regression lines have to be used for linear and branched alkanes. Furthermore, often the smallest members of a compound class have to be excluded to derive best results of the correlation lines as in the case of carboxylic acids. …

Deleted: Dicarboxylic acids follow a sigmoidal rather than a linear regression as explained in section S2.2 of

Deleted: The regression yields negative rate constant values for the smallest members oxalate and malonate.

Deleted: these species have been excluded in the evaluation of homologous series in Figure 1. Combined with the fact that only a small dataset of aqueous rate constants exists, overfitting

Deleted: likely and the predicted correlations should be handled with care.
In reactivity comparisons, where the rate constants of different radical oxidants in the aqueous phase are compared and correlated, a large kinetic data set with a sufficient intersect of organic reactants for the radical oxidants is needed to derive reliable

Deleted: . While this goal is already only partially achieved for a limited set of structures, the method completely disqualifies for mechanism auto-generation as kinetic measurements are of one radical oxidant are needed to predict rate constants of another. Kinetic datasets are too small to ensure a functional predication in automated mechanism generators. An analysis with box plots was not performed due to the limited data points. Due to their limited applicability, the

Deleted: are briefly described in the ESM, correlations are provided, but are not considered for use in CAPRAM/GECKO-A

Deleted: ·exp(-

Deleted:)

Deleted: -atoms

Deleted: will be abstracted during a reaction

Deleted: if

Deleted: are used

Deleted: ,

Deleted: of the prediction method are resulting

Deleted: correlation

Deleted: in such a plot.

Deleted: of

Deleted: correlation coefficients

Figure 3 shows that, except for the pure hydrocarbons, rate constants of fast reacting compounds are underpredicted while rate constants of smaller compounds are overpredicted. This fact demonstrates the limitations of the current Evans-Polanyi-type correlations to accurately predict rate constants of larger compounds as it was already seen during the derivation of the correlation. Faster rate constants in the dataset belong to larger compounds. Hence, the increase of their observed rate constants is larger than the increase expected from their lowest BDE due to increased side attacks of the hydroxyl radical at the remaining carbon skeleton. As these side attacks are not considered in the correlation, where only the weakest bound H-atoms of the major reaction pathway are correlated against log(k_H), an underprediction is inevitable. As a consequence, the regression line of the correlation is tilted resulting in an overprediction of smaller or slow reacting compounds.

2.3.2 NO_3 rate constant prediction

The much smaller dataset of available NO_3 reactions of aliphatic compounds further reduces the accuracy of Evans-Polanyi-type correlations. It is considerably harder to derive reliable correlations, which can be achieved only for alcohol compounds and carboxylic acid with an appreciable coefficient of determination R^2 between 0.6 and 0.7. Correlations are shown in Figure 4a with the respective statistical data given in Table S9 in the ESM.

Deleted: for reactions of organic compounds with this radical oxidant.…

Deleted: correlation coefficients

Predictions of NO_3 reactions with organic compounds inherit large errors. For a large fraction, the right order of magnitude is not even predicted. Again, an underprediction of fast reactions (or large molecules) is observed, while the rate constants of smaller or slow reacting compounds are overpredicted (see Figure 4a) as discussed for OH in the previous subsection.

Deleted:)

2.3.3 Advanced Evans-Polanyi-type correlations

The evaluation of current Evans-Polanyi-type correlations has shown strong limitations for the use of automated prediction methods, which aims at large molecules, where the formation of many intermediate compounds makes manual mechanism construction infeasible. As the accuracy of the predictions of rate constants for these compounds is significantly reduced, a revision and improvement of the current correlations is needed and is described in this subsection.

Deleted: a

Deleted: are

Deleted: are

Development of improved Evans-Polanyi-type correlations

The need to improve Evans-Polanyi-type correlations for larger compounds, where minor reaction channels become increasingly important as outlined in the preceding subsections, led to a revised correlation method, where the sum of all BDEs of bonds including hydrogen atoms (∑BDE) was correlated against the overall second order rate constant:

$$\log(k_{exp}) = a - b \cdot \sum BDE \qquad (3)$$

The consideration of minor pathways is achieved by including all BDEs rather than only the weakest ones and the overall second order rate constant instead of the second order rate constants scaled to the number of weakest H-atoms. A certain disadvantage of this method is that information about branching ratios and reaction products cannot be provided.

Deleted: is lost

OH radical rate constant predictions

Compared to previous Evans-Polanyi-type correlations, significant changes are observed as can be seen from

Formatted: Don't keep with next

Figure 5. The range of ∑BDE is much broader ranging from about 500 to 8000 kJ mol^{-1} compared to a BDE range of about 360 – 440 kJ mol^{-1}. More importantly, in the new correlation there is a positive correlation between ∑BDE and k_{exp}. The positive correlation derives from the fact that ∑BDE is correlated to all abstractable H-atoms and that k_{exp} increases with larger molecules, i.e. an increasing number of H-atoms or ∑BDE. In the original Evans-Polanyi-type correlations, a negative correlation is observed due to higher reactivities at molecular sites with low BDEs. The most striking difference are quadratic correlations in the advanced Evans-Polanyi-type correlations compared to linear correlations previously. In the new

correlations, rate constants plotted over ∑BDE follow downward-opened parabolas. All data fits with in an upper and lower parabola, which converge towards log(k_{exp} / M^{-1} s^{-1}) = 10 and ∑BDE = 8000 kJ mol^{-1} in the log(k_{exp}) over ∑BDE diagram.

A likely reason for the different behaviour of the old and the new regressions is the diffusion limit of reactions. The diffusion limit does not come into effect in the old correlation, where the partial rate constant (k_H) refers to only the weakest bound H-atoms. When the overall rate constant is considered, the diffusion limit is reached for high values of ∑BDE. Thus, despite an increasing ∑BDE due to an increasing number of abstractable H-atoms, the rate constants might not increase accordingly as they are levelling off and undergo a transition to control by diffusion rather than by chemical control. This view is supported by the upper limit of all data around log(k_{exp} / M^{-1} s^{-1}) = 10, the approximate diffusion limit of rate constants of OH with organic compounds (see, e.g., Haag and Yao, 1992; Schöne et al., 2014).

The correlations show significant improvements with coefficients of determination R^2 up to 0.99 (see Figure S6 and Table S10 in the ESM). A weak correlation is still observed for ketones (R^2 = 0.24) and alcohol compounds except linear terminal alcohols (R^2 = 0.35). Monocarboxylic acids show only a moderate correlation (R^2 = 0.55). The better performance can also be evaluated from the absolute errors analysed as box plots in Figure 6. Almost all data are predicted with the correct order of magnitude. The weak correlations of the above-mentioned compound classes are reflected by larger errors. More importantly, the objective to reduce biases of larger molecules was achieved as can be observed from the scatter plot of the calculated over experimental data in Figure S7 in the ESM. Except for ketones, regression lines now have a slope close to 1 (between 0.76 and 1.16). Omitting the outlier acetylacetone in the analysis of ketones gives a slope of the regression line of 0.54, which is still a big improvement compared to the original correlation. Although an omission of data points for the derivation of a correlation is not ideal, a large modified Z score after Iglewicz and Hoaglin (1993) (see equation 4) of 4.21 justifies the removal of the data point from the dataset. Acetylacetone is the only compound, which has a modified Z score well above the suggested threshold of 3.5 (Iglewicz and Hoaglin, 1993).

Deleted: correlation

$$Z_i = \frac{0.6745(x_i - \tilde{x})}{MAD} \quad (4)$$

In equation 4, x_I is the individual measurement, $\tilde{x}$ the median, and MAD the median absolute deviation.

NO_3 radical rate constant predictions

When deriving the advanced Evans-Polanyi-type correlations for nitrate radical reactions with organic compounds, a major difference to hydroxyl radical reactions is observed. NO_3 reactions follow a linear trend rather than a quadratic correlation. The additional quadratic polynomial does not reduce errors significantly. An explanation for the different behaviour can be found again in the diffusion limit of both reactions. The diffusion limit of nitrate radical reactions is only insignificantly smaller compared to hydroxyl radical reactions (~$9.5 \cdot 10^9$ M^{-1} s^{-1} vs. ~10^{10} M^{-1} s^{-1}). However, rate constants for nitrate radical reactions are in the order $10^4 – 10^8$ M^{-1} s^{-1}. Most reactions are below 1% of their diffusion-controlled limit. Therefore, the diffusion limit does not affect the correlation. Even though a quadratic correlation could be applied, values are so far away from the maximum of the parabola, that a linear equation is an equally valid approximation.

The correlations are shown in Figure 7 with the raw data in subfigure (a) and the final correlations in subfigure (b). The respective statistical data is provided in Table S11 and S12 in the ESM. Both linear (solid lines) and quadratic regressions (dashed lines) are shown in Figure 7b. Another advantage of the advanced Evans-Polanyi-type correlations is that certain compound classes can be grouped together without a loss of accuracy. This increases the number of data points used for each regression and, therefore, its reliability. For the derivation of the final correlations, data from tert-butanol and acetone have not been considered due to their high modified Z scores of 5.55 and 4.57, respectively, well above the suggested threshold of 3.5 (Iglewicz and Hoaglin, 1993).

Deleted: suggest

As can be seen from Figure 7b and the statistical data in Table S11 and S12 in the ESM, only a weak correlation with large associated errors is observed for carboxylic acids. Moreover, for this compound class, a negative correlation is observed for which the reasons remain unclear. More data are needed to constrain a more reliable correlation for these types of molecules and their respective NO_3 reactions.

Overall, the advanced Evans-Polanyi-type correlations perform well with significantly reduced errors as can be seen from the box plot analysis in Figure S8 in the ESM. The correct order of magnitude is met for almost all compounds and usually errors are much smaller. Only one carboxylic and two dicarboxylic acids are not predicted within the correct order of magnitude. Biases of the slopes of the regression lines in the scatter plot of the calculated over experimental data are significantly reduced except for the very uncertain correlation of carboxylic acids (see Figure S7 in the ESM).

2.4 Structure-activity relationships

A more sophisticated prediction of rate constants of the hydroxyl radical with organic compounds can be achieved by means of structure-activity relationships (SARs). In an SAR, the assumption is made that a molecule can be split into increments. Rate constants are assigned to the individual increments, which are modulated by the effects of the neighbouring groups in α- and, in the case of the SAR by Doussin and Monod (2013), in β-position as well as ring effects of the molecule. The overall reaction rate is the sum of the incremental rate constants. Two structure-activity relationships from the literature have been compared – the SAR by Minakata et al. (2009) and the one by Monod and Doussin (2008) with updates by Doussin and Monod (2013).

Deleted: and the overall reaction rate is the sum of the individual reaction rates of each increment

2.4.1 SAR by Minakata et al.

A big advantage of the SAR of Minakata et al. (2009) is the large dataset of 434 aqueous-phase reaction rate constants covering all important compound classes for tropospheric aqueous-phase chemistry including alkanes, alcohols, carbonyl compounds, carboxylic acids, ethers, esters, sulphur-, nitrogen- and phosphorus-containing species, polyfunctionals, unsaturated compounds, and aromatics. Their dataset was split in a training set of 310 reactions to derive the SAR and a test set of 124 reactions for validation. The large dataset enables a robust prediction of aqueous hydroxyl radical reaction rates with all organic compounds of atmospheric relevance. The authors were able to achieve a high accuracy and predict rate constants of 83% of the compounds in their training set and 62% of the compounds in their test set within a factor of 2.

Deleted: phosphorous

2.4.2 SAR by Monod and Doussin

The structure-activity relationship by Monod and Doussin (2008) covers the prediction of OH rate constants for alkanes, alcohols, carboxylic acids and bases as well as polyfunctional compounds derived from these functions. 72 compounds were used to derive the SAR. A major improvement of the SAR by Monod and Doussin (2008) is the introduction of a second correction factor for the incremental rate constants taking the effects of the β-neighbours into account. However, this improvement is also one of its biggest weaknesses as over-fitting becomes likely. With the dataset of 72 compounds, 22 descriptors have been defined. Moreover, a wide range of atmospherically relevant compounds is still missing and currently only H-abstraction reactions are possible to predict with this SAR. Yet, high accuracy is achieved and according to their own validation, Monod and Doussin (2008) predicted 60% of their compounds tested within the range of 80% of the experimental value.

The original SAR by Monod and Doussin (2008) was extended to include carbonyl compounds by Doussin and Monod (2013). The original parameters were kept constant and new parameters have been introduced to describe the partial rate constant at aldehyde groups and α- and β-effects of carbonyl (keto and aldehyde) groups. Moreover, a modulating factor for gem-diol groups in hydrated carbonyls was introduced.

Deleted: introduce

2.4.3 Comparison of both SARs

In general, both SARs by Minakata et al. (2009) and Monod and Doussin (2008) with updates by Doussin and Monod (2013) are suitable tools for automated rate constant prediction of aqueous-phase hydroxyl radical reactions with organic compounds with the above-mentioned strengths and restrictions. The accuracy is high and implementation in computer-assisted tools is easy. All parameters are delivered by the structure-activity relationships and the only input variable is the chemical structure of the organic compound. Both SARs were tested using the kinetics database described in section 2.1. They show a very good agreement with the experimental values, especially for simple molecules (see scatter plots in Figure 8). Best results are achieved for pure hydrocarbons and errors increase when introducing substituents. Largest errors occur for polyfunctional compounds. The box plots of the absolute errors of both SARs compared to the experimental values demonstrate these facts (see Figure 9). More detailed information on the statistical data of the evaluation for every compound class can be found in the review by Herrmann et al. (2010).

The box plots in Figure 9 show that both SARs have difficulties predicting the hydroxyl radical rate constants for dicarbonyl compounds (compound class 5). There is a large variation of about 3 orders of magnitude in the absolute errors between the minimum and the maximum value. Both SARs underpredict the rate constants. The difficulties may be caused by the small dataset of only 5 dicarbonyl compounds.

In general, errors are smaller in the SAR by Doussin and Monod (2013) due to the second descriptor for β-neighbours; however, it is noted again that over-fitting might be a problem in the SAR of these authors. Errors in both SARs are very small and besides a few exceptions well within one order of magnitude.

Deleted: ,

3 Sensitivity runs of crucial parameters

Based on the evaluation of the kinetic data and prediction methods for aqueous-phase rate constants a preliminary protocol has been designed for mechanism auto-generation. The protocol uses SARs for hydroxyl radical reactions with organic compounds and the linear correlations of the refined Evans-Polanyi-type correlations for nitrate radical reactions with organic compounds. For uptake, the structure-activity relationship GROMHE (GROup contribution Method for Henry's law Estimate, Raventos-Duran et al., 2010) was used and dissociations of carboxylic acids have been estimated with the method by Perrin et al. (1981). Fixed rate constants and branching ratios have been used for radical species. A more detailed description of all processes implemented in the protocol in its final state can be found in Table 2 in section 4.

Deleted: structure-activity relationships

With the preliminary protocol, test mechanisms have been designed and evaluated focusing on the influence of critical parameters or the quality of estimates of parameters, where the scarcity of data allowed only rough estimates. All sensitivity studies have been performed with the parcel model SPACCIM (SPectral Aerosol Cloud Chemistry Interaction Model; Wolke et al., 2005) in a general, non-specific urban environment. Model runs are for 4.5 days at 45ºN in mid-June. The trajectory of the parcel model involves 8 cloud passages for about 2 hours at noon and midnight of each day (marked by a blue shaded area in the results plots given in the following). This scenario allows a detailed investigation of either particle or cloud chemistry and interactions between both (see Tilgner et al., 2013 for further information on the model scenario).

3.1 Degradation of polycarbonyl compounds

In a first sensitivity test, the formation of polycarbonyl compounds mostly in their hydrated form was observed in high concentrations. Diol functional groups were found at every site of the molecule, which is an unstable structure and should decompose thermally and, therefore, not exist in high concentrations. Hence, a decay of polycarbonyl compounds by C–C bond breaking has been introduced to the protocol when at least three carbonyl groups (hydrated or unhydrated) are found within four adjacent carbon atoms. The rule is based on considerations in the gas-phase mechanism MCMv3.2 (Master

Deleted: functions

Deleted: 3

Chemical Mechanism, http://mcm.leeds.ac.uk/MCMv3.2/), where in the n-alkane oxidation series no more than 3 carbonyl groups are found within four adjacent carbon atoms independently of the chain length of the parent molecule.

For the estimation of the decay rate, sensitivity studies have been performed, where the first order rate constant was varied between 0.01 and 1 s^{-1}. Moreover, the importance of OH radical induced oxidation of polycarbonyl compounds and the monomolecular decay has been investigated by allowing only molecular decay in the protocol or by treating both processes in parallel. The set of sensitivity studies was compared to the base case, which treats only the OH attack of polycarbonyl compounds. A short description of all sensitivity studies and the nomenclature used in the following is given in Appendix A.2. In the sensitivity runs, GECKO-A with a preliminary aqueous-phase protocol was used to extend CAPRAM 3.0n. The generator was used to revise the chemistry of all stable organic compounds in CAPRAM 3.0n and introduce branching ratios for their degradation reactions. The preliminary protocol was applied to all newly evolving intermediates, but was stopped at radical species, which were already previously defined in CAPRAM, to reduce the size of the mechanism. Besides a more detailed chemical scheme due to the treatment of minor reaction pathways in contrast to most reactions in the previous CAPRAM version, the hydration of carbonyl compounds is treated with greater complexity allowing the hydration of keto functionalities according to GROMHE.

Figure 10 shows the concentrations of 2-oxo-3-hydroxy-succinaldehyde (2O3H-SA), which illustrates the effects of the new protocol as it was already part of CAPRAM 3.0n. In this Figure and all other Figures, a '∑' before a species names or chemical formula in the unhydrated and protonated form means that the sum of the concentrations of all hydration and dissociation states of a given species are shown. Hydration is only considered in the sensitivity runs with the new protocol rules. Figure 10 shows that negligible concentrations are reached for the highly oxidised polycarbonyl compounds with rate constants of at least 0.1 s^{-1}. Additional oxidation by hydroxyl radicals seems negligible as concentrations of the sensitivity runs with and without oxidation by OH radicals are indistinguishable from each other. However, product distributions are affected by the additional oxidation of OH radicals as can be seen from Figure 11. The two acids shown in Figure 11a/b are the main degradation product of the OH-initiated oxidation of 2O3H-SA. While bond breaking reduces their concentrations compared to the base run with no monomolecular decay of polycarbonyls (woBB), this effect is counteracted in the runs with additional oxidation treated in the protocol especially for the run with the slow decay rate of 10^{-2} s^{-1} (BBe-2+OH). Figure 11c/d shows the concentration-time profiles of oxo-lactic and tartronic acid, the major first- and second-generation products of the monomolecular decay of 2O3H-SA. It can be seen that the order of magnitude of the reaction rate constant has little effect on the concentrations of these products. Moreover, additional oxidation by hydroxyl radicals does not affect the formation of oxo-lactic acid and tartronic acid.

Finally, the implemented additional monomolecular decay of polycarbonyl compounds does not significantly increase the oxidation capacity of the aqueous phase. Macroscopic particle properties such as pH or organic particle mass are not affected by the additional decay channel. However, the high concentrations of highly oxidised and thermally unstable polycarbonyl compounds can be effectively suppressed with this new reaction type in the protocol. Therefore, it has been added to the final protocol. A decay rate of 0.1 s^{-1} was chosen as an ideal compromise between the suppression of high concentrations of polycarbonyls and an increased oxidation capacity of the aqueous phase. For complete description in the final aqueous-phase protocol of GECKO-A, additional oxidation by hydroxyl radicals is considered as well to determine the product distribution with the best current knowledge.

3.2 Influence of the chosen SAR

SARs form the basis of the protocol for automated mechanism generation. Therefore, their influence on the oxidation mechanism and modelled concentrations of important constituents of the tropospheric aqueous phase has been investigated thoroughly. Figure S9 in the ESM shows the concentrations of selected organic compounds in the aqueous phase. Concentrations of compounds whose major source is the uptake from the gas phase are in excellent agreement for the two

Deleted: Table 1.

Deleted: the structure-activity relationship

Deleted: ,

Deleted: compound for

Deleted:

Deleted: show

Deleted: acid

Deleted: 2-oxo-3-hydroxy succinaldehyde

Formatted: English (UK)

investigated SARs by Minakata et al. (2009) and Doussin and Monod (2013). However, significant differences in concentration-time profiles can be observed for second or older generation products mainly produced by aqueous-phase processes (see Figure S9).

This behaviour is explained by two facts. First, errors in the SARs increase with increasing complexity of the molecule and, hence, with more oxidised compounds in the aqueous phase. More importantly, this behaviour is a result of the excellent prediction of the overall rate constants by SARs in general, but significant uncertainties in the predicted products of aqueous-phase SARs due to missing experimental determinations of products and their branching ratios. Therefore, significant differences can be observed in the branching ratios while the rate constants of the overall decay compare well. More experimental data is needed to derive more reliable product distributions in aqueous-phase SARs. The macroscopic properties of particles such as pH and organic particle mass are not affected by these uncertainties (see Figure S9 in the ESM), but significant differences in the prediction of the concentrations of single species might be observed between the two SARs.

3.3 Processing of the organic mass fraction

As the focus of this study is the aqueous-phase processing of organic particulate matter, a more detailed investigation has been performed for an urban environment with the improved mechanism from section 3.1. From Figure 12, two deficits of the current protocol can be seen. For such a polluted environment the growth of the organic mass fraction is too small. A significant mass increase of 166 µg m^{-3} is observed in the base model run as seen in Figure S10 of the ESM, while the organic mass increases by only 1.7 µg m^{-3} contributing less than 5% to the total mass at the end of the model run. This is significantly less than observed all around the world (Jimenez et al., 2009). The organic mass increase is significantly less than observed previously (Brégonzio-Rozier et al., 2016; Ervens and Kreidenweis, 2007). Secondly, unrealistically high concentrations of organic nitrates are observed during non-cloud periods. During non-cloud periods, the majority (>80%) of the particle mass of the explicit scheme (excluding the generic model species HULIS, WSOC, and WISOC) consists of organic nitrates. In general, organic nitrate fraction of up to 20% are observed (Day et al., 2010) and up to 45% in submicron aerosol and PM1 (Bean et al., 2016; Kiendler-Scharr et al., 2016). To address these issues, further investigations were performed on the processing of the organic particulate matter with a focus on organic nitrates. A series of test studies were performed, which led to a significant improvement of the description of the processing and the composition of organic particulate matter. These studies are described in the following subsections. The best estimates of each test scenario are taken over and included in the following model runs unless stated otherwise.

Deleted: (submircron

Deleted: ;

3.3.1 Proxy reactions for OH and NO_3 radical reactions with residual OM

Despite its great level of detail, the mechanism generated by the preliminary protocol for these sensitivity studies is still limited as it only treats the chemistry of compounds with up to four carbon atoms explicitly. Therefore, radical concentrations might be overestimated due to missing scavenging by larger organic compounds, which further affects important particle properties and particle growth. Therefore, proxy reactions for the processing of the generic water-soluble organic compounds (WSOC) and humic-like substances (HULIS/$HULIS^-$) have been introduced to CAPRAM 3.0n to account for the interactions of hydroxyl and nitrate radicals with longer-chained organic compounds. The generic model species WSOC, HULIS/$HULIS^-$ as well as water-insoluble organic matter (WISOC) are referred to as residual organic matter (residual OM) in the following. All proxy reactions are given in Table 1. Besides the oxidation by OH and NO_3, photolysis of humic-like substances is included to account for an accurate description of the iron(II) to iron(III) ratio.

The new proxy reactions decrease radical oxidant concentrations as expected (see Figure S11 in the ESM for OH and NO_3 concentrations in the run WSOC). Daytime OH radical concentrations are decreased by more than one order of magnitude and nitrate radical concentrations by almost one order of magnitude by the end of the simulation after 4.5 simulated days. Reduced radical oxidant concentrations cause an increase in organic particulate matter as a result of decreased sinks and equal sources

Deleted: daytime

Deleted: an

Deleted: Consequently, particle growth increases

Deleted: can be seen from

of the dissolved organic matter compared to previous model runs. Figure 13 illustrates the mass increase showing the total organic particle mass for the scenarios with (WSOC) and without (orig) reactions of radical oxidants with the residual OM as well as the organic nitrates and the residual OM fraction. As the sensitivity runs focus on non-cloud periods, high concentrations during cloud periods are not shown in Figure 13 and all other Figures of this subsection for a better resolution of the differences during non-cloud periods.

Figure 13 shows that previously particle growth was observed only during cloud periods, while the organic mass during non-cloud periods decreased. With decreased OH and NO_3 radical concentrations from the WSOC and HULIS proxy reactions, less oxidation is observed. The reason for this behaviour is that the current protocol consists mainly of fragmentation reactions, which produce mainly high volatility products. Thus, the decreased oxidation in the WSOC runs suppresses the production of volatile organic compounds and reduces their release to the gas phase. As a consequence, the observed decrease in organic particle mass during non-cloud periods is less with the proxy reactions for WSOC and HULIS species.

These sensitivity runs also demonstrate a weakness of the current protocol, which only includes oxidative processes. Non-oxidative processes, such as accretion reactions are currently not considered. This is partly owed to very limited experimental data and partly due to the fact that non-oxidative processes will rapidly lead to very large products, which require large explicit oxidation schemes. With the currently very comprehensive protocol, the mechanism size would increase beyond the capabilities of current numeric models. Furthermore, fragmentation seems overestimated in the current protocol, a fact that is addressed in another sensitivity study introduced in section 3.3.3. While the new proxy reactions help to increase organic particle growth rates to more realistic values, they do not affect particle composition. Therefore, the overestimation of organic nitrate concentrations remains. Therefore, further tests are introduced in the next subsection to investigate the formation and degradation of organic nitrates and identify missing processes in the current protocol.

3.3.2 Detailed studies of organic nitrate sinks and sources

Further tests have been performed on the sinks and sources of organic nitrates to investigate the cause of their high concentrations in the model simulations. In the current protocol, photolysis is excluded due to the very limited data, which makes it hard to determine rules for automated prediction of photolysis rates. To evaluate effects on the processing of organic nitrates in the aqueous phase, photolysis has been included for this compound class leading to alkoxy radicals and NO_2:

$$RONO_2 \longrightarrow RO + NO_2 \qquad (5)$$

For estimating a maximum photolysis efficiency, the photolysis rate was estimated twice as high as gas-phase photolysis of typical organic nitrates. This estimate recognises the lens effects deriving from the spherical shape of cloud droplets and particles (e.g., Mayer and Madronich, 2004), but fully neglects any solvent cage effects to have an upper limit of the sink effects of photolysis on organic nitrate concentrations in the aqueous phase. For neutral photofragments, effective quantum yields similar to their gas-phase counterparts have been discussed before (Herrmann, 2007).

Only minor effects from additional photolysis of organic nitrates (even using the upper limit estimates) are observed in the scenario 'Phot' compared to scenario 'WSOC' (see Figure 14). Organic nitrates remain the dominant fraction and their reduction is negligible. Therefore, photolysis for organic nitrates has been neglected in the final protocol (and the following sensitivity studies) to be more consistent with the other compound classes and until the development of a more vigorously tested photolysis protocol for all chromophores.

Further investigation focused on possible overestimations of the sources of organic nitrates. The only aqueous-phase source of organic nitrates besides possible uptake from the gas phase is the addition of nitrate radicals to double bonds of unsaturated organic compounds. Therefore, a sensitivity study has been performed with reduced rate constants of the addition reaction. In the original protocol, different estimates for different compound classes were made based on experimental determinations by Alfassi et al. (1993) as given in Table S2 in the ESM. Their measurements indicate high reaction rate constants in the order of 10^9 M^{-1} s^{-1} for unsaturated compounds and rate constants in the order of 10^7 M^{-1} s^{-1} for carboxylic acids. However, recent

Deleted: . In this plot,

Deleted: is given

Deleted: mass of all

Deleted: for the runs with the initial mechanism from section 3.1 and the sensitivity run (WSOC).

Deleted: RONO2 →

Deleted: The scenario 'Phot' in Figure 14 indicates that

Deleted: of photolysis in a sensitivity run with these

Deleted: reactions are minor

Deleted: with

Deleted: described here. Only little reduction in organic nitrate concentrations is resulting and these compounds

Deleted: constituents of the particle phase measurements by Schöne et al. (2014) indicate reduced rate constants for unsaturated compounds. Therefore, rate constants of unsaturated compounds with nitrate radicals were restricted to 10^7 M^{-1} s^{-1} in another sensitivity study labelled with ‘NO3add' in Figure 14.

The reduction of the rate constants of NO_3 addition reactions significantly reduces the mass fraction of organic nitrates, but consequently also suppresses particle growth (see scenario ‘NO3add’ in Figure 14). The described attempts have been unable to resolve the opposing effects of overestimated organic nitrate concentrations and underestimated particle growth in an accurate description of the processing of the organic particle mass. Therefore, further investigations were performed aiming at the phase transfer in the aqueous-phase protocol of GECKO-A.

3.3.3 Phase transfer of oxygenated organic compounds

GECKO-A uses the structure-activity relationship GROMHE (Raventos-Duran et al., 2010) to estimate Henry’s Law coefficients (HLCs) needed to describe the uptake process. However, recent research indicates that due to the data used to derive the SAR, HLCs might be underestimated in GROMHE (Compernolle and Müller, 2014b, 2014a). To address a possible overestimated release of organic particulate constituents to the gas phase, a sensitivity study (‘O:C=1’) has been performed, where the HLC of all compounds with an O:C ratio greater or equal to one has been set to a fixed value of $1\cdot10^9$ M atm^{-1}.

Deleted: structure-activity relationship

The results are shown in Figure 15. The new estimates increase the organic mass concentration during non-cloud periods to values between 9 and 13 µg m^{-3}. A noticeable difference is the faster particle growth during non-cloud periods in the model run with the revised uptake, reaching the (non-cloud) peak value of 13 µg m^{-3} directly after the daytime cloud on the second model day. Thereafter, peak values after cloud periods are stagnant or slightly decreasing. This is in contrast to the model runs that use only the GROMHE estimates, where a smaller particle growth is observed, however, with constantly increasing peak values after cloud periods. The new estimates lead to an increase in organic particulate mass of 2 µg m^{-3} at the end of the model run.

Deleted: Results

Other studies have previously shown that different estimation methods of HLCs lead to important differences of several orders of magnitude (Wang et al., 2017). The current deficits can only be overcome with further development of the estimation methods for HLCs using an updated database of experimentally determined Henry’s Law coefficients. For the current study, HLCs of species with an O:C ratio larger or equal to 1 are set to $1\cdot10^9$ M atm^{-1}. However, uptake processes are currently the source for one of the largest uncertainties in the protocol.

Deleted: shown

Deleted: the description of

Deleted: still inherits

3.3.4 Decay of alkoxy radicals

Further investigation focused at the chemistry of alkoxy radicals in the database. Previous CAPRAM estimates derived from the MOST Project (George et al., 2005) considered two degradation pathways with the following rate constants:

$$R_1R_2O^{\cdot} \longrightarrow R_1^{\cdot} + R_2{=}O \quad (5\cdot10^5\ s^{-1}) \qquad (6)$$

$$RO^{\cdot} + O_2 \longrightarrow R{=}O + HO_2^{\cdot} \quad (5\cdot10^6\ M^{-1}\ s^{-1}) \qquad (7)$$

With typical modelled aqueous-phase oxygen concentrations of 3.5 – $4.0\cdot10^{-4}$ M, this means that almost all alkoxy radicals decay by C–C bond breaking as the pseudo first order reaction rate constant of the oxygen channel is about a factor of 250 smaller. Therefore, this estimate favours fragmentation over the oxidation to more polar products with an increased O:C ratio whose further oxidation can potentially lead to highly soluble multifunctional compounds. Hence, the degradation reaction has been re-investigated by varying the decay rate of the fragmentation channel over 5 orders of magnitude from $5\cdot10^0$ to $5\cdot10^5$ s^{-1}. The results are shown in Figure 16. As expected, a big increase in particulate matter is observed in the sensitivity run with a decay rate of $5\cdot10^2$ s^{-1}, where the ratio of the rate constant of the fragmentation channel to the pseudo first order rate constant of the oxygen channel decreases to 0.25. With the competitiveness of the oxygen channel, particle growth increases by about 3 µg m^{-3} in 4.5 days (see Figure 16). Further reductions of the rate constant of the monomolecular decay channel affect particle

Deleted: s^{-}

Deleted: Results

growth less leading to the production of one additional µg m^{-3} at the end of the model run. Therefore, $5\cdot10^{2}$ s^{-1} has been used as the best estimate for the degradation channel in the final protocol. However, measurements of the decay of alkoxy radicals are urgently needed for a wider range of compounds and, in particular, for the ratio of the different product channels. The current mechanism is based on just two measurements of aliphatic alkoxy radicals – the methoxy radical (Schuchmann and von Sonntag, 1984) and the ethoxy radical (Bonifačić et al., 2003).

3.4 Influence of nitrate radical chemistry

The explicit description of nitrate radical chemistry can lead to an increase in the size of the generated mechanisms, in particular, when unsaturated organic compounds are involved. Unsaturated compounds preferably react by addition reactions with the attacking radicals. Therefore, organic nitrates are formed in reactions of NO_3 radicals with unsaturated compounds, which were not treated in previous CAPRAM mechanisms. For each new organic nitrate, a complete oxidation scheme has to be generated up to CO_2. Only one reaction type has been implemented to remove the nitrate group from the carbon skeleton: the hydrolysis of carbonyl nitrates, which was estimated in accord with peroxyacyl nitrate (PAN) hydrolysis:

$$\mathrm{RC(=O)ONO_2} \xrightarrow{\mathrm{H_2O}} \mathrm{RC(=O)OH} + \mathrm{NO_3^-} + \mathrm{H^+} \qquad (8)$$

However, with estimated rate constants of $k_{2nd} = 7.6\cdot10^{-6}$ M^{-1} s^{-1} and $E_A/R = 6600$ K (Kames and Schurath, 1995) from PAN hydrolysis, this process is very slow and only important for highly oxidised species, which possess no carbon bound H-atoms and can therefore not be oxidised by radical attack. Therefore, the nitrate function is likely to remain in the molecular structure throughout the whole oxidation process to small molecules. Hence, a large additional reaction scheme is needed. The sensitivity runs in subsection 3.3 have demonstrated the need to include these reactions in polluted environments. However, in clean environments or for chamber modelling under low-NOx conditions, such detailed chemistry might not be needed. Therefore, GECKO-A has been equipped with 3 options to treat nitrate radical chemistry. For every chemical mechanism, 3 levels of reduction are generated:

- *α version*: Treatment of complete nitrate radical chemistry. Full mechanism generated.
- *β version*: Reactions with unsaturated compounds prohibited to suppress organic nitrate formation. H-atom abstraction reactions are allowed with saturated compounds, but not with unsaturated compounds to prevent a shift in the reaction products.
- *γ version*: No nitrate radical chemistry allowed at all except for the chemistry already treated in previous CAPRAM versions.

Sensitivity studies have been performed under urban and remote conditions, which confirm the importance of nitrate radical chemistry in highly polluted regimes and the necessity for a complete treatment of these compounds as stressed in subsection 3.3. Under remote conditions, organic nitrate formation is negligible with a total organic nitrate mass of less than $5\cdot10^{-12}$ g m^{-3}. Therefore, it is safe to use the β version of the generated mechanism in these environments. The significance of nitrate radical chemistry is low in general in these environments according to the model simulations. Differences in the concentration-time profiles between the β and the γ version are only observed for highly oxidised dicarboxylic acids, where electron transfer dominates over H-abstraction reactions. Results for these remote conditions are presented for selected organic compounds in Figure S12 in the ESM. Therefore, for pristine environments or very clean chamber conditions, the γ version of the mechanism might be suitable as well; however, errors increase, especially for highly oxidised organic compounds. Moreover, the potential for mechanism reduction is much smaller for the omission of H-abstraction reactions as in general the same products are produced in these reactions as for the hydroxyl radical attack. Therefore, the generator does not create new reaction schemes for new intermediate compounds and the mechanisms are only reduced for the nitrate radical reactions themselves.

Deleted: ,

3.5 Investigation of further parameters in the protocol

Further sensitivity studies have been employed to investigate the sensitivity of the generated mechanisms towards the mass accommodation coefficient α in the uptake process and the choice of the threshold percentage to omit minor reactions pathways. These results are outlined here only in brief.

Uptake parameters

Only very few experimental determinations of mass accommodation coefficients exist in the literature (see, e.g., the most recent IUPAC recommendation by Ammann et al., 2013; or the compilations by Davidovits et al., 2006, 2011). Therefore, it is impossible to derive advanced estimation methods for this parameter. Previous CAPRAM and GECKO-A (Mouchel-Vallon et al., 2013) estimates used a fixed estimate of 0.1. To evaluate the sensitivity of this parameter, different model runs with varying mass accommodation coefficient estimates from the lowest value in the CAPRAM database of 0.0067 for methyl hydroperoxide to the highest value of 0.5 for HONO.

Deleted: little

No effects on any concentration-time profile could be detected. Therefore, this parameter seems insensitive in the typical range found for organic compounds relevant for tropospheric multiphase chemistry and the previous CAPRAM estimate of 0.1 has been taken over in the GECKO-A protocol.

Cut-off thresholds

Furthermore, thresholds for the cut-off of minor reaction pathways have been investigated as a means of mechanism reduction. In the aqueous-phase protocol of GECKO-A, a choice of different cut-off parameters is possible. The generator also ensures that the omission of minor reaction pathways does not result in the loss of too many reaction pathways as described in detail in the next section. As shown in Figure S13 in the ESM, the number of reduced reactions increases linearly with the percentage of the cut-off parameter. Significant differences occur mainly for very crude thresholds of 10% or higher (see Figure S14 in the ESM). In the current protocol, a 3% threshold was chosen as standard value to compromise between a most detailed description of the chemistry in benchmark mechanisms and a reduced mechanism size for better numerical processing.

Deleted: for

Deleted: use as

Deleted: mechanism

Deleted: the reduction of the

4 The new multiphase mechanism generator GECKO-A

Based on the evaluation of kinetic data and prediction methods in section 2 and the sensitivity studies in section 3, a protocol for aqueous-phase mechanism auto-generation has been defined. The final protocol is described in section 4.1. Its implementation in CAPRAM/GECKO-A and the workflow of the new multiphase mechanism generator are explained in section 4.2.

Deleted: automated

Deleted: GECKO-A

4.1 The new aqueous-phase protocol for GECKO-A

This section details the rules defined to predict mechanistic, kinetic, and thermodynamic data for mechanism auto-generation in GECKO-A. An overview of all processes in the new aqueous-phase protocol and the estimates used to derive rate constants and further kinetic and thermodynamic parameters is given in Table 2.

SARs form the basis of the protocol due to the highest accuracy and the ease to implement them in automated computer tools. Furthermore, a major advantage over all other estimation methods is the ability to predict reaction products. In the current protocol, the SAR by Doussin and Monod (2013) is preferred over the SAR by Minakata et al. (2009). Despite a similarly successful generation of overall rate constants, attempts have been made to acknowledge branching ratios from measurements by Asmus et al. (1973) in the SAR by Monod and Doussin (2008) (pers. comm. with A. Monod). Therefore, the SAR was chosen for a best possible description of the product distribution. In the protocol, the SAR is supplemented with parameters from the SAR by Minakata et al. (2009) for unsaturated compounds or H-atom abstraction reactions on carboxyl groups, which is neglected in the SAR by Monod and Doussin (2008) due to the very low partial rate constants. Hence, it is possible to have a mixture of different SARs used to predict the rate constant for one compound. In the generator, molecules are treated group-

Deleted: Structure-activity relationships

Deleted: Inspite

Deleted: structure-activity relationships wise for every carbon atom bearing group. Where possible, the SAR by Doussin and Monod (2013) is used and only those groups are supplemented with the SAR by Minakata et al. (2009) were the SAR by Doussin and Monod (2013) fails (see also Table 2).

Branching ratios for the various product channels are determined by scaling the individual rate constants, which have been modulated by the effects of the neighbouring groups, to the overall rate constant. Immediate oxygen addition to alkyl radicals resulting from H-atom abstraction is assumed in GECKO-A directly producing peroxy radicals. A threshold to omit minor reaction pathways and reduce mechanism size is implemented in GECKO-A where the current protocol uses 3% as standard. When minor branches are omitted in the generator, the overall rate constant is reduced. No attempts are made to rescale the remaining reaction pathways to the overall rate constant, hence, reducing the rate constant when minor reaction pathways are omitted. This could result in a sufficient loss of reactivity, if too many minor reaction pathways are omitted, which accumulate to a significant portion of the overall reaction. Therefore, a second parameter is introduced, which ensures that the overall reactivity stays above a defined percentage (80% as standard). In GECKO-A, 10 levels of accuracy exist for the thresholds of minor reaction pathways ranging from 0.1 to 25%. If the overall reactivity is reduced below the threshold of 80% (or any other user input), then the generator automatically switches to the next more accurate threshold level for minor branches until the reactivity stays above the defined threshold or the highest accuracy of 0.1% cut-off for minor branches is reached. This is a major improvement to previous CAPRAM versions, where only a few branching ratios with experimental evidence had been implemented in the mechanism. The approach is similar to that by Mouchel-Vallon et al. (2017) in the CLEPS 1.0 model, where branching ratios are determined by an SAR and a reduction was applied, where the contribution of each reaction pathway was determined to maintain at least 75% of the total reactivity. After the reduction, branching ratios were recalculated to maintain the global rate constant (Mouchel-Vallon et al., 2017).

Deleted: define

Nitrate radical reactions are estimated with the new advanced Evans-Polanyi-type correlations introduced in section 2.3.3. Evans-Polanyi correlations are designed for gas-phase H-atom abstraction reactions only, but have proven to work equally well in the aqueous phase (e.g., Hoffmann et al., 2009). However, this results in limitations of the applicability of Evans-Polanyi-type correlations as they are unsuitable for unsaturated compounds and ions. Therefore, estimates with fixed rate constants of $1\cdot10^{7}$ M^{-1} s^{-1} had to be used for these compounds based on the sensitivity studies described in section 3. Moreover, no branching ratios can be derived from these estimates. Therefore, branching ratios from hydroxyl radical reactions have been taken over except for reactions with carboxylates, where electron transfer is assumed to be the only process. For unsymmetrical dicarboxylates, equal branching is assumed. There is a need for further development of a prediction method for kinetic and mechanistic data of nitrate radical reactions with organic compounds. However, for more advanced predication methods such as SARs, a more comprehensive experimental database is needed.

Deleted: above.

Uptake is described with GROMHE. Due to the large uncertainties, which derive from the experimental data used to obtain the relationship, the SAR is only applied to compounds with an O:C ratio below one. Higher oxidised compounds are assumed to remain in the aqueous phase until a SAR becomes available based on recent findings. Furthermore, uptake is restricted to species with an HLC between 10^{2} and 10^{12} M atm^{-1}. This measure has been taken to reduce the size of the generated mechanism as species below the lower threshold will predominantly exist in the gas phase and above the range, species will almost exclusively remain in the aqueous phase (see also discussions by Mouchel-Vallon et al., 2013). Therefore, reaction schemes for these compounds can be omitted in the corresponding phases with only small errors.

Deleted: the structure-activity relationship

Deleted: refined structure-activity relationship

Deleted: a Henry's Law constants

Further parameters needed to describe the phase transfer process are the gas-phase diffusion coefficient D_g and the mass accommodation coefficient α. D_g can be calculated from the molecular diffusion volumes with the FSG method as described by Fuller (1986). For α, a fixed value of 0.1 is applied in the new aqueous-phase protocol based on previous CAPRAM estimates and the sensitivity studies presented in section 3.

For the estimation of hydration equilibrium constants of carbonyl compounds, GROMHE can be used as well. Hydrations are important to determine the effective HLCs. Therefore, their prediction is already incorporated in GROMHE and can directly

Deleted: Henry's Law constants.

be used for the new GECKO-A protocol. To reduce the size of the generated mechanisms, hydration channels are omitted for equilibria, where the hydration equilibrium constant for a channel is below 5% of the overall equilibrium constant k^*_{hyd} taking all possible hydration forms into account.

Dissociation of carboxylic acids is estimated using the method by Perrin et al. (1981). No threshold for minor dissociation states is currently used in the standard mode of GECKO-A as the threshold is highly dependent on particle and cloud droplet pH. With varying pH in the model scenarios with non-permanent clouds as applied in this study, this can lead to significant inaccuracies. Furthermore, different dissociation states possess different reactivities. Dissociated carboxylic acids are likely to react by electron transfer reaction (ETR), which is generally faster than H-abstraction reactions (see also Table S1 and S2 in the ESM). Therefore, with increased reactivities of the products of minor branches, significant turnovers can still be achieved through these reaction pathways. These considerations apply also to hydration processes, but are less critical for this equilibrium type with less variation of the reaction rate constants between the different hydration forms. Future versions of the generator should use more advanced determinations of the threshold for minor reaction pathways, which include the consideration of the reactivities of the products in each channel. However, these estimates would depend on typical radical oxidant concentrations and pH and, hence, would be environment specific.

Deleted: are

Deleted: estimation

For highly oxidised polycarbonyl compounds, a monomolecular decay has been implemented in addition to the radical attack, if three carbonyl groups are found within four adjacent carbon atoms. Bond breaking occurs always between two carbonyl groups. If three carbonyl groups are directly adjacent to each other, equal branching is assumed leading to a maximum of four fragments. The decay rate is estimated as 0.1 s^{-1} based on the sensitivity studies in section 3.

Deleted: with

For organic nitrates with an α-carbonyl group, hydrolysis is assumed in addition to radical attack. The second order rate constant is assumed equal to PAN hydrolysis with an estimated second order rate constant of $k_{2nd} = 7.6\cdot10^{-6}$ M^{-1} s^{-1} and $E_A/R =$ 6600 K (Kames and Schurath, 1995). Products formed are a carboxylic acid and dissociated nitric acid.

Due to the experimental difficulties to determine the very fast reaction rate constants of organic radical compounds, measurements are scarce. Therefore, no sophisticated estimation method could be derived for these compounds and estimates use fixed rate constants and branching ratios based on previous CAPRAM estimates. Organic peroxy radical reactions are based on the mechanism proposed by von Sonntag (1987) and von Sonntag and Schuchmann (1991) with updated mechanistic and kinetic data by Schaefer et al. (2012) and include the reactions and estimated rate constants as given in Table 2. Peroxy radical reactions are included as pseudo first order reactions based on the methodology of the gas-phase mechanism MCM (Jenkin et al., 1997; Saunders et al., 2003), where a given peroxy radical reacts with the sum of concentrations of all peroxy radicals to account for recombinations and cross-reactions. Several exceptional reaction pathways of certain peroxy radicals have been included in the protocol. Peroxy radicals bearing a hydroxyl group in α-position solely decay by HO_2 elimination to form a carbonyl compound and a hydroperoxyl radical in a unimolecular decay. Decay rates are estimated with 200 s^{-1} for one hydroxyl group in α-position and with 1000 s^{-1} for a gem-diol function in α-position based on previous CAPRAM estimates (Tilgner and Herrmann, 2010). Recombination and cross-reactions are neglected for this type of peroxy radicals due to the considerations given in section S3.5 of the ESM. Peroxy radicals with an adjacent carboxyl or carboxylate group decay by CO_2 elimination in addition to the recombination- and cross-reactions (see Table 2 for more details on mechanistic and kinetic data). Decay rates are estimated based on the measurements of the acetate peroxy radical ($CH_2(OO\cdot)C(=O)O^-$) by Schuchmann et al. (Schuchmann et al., 1985).

Deleted: dial

Alkoxy radicals decay by reaction with O_2 or by monomolecular decay have been implemented in the new protocol with the rate constants determined in subsection 3.3. Immediate oxygen addition is assumed for any carbon centred radical fragments, which will directly lead to the formation of peroxy radicals. For acyloxy radicals, a monomolecular decay by C–C bond breaking of the acyloxy group is assumed leading to dissolved carbon dioxide and a peroxy radical as immediate oxygen addition is assumed for the resulting alkyl radical. In contrast to previous CAPRAM estimates, a reduced decay rate of $5\cdot10^2$ s^{-1} is assumed in the current protocol in accord with the reduced bond breaking rates of alkoxy radicals.

Deleted: radical

Deleted: braking

For every auto-generated CAPRAM version, three sub-versions are created. The standard α version describes the full nitrate radical chemistry. The β mechanism includes the full inorganic and organic nitrate radical chemistry of the CAPRAM core mechanism 3.0n, but omits any reactions of nitrate radicals with unsaturated organic compounds. This measure significantly reduces the size of the mechanism as organic nitrate formation is suppressed resulting in a significantly reduced number of intermediate species in the oxidation chain of organic compounds. In the most reduced γ mechanism, only nitrate radical chemistry of the core mechanism CAPRAM 3.0n is allowed, while nitrate radical chemistry in the auto-generated mechanism part is suppressed. The potential for a significant reduction in mechanism size is far less for the γ-version than for the β-version of the mechanism as in the γ mechanism the same intermediates are produced as in the corresponding hydroxyl radical reactions. Thus, the mechanism is only reduced by the number of nitrate radical reactions, but no reduction in the number of species is achieved. The latter two sub-versions of the mechanism are meant for modeling in clean environments or for low-NOx chamber simulations.

Two modes of operation exist in CAPRAM/GECKO-A. In the first option, the generator produces mechanisms entirely based on the protocol rules. For every parent compound, a complete mechanism is auto-generated up to the final products CO/CO_2. In the second option, the generator produces supplementary modules for a parent mechanism and can be used to extend CAPRAM 3.0n or higher versions. In this mode, the generator stops the auto-generation when compounds of the parent mechanism are reached.

4.2 Implementation of the protocol in GECKO-A

The above protocol rules have been implemented as a new module in the existing gas-phase mechanism generator GECKO-A. The gas-phase mechanism generator is described in detail by Aumont et al. (2005). This section details the incorporation of the new aqueous-phase protocol. The workflow of the aqueous-phase module of GECKO-A is schematically shown in Figure 17. GECKO-A will always be initialised in the gas phase as most organic compounds are emitted as trace gases. However, it is possible to extract just the aqueous-phase mechanism from GECKO-A and couple it to further mechanisms as it was done in this study.

To generate oxidation schemes with GECKO-A, any number of 'primary gas-phase species', for which an oxidation mechanism is desired, can be added to the 'primary stack'. The mechanism generator will start with the first species in this stack and generate all possible gas-phase reactions as described by Aumont et al. (2005). In a second step, HLCs will be generated by the GROMHE subroutine and phase transfer will be described in the generated mechanisms if the HLC is above a given threshold. Otherwise, the assumption is made that the compound is insoluble and exclusively available in the gas phase. Therefore, uptake is suppressed to reduce the aqueous-phase mechanism size.

In the next step, the protocol rules described in subsection 4.1 will be applied (see also Figure 17). This includes checks for radical functions and any other functional groups in the molecule and the application of the appropriate rules from the protocol as schematically depicted in Figure 17. The generator determines any mechanistic, kinetic, and thermodynamic data for the given compound. It furthermore checks whether reaction products have previously been treated. New intermediate species will be added to an 'aqueous stack' for later treatment. Before the data is written into a mechanism, the solubility of the compound is checked again. If the HLC is below a pre-defined threshold, release to the gas phase is treated. The compound will be checked for its treatment in the gas phase. Untreated species will be added to a *gaseous stack* for later treatment in the gas-phase mechanism. If a compound exceeds the HLC limit, exclusive existence in the aqueous phase is assumed to reduce the size of the gas-phase mechanism.

In a last check, GECKO-A consults an experimental database. Any available experimental kinetic or thermodynamic data is preferred over theoretically predicted data. All reactions for the given compound are written into a mechanism as determined by GECKO-A. The generator then returns to the 'aqueous stack' for untreated species and generates reactions for these compounds as well. Thus, the *aqueous stack* will be filled by new intermediate species from the generated reactions. After the

Deleted: subversions

Deleted: Reduction

Deleted: as

Deleted: first reduction step as generally

Deleted: in reactions of nitrate radicals with saturated organic compounds…

Formatted: English (UK)

Deleted: products

Formatted: English (UK)

Formatted: English (UK)

Deleted: subversions

Deleted: The

Deleted: can either be used to produce "stand-alone

Deleted: ", where the generator creates

Deleted: oxidation mechanisms

Deleted: product

Deleted: solely based on the rules of the protocol described above. As…

Deleted: other

Deleted: may be used to produce

Deleted: to

Deleted: This

Deleted: uses

Deleted: CAPRAM

Deleted: as core and new oxidation schemes

Deleted: only created by GECKO-A for those species not yet described in CAPRAM. Thus, the generator will stop for any species already present in CAPRAM and acknowledge the chemistry of CAPRAM rather than producing own oxidation schemes

Deleted: to

Deleted: for mechanism auto-generation

Deleted: Henry's Law constants (

Deleted:)

Deleted: a

treatment of a species it will be marked to avoid double treatment of species generated in several reactions. GECKO-A proceeds with all unmarked species in the aqueous stack until every species in the stack is marked and the products of a current reaction are only species already treated previously or the end product CO/CO_2. In this case, the generator returns to the gas-phase stack and continues to generate gas-phase reactions for any unmarked species in this stack. The gas and aqueous-phase mechanism will be generated alternately in this way until a complete multiphase mechanism is generated for the species of the 'primary stack' and all intermediate products.

After the generation of a complete multiphase oxidation scheme for a species of the *primary stack*, the generator returns to this stack to treat the next species in it. The reaction mechanism for this compound will complement the mechanism of the previous species of this stack. Therefore, species of the *gaseous* and *aqueous stack* will not be emptied until the complete treatment of the 'primary stack'. Instead, they will be used as markers to indicate previous treatment in the generator and avoid double reactions. GECKO-A finishes, when all species of the 'primary', 'gas', and 'aqueous stack' are marked as treated and a complete multiphase reaction scheme has been generated for these species.

5 Validation of the CAPRAM/GECKO-A protocol against aerosol chamber experiments

5.1 Chamber experiments

The oxidation of 1,3,5-trimethyl benzene (TMB) was conducted in the aerosol chamber LEAK (Leipziger Aerosolkammer). A detailed description of LEAK can be found elsewhere (Mutzel et al., 2016 and references therein). The experiments were conducted in the presence of sodium sulfate seed particles mixed with 30% sodium peroxide. The photolysis of ozone with UV-C light (λ = 254 nm) served as gas-phase OH radical source (see reactions 9 and 10). Ozone was generated by UV irradiation of O_2 using a flow rate of 3 L minute^{-1}.

Deleted: , mesitylene

Deleted: .

$$O_3 + h\nu \longrightarrow O_2 + O(\,^1D) \qquad (9)$$

$$O(\,^1D) + H_2O \longrightarrow 2\,^{\cdot}OH \qquad (10)$$

Furthermore, sodium peroxide was used as OH radical in-situ source in the particle phase via the reaction sequence:

$$Na_2O_2 + 2H_2O \longrightarrow 2\,NaOH + H_2O_2 \qquad (11)$$

$$H_2O_2 + h\nu \longrightarrow 2\,^{\cdot}OH \qquad (12)$$

Deleted: 9

Deleted: 10

TMB (≈ 85.5 ppb) was injected into LEAK with a microliter-syringe. The oxidation of TMB was conducted at a relative humidity of 75% and room temperature. The consumption of the precursor compound (ΔHC) was monitored with a proton-transfer-reaction mass spectrometer (PTR-MS) over a reaction time of 210 minutes. The volume size distribution of the seed particles was measured with a scanning mobility particle sizer (SMPS). An average density of 1 g cm^{-3} was used to calculate the produced organic particle mass (ΔM). The particle phase was sampled after the experiments. 1.8 m³ and 0.6 m³ of the chamber volume was collected on a PTFE filter (borosilicate glass fiber filter coated with fluorocarbon, 47 mm in diameter, PALLFLEX T60A20, PALL, NY, USA), which was connected to a denuder (URG-2000-30B5, URG Corporation, Chapel Hill, NC, USA; Kahnt et al., 2011) to avoid gas-phase artefacts. The particle-phase products were also collected with a condensation growth and impaction system (C-GIS, Sierau et al., 2003) with a time resolution of 15 min. Particle mass was monitored by an aerosol mass spectrometer (High-Resolution Time-of-Flight Aerosol Mass Spectrometer; HR-ToF-AMS).

Deleted: 1,3,5-

Deleted: 1,3,5-

5.2 Model setup

For the gas-phase description of the chemistry, the MCMv3.2 was used (http://mcm.leeds.ac.uk/MCMv3.2/; Jenkin et al., 2003; Saunders et al., 2003). GECKO-A was initialised only with methylglyoxal as both, the chamber and model results (see results in section 5.3), did not show significant concentrations of any other intermediate compound in the oxidation chain between TMB and methylglyoxal. The final version of GECKO-A as described above was used to generate the aqueous-phase oxidation scheme including phase transfers (with HLCs set to 1·10^9 M atm^{-1} for species with an O:C greater or equal to 1).

Deleted: 1,3,5-

Deleted: Henry's Law coefficients

Deleted: $^{-1}$ s

The generated scheme includes important aqueous-phase compounds such as oxalate, pyruvate, acetate, formate, formaldehyde or several di- and polycarbonyls. The total aqueous-phase scheme comprises 264 species, 596 reactions and 25 phase transfers. The mechanism is supplied as SPACCIM input file in the ESM.

Despite very low gas-phase concentrations, chemical turnovers can be substantial for some of the larger TMB oxidation products. Furthermore, some of the larger intermediates are already very oxidised with high O:C ratios and the aqueous-phase might be a potent sink for them. Therefore, several sensitivity studies have been conducted, where uptake into the aqueous phase was considered for 20 additional intermediates. As some of the intermediates were still very large with carbon numbers up to 9, an explicit description model with the currently very detailed protocol is beyond the capabilities of the current box with its detailed microphysical scheme. Therefore, the generic model species WSOC was used as a reaction product for those intermediates in the sensitivity run UPT.

As the majority of those intermediates bear double bonds, carbonyl and/or carboxyl functional groups, reactive uptake is possible due to the fast kinetics (addition reactions, hydrolysis, and dissociations) of those compound classes. Therefore, another sensitivity run ("RXN") was performed, where the initial aqueous-phase reactions were described explicitly following the generator protocol rules. Reaction products were described only, if they were part of the explicit methylglyoxal oxidation scheme, otherwise WSOC was used as a reaction product. In a last sensitivity run, WSOC yields in the additional reaction scheme of the "RXN" run were reduced to 0.4 to match the model predictions of the particle mass with the AMS and SMPS measurements. The additional species and reactions of the sensitivity runs UPT, RXN, and RXN$_{0.4}$ alongside the kinetic and thermodynamic data used can be found in Table S15 in the ESM.

Deleted: functions,

Deleted: functions

Deleted: with

Model runs were performed with the box model SPACCIM (Wolke et al., 2005) with a detailed description of microphysical and chemical processes. The model was initialised with $2.14\cdot10^{12}$ molecules cm^{-3} of TMB, $3.11\cdot10^{10}$ molecules cm^{-3} of Ozone and traces of NO and NO_2 to account for any background chemistry (1.5 and $2.0\cdot10^{10}$ molecules cm^{-3}, respectively). The aqueous-phase was initialised with sodium sulfate particles and 30% sodium peroxide. OH concentrations were held constant in both phases at a gas-phase concentration level of $5\cdot10^{6}$ molecules cm^{-3} and an aqueous concentration of 10^{-11}M. This was necessary as the current model version is designed specifically for atmospheric applications with a solar radiation spectrum under tropospheric conditions. Thus, it was not possible to simulate a constant light source from non-solar irradiation. The same microphysical conditions as in the chamber experiments were used with constant relative humidity of 75% and a constant temperature of 298K.

Deleted: 1,3,5-

5.3 Comparison of chamber and model results

Figure 18 shows the gas-phase concentration time profiles of TMB and its major oxidation products methylglyoxal and acetic acid as monitored by PTR-MS (squares) or simulated in the model run RXN$_{0.4}$. It should be noted that concentrations for methylglyoxal and acetic acid had to be scaled by a factor of 1.35 and 0.14, respectively, which can at least in part be explained by different protonation efficiencies for different molecules in the PTR-MS. This leads to inaccuracies in the PTR-MS measurements, which justify a re-scaling. Another, yet more unlikely, source of error would be another overlying compound with the same mass-to-charge ratio, which modifies the PTR-MS measurements for the respective *m/z*.

Deleted: mesitylene

With the rescaled concentrations, however, the MCMv3.2 is able to explain the measured concentrations well. The general degradation of TMB and the subsequent formation of methylglyoxal and acetic acid are well captured by the model. The concentration-time profile of TMB shows a slightly steeper curve in the model results with slightly stronger degradation rates in the first 1.5 hours and slower degradation rates thereafter. Up to 15 ppb less TMB are observed in the model compared to the experiment in the first hour. Consequently, methylglyoxal production is slightly over-predicted in the first 1.5 hours leading to ~2 – 3 ppb more methylglyoxal in the model compared to the measurements and the magnitude of the decay of methylglyoxal towards the end of the experiment is smaller in the model than in the measured concentration-time profile. At the end of the

Deleted: mesitylene

Deleted: mesitylene

Deleted: mesitylene

experiment, the model overpredicts the experimental results by about 3 ppb. Agreement of acetic acid concentrations between model and experiment is very good with slightly lower modelled concentrations towards the end of the experiment (2 – 3 ppb). Possible explanations for the discrepancies between measured and modelled concentrations in Figure 18 are uncertainties in the mechanistic and kinetic data either directly in the gas phase or indirectly in the aqueous phase influencing gas-phase concentrations through reactive uptake. Even though, only TMB, methylglyoxal and acetic acid have been measured in significant concentrations, it is likely that uptake of further intermediates in the oxidation chain of TMB to methylglyoxal influence the concentration profiles. Despite minor concentrations, large uptake fluxes into aerosol particle are modelled for the highly oxidised intermediates. With uptake processes having one of the most uncertain estimates in the CAPRAM/GECKO-A protocol (see section 3), they are another likely source for the observed discrepancies between modelled and measured concentrations.

Deleted: Figure 18

Deleted: Furthermore, uptake processes of intermediates in the aqueous-phase oxidation chain are a likely explanation for the discrepancies as the sensitivity studies have shown large uncertainties for these processes (see section 3).

In the aqueous phase, methylglyoxal chemistry alone fails to predict an increase in particulate matter (PM) by approximately 50 µg m^{-3} as seen by the SMPS and AMS (see Figure 19). Particle growth is negligible in the model run TMB. Therefore, more sensitivity runs have been performed as introduced in section 5.2, where uptake of further precursors of methylglyoxal and their initial reaction steps in the aqueous phase are considered. The influence of uptake alone in the sensitivity run UPT is negligible and the concentration-time profile of the overall dry particle mass is indistinguishable from the base run TMB.

Aqueous-phase chemistry has a big influence on particle growth. In the simulation RXN, where besides uptake, initial reactions are also considered assuming 100% water-soluble organic carbon (WSOC) as the reaction product, model predictions of PM at the end of the experiment are at ~130 µg m^{-3} about twice as high as seen by the SMPS or AMS. Reasonable agreement between modelled and measured concentrations is reached only when the reaction product WSOC is reduced by an artificial stoichiometric index of 0.4. This rescaling also has an impact on gas-phase concentrations, decreasing the concentrations of methylglyoxal and, consequently, acetic acid. To match the concentrations in the best scenario RXN$_{0.4}$ to experimental results, scaling factors for methylglyoxal in the gas phase were improved from 2.5 to 1.35 while acetic acid decreased from 0.23 to 0.14. The comparison of all gas-phase concentrations of methylglyoxal and acetic acid can be found in Figure S18 in the ESM.

Deleted: with

Deleted: has

Hence, large oxidation products are needed to explain the particle growth seen in the experiment, despite their negligible concentrations in the gas phase. The scaling factor for WSOC of 0.4 in the scenario RXN$_{0.4}$ could be interpreted in a way that subsequent aqueous-phase chemistry produces a mixture of soluble, semi-volatile, and volatile products of which 40% will remain in the aqueous phase and 60% are released back to the gas phase. This interpretation might also be used as a justification for the newly introduced degradation rates for alkoxy radicals. While previous CAPRAM mechanisms used fragmentation as the predominant degradation pathway, products are shifted towards carbonyl formation with a ratio of 73% carbonyl formation and 27% fragmentation under the conditions of the experiment. As carbonyl formation decreases volatility in contrast to fragmentation, the new product distribution is in better agreement with the above results from the sensitivity runs RXN and RXN$_{0.4}$ assuming that not all carbonyl compounds will remain completely in the aqueous phase.

However, even in the final re-scaled sensitivity run RXN$_{0.4}$, some discrepancies can be observed. The increase in PM is delayed by about 20 minutes in the model run. Furthermore, the model does not predict a slight decrease in PM towards the end of the model run as seen by the SMPS and AMS. The delayed increase is somewhat surprising and its reason remains unclear as an increased degradation of TMB was observed in the first 1.5 hours of the experiment in Figure 18, which would imply an increased particle formation in the model runs compared to the measurements. However, even in the run RXN, where 100% WSOC formation is assumed, PM formation is slightly lower in the first 40 minutes of the experiment than observed by the AMS and SMPS. It should also be mentioned that no wall losses of particles and oxidised organic compounds were implemented in the model as SPACCIM mainly targets atmospheric applications. Missing consideration of chamber background chemistry is another source for discrepancies. Moreover, currently no non-radical chemistry, such as accretion reactions are implemented in the CAPRAM/GECKO-A protocol, albeit, no oligomers were observed in the experimental particle analysis.

Deleted: mesitylene

Further investigations of the microphysical parameters liquid water content (LWC) and mean particle radius in Figure 20 show more interesting aspects of the influence of aqueous chemistry on particle growth. It seems that particle chemistry is necessary to initiate particle growth. Without aqueous-phase chemistry of the larger intermediates, no particle growth is observed in the run TMB. Uptake of these compounds alone is not sufficient to overcome the curvature effect of the relatively small seed particles with a mean radius of 55 nm. However, if chemistry is treated in the runs RXN and $RXN_{0.4}$, particle radii and, hence, LWC increase rapidly. The chemistry is needed as a trigger for the initial growth. With growing radii and decreasing curvature effect, LWC increases and uptake processes have an increased importance for the particle composition.

The increased uptake of organic compounds and, hence, increased carboxylic acid formation in the scenarios RXN and $RXN_{0.4}$ causes a decrease in pH by about 1 unit. The decrease from near neutral concentration is strongest in the first minutes of the experiments and levels of after 1 to 2 hours as can be seen in Figure S16 of the ESM.

Attempts were made to identify concentrations of the expected aqueous-phase products by offline analysis of C-GIS and PTFE filter samples. However, concentrations were close to the detection limit or within the noise of the expected background chemistry as can be seen from Table 3. In this table, the first sample represents background concentrations prior to the injection of 1,3,5-TMB and ozone. Moreover, large differences are seen in the concentrations for some of the compounds determined from samples using the different sampling techniques. For example, oxalate concentrations from filter samples were with 6.8 µg m^{-3} almost 10 times as high as determined from the C-GIS samples (0.7 µg m^{-3}). Therefore, a direct comparison of concentrations of individual species of experimental and modelled results is difficult.

It should be mentioned that large amounts of malic acid were detected in the gas and the aqueous phase throughout the experiment as shown for the gas phase in Figure S17 in the ESM and for the aqueous phase in Table 3. However, there is currently no information about formation pathways of malic acid from TMB oxidation and concentrations are attributed to background chemistry. Consequently, the MCMv3.2 does not predict the formation of malic acid in any of the sensitivity runs.

Deleted: mesitylene

For a thorough analysis, modelled chemical fluxes from the explicit scheme in scenario $RXN_{0.4}$ have been analysed and averages over the whole 3.5 hours of the experiments are shown in Figure 21. In addition, final aqueous-phase concentrations after 3.5 hours are shown for each species. Figure 21 shows that less than 3% of methylglyoxal is oxidised to acetic acid in the aqueous phase and gas-phase oxidation is the main sink. In the aqueous phase, 75% of the acetic acid is formed directly from methyl glyoxal while 25% is formed with pyruvic acid as intermediate, which is the major first generation aqueous-phase oxidation product. Oxidation of pyruvate leads mainly to oxo-pyruvic acid, which is subsequently degraded to mesoxalic acid and oxalate in the model and finally to formate. The formation of these highly oxidised dicarboxylic acids is a direct consequence of the revision of the radical protocol in the CAPRAM/GECKO-A mechanism generation process. The revised monomolecular decay of alkoxy radicals after the hydroxyl radical attack of pyruvic acid leads to an increased formation of oxo-pyruvic acid in favour of fragmentation. Previous CAPRAM mechanisms would have favoured the formation of more acetic acid. Thus, the new protocol favours particle growth, as mesoxalic and oxalic acid are far less volatile than acetic acid. The modelled concentrations in Figure 21 (in ng m^{-3}) are lower than those seen in the filter and C-GIS samples (see Table 3), but are generally within the experimental error. An exception is methylglyoxal with concentration modelled somewhat higher (78 ng m^{-3}) compared to measurements (48 ng m^{-3}).

Deleted: Modelled

Despite the difficulties to conduct experiments with sufficient bulk aqueous-phase chemistry, the plausibility of the new CAPRAM/GECKO-A protocol could be proven while further validation from model simulations with larger mechanisms under real tropospheric conditions is needed. These studies will be presented in a companion paper.

Deleted: are

6 Conclusions

A new protocol for mechanism auto-generation within the expert system GECKO-A has been developed and tested. The protocol was developed to supplement the mechanism generation process of the aqueous-phase benchmark mechanism CAPRAM.

Deleted: a

Following an extensive evaluation of existing kinetic data and prediction methods for aqueous-phase mechanistic, thermodynamic and kinetic data, Evans-Polanyi-type correlations have been further improved. The advanced correlations consider all bonds in a molecule connected to an H-atom rather than the weakest bonds only. This way, minor channels are considered in the correlation, which decreases biases especially for compounds, where measurements are typically scarce. Interesting effects were observed, especially for hydroxyl radical reactions. While previously, BDE and second order rate constants were anti-correlated due to an increased reactivity of weaker bonds, the new correlation shows a positive relationship due to increased side attacks on larger molecules, which have a larger accumulated bond dissociation enthalpy ($\sum$BDE). Moreover, for hydroxyl radicals, quadratic relationships were seen, while nitrate radical reactions can still be described with linear relationships. The most likely explanation for this behaviour is that for larger organic compounds the diffusion limit of the reaction with OH is reached and the levelling off of the rate constants can best be described with quadratic relationships while nitrate radical reactions are well below a diffusion-controlled range, where linear relationships are still applicable.

The evaluation process led to a new CAPRAM/GECKO-A protocol for mechanism auto-generation, where hydroxyl radical reactions are estimated with structure-activity relationships by Doussin and Monod (2013) supplemented by SARs from Minakata et al. (2009). The advanced Evans-Polanyi-type correlations were used to describe nitrate radical reactions with organic compounds and estimates with fixed rate constants and branching ratios were used to predict reactions of organic radicals. Hydrations are estimated with the SAR GROMHE and dissociations using Taft parameters with the method by Perrin et al. (1981). Uptake is described with the Schwartz approach (Schwartz, 1986) using GROMHE for the estimation of HLCs, the FSG method (Fuller, 1986) for the estimation of gas-phase diffusion coefficients and constant mass accommodation coefficients $\alpha = 0.1$.

Deleted: Henry's Law coefficients

Rigorous testing in sensitivity studies led to further improvements of the protocol, such as a monomolecular decay channel of polycarbonyl compounds with at least 3 carbonyl groups within 4 carbon-containing groups. Furthermore, the largest uncertainties in current estimation methods were identified and led to further improvements of the protocol. These were found for (i) uptake processes and (ii) radical reactions. While uncertainties in uptake processes are generally high, recent research seems to additionally indicate that GROMHE is underestimating uptake. Therefore, the current protocol refrains from using GROMHE for very polar molecules with an O:C ratio of one or greater. Instead, an HLC of $1 \cdot 10^9$ M atm^{-1} is used. Moreover, radical reactions are based on only a very few measurements for peroxy radicals and recent estimates from previous CAPRAM studies for alkoxy radicals. The latter radicals are either fragmenting or reacting with dissolved oxygen to form carbonyl compounds. The ratio has a large impact on particle growth as carbonyl formation leads to less volatile products than fragmentation. Therefore, the ratio was refined to best resemble experimental findings. Further sensitivity studies focused on organic nitrate formation in the aqueous phase as alkyl nitrate concentrations are at the upper end of observations or overestimated in the current sensitivity studies.

Deleted: let

Deleted: a Henry's Law coefficient

A TMB oxidation experiment was conducted at the aerosol chamber LEAK, which could prove the plausibility of the current protocol for automated mechanism construction. Modelled gas-phase concentrations of TMB, methylglyoxal, and acetic acid are in good agreement with the PTR-MS measurements. Sensitivity studies have shown, that the uptake and aqueous-phase chemistry of larger methylglyoxal precursor species are needed to accurately describe particle growth. However, the currently very explicit protocol would lead to very large and detailed mechanisms for the considered compounds with up to 9 carbon atoms and tests are infeasible for the current version of the box model SPACCIM.

Deleted: mesitylene

Deleted: mesitylene

Therefore, more model studies with more comprehensive mechanisms under real atmospheric conditions are needed for the validation of the protocol. The studies are part of a companion paper with further CAPRAM mechanism development.

A List of abbreviations and acronyms

A.1 General abbreviations

BDE	bond dissociation enthalpy
ESM	electronic supplementary material
ETR	electron transfer reaction
HLC	Henry’s Law coefficient
SAR	structure-activity relationship

A.2 Scenarios names

Sensitivity studies on monomolecular decay of polycarbonyl compounds

woBB	no bond breaking, oxidation by OH radicals
BBe-2+OH	bond breaking with 10^{-2} s^{-1}, additional oxidation by OH radicals
BBe-2woOH	bond breaking with 10^{-2} s^{-1}, no additional oxidation by OH radicals
BBe-1+OH	bond breaking with 10^{-1} s^{-1}, additional oxidation by OH radicals
BBe-1woOH	bond breaking with 10^{-1} s^{-1}, no additional oxidation by OH radicals
BBe0+OH	bond breaking with 1 s^{-1}, additional oxidation by OH radicals
BBe0woOH	bond breaking with 1 s^{-1}, no additional oxidation by OH radicals

Sensitivity studies on processing of organic mass fraction

orig	Base scenario, where chemistry of stable compounds in CAPRAM 3.0n has been replaced by a preliminary CAPRAM GECKO-A protocol
WSOC	Base with additional chemistry of residual OM (WSOC/WISOC/HULIS species)
Phot	Scenario WSOC with additional upper limit estimates for organic nitrate photolysis
NO3add	Scenario WSOC with updated reaction rate constants of NO_3 radicals with unsaturated organic compounds
O:C=1	Scenario NO3add with HLCs set to 10^9 M atm^{-1} for organic compound with and O:C ratio of one or larger

Chamber experiments

TMB	Base run for LEAK TMB oxidation experiment using ozone photolysis to generate OH radical oxidants
UPT	Base run with additional uptake processes for larger organic compounds, but no additional aqueous phase chemistry
RXN	Scenario UPT with the first reaction step protocol in the mechanism described by the new CAPRAM/ GECKO-A protocol leading to WSOC for products not defined in the explicit chemical scheme
$RXN_{0.4}$	Same as scenario RXN, but with WSOC products scaled by a factor of 0.4

A.3 Model and mechanism names

CAPRAM	Chemical Aqueous Phase RAdical Mechanism (http://projects.tropos.de/capram/)
GECKO-A	Generator for Explicit Chemistry and Kinetics of Organics in the Atmosphere (http://geckoa.lisa.u-pec.fr/index.php)
GROMHE	GROup contribution Method for Henry’s law Estimate (SAR by Raventos-Duran et al., 2010)
MCM	Master Chemical Mechanism (http://mcm.leeds.ac.uk/)
SPACCIM	SPectral Aerosol Cloud Chemistry Interaction Model

A.4 Chamber and instrumentation abbreviations

AMS	aerosol mass spectrometer
C-GIS	condensation growth and impaction system
LEAK	LEipziger Aerosol Kammer
PTFE	polytetrafluoroethylene
PTR-MS	proton-transfer-reaction mass spectrometer
SMPS	scanning mobility particle sizer

A.5 Organic compound names

HULIS/HULIS$^-$	humic-like substances (fully protonated and deprotonated)
OM	organic matter
TMB	1,3,5-trimethylbenzene
WISOC	water-insoluble organic compounds
WSOC	water-soluble organic compounds
2O3H-SA	2-oxo-3-hydroxy-succinaldehyde

Author contributions.

P.B., C.M.V., A.T, B.A. and H.H. developed the protocol for mechanism auto-generation

Deleted:]

P.B., C.M.V., A.T., R.W., B.A. and H.H. designed the model experiments.
P.B., C.M.V., and B.A. did model development on GECKO-A.
P.B. and R.W. did model development on SPACCIM.
P.B., A.T., A.M., O.B., M.R., L.P., D.v.P., and H.H. designed the aerosol chamber experiments.
M.R., A.M., O.B., L.P., and D.v.P. performed the aerosol chamber experiments and analysed the data.
PB, A.T., and H.H analysed model results.
P.B., A.T., and H.H. wrote the paper.

Competing interests. The authors declare that they have no competing interests.

Acknowledgements. This work was performed within the project ATMOCHEM funded by the German Research Foundation (Deutsche Forschungsgemeinschaft, DFG) under the project number BO 1714/3-1. Support was also received from the European Commission within EUROCHAMP-2020 under the EUROCHAMP Grant Agreement No. 730997.

Deleted: Co-funding

References

Alfassi, Z. B., Padmaja, S., Neta, P. and Huie, R. E.: Rate constants for reactions of nitrate (NO_3) radicals with organic compounds in water and acetonitrile, J. Phys. Chem., 97(15), 3780–3782, doi:10.1021/j100117a025, 1993.

Ammann, M., Cox, R. A., Crowley, J. N., Jenkin, M. E., Mellouki, A., Rossi, M. J., Troe, J. and Wallington, T. J.: Evaluated kinetic and photochemical data for atmospheric chemistry: Volume VI – heterogeneous reactions with liquid substrates, Atmos. Chem. Phys., 13(16), 8045–8228, doi:10.5194/acp-13-8045-2013, 2013.

Arakaki, T., Saito, K., Okada, K., Nakajima, H. and Hitomi, Y.: Contribution of fulvic acid to the photochemical formation of Fe(II) in acidic Suwannee River fulvic acid solutions, Chemosphere, 78(8), 1023–1027, doi:10.1016/j.chemosphere.2009.11.035, 2010.

Arakaki, T., Anastasio, C., Kuroki, Y., Nakajima, H., Okada, K., Kotani, Y., Handa, D., Azechi, S., Kimura, T., Tsuhako, A. and Miyagi, Y.: A general scavenging rate constant for reaction of hydroxyl radical with organic carbon in atmospheric waters, Environ. Sci. Technol., 47(15), 8196–8203, doi:10.1021/es401927b, 2013.

Asmus, K. D., Möckel, H. and Henglein, A.: Pulse radiolytic study of site of OH radical attack on aliphatic alcohols in aqueous solution, J. Phys. Chem., 77(10), 1218–1221, doi:10.1021/j100629a007, 1973.

Aumont, B., Szopa, S. and Madronich, S.: Modelling the evolution of organic carbon during its gas-phase tropospheric oxidation: development of an explicit model based on a self generating approach, Atmos. Chem. Phys., 5(9), 2497–2517, doi:10.5194/acp-5-2497-2005, 2005.

Bean, J. K., Faxon, C. B., Leong, Y. J., Wallace, H. W., Cevik, B. K., Ortiz, S., Canagaratna, M. R., Usenko, S., Sheesley, R. J., Griffin, R. J. and Ruiz, L. H.: Composition and sources of particulate matter measured near Houston, TX: Anthropogenic-biogenic interactions, Atmosphere, 7(5), doi:10.3390/atmos7050073, 2016.

Benson, S. W.: Thermochemical kinetics: methods for the estimation of thermochemical data and rate parameters, 2nd ed., edited by S. W. Benson, John Wiley & Sons, Inc., New York., 1976.

Bonifačić, M., Armstrong, D. a., Štefanić, I. and Asmus, K.-D.: Kinetic isotope effect for hydrogen abstraction by ·OH radicals from normal and carbon-deuterated ethyl alcohol and methylamine in aqueous solutions, J. Phys. Chem. B, 107(30), 7268–7276, doi:10.1021/jp027790e, 2003.

Boucher, O., Randall, D., Artaxo, P., Bretherton, C., Feingold, G., Forster, P., Kerminen, V.-M., Kondo, Y., Liao, H., Lohmann, U., Rasch, P., Satheesh, S. K., Sherwood, S., Stevens, B. and Zhang, X. Y.: Clouds and Aerosols, in Climate Change 2013: The Physical Science Basis. Contribution of Working Group I to the Fifth Assessment Report of the Intergovernmental Panel on Climate Change, edited by T. F. Stocker, D. Qin, G.-K. Plattner, M. Tignor, S. K. Allen, J. Boschung, and V. B. and P. M. M. A. Nauels, Y. Xia, pp. 571–658, Cambridge University Press, Cambridge, UK., 2013.

Brasseur, G. P., Artaxo, P., Barrie, L. A., Delmas, R. J., Galbally, I. E., Hao, W. M., Harriss, R. C., Isaksen, I. S. A., Jacob, D. J., Kolb, C. E., Prather, M., Rodhe, H., Schwela, D., Steffen, W. and Wuebbles, D. J.: Chapter 7 An Integrated View of Causes and Impacts of Atmospheric Changes, in Atmospheric Chemistry in a Changing World – An Integration and Synthesis of a Decade of Tropospheric Chemistry Research, edited by G. P. Brasseur, R. G. Prinn, and A. A. R. Pszenny, Springer Verlag, Berlin, Germany., 2003.

Bräuer, P., Tilgner, A., Wolke, R. and Herrmann, H.: Mechanism development and modelling of tropospheric multiphase halogen chemistry: The CAPRAM Halogen Module 2.0 (HM2), J. Atmos. Chem., 1–34, doi:10.1007/s10874-013-9249-6, 2013.

Brégonzio-Rozier, L., Giorio, C., Siekmann, F., Pangui, E., Morales, S. B., Temime-Roussel, B., Gratien, A., Michoud, V., Cazaunau, M., DeWitt, H. L., Tapparo, A., Monod, A. and Doussin, J.-F.: Secondary organic aerosol formation from isoprene photooxidation during cloud condensation–evaporation cycles, Atmos. Chem. Phys., 16(3), 1747–1760, doi:10.5194/acp-16-1747-2016, 2016.

Buxton, G. V., Greenstock, C. L., Helman, W. P. and Ross, A. B.: Critical review of rate constants for reactions of hydrated electrons, hydrogen atoms and hydroxyl radicals (OH/O-) in aqueous solution, J. Phys. Chem. Ref. Data, 17(2), 513–886, 1988.

Compernolle, S. and Müller, J.-F.: Henry's law constants of diacids and hydroxy polyacids: Recommended values, Atmos. Chem. Phys., 14(5), 2699–2712, doi:10.5194/acp-14-2699-2014, 2014a.

Compernolle, S. and Müller, J.-F.: Henry's law constants of polyols, Atmos. Chem. Phys., 14(9), 12815–12837, doi:10.5194/acp-14-12815-2014, 2014b.

Davidovits, P., Kolb, C. E., Williams, L. R., Jayne, J. T. and Worsnop, D. R.: Mass Accommodation and Chemical Reactions at Gas−Liquid Interfaces, Chem. Rev., 106(4), 1323–1354, doi:10.1021/cr040366k, 2006.

Davidovits, P., Kolb, C. E., Williams, L. R., Jayne, J. T. and Worsnop, D. R.: Update 1 of: Mass Accommodation and Chemical

Reactions at Gas−Liquid Interfaces, Chem. Rev., 111(4), doi:10.1021/cr100360b, 2011.

Day, D. A., Liu, S., Russell, L. M. and Ziemann, P. J.: Organonitrate group concentrations in submicron particles with high nitrate and organic fractions in coastal southern California, Atmos. Environ., 44(16), 1970–1979, doi:10.1016/J.ATMOSENV.2010.02.045, 2010.

Doussin, J.-F. and Monod, A.: Structure–activity relationship for the estimation of OH-oxidation rate constants of carbonyl compounds in the aqueous phase, Atmos. Chem. Phys., 13(23), 11625–11641, doi:10.5194/acp-13-11625-2013, 2013.

Dunmore, R. E., Hopkins, J. R., Lidster, R. T., Lee, J. D., Evans, M. J., Rickard, a. R., Lewis, a. C. and Hamilton, J. F.: Diesel-related hydrocarbons can dominate gas phase reactive carbon in megacities, Atmos. Chem. Phys., 15(17), 9983–9996, doi:10.5194/acp-15-9983-2015, 2015.

Ervens, B.: Modeling the Processing of Aerosol and Trace Gases in Clouds and Fogs, Chem. Rev., 115(10), 4157–4198, doi:10.1021/cr5005887, 2015.

Ervens, B. and Kreidenweis, S. M.: SOA Formation by Biogenic and Carbonyl Compounds : Data Evaluation and Application, 41(11), 3904–3910, doi:10.1021/es061946x, 2007.

Ervens, B., Turpin, B. J. and Weber, R. J.: Secondary organic aerosol formation in cloud droplets and aqueous particles (aqSOA): a review of laboratory, field and model studies, Atmos. Chem. Phys., 11(21), 11069–11102, doi:10.5194/acp-11-11069-2011, 2011.

Evans, M. G.: Thermodynamical treatment of transition state, Trans. Faraday Soc., 34, 49–57, doi:10.1039/TF9383400049, 1938.

Fuller, E. N.: Diffusion coefficients for binary gas systems at low pressures: Empirical correlations, McGraw Hill, New York., 1986.

George, C., Sidebottom, H. W., Mellouki, A., Barnes, I., Pilling, M. J., Herrmann, H., Wortham, H., Kirchner, F., Wirtz, K., Zetzsch, C. and Kanakidou, M.: Final report (sections 1 – 6), Fifth Framework Programme 1998 – 2002, Thematic Programme: Environment and Sustainable Development, Project number EVK2-CT-2001-00114., 2005.

Goldstein, A. H. and Galbally, I. E.: Known and unexplored organic constituents in the earth's atmosphere, Environ. Sci. Technol., 41(5), 1514–1521, doi:10.1021/es072476p, 2007.

Haag, W. R. and Yao, C. C. D.: Rate constants for reaction of hydroxyl radicals with several drinking water contaminants, Environ. Sci. Technol., 26(5), 1005–1013, doi:10.1021/es00029a021, 1992.

Hallquist, M., Wenger, J. C., Baltensperger, U., Rudich, Y., Simpson, D., Claeys, M., Dommen, J., Donahue, N. M., George, C., Goldstein, A. H., Hamilton, J. F., Herrmann, H., Hoffmann, T., Iinuma, Y., Jang, M., Jenkin, M. E., Jimenez, J. L., Kiendler-Scharr, A., Maenhaut, W., McFiggans, G., Mentel, T. F., Monod, A., Prevot, A. S. H., Seinfeld, J. H., Surratt, J. D., Szmigielski, R. and Wildt, J.: The formation, properties and impact of secondary organic aerosol: current and emerging issues, Atmos. Chem. Phys., 9(14), 5155–5236, 2009.

Herrmann, H.: Kinetics of Aqueous Phase Reactions Relevant for Atmospheric Chemistry, Chem. Rev., 103(12), 4691–4716, doi:10.1021/cr020658q, 2003.

Herrmann, H.: On the photolysis of simple anions and neutral molecules as sources of O^-/OH, SO_x^- and Cl in aqueous solution, Phys. Chem. Chem. Phys., 9(30), 3935–3964, doi:10.1039/B618565G, 2007.

Herrmann, H. and Zellner, R.: Reactions of $NO_3^\bullet$-radicals in aqueous solution, edited by Z. B. Alfassi, pp. 291–343, Wiley, New York., 1998.

Herrmann, H., Tilgner, A., Barzaghi, P., Majdik, Z., Gligorovski, S., Poulain, L. and Monod, A.: Towards a more detailed description of tropospheric aqueous phase organic chemistry: CAPRAM 3.0, Atmos. Environ., 39(23--24), 4351–4363, doi:10.1016/j.atmosenv.2005.02.016, 2005.

Herrmann, H., Hoffmann, D., Schaefer, T., Bräuer, P. and Tilgner, A.: Tropospheric Aqueous-Phase Free-Radical Chemistry: Radical Sources, Spectra, Reaction Kinetics and Prediction Tools, ChemPhysChem, 11(18), 3796–3822, 2010.

Hoffmann, D., Weigert, B., Barzaghi, P. and Herrmann, H.: Reactivity of poly-alcohols towards OH, NO_3 and SO_4^- in aqueous solution, Phys. Chem. Chem. Phys., 11(41), 9351, doi:10.1039/b908459b, 2009.

Iglewicz, B. and Hoaglin, D.: Volume 16: How to Detect and Handle Outliers, The ASQC Basic References in Quality Control: Statistical Techniques, Edward F. Mykytka, Ph.D., Editor., 1993.

Jenkin, M. E., Saunders, S. M. and Pilling, M. J.: The tropospheric degradation of volatile organic compounds: A protocol for mechanism development, Atmos. Environ., 31(1), 81–104, doi:10.1016/S1352-2310(96)00105-7, 1997.

Jenkin, M. E., Saunders, S. M., Wagner, V. and Pilling, M. J.: Protocol for the development of the Master Chemical Mechanism, MCM v3 (Part B): Tropospheric degradation of aromatic volatile organic compounds, Atmos. Chem. Phys., 3(1), 181–193, doi:10.5194/acp-3-181-2003, 2003.

Jimenez, J. L., Canagaratna, M. R., Donahue, N. M., Prevot, A. S. H., Zhang, Q., Kroll, J. H., DeCarlo, P. F., Allan, J. D., Coe, H., Ng, N. L., Aiken, A. C., Docherty, K. S., Ulbrich, I. M., Grieshop, A. P., Robinson, A. L., Duplissy, J., Smith, J. D., Wilson, K. R., Lanz, V. A., Hueglin, C., Sun, Y. L., Tian, J., Laaksonen, A., Raatikainen, T., Rautiainen, J., Vaattovaara, P., Ehn, M., Kulmala, M., Tomlinson, J. M., Collins, D. R., Cubison, M. J., Dunlea, J., Huffman, J. A., Onasch, T. B., Alfarra, M. R., Williams, P. I., Bower, K., Kondo, Y., Schneider, J., Drewnick, F., Borrmann, S., Weimer, S., Demerjian, K., Salcedo, D., Cottrell, L., Griffin, R., Takami, A., Miyoshi, T., Hatakeyama, S., Shimono, A., Sun, J. Y., Zhang, Y. M., Dzepina, K., Kimmel, J. R., Sueper, D., Jayne, J. T., Herndon, S. C., Trimborn, A. M., Williams, L. R., Wood, E. C., Middlebrook, A. M., Kolb, C. E., Baltensperger, U. and Worsnop, D. R.: Evolution of Organic Aerosols in the Atmosphere, Science, 326(5959), 1525–1529, doi:10.1126/science.1180353, 2009.

Kames, J. and Schurath, U.: Henry's Law and hydrolysis-rate constants for peroxyacyl nitrates (PANS) using a homogeneous gas-phase source, J. Atmos. Chem., 21(2), 151–164, doi:10.1007/BF00696578, 1995.

Kiendler-Scharr, A., Mensah, A. A., Friese, E., Topping, D., Nemitz, E., Prevot, A. S. H., Äijälä, M., Allan, J., Canonaco, F., Canagaratna, M., Carbone, S., Crippa, M., Dall Osto, M., Day, D. A., De Carlo, P., Di Marco, C. F., Elbern, H., Eriksson, A., Freney, E., Hao, L., Herrmann, H., Hildebrandt, L., Hillamo, R., Jimenez, J. L., Laaksonen, A., McFiggans, G., Mohr, C., O'Dowd, C., Otjes, R., Ovadnevaite, J., Pandis, S. N., Poulain, L., Schlag, P., Sellegri, K., Swietlicki, E., Tiitta, P., Vermeulen, A., Wahner, A., Worsnop, D. and Wu, H. C.: Ubiquity of organic nitrates from nighttime chemistry in the European submicron aerosol, Geophys. Res. Lett., 43(14), 7735–7744, doi:10.1002/2016GL069239, 2016.

La, Y. S., Camredon, M., Ziemann, P. J., Valorso, R., Matsunaga, A., Lannuque, V., Lee-Taylor, J., Hodzic, A., Madronich, S. and Aumont, B.: Impact of chamber wall loss of gaseous organic compounds on secondary organic aerosol formation: Explicit modeling of SOA formation from alkane and alkene oxidation, Atmos. Chem. Phys., 16(3), 1417–1431, doi:10.5194/acp-16-1417-2016, 2016.

Lee-Taylor, J., Hodzic, A., Madronich, S., Aumont, B., Camredon, M. and Valorso, R.: Multiday production of condensing organic aerosol mass in urban and forest outflow, Atmos. Chem. Phys., 15(2), 595–615, doi:10.5194/acp-15-595-2015, 2015.

Li, K. and Crittenden, J.: Computerized pathway elucidation for hydroxyl radical-induced chain reaction mechanisms in aqueous phase advanced oxidation processes, Environ. Sci. Technol., 43(8), 2831–2837, doi:10.1021/es802039y, 2009.

Mayer, B. and Madronich, S.: Photolysis frequencies in water droplets: Mie calculations and geometrical optics limit, Atmos. Chem. Phys., 4(8), 4105–4130, doi:10.5194/acp-4-2241-2004, 2004.

McVay, R. C., Zhang, X., Aumont, B., Valorso, R., Camredon, M., La, Y. S., Wennberg, P. O., Seinfeld, J. H., Insu, U. M. R. C., Paris, U., Créteil, E., Diderot, P., Pierre, I. and Laplace, S.: SOA formation from the photooxidation of α-pinene : systematic exploration of the simulation of chamber data, Atmos. Chem. Phys., 16(5), 2785–2802, doi:10.5194/acp-16-2785-2016, 2016.

Minakata, D., Li, K., Westerhoff, P. and Crittenden, J.: Development of a group contribution method to predict aqueous phase hydroxyl radical (HO) reaction rate constants, Environ. Sci. Technol., 43(16), 6220–6227, doi:10.1021/es900956c, 2009.

Monod, A. and Doussin, J. F.: Structure-activity relationship for the estimation of OH-oxidation rate constants of aliphatic organic compounds in the aqueous phase: alkanes, alcohols, organic acids and bases, Atmos. Environ., 42(33), 7611–7622,

Deleted: Mcvay

doi:10.1016/j.atmosenv.2008.06.005, 2008.

Mouchel-Vallon, C., Bräuer, P., Camredon, M., Valorso, R., Madronich, S., Herrmann, H. and Aumont, B.: Explicit modeling of volatile organic compounds partitioning in the atmospheric aqueous phase, Atmos. Chem. Phys., 13(2), 1023–1037, doi:10.5194/acp-13-1023-2013, 2013.

Mouchel-Vallon, C., Deguillaume, L., Monod, A., Perroux, H., Rose, C., Ghigo, G., Long, Y., Leriche, M., Aumont, B., Patryl, L., Armand, P. and Chaumerliac, N.: CLEPS 1.0: A new protocol for cloud aqueous phase oxidation of VOC mechanisms, Geosci. Model Dev., 10(3), 1339–1362, doi:10.5194/gmd-10-1339-2017, 2017.

Pereira, K. L., Dunmore, R., Whitehead, J., Rami Alfarra, M., Allan, J. D., Alam, M. S., Harrison, R. M., McFiggans, G. and Hamilton, J. F.: Technical note: Use of an atmospheric simulation chamber to investigate the effect of different engine conditions on unregulated VOC-IVOC diesel exhaust emissions, Atmos. Chem. Phys., 18(15), 11073–11096, doi:10.5194/acp-18-11073-2018, 2018.

Perrin, D. D., Dempsey, B. and Serjeant, E. P.: pKa prediction for organic acids and bases, Chapman and Hall, London, UK, 1981.

Raventos-Duran, T., Camredon, M., Valorso, R., Mouchel-Vallon, C. and Aumont, B.: Structure-activity relationships to estimate the effective Henry's law constants of organics of atmospheric interest, Atmos. Chem. Phys., 10(16), 7643–7654, doi:10.5194/acp-10-7643-2010, 2010.

Ross, A. B., Bielski, B. H. J., Buxton, G. V, Cabelli, D. E., Helman, W. P., Huie, R. E., Grodkowski, J., Neta, P., Mulazzani, Q. G. and Wilkinson, F.: NIST Standard Reference Database 40, Version 3.0, Gaithersburg, MD, USA., 1998.

Salma, I. and Láng, G. G.: How many carboxyl groups does an average molecule of humic-like substances contain?, Atmos. Chem. Phys., 8(20), 5997–6002, doi:10.5194/acp-8-5997-2008, 2008.

Saunders, S. M., Jenkin, M. E., Derwent, R. G. and Pilling, M. J.: Protocol for the development of the Master Chemical Mechanism, MCM v3 (Part A): Tropospheric degradation of non-aromatic volatile organic compounds, Atmos. Chem. Phys., 3(1), 161–180, 2003.

Schaefer, T., Schindelka, J., Hoffmann, D. and Herrmann, H.: Laboratory kinetic and mechanistic studies on the OH-initiated oxidation of acetone in aqueous solution, J. Phys. Chem. A, 116(24), 6317–6326, doi:10.1021/jp2120753, 2012.

Schöne, L., Schindelka, J., Szeremeta, E., Schaefer, T., Hoffmann, D., Rudzinski, K. J., Szmigielski, R. and Herrmann, H.: Atmospheric aqueous phase radical chemistry of the isoprene oxidation products methacrolein, methyl vinyl ketone, methacrylic acid and acrylic acid - kinetics and product studies, Phys. Chem. Chem. Phys., 16(13), 6257–6272, doi:10.1039/C3CP54859G, 2014.

Schuchmann, H. P. and von Sonntag, C.: Methylperoxyl Radicals: A Study of the γ-Radiolysis of Methane in Oxygenated Aqueous Solutions, Zeitschrift fur Naturforsch. - Sect. B J. Chem. Sci., 39(2), 217–221, doi:10.1515/znb-1984-0217, 1984.

Schuchmann, M. N., Zegota, H. and von Sonntag, C.: Acetate peroxyl radicals, O2CH2CO2- – A study on the gamma radiolysis and pulse-radiolysis of acetate in oxygenated aqueous solutions, Zeitschrift f\"ur Naturforsch. Sect. B -- A J. Chem. Sci., 40(2), 215–221, 1985.

Schwartz, S. E.: Mass transport considerations pertinent to aqueous phase reactions of gases in liquid water clouds, edited by W. Jaeschke, pp. 415–471, Springer, Berlin, Germany., 1986.

von Sonntag, C.: The chemical basis of radiation biology, Taylor and Francis, London, Great Britain., 1987.

von Sonntag, C. and Schuchmann, H. P.: The elucidation of peroxyl radical reactions in aqueous solution with the help of radiation chemical methods, Angew. Chemie -- Int. Ed. English, 30(10), 1229–1253, doi:10.1002/anie.199112291, 1991.

von Sonntag, C., Dowideit, P., Fang, X. W., Mertens, R., Pan, X. M., Schuchmann, M. N. and Schuchmann, H. P.: The fate of peroxyl radicals in aqueous solution, Water Sci. Technol., 35(4), 9–15, doi:10.1016/S0273-1223(97)00003-6, 1997.

Tilgner, A. and Herrmann, H.: Radical-driven carbonyl-to-acid conversion and acid degradation in tropospheric aqueous systems studied by CAPRAM, Atmos. Environ., 44(40), 5415–5422, 2010.

Tilgner, A., Bräuer, P., Wolke, R. and Herrmann, H.: Modelling multiphase chemistry in deliquescent aerosols and clouds using CAPRAM3.0i, J. Atmos. Chem., 70(3), 221–256, doi:10.1007/s10874-013-9267-4, 2013.

Vereecken, L., Aumont, B., Barnes, I., Bozzelli, J. W., Goldman, M. J., Green, W. H., Madronich, S., Mcgillen, M. R., Mellouki, A., Orlando, J. J., Picquet-Varrault, B., Rickard, A. R., Stockwell, W. R., Wallington, T. J. and Carter, W. P. L.: Perspective on Mechanism Development and Structure-Activity Relationships for Gas-Phase Atmospheric Chemistry, Int. J. Chem. Kinet., 50(6), 435–469, doi:10.1002/kin.21172, 2018.

Wang, C., Yuan, T., Wood, S., Goss, K. U., Li, J., Ying, Q. and Wania, F.: Uncertain Henry's law constants compromise equilibrium partitioning calculations of atmospheric oxidation products, Atmos. Chem. Phys., 17(12), 7529–7540, doi:10.5194/acp-17-7529-2017, 2017.

Wolke, R., Sehili, A. M., Simmel, M., Knoth, O., Tilgner, A. and Herrmann, H.: SPACCIM: A parcel model with detailed microphysics and complex multiphase chemistry, Atmos. Environ., 39(23–24), 4375–4388, doi:10.1016/j.atmosenv.2005.02.038, 2005.

Tables

Table 1
Parameterisations for the aqueous-phase chemistry of WSOC and HULIS compounds.

Formatted: Font: Not Bold

Process	$k_{298}/K/j_{max}$ (a)	Reference/comment
$WSOC + OH \rightarrow WSOC + HO_2$	$3.8 \cdot 10^{8}$	Estimated after Arakaki et al. (2013)
$HULIS + OH \rightarrow HULIS + HO_2$	$3.8 \cdot 10^{8}$	Estimated after Arakaki et al. (2013)
$HULIS^{-} + OH \rightarrow HULIS^{-} + HO_2$	$3.8 \cdot 10^{8}$	Estimated after Arakaki et al. (2013)
$WSOC + NO_3 \rightarrow WSOC + HO_2 + NO_3^{-} + H^{+}$	$1.0 \cdot 10^{7}$	Estimated in accord with subsection 3.3.1
$HULIS + NO_3 \rightarrow HULIS + HO_2 + NO_3^{-} + H^{+}$	$1.0 \cdot 10^{7}$	Estimated in accord with subsection 3.3.1
$HULIS^{-} + NO_3 \rightarrow HULIS + HO_2 + NO_3^{-}$	$5.0 \cdot 10^{7}$	Estimated in accord with subsection 3.3.1
$HULIS \rightleftharpoons HULIS^{-} + H^{+}$	$3.98 \cdot 10^{-4}$ (b)	Estimated with pK_a of fulvic acid after Salma and Láng (2008)
$Fe^{3+} + HULIS^{-} \rightleftharpoons [FeHULIS]^{2+} + 0.5\,HO_2$	$1.0 \cdot 10^{9}$ (c)	Estimated after iron-oxalato complex formation
$Fe^{2+} + HULIS^{-} \rightleftharpoons [FeHULIS]^{+}$	$1.0 \cdot 10^{9}$ (c)	Estimated after iron-oxalato complex formation
$[FeHULIS]^{2+} \xrightarrow{h\nu} Fe^{2+} + HULIS + 0.5\,HO_2$	$2.0 \cdot 10^{-2}$	Estimated after iron-hydroxy complex photolysis (see Arakaki et al., 2010)

(a) k_{298} is given for irreversible reactions (indicated by $\rightarrow$) in $M^{-1}\,s^{-1}$, K is given for equilibria (indicated by $\rightleftharpoons$) in M^{-1}. For photolysis (indicated by $\xrightarrow{h\nu}$), j_{max} is given in s^{-1}. (b) $k_{backward} = 5.0 \cdot 10^{9}\,s^{-1}$; (c) $k_{backward} = 3.0 \cdot 10^{-3}\,s^{-1}$

Table 2 Processes implemented in the final GECKO-A aqueous-phase protocol for mechanism auto-generation.

Deleted: automated

Deleted: self

Process	Estimation/comment
Organic compounds + OH	SAR by Doussin and Monod (2013) accompanied by SAR by Minakata et al. (2009) for carboxyl/carboxylate groups and unsaturated carbon atoms with a double bond or groups in α- and β-position to unsaturated carbon atoms. For organic nitrate functions the same group contribution factors for α- and β-effects are assumed as for OH-functions. Immediate oxygen addition is assumed to formed alkyl radicals. 3% cut-off for minor branches.
Neutral saturated organic compounds + NO_3	Advanced Evans-Polanyi-type correlations using product determinations from the SAR of the corresponding hydroxyl radical reaction.
Unsaturated organic compounds + NO_3	$k_{2nd} = 1 \cdot 10^{7}$ M^{-1} s^{-1} based on subsection 3.3.2.
Dissociated carboxylic acids and diacids + NO_3	k_{2nd}(monocarboxylates + NO_3) = $2 \cdot 10^{7}$ M^{-1} s^{-1}, k_{2nd}(DCA mono-anion + NO_3) = $2.5 \cdot 10^{7}$ M^{-1} s^{-1}, and k_{2nd}(DCA dianion + NO_3) = $7.75 \cdot 10^{7}$ M^{-1} s^{-1} with ETR assumed as only reaction pathway and equal branching for unsymmetrical dicarboxylates. Nitrate radical addition to double bonds is assumed for unsaturated organic acids as only reaction pathway instead of ETR with $k_{2nd} = 1 \cdot 10^{7}$ M^{-1} s^{-1}.
Monomolecular decay of polycarbonyl compound	Monomolecular decay of polycarbonyls with 3 carbonyl groups within 4 adjacent carbon atoms with $k_{1st} = 0.1$ s^{-1}. Fragmentation is always between 2 carbonyl groups. Equal branching is assumed for unsymmetrical polycarbonyls with 3 adjacent carbonyl groups.
Hydrolysis of carbonyl nitrates	Hydrolysis of nitrates with an adjacent carbonyl group is assumed with $k_{2nd} = 7.5 \cdot 10^{-6}$ M^{-1} s^{-1} and $E_A/R = 6600$ K based on PAN hydrolysis by Kames and Schurath (1995).
$RO_2 \xrightarrow{R'O_2} 0.4\ RO + 1.1\ R{=}O + 0.5\ ROH + 0.7\ O_2 + 0.3\ H_2O_2$	Peroxy radical (RO_2) recombinations based on mechanism by von Sonntag and Schuchmann (1991) and von Sonntag et al. (1997) leading to alkoxy radicals (RO), carbonyl (R=O) and alcohol (ROH) compounds with updated kinetic and mechanistic data for the acetonyl peroxy radical by Schaefer et al. (2012) using the given fixed branching ratios and $k_{2nd} = 7.3 \cdot 10^{8}$ M^{-1} s^{-1}.
Peroxy radicals with OH in α -position	HO_2 elimination assumed as only process with $k_{1st} = 200$ s^{-1}. For a gem-diol function in α-position, an increased k_{1st} of 1000 s^{-1} is assumed.
$2\ RCH(O_2\cdot)COOH \rightarrow 2\ RCHO + 2\ CO_2 + H_2O_2$ $2\ RCH(O_2\cdot)COO^{-} \xrightarrow{2H_2O} \rightarrow 2\ RCHO + 2\ CO_2 + H_2O_2 + 2\ OH^{-}$	Additional reaction pathway to recombination and cross-reactions for peroxy radicals with COOH/COO^{-} in α-position with estimated k_{2nd} = 200 s^{-1} leading to a carbonyl compound, H_2O_2, and dissolved CO_2.

$RCO_3 \xrightarrow{H_2O} RCOOH + HO_2$	Immediate hydration of acylperoxy radicals (RCO_3) and HO_2 elimination with $k_{1st} = 1000\ s^{-1}$ is assumed leading to carboxylic acid formation (RCOOH).
Monomolecular decay of alkoxy radicals	C–C bond breaking with equal branching for unsymmetrical molecules is assumed for alkoxy radicals with and estimated k_{1st} of $5{\cdot}10^{2}\ s^{-1}$.
Alkoxy radicals + O_2	Formation of HO_2 and carbonyls with an estimated k_{2nd} of $5{\cdot}10^{6}\ s^{-1}$.
Decomposition of acyloxy radicals	Decarboxylation by C–C bond breaking of acyloxy radicals leading to dissolved CO_2 and a peroxy radical (as immediate oxygen addition is assumed for the alkyl radical formed).
Hydration of carbonyl compounds	Hydration constants calculated with GROMHE (Raventos-Duran et al., 2010). Estimated k_b of $5.69{\cdot}10^{-3}\ s^{-1}$; k_f calculated from K and k_b. 5% cut-off for minor hydration forms.
Dissociations of carboxylic acids	Calculated using pK_a prediction method with Taft parameters by Perrin et al. (1981) and an estimated backward rate constant of $5{\cdot}10^{10}\ M^{-1}\ s^{-1}$; k_f calculated from pK_a and k_b. Currently no cut-off for minor dissociation states.
Phase transfer	HLC calculated using GROMHE; D_g calculated with FSG method (Fuller, 1986); α assumed 0.1.

Deleted: braking

Deleted: braking

Table 3 Measured uncorrected concentrations in µg m^{-3} from C-GIS and the PTFE filter samples for identified products. Times given in the first column refer to measurement points in hours and minutes after the injection of ozone and the start of the UV-C photolysis.

Sample	[TIME]	Methyl-glyoxal	Formate	Acetate	Pyruvate	Oxalate	Malonate	Succinate	Malate
C-GIS samples (times correspond to the start of experiment, sample A00 is used to correct for background chemistry)									
A00[(a)]	[-00:27]	—	0.230	0.395	—	0.199	0.019	0.049	0.422
A01[(b)]	[00:01]	—	0.328	0.512	—	0.212	0.016	0.105	0.748
A02	[00:16]	—	0.266	0.433	—	0.213	0.022	0.074	0.475
A03	[00:31]	—	0.340	0.783	—	0.355	0.046	0.130	0.475
A04	[00:46]	—	0.159	0.427	—	0.178	0.017	0.048	0.149
A05	[01:01]	—	0.026	0.630	—	0.185	0.014	0.150	0.004
A06	[01:16]	—	0.230	0.570	—	0.237	0.018	0.116	0.083
A07	[01:31]	—	0.137	0.436	—	0.189	0.018	0.044	0.052
A08	[01:46]	—	0.230	0.798	—	0.315	0.016	0.023	0.055
A09	[02:01]	—	0.374	1.469	—	0.651	0.043	0.087	0.079
A10	[02:16]	—	0.230	0.887	—	0.355	0.031	0.058	0.026
A11	[02:31]	—	0.477	2.169	—	0.824	0.039	0.070	0.064
A12	[02:46]	—	0.170	0.908	—	0.260	0.037	0.098	0.027
A13	[03:01]	—	0.307	1.798	—	0.474	0.028	0.021	0.018
A14	[03:16]	—	0.362	2.194	—	0.703	0.043	0.087	0.037
PTFE filter samples (collected after the end of the experiment at 3:30)									
FS[(c)]	[-00:27]	0.048	0.646	0.810	0.280	6.819	0.354	—	5.640

[(a)] Sample A00 was collected after the injection of seed particles, when conditions were stable, but prior to the injection of TMB and ozone and the start of the UV-C photolysis.

[(b)] Sample A01 was collected directly after the start of the experiment with the injection of TMB and ozone and the start of the UV-C photolysis.

[(c)] The experiment was ended by switching of the UV-C lights at 03:30. Filter samples were taken at 03:36.

Deleted: UC

Figures

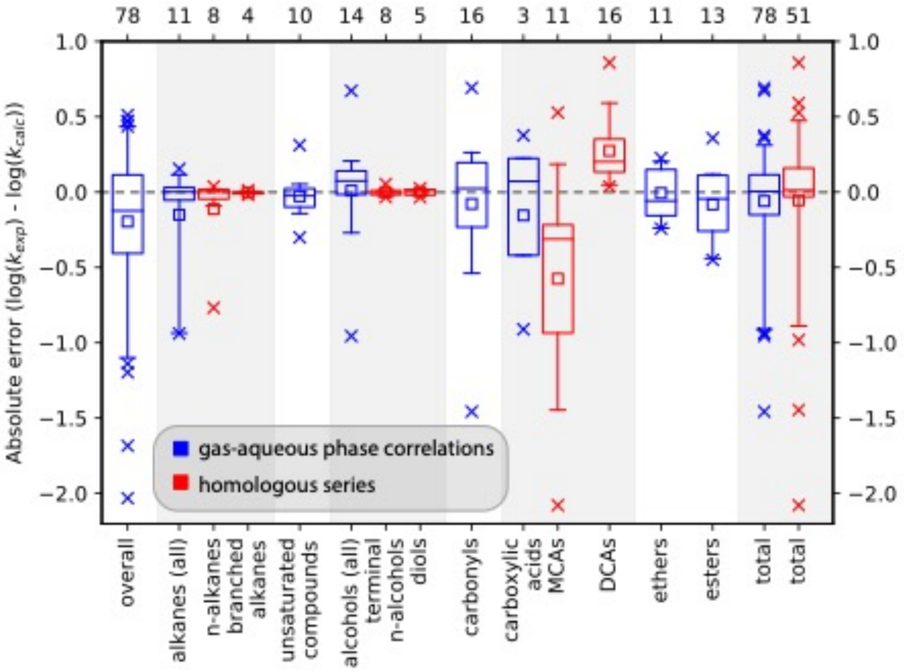

Figure 1 Box plots of the absolute errors of the logarithmised experimental versus predicted OH rate constants for the prediction of OH rate constants with gas-aqueous phase correlations (blue boxes) and extrapolations of homologous series (red boxes). Boxes represent the quartiles of the absolute errors, whiskers the 95% confidence interval, data points outside this are shown explicitly. The arithmetic mean is represented by a square. The 'overall'-box represents absolute errors from a gas-aqueous phase correlation derived from a fit of all data, while the total column denotes the evaluation of all errors compiled from the analysis of the various compound classes.

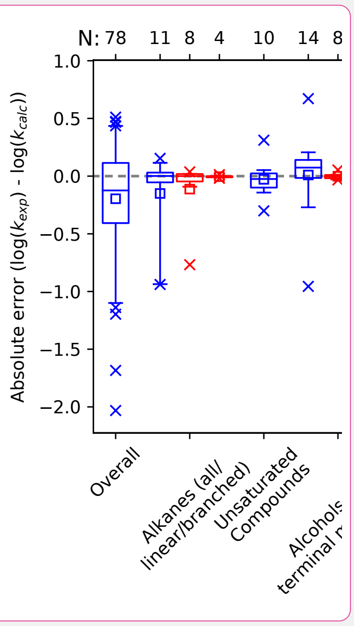

Deleted:

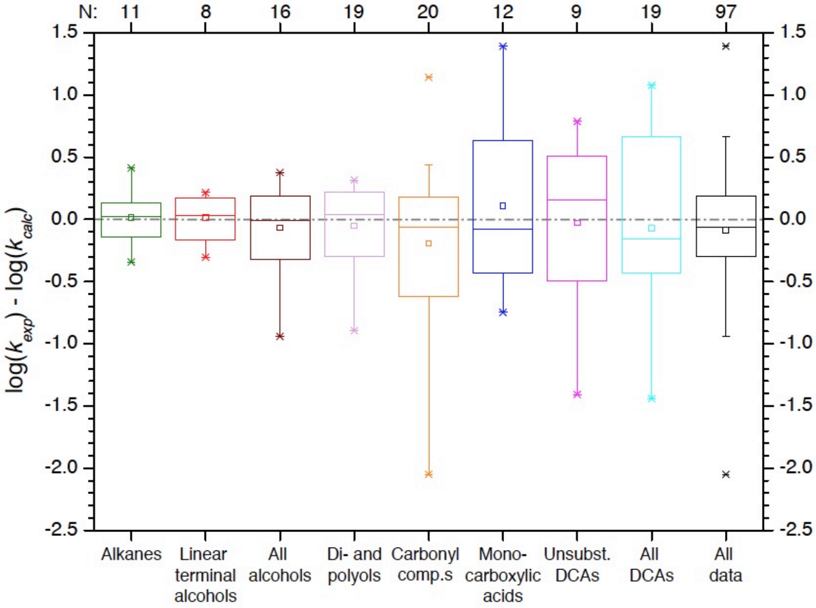

Figure 2 Box plots of the absolute errors of Evans-Polanyi-type correlations of hydroxyl radical reactions with organic compounds distinguished by compound class.

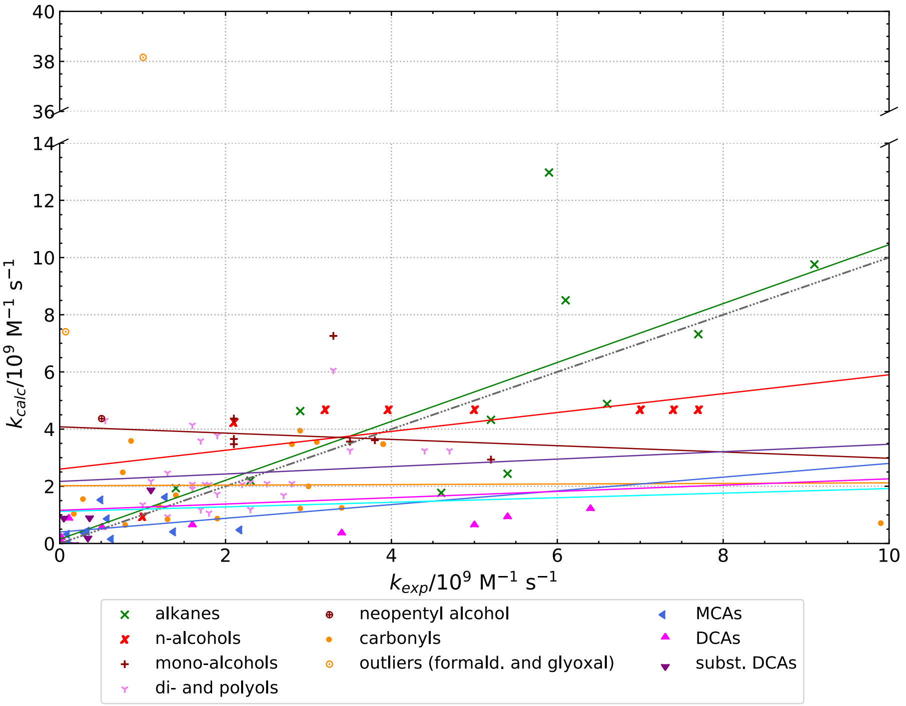

Figure 3 Plot of predicted versus experimental data for Evans-Polanyi correlations of OH radical reactions with organic compounds differentiated by compound class. Parameters of the regression lines are given in Table S8 in the ESM. The regression lines have the same colour code as the data points. The black dashed-dotted line is the line of same reactivity.

Deleted:

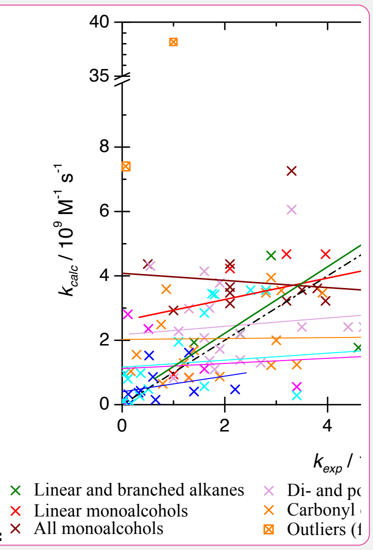

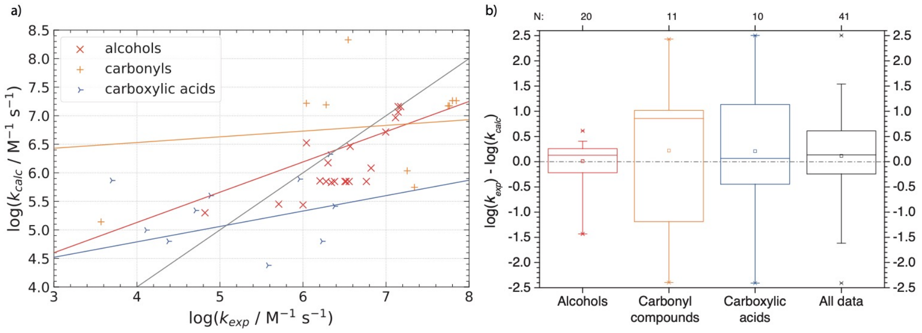

Figure 4 Evaluation of predicted versus experimental data for Evans-Polanyi-type correlations of NO_3 radical reactions with organic compounds using scatter plots (a) and analysis of absolute errors (b) distinguished by compound class. Parameters for the linear regression lines are given in Table S9 in the ESM.

Deleted:

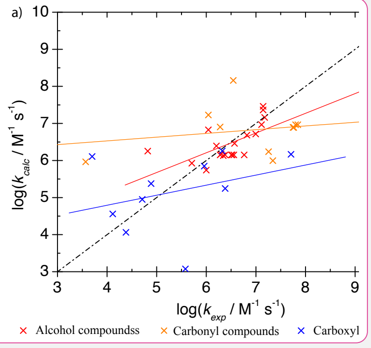

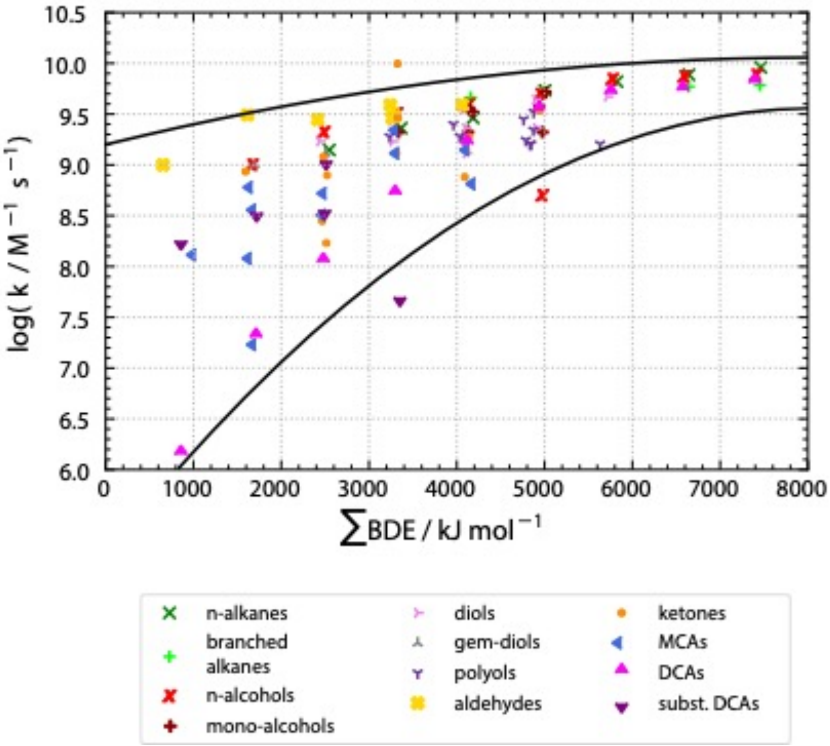

Figure 5 **Plot of experimentally determined second order rate constants versus accumulated bond strengths of all bonds containing hydrogen atoms in a molecule (ΣBDE) distinguished by compound classes. Black lines mark upper and lower boundary parabolas with most of the data lying within these boundaries.**

Deleted: ¶
¶

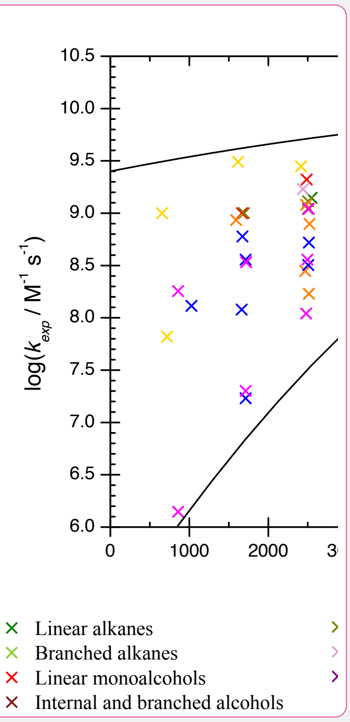

Formatted: Don't keep with next

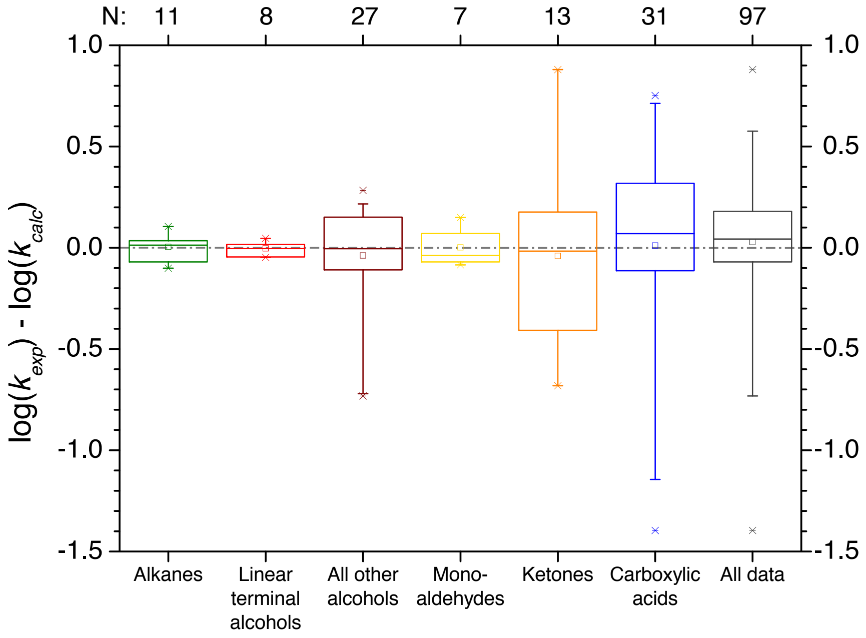

Figure 6 Box plots of absolute errors of second order OH rate constants predicted with the advanced Evans-Polanyi-type correlations versus experimental data for the various compound classes as well as all data.

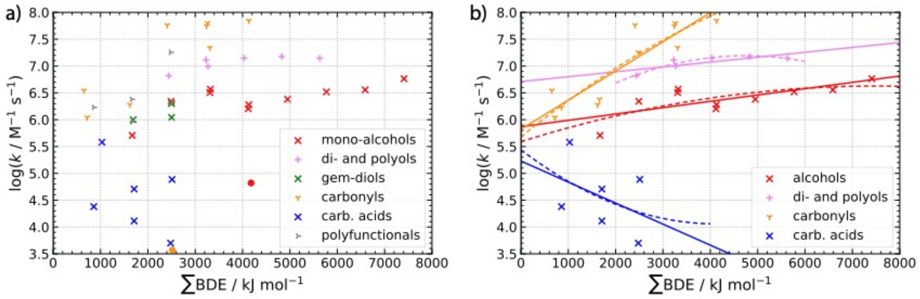

Figure 7 Experimental second order rate constants versus accumulated bond dissociation enthalpies of all bonds in molecules containing H-atoms (ΣBDE). Subfigure a shows the raw data and subfigure b the final datasets of the combined compound classes and their linear and quadratic regressions.

5

Deleted:

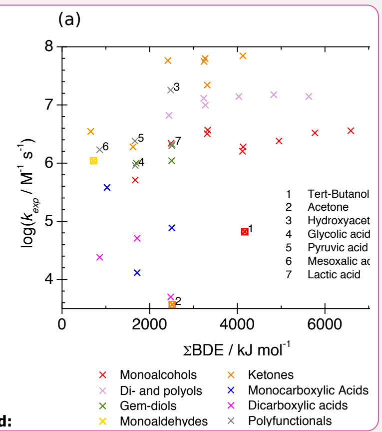

Deleted: there

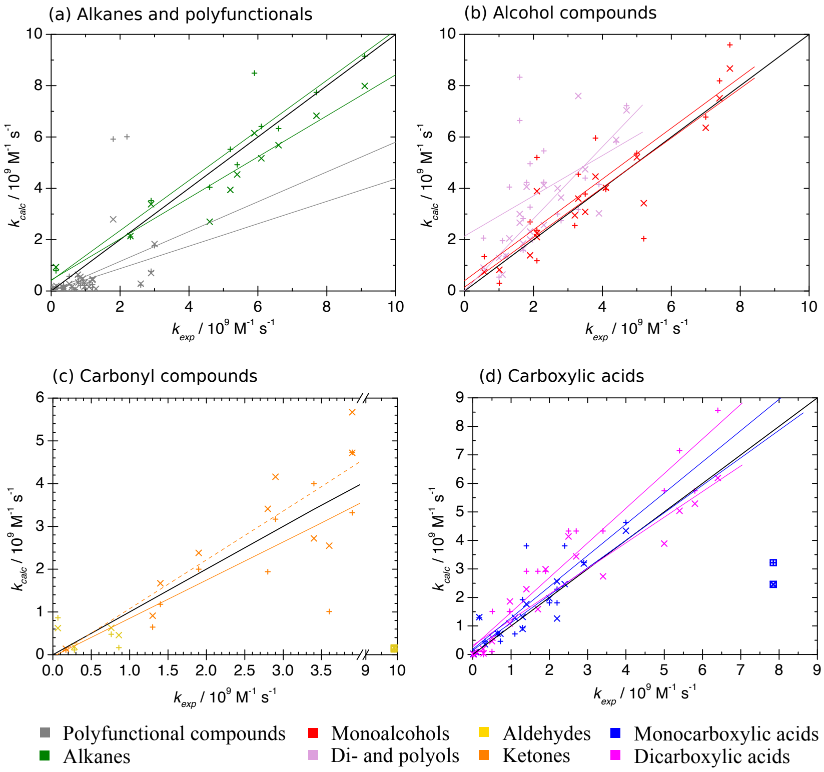

Figure 8 Scatter plots of predicted versus experimental data for the two SARs by Doussin and Monod (2013) and Minakata et al. (2009). Oblique crosses indicate predicted data by the SAR of Doussin and Monod (2013) with solid regression lines in the same colour. Upright crosses are data predicted with the SAR by Minakata et al. (2009) and dashed regression lines in the same colour. The boxed value in subfigure c has been excluded as an outlier in the regressions. Regressions in subfigure c include both, aldehyde and ketone data. Parameters for regression lines are given in Table S13 and S14 in the ESM for the data by Doussin and Monod (2013) and Minakata et al. (2009), respectively.

Deleted: cross

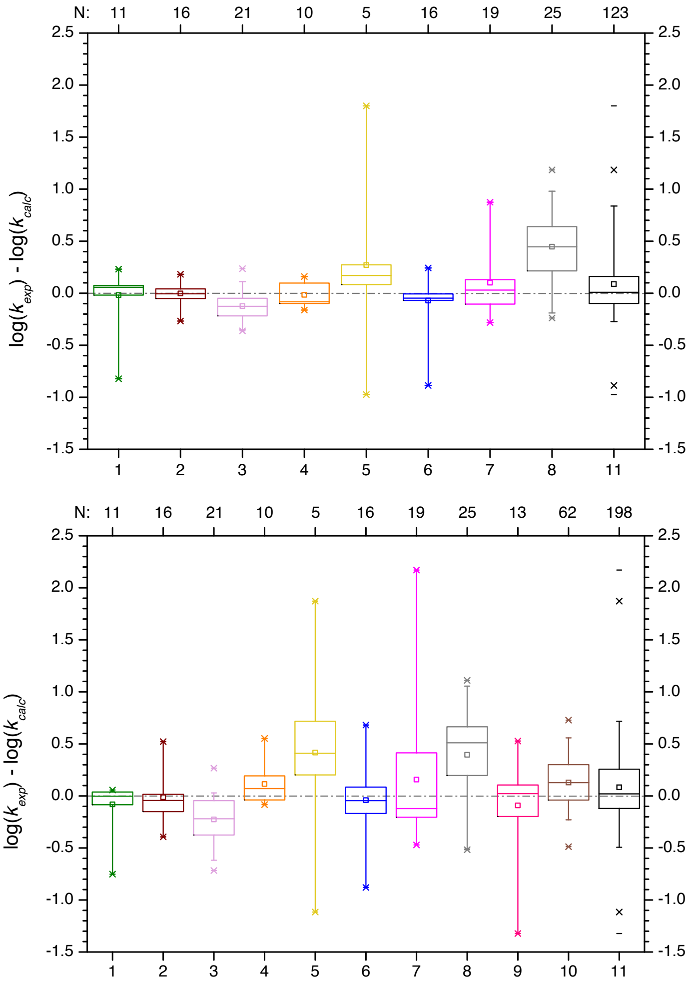

Figure 9 Box plots of the absolute errors of the logarithmised experimental versus predicted rate constants for the prediction with the SAR of Doussin and Monod (2013 (top) and Minakata et al. (2009) (bottom). Numbers at the abscissa refer to the compound class: 1 – alkanes, 2 – mono-alcohols, 3 – di- and polyols, 4 – carbonyls, 5 – dicarbonyls, 6 – mono-carboxylic acids, 7 – di-carboxylic acids, 8 – polyfunctionals, 9 – unsaturated compounds, 10 – aromatics, 11 – all data.

Deleted: bicarbonyls

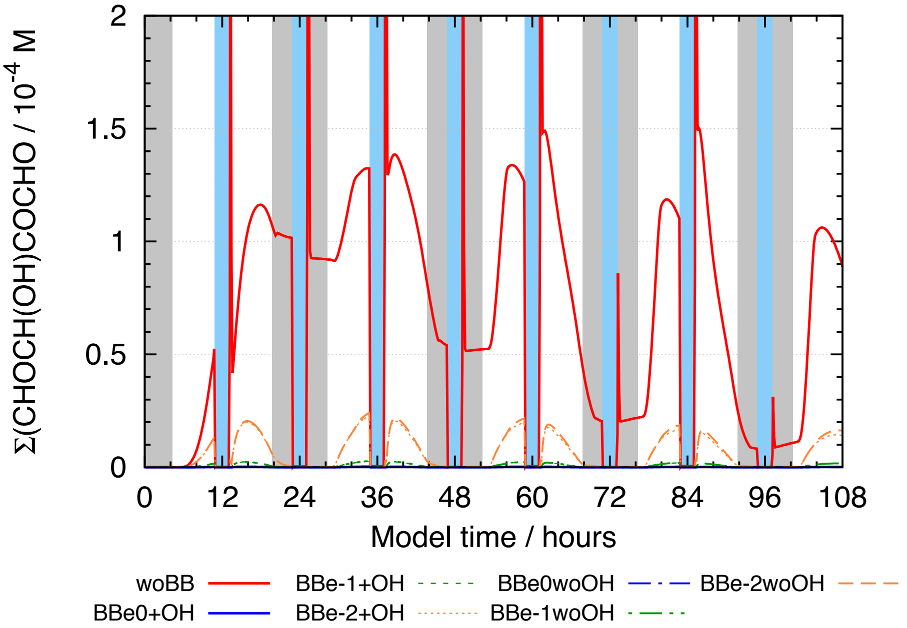

Figure 10 Concentration-time profiles of aqueous 2-oxo-3-hydroxy-succinaldehyde in all hydration forms in the sensitivity runs investigating the decay of polycarbonyl compounds under urban summer conditions with 8 cloud passages using the preliminary CAPRAM/GECKO-A protocol described in the text. Cloud passaged are marked with a blue shade and night-time periods with a grey shade. Scenario names of the legend are explained in Appendix A.2.

Deleted:

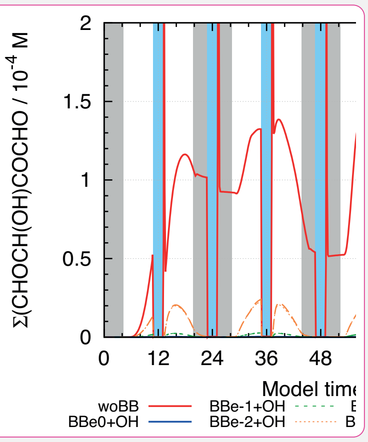

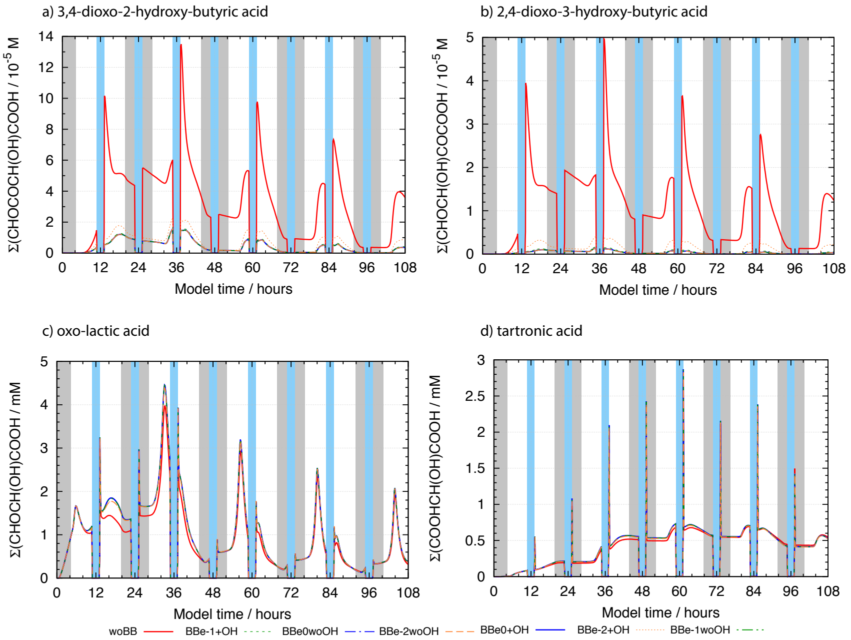

Figure 11 Accumulated concentration-time profiles of all hydration and dissociation forms of products of 2-oxo-3-hydroxy-succinaldehyde in the sensitivity runs investigating the decay of polycarbonyl compounds under urban summer conditions with 8 cloud passages using the preliminary CAPRAM/GECKO-A protocol described in the text. Cloud passaged are marked with a blue shade and night-time periods with a grey shade. Scenario names of the legend are explained in Appendix A.2.

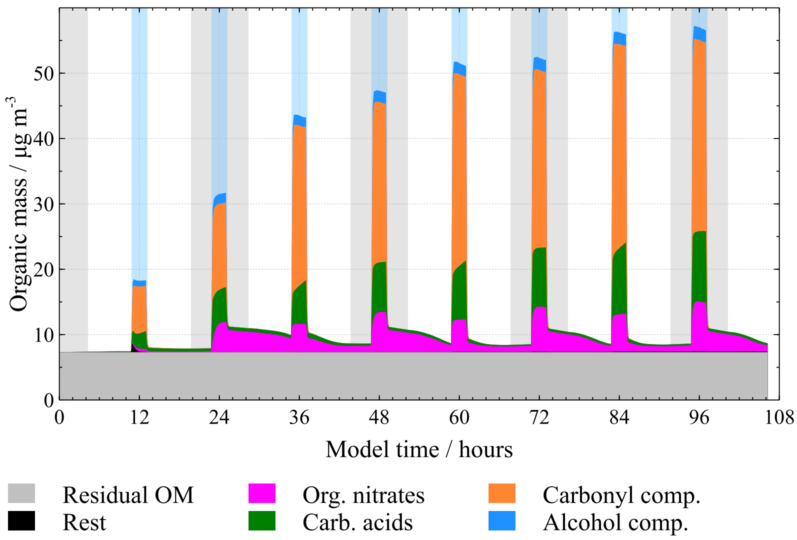

Figure 12 Particulate organic mass fraction distinguished by constituents in the base scenario ‘orig’ using the preliminary mechanism from Section 3.1 under urban summer conditions with 8 cloud passages. Cloud passaged are marked with a blue shade and night-time periods with a grey shade.

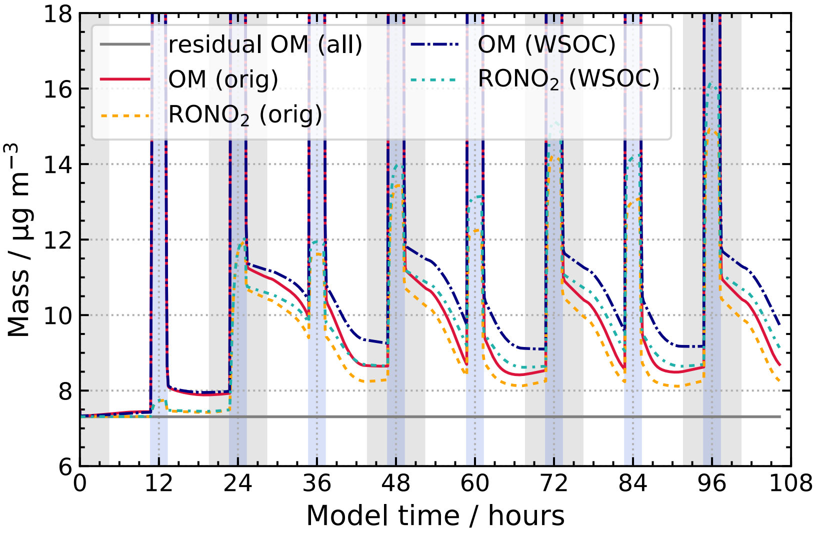

Figure 13 Processing of the organic mass fraction in the sensitivity runs investigating the influence of parameterisations for WSOC and HULIS chemistry on aqueous-phase chemistry and composition using the same conditions as in the base scenario with additional reactions given in Table 4. Cloud passaged are marked with a blue shade and night-time periods with a grey shade. Scenario names of the legend are explained in Appendix A.2.

Deleted: Column Break ... [3]

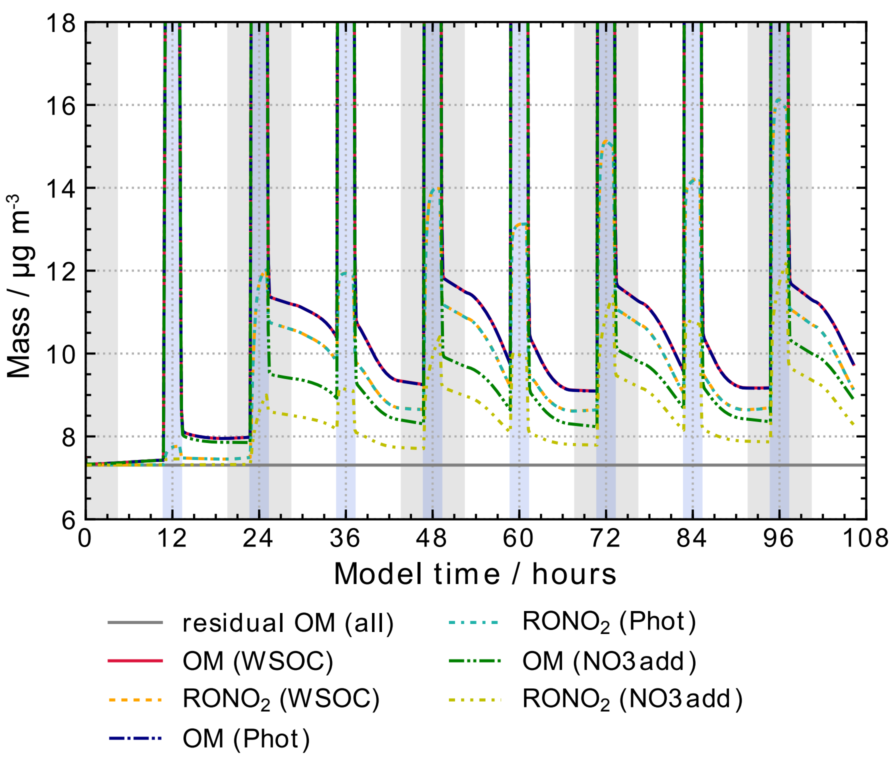

Figure 14 Processing of the organic mass fraction in the sensitivity runs investigating the influence of sink and source reactions for organic nitrates on aqueous-phase chemistry and composition. In addition to the scenario 'WSOC', rate constants of all NO_3 reactions with unsaturated organic compounds have been set to 10^7 M^{-1} s^{-1} in scenario 'NO3add' and photolysis reactions with $j = 3.6 \cdot 10^{-7}$ s^{-1} have been added in scenario 'Phot'. Cloud passaged are marked with a blue shade and night-time periods with a grey shade. Scenario names of the legend are explained in Appendix A.2.

Deleted: Column Break ... [4]

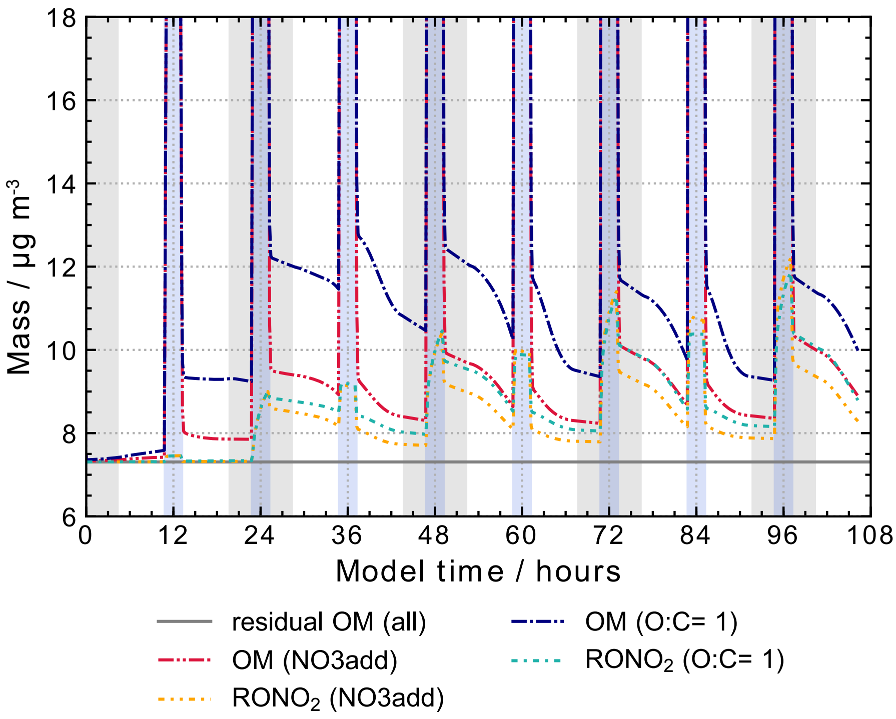

Figure 15 Processing of the organic mass fraction in the sensitivity runs investigating the influence of the phase transfer of oxygenated organic compounds on aqueous-phase chemistry and composition with the same conditions as in scenario 'NO3add', but with HLCs set to $1 \cdot 10^9$ M amt^{-1} for species with an O:C ratio greater or equal to one. Cloud passaged are marked with a blue shade and night-time periods with a grey shade. Scenario names of the legend are explained in Appendix A.2.

Deleted: Column Break ... [5]

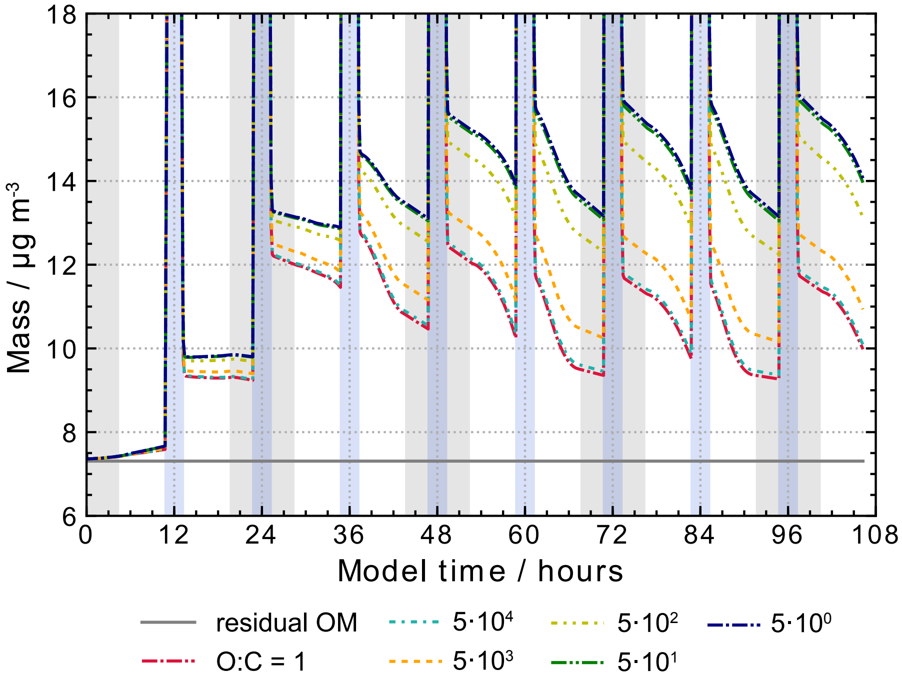

Figure 16 Processing of the organic mass fraction in the sensitivity runs investigating the influence of alkoxy radical chemistry on aqueous phase chemistry and composition, using the same conditions as in the scenario with O:C = 1, but varying the mono-molecular decay rate of alkoxy radicals as given in the figure legend (in s^{-1}). Cloud passaged are marked with a blue shade and night-time periods with a grey shade.

Deleted: . The terms in parentheses indicate

Deleted: order of magnitude of

Deleted: estimate for

Deleted: bimolecular reaction

Deleted: with dissolved oxygen

Deleted: $5\cdot10^{x}$ M^{-1}

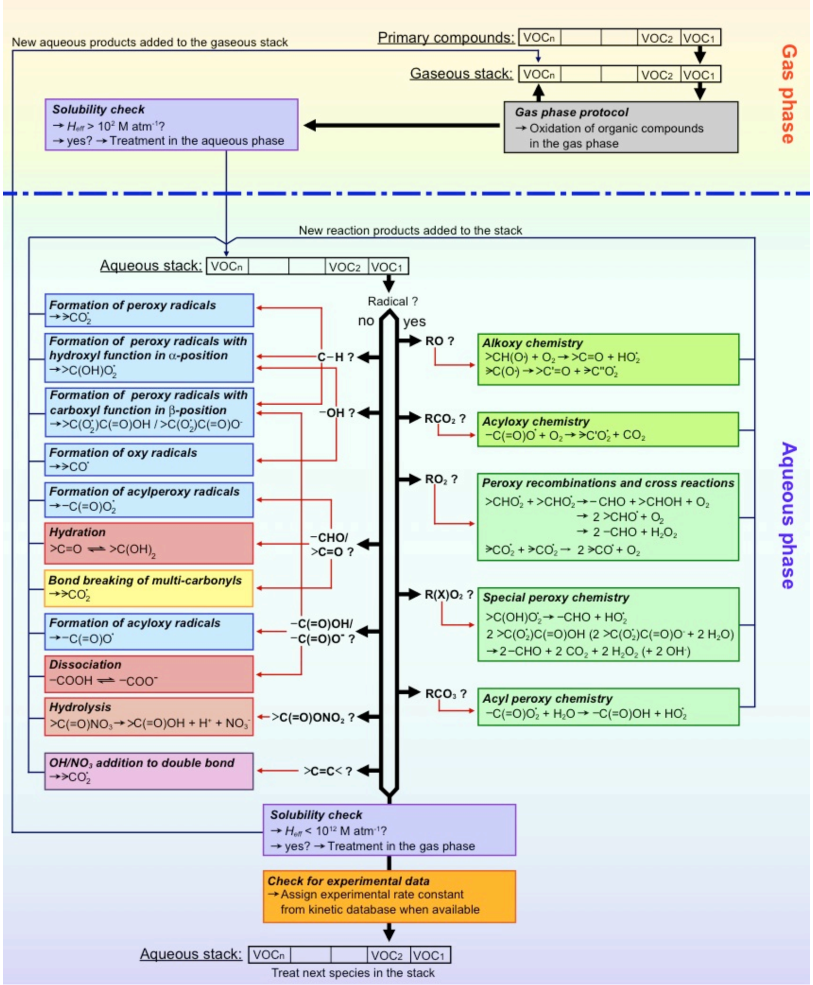

Figure 17 Workflow of the generator GECKO-A with the processes implemented in the aqueous phase protocol. Blue boxes represent H-abstraction reactions, the pink box represents radical addition to double bonds of unsaturated organic compounds, red boxes represent equilibria, the yellow box represents C–C bond breaking of poly-carbonyls, the light brown box represents the hydrolysis of carbonyl nitrates, and green boxes represent radical chemistry (different shades differentiate between oxy and peroxy radical chemistry).

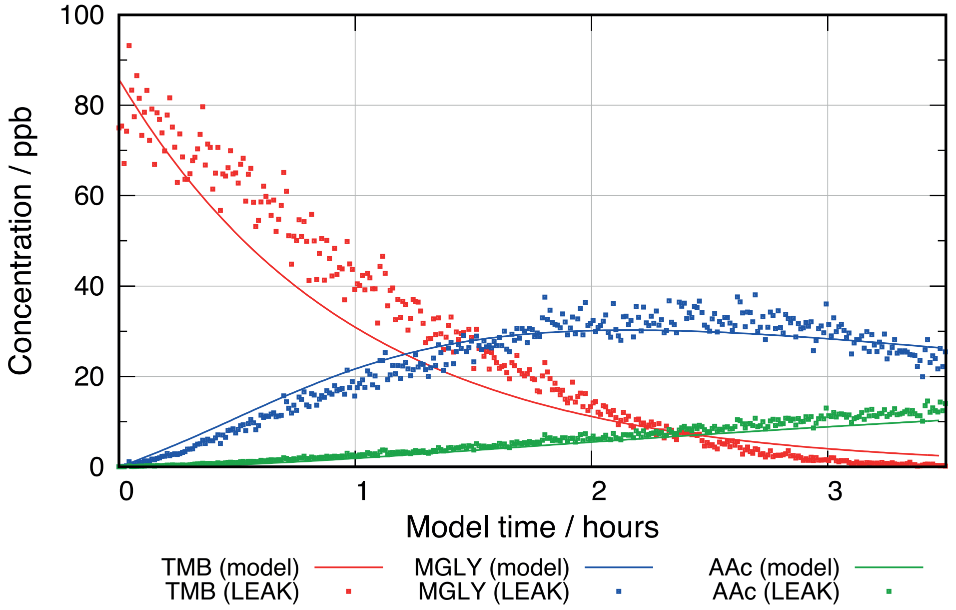

Figure 18 Comparison of measured (squares) and modelled (lines) gas-phase volume mixing ratios for 1,3,5-trimethyl benzene (TMB, red), methylglyoxal (MGLY, blue), and acetic acid (AAc, green) in the model scenario RXN$_{0.4}$.

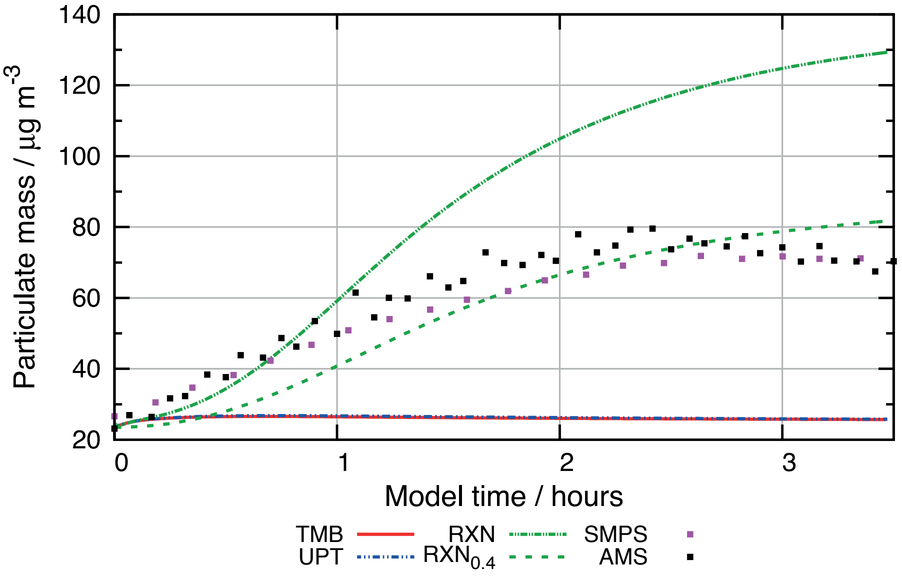

Deleted:

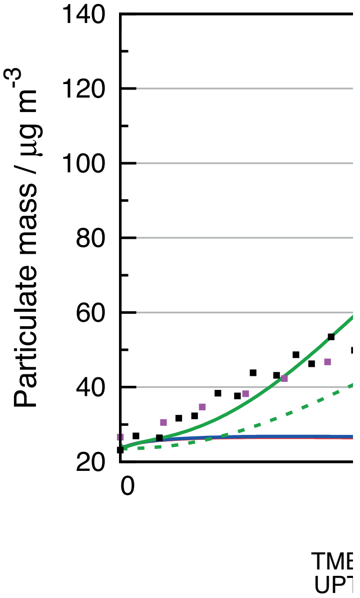

Figure 19 Comparison of dry particle mass in the various sensitivity studies against SMPS and AMS measurements.

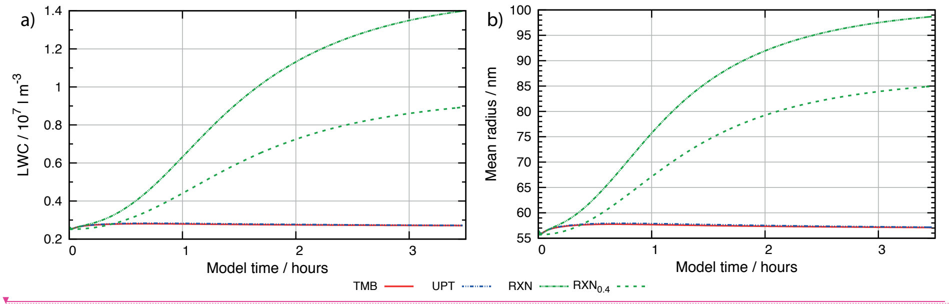

Figure 20 Profiles of the liquid water content (LWC, subplot a) and mean particle radius (b) for the various model runs.

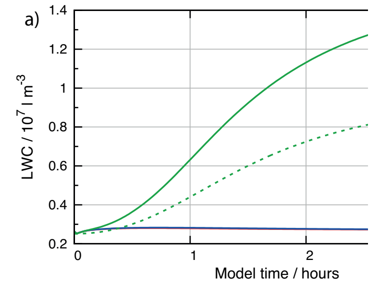

Deleted:

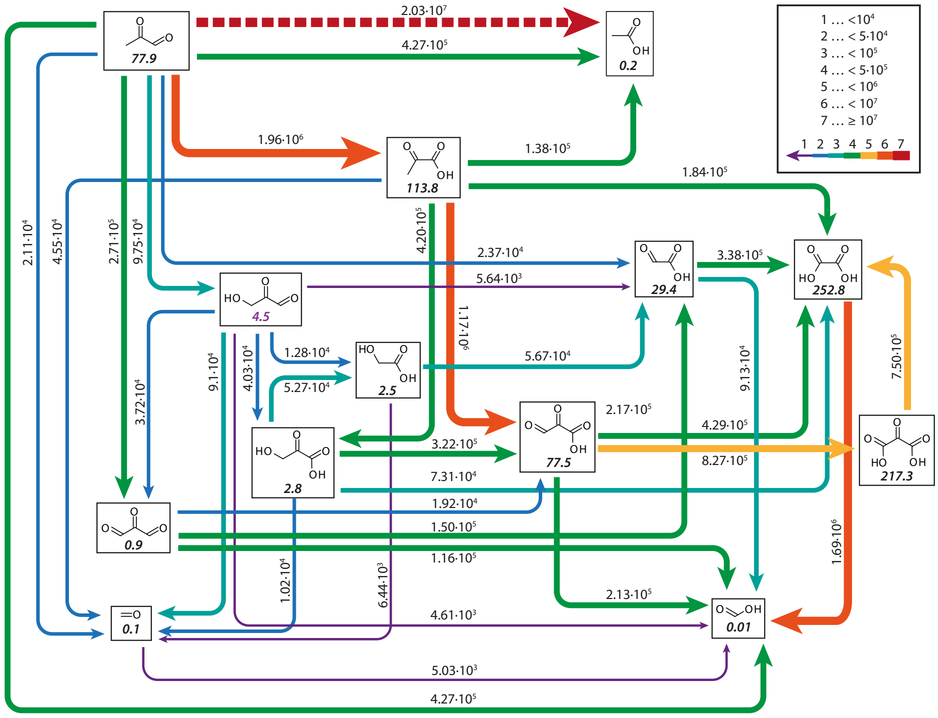

Figure 21 Chemical fluxes in the TMB oxidation experiments modelled in the scenario $RXN_{0.4}$ averaged over the whole 3.5 hours of the experiment. Numbers above the arrows correspond to fluxes in molecules cm^{-3} s^{-1}, bold numbers in the species boxes are concentrations in ng m^{-3} at the end of the experiment.

Deleted: mesitylene

S1 Kinetic data used to design the protocol for mechanism auto-generation

and show recommended values of reactions of hydroxyl and nitrate radicals, respectively, with organic compounds. The data have been used to validate existing prediction methods for reactions of OH/NO_3 radicals with organic compounds, improve or develop new prediction methods and are used directly in the new protocol for mechanism auto-generation as preferred values over theoretically predicted values.

Deleted: **self-generation used to design the protocol for mechanism self…**

Field Code Changed

Field Code Changed

Deleted: self

Table S1 Recommended kinetic data for OH reactions with organic compounds.

Reactant	SMILES	GECKO-A	k298 [$M^{-1}s^{-1}$]	A [$M^{-1}s^{-1}$]	E_a / R [K]	Reference/remarks	n = 467 (282 aliphatic/185 aromatic)
Alkanes							n = 12
Methane	C	CH4	$1.1\cdot10^{8}$			Buxton et al. (1988)	
Ethane	CC	CH3CH3	$1.4\cdot10^{9}$			Getoff (1989)[1]	
Propane	CCC	CH3CH2CH3	$2.3\cdot10^{9}$			Getoff (1989)[1]	
Butane	CCCC	CH3CH2CH2CH3	$2.9\cdot10^{9}$			Getoff (1989)[1]	
Pentane	CCCCC	CH3CH2CH2CH2CH3	$5.4\cdot10^{9}$			Rudakov et al. (1981)[2]	
Hexane	CCCCCC	CH3CH2CH2CH2CH2CH3	$6.6\cdot10^{9}$			Rudakov et al. (1981)[2]	
Heptane	CCCCCCC	CH3CH2CH2CH2CH2CH2CH3	$7.7\cdot10^{9}$			Rudakov et al. (1981)[2]	
Octane	CCCCCCCC	CH3CH2CH2CH2CH2CH2CH2CH3	$9.1\cdot10^{9}$			Rudakov et al. (1981)[2]	
Iso-butane	CC(C)C	CH3CH(CH3)CH3	$4.6\cdot10^{9}$			Rudakov et al. (1981)[2]	
2-methyl butane	CCC(C)C	CH3CH2CH(CH3)CH3	$5.2\cdot10^{9}$			Rudakov et al. (1981)[2]	
3-ethyl pentane	CCC(CC)CC	CH3CH2CH(CH2CH3)CH2CH3	$5.9\cdot10^{9}$			Rudakov et al. (1981)[2]	
2,2,4-trimethyl pentane	CC(C)CC(C)(C)C	CH3CH(CH3)CH2C(CH3)(CH3)CH3	$6.1\cdot10^{9}$			Rudakov et al. (1981)[2]	
Alkenes and alkynes							n = 7
Ethylene	C=C	CdH2=CdH2	$3.1\cdot10^{9}$			Thomas (1967) with updated k_{ref} from NIST database	
Propylene	CC=C	CH3CdH=CdH2	$7.0\cdot10^{9}$			Thomas (1967) with updated k_{ref} from NIST database	
1-butene	CCC=C	CH3CH2CdH=CdH2	$7.0\cdot10^{9}$			Thomas (1967) with updated k_{ref} from NIST database	
Butadien	C=CC=C	CdH2=CdHCdH=CdH2	$7.0\cdot10^{9}$			Thomas (1967) with updated k_{ref} from NIST database	
2,3-dimethyl butadiene	C=C(C)C(C)=C	CdH2=Cd(CH3)Cd(CH3)=CdH2	$3.1\cdot10^{10}$			Moise et al. (2005)	
Isobutylene	CC(=C)C	CH3Cd(CH3)=CdH2	$5.4\cdot10^{9}$			Thomas (1967) with updated k_{ref} from NIST database	
Acetylene	C#C		$4.7\cdot10^{9}$			Average of Anderson and Schulte-Frohlinde (1978)[1] values	
N- and S-substituted alkanes and alkenes							n = 16
Methyl nitrite	CN(=O)(=O)	CH3(NO2)	$1.85\cdot10^{8}$			Anbar et al. (1966a)	
Methylene nitrtite	C=N(=O)(=O)		$8.5\cdot10^{9}$			Asmus and Taub (1968)[2]	
Nitroso tert-butane	CC(C)(C)N=O	CH3C(NO)(CH3)CH3	$4.0\cdot10^{8}$			Bakalik and Thomas (1977)[2]	
Methanesulfinate	CS(=O)[O-]		$5.3\cdot10^{9}$			Flyunt et al. (2001)	
Methanesulfonate	CS(=O)(=O)[O-]		$1.3\cdot10^{9}$			Lind and Eriksen (1977)[2]	
Methylsulfate	COS(=O)(=O)[O-]		$5.0\cdot10^{7}$			Almgren et al. (1979)[2]	
Hydroxymethylsulfate (HMS$^-$)	OCS(=O)(=O)[O-]		$3.0\cdot10^{8}$			Barlow et al. (1997)[3]	
Methyldisulfonate monoanion	OS(=O)(=O)CS(=O)(=O)[O-]		$2.5\cdot10^{7}$			Lind and Eriksen (1977)[2]	
Methyldisulfonate dianion	[O-]S(=O)(=O)CS(=O)(=O)[O-]		$4.3\cdot10^{7}$			Lind and Eriksen (1977)[2]	
Ethyl sulfonate	CCS(=O)(=O)[O-]		$1.0\cdot10^{8}$			Balazs et al. (1968)[2]	
Ethyl sulphate	CCOS(=O)(=O)[O-]		$3.5\cdot10^{8}$			Almgren et al. (1979)[2]	
Butyl sulphate	CCCCOS(=O)(=O)[O-]		$1.0\cdot10^{9}$			Almgren et al. (1979)[2]	
Hexyl sulphate	CCCCCCOS(=O)(=O)[O-]		$2.5\cdot10^{9}$			Almgren et al. (1979)[2]	
Octyl sulphate	CCCCCCCCOS(=O)(=O)[O-]		$6.5\cdot10^{9}$			Almgren et al. (1979)[2]	
Decyl sulphate	CCCCCCCCCCOS(=O)(=O)[O-]		$8.2\cdot10^{9}$			Buxton et al. (1988)	
Methylene sulfonate	C=CS(=O)(=O)[O-]		$3.5\cdot10^{9}$			Behar et al. (1982)[2]	
Monoalcohols							n = 19
Methanol	CO	CH3OH	$1.0\cdot10^{9}$	$7.0\cdot10^{9}$	580	Average of George et al. (2003); Alam et al. (2003); and Janata (2002) with E/R value of Elliot and McCracken (1989)	
Ethanol	CCO	CH3CH2OH	$2.1\cdot10^{9}$	$1.02\cdot10^{11}$	1200	Ervens et al. (2003)	
Propanol	CCCO	CH3CH2CH2OH	$3.2\cdot10^{9}$	$5.6\cdot10^{10}$	1000	Ervens et al. (2003)	
Butanol	CCCCO	CH3CH2CH2CH2OH	$3.96\cdot10^{9}$	$1.0\cdot10^{11}$	1000	Hesper (2003)[4]	
Pentanol	CCCCCO	CH3CH2CH2CH2CH2OH	$5.0\cdot10^{9}$			Stemmler and von Gunten (2000)	
Hexanol	CCCCCCO	CH3CH2CH2CH2CH2CH2OH	$7.0\cdot10^{9}$			Scholes and Willson (1967)[2]	
Heptanol	CCCCCCCO	CH3CH2CH2CH2CH2CH2CH2OH	$7.4\cdot10^{9}$			Scholes and Willson (1967)[2]	
octanol	CCCCCCCCO	CH3CH2CH2CH2CH2CH2CH2CH2OH	$7.7\cdot10^{9}$			Scholes and Willson (1967)[2]	
Iso-propanol	CC(O)C	CH3CH(OH)CH3	$2.1\cdot10^{9}$	$6.1\cdot10^{10}$	962	Hesper (2003)[4]	
2-butanol	CCC(O)C	CH3CH2CH(OH)CH3	$3.5\cdot10^{9}$	$7.4\cdot10^{10}$	910	Hesper (2003)[4]	
3-pentanol	CCC(O)CC	CH3CH2CH(OH)CH2CH3	$2.1\cdot10^{9}$			Snook and Hamilton (1974)	
Iso-butanol	CC(C)CO	CH3CH(CH3)CH2(OH)	$3.3\cdot10^{9}$			Buxton et al. (1988)	
Tert-butanol	CC(C)(C)O	CH3C(OH)(CH3)CH3	$5.0\cdot10^{8}$	$3.3\cdot10^{10}$	1200	Ervens et al. (2003)	
2,2-dimethyl propanol	CC(C)(C)CO	CH3C(CH3)(CH3)CH2(OH)	$5.2\cdot10^{9}$			Walling (1975) with updated k_{ref} from NIST database	
1,1-dimethyl propanol	CCC(C)(C)O	CH3CH2C(OH)(CH3)CH3	$1.9\cdot10^{9}$			Anbar et al. (1966a)	
Isoamyl alcohol	CC(C)CCO	CH3CH(CH3)CH2CH2(OH)	$3.8\cdot10^{9}$			Buxton et al. (1988)	
Allyl alcohol	C=CCO	CH2(OH)CdH=CdH2	$5.9\cdot10^{9}$			Maruthamuthu (1980)[1, 2]	

Reactant	SMILES	GECKO-A	k298 [M^{-1}s^{-1}]	A [M^{-1}s^{-1}]	E_a / R [K]	Reference/remarks	n = 467 (282 aliphatic/185 aromatic)
3-hydroxy-1,4-pentadien	C=CC(O)C=C	CdH2=CdHCH(OH)CdH=CdH2	$1.0\cdot10^{10}$			Simic et al. (1973b)[2]	
2,4-hexadienol	CC=CC=CCO	CH3CdH=CdHCdH=CdHCH2(OH)	$9.8\cdot10^{9}$			Simic et al. (1973b)[2]	
Diols							n = 13
ethylene glycol	OCCO	CH2(OH)CH2(OH)	$1.7\cdot10^{9}$	$9.0\cdot10^{10}$	1191	Hoffmann et al. (2009)	
1,3-propanediol	OCCCO	CH2(OH)CH2CH2(OH)	$2.7\cdot10^{9}$	$2.5\cdot10^{11}$	1371	Hoffmann et al. (2009)	
1,4-butanediol	OCCCCO	CH2(OH)CH2CH2CH2(OH)	$3.5\cdot10^{9}$	$2.0\cdot10^{11}$	1203	Hoffmann et al. (2009)	
1,5-pentanediol	OCCCCCO	CH2(OH)CH2CH2CH2CH2(OH)	$4.4\cdot10^{9}$	$3.1\cdot10^{11}$	1275	Hoffmann et al. (2009)	
1,6-hexanediol	OCCCCCCO	CH2(OH)CH2CH2CH2CH2CH2(OH)	$4.7\cdot10^{9}$			Anbar et al. (1966a)	
1,2-propanediol	CC(O)CO	CH3CH(OH)CH2(OH)	$1.7\cdot10^{9}$	$1.9\cdot10^{11}$	1383	Hoffmann et al. (2009)	
1,2-butanediol	CCC(O)CO	CH3CH2CH(OH)CH2(OH)	$2.3\cdot10^{9}$	$5.2\cdot10^{11}$	1600	Hoffmann et al. (2009)	
1,3-butanediol	CC(O)CCO	CH3CH(OH)CH2CH2(OH)	$1.8\cdot10^{9}$			Average of Anbar et al. (1966a) and Adams et al. (1965a)[2]	
2,3-butanediol	CC(O)C(O)C	CH3CH(OH)CH(OH)CH3	$1.3\cdot10^{9}$			Adams et al. (1965a)[2]	
2,4-pentanediol	CC(O)CC(O)C	CH3CH(OH)CH2CH(OH)CH3	$2.3\cdot10^{9}$			Ulanski et al. (1994)[1]	
2,3-dimethyl- 2,3-butanediol	OC(C)(C)C(C)(C)O	CH3C(OH)(CH3)C(OH)(CH3)CH3	$5.5\cdot10^{8}$			Anbar et al. (1966a)	
2-butyne-1,4-diol	OCC#CCO		$7.2\cdot10^{9}$			Gilbert and Whitwood (1989)[8]; 78% H-Abs, 22% OH addition	
2,5-dimethyl-3-hexyne-2,5-diol	OC(C)(C)C#CC(C)(C)O		$3.3\cdot10^{9}$			Walling and El-Taliawi (1973a)[2]	
Aldehydes and gem-diols							n = 13
Formaldehyde	C=O	CH2O	$1.0\cdot10^{9}$			Witter and Neta (1973)[5]	
Hydrated formaldehyde	OCO	CH2(OH)(OH)	$1.0\cdot10^{9}$	$3.1\cdot10^{10}$	1022	Hart et al. (1964)[5]; Chin and Wine (1992)	
Acetaldehyde	CC=O	CH3CHO	$3.1\cdot10^{9}$			Average of overall rates of Schuchmann and von Sonntag (1988) and Monod et al. (2005); 2.7% H-Abs on methyl group	
Hydrated acetaldehyde	CC(O)O	CH3CH(OH)(OH)	$1.3\cdot10^{9}$			Schuchmann and von Sonntag (1988); 7,7% H-Abs on methyl group	
Propionaldehyde	CCC=O	CH3CH2CHO	$2.8\cdot10^{9}$	$2.6\cdot10^{11}$	1300	Overall rate constant of Hesper (2003)	
Butyraldehyde	CCCC=O	CH3CH2CH2CHO	$3.9\cdot10^{9}$	$8.1\cdot10^{10}$	900	Overall rate constant of Hesper (2003)	
Valeraldehyde	CCCCC=O	CH3CH2CH2CH2CHO	$3.9\cdot10^{9}$			Overall rate constant of Monod et al. (2005)	
Isobutyraldehyde	CC(C)C=O	CH3CH(CH3)CHO	$2.9\cdot10^{9}$	$3.0\cdot10^{10}$	700	Gligorovski and Herrmann (2004)	
Acrolein	C=CC=O	CHOCdH=CdH2	$7.0\cdot10^{9}$			Lilie and Henglein (1970)[1,2]	
Crotonaldehyde	CC=CC=O	CH3CdH=CdHCHO	$5.8\cdot10^{9}$			Lilie and Henglein (1970)[2]	
Methacrolein	C=C(C)C=O	CH3Cd(CHO)=CdH2	$9.4\cdot10^{9}$	$5.6\cdot10^{11}$	1200	Schöne et al. (2014)	
Glyoxal	O=CC=O	CHOCHO	$6.6\cdot10^{7}$			Draganic and Marcovic, unpublished data[1,2]	
Hydrated glyoxal	OC(O)C(O)O	CH(OH)(OH)CH(OH)(OH)	$1.1\cdot10^{9}$	$1.8\cdot10^{11}$	1516	Buxton et al (1997)	
Ketones							n = 12
Acetone	CC(=O)C	CH3COCH3	$1.7\cdot10^{8}$	$6.9\cdot10^{10}$	1788	Average of measurements within MOST[6]	
Methyl ethyl ketone	CC(=O)CC	CH3CH2COCH3	$1.3\cdot10^{9}$	$1.7\cdot10^{11}$	1451	Average of measurement within the MOST project[6]; 10% $CH_2COCH_2CH_3$ and 90% $CH_3COCHCH_3$[6]	
Methyl propyl ketone	CC(=O)CCC	CH3CH2CH2COCH3	$1.9\cdot10^{9}$			Adams et al. (1965b)[2]	
Diethyl ketone	CCC(=O)CC	CH3CH2COCH2CH3	$1.4\cdot10^{9}$			Adams et al. (1965b)[2]	
Methyl vinyl ketone	CC(=O)C=C	CH3COCdH=CdH2	$7.3\cdot10^{9}$	$9.0\cdot10^{11}$	1443	Schöne et al. (2014)	
Methyl iso-butyl ketone	CC(C)CC(=O)C	CH3COCH2CH(CH3)CH3	$3.4\cdot10^{9}$			Average of measurements within the MOST project[6]; 30% $CH_3C(CH_3)CH_2C(=O)CH_3$ and 70% $CH_3CH(CH_3)CHC(=O)CH_3$[6]	
Methylglyoxal	CC(=O)C=O	CH3COCHO	$8.6\cdot10^{8}$	$8.0\cdot10^{10}$	1350	Average of Monod et al. (2005); Park et al. (2003)[7] ; Stefan and Bolton (1999); and TROPOS measurements	
Hydrated methylglyoxal	CC(=O)C(O)O	CH3COCH(OH)(OH)	$7.9\cdot10^{8}$	$1.6\cdot10^{11}$	1589	Average of measurement within the MOST project[6]	
Diacetyl	CC(=O)C(=O)C	CH3COCOCH3	$2.8\cdot10^{8}$	$4.3\cdot10^{12}$	2880	Gligorovski and Herrmann (2004)	
Acetylacetone	CC(=O)CC(=O)C	CH3COCH2COCH3	$9.9\cdot10^{9}$			Broszkiewicz et al. (1982)[2]	
Acetylacetone, conjugate base	CC([O-])=CC(=O)C		$7.4\cdot10^{9}$			Broszkiewicz et al. (1982)[2]	
Acetonyl acetone	CC(=O)CCC(=O)C	CH3COCH2CH2COCH3	$7.6\cdot10^{8}$	$1.1\cdot10^{11}$	1485	Gligorovski and Herrmann (2004)	
Monocarboxylic acids (undissociated and dissociated)							n = 28
Formic acid	C(=O)O	CHO(OH)	$1.3\cdot10^{8}$	$3.7\cdot10^{9}$	1000	Buxton et al. (1988) with rounded E/R values of Chin and Wine (1992)/ Adams et al. (1965a)	
Formate	C(=O)[O-]	CHO(Om)	$3.2\cdot10^{9}$	$9.2\cdot10^{10}$	1000	Buxton et al. (1988); Elliot and Simsons (1984)	
Acetic acid	CC(=O)O	CH3CO(OH)	$1.7\cdot10^{7}$	$1.5\cdot10^{9}$	1330	Chin and Wine (1992)	
Acetate	CC(=O)[O-]	CH3CO(Om)	$7.3\cdot10^{7}$	$2.8\cdot10^{10}$	1770	Chin and Wine (1992)	
Propionic acid	CCC(=O)O	CH3CH2CO(OH)	$3.2\cdot10^{8}$	$7.6\cdot10^{11}$	2300	Ervens et al. (2003)	
Propionate	CCC(=O)[O-]	CH3CH2CO(Om)	$7.2\cdot10^{8}$	$3.2\cdot10^{11}$	1800	Ervens et al. (2003)	
Butyric acid	CCCC(=O)O	CH3CH2CH2CO(OH)	$2.2\cdot10^{9}$			Scholes and Willson (1967)[2]	
Butyrate	CCCC(=O)[O-]	CH3CH2CH2CO(Om)	$2.0\cdot10^{9}$			Anbar et al. (1966a)	
N-valerate	CCCCC(=O)[O-]	CH3CH2CH2CH2CO(Om)	$2.9\cdot10^{9}$			Anbar et al. (1966a)	

Reactant	SMILES	GECKO-A	k298 [$M^{-1}s^{-1}$]	A [$M^{-1}s^{-1}$]	E_a / R [K]	Reference/remarks n = 467 (282 aliphatic/185 aromatic)
Hexanate	CCCCCC(=O)[O-]	CH3CH2CH2CH2CH2CO(Om)	$4.0\cdot10^{9}$			Anbar et al. (1966a)
Iso-butyrate	CC(C)C(=O)[O-]	CH3CH(CH3) CO(Om)	$1.3\cdot10^{9}$			Anbar et al. (1966a)
Iso-valeric acid	CC(C)CC(=O)O	CH3CH(CH3)CH2CO(OH)	$1.4\cdot10^{9}$			Merz and Waters (1949)[1]
Iso-valerate	CC(C)CC(=O)[O-]	CH3CH(CH3)CH2CO(Om)	$2.4\cdot10^{9}$			Anbar et al. (1966a)
2-methyl-butyrate	CCC(C)C(=O)[O-]	CH3CH2CH(CH3) CO(Om)	$2.2\cdot10^{9}$			Anbar et al. (1966a)
Pivalic acid	CC(C)(C)C(=O)O	CH3C(CH3)(CH3)CO(OH)	$6.5\cdot10^{8}$			Nauser and Bühler (1994)
Pivalate	CC(C)(C)C(=O)[O-]	CH3C(CH3)(CH3)CO(Om)	$1.1\cdot10^{9}$			Average of Nauser and Bühler (1994) and Anbar et al. (1966a)
2,2-dimethyl butyrate	CC(C)(C)CC(=O)[O-]	CH3C(CH3)(CH3)CH2CO(Om)	$1.7\cdot10^{8}$			Anbar et al. (1966a)
Acrylic acid	C=CC(=O)O	CO(OH)CdH=CdH2	$5.1\cdot10^{9}$	$9.4\cdot10^{10}$	842	Schöne et al. (2014)
Acrylate	C=CC(=O)[O-]	CO(Om)CdH=CdH2	$5.9\cdot10^{9}$	$1.8\cdot10^{10}$	360	Schöne et al. (2014)
Crotonic acid	CC=CC(=O)O	CH3CdH=CdHCO(OH)	$2.9\cdot10^{9}$			Walling and El-Taliawi (1973b)[2]
Crotonate	CC=CC(=O)[O-]	CH3CdH=CdHCO(Om)	$5.0\cdot10^{9}$			Lilie and Henglein (1970); Maruthamuthu and Dhandavel (1980)[2]
Methacrylic acid	C=C(C)C(=O)O	CH3Cd(CO(OH))=CdH2	$1.1\cdot10^{10}$	$1.0\cdot10^{12}$	1320	Schöne et al. (2014)
Methacrylate	C=C(C)C(=O)[O-]	CH3Cd(CO(Om))=CdH2	$1.1\cdot10^{10}$	$8.0\cdot10^{12}$	1924	Schöne et al. (2014)
Methylcrotonic acid	CC(C)=CC(=O)O	CH3Cd(CH3)=CdHCO(OH)	$9.0\cdot10^{9}$			Kumar and Rao (1991)[1]
Methylcrotonate	CC(C)=CC(=O)[O-]	CH3Cd(CH3)=CdHCO(Om)	$5.9\cdot10^{9}$			Average of different measurements of Kumar and Rao (1991)[1]
Sorbic acid	CC=CC=CC(=O)O	CH3CdH=CdHCdH=CdHCO(OH)	$9.8\cdot10^{9}$			Simic et al. (1973b)[1]
Linoleate	CCCCCC=CCC=CCCCCCCCC(=O)O	CH3CH2CH2CH2CH2CdH=CdHCH2CdH=CdH... ...CH2CH2CH2CH2CH2CH2CH2CO(OH)	$1.0\cdot10^{10}$			Al-Sheikhly et al. (2004)
Linolenic acid	CCC=CCC=CCC=CCCCCCCCC(=O)[O-]	CH3CH3CdH=CdHCH2CdH=CdHCH2CdH=CdH... ...CH2CH2CH2CH2CH2CH2CH2CO(Om)	$9.9\cdot10^{9}$			Patterson and Hasegawa (1978)[2]; value scaled by a factor of 1.35 based on the ratio of the values of Patterson and Hasegawa (1978) and Al-Sheikhly et al. (2004) for linoleate
Dicarboxylic acids (undissociated and dissociated)						n = 26
Oxalic acid	OC(=O)C(=O)O	CO(OH)CO(OH)	$1.4\cdot10^{6}$			Getoff et al. (1971)
Oxalate monoanion	OC(=O)C(=O)[O-]	CO(Om)CO(OH)	$1.9\cdot10^{8}$	$2.5\cdot10^{12}$	2800	Ervens et al. (2003)
Oxalate dianion	[O-]C(=O)C(=O)[O-]	CO(Om)CO(Om)	$1.6\cdot10^{8}$	$4.6\cdot10^{14}$	4300	Ervens et al. (2003)
Malonic acid	OC(=O)CC(=O)O	CO(OH)CH2CO(OH)	$2.0\cdot10^{7}$			Buxton et al. (1988)
Malonate monoanion	OC(=O)CC(=O)[O-]	CO(Om)CH2CO(OH)	$6.0\cdot10^{7}$	$3.2\cdot10^{9}$	1300	Ervens et al. (2003)
Malonate dianion	[O-]C(=O)CC(=O)[O-]	CO(Om)CH2CO(Om)	$2.7\cdot10^{8}$			Average of Logan (1989) and Adams et al. (1965a)
Succinic acid	OC(=O)CCC(=O)O	CO(OH)CH2CH2CO(OH)	$1.1\cdot10^{8}$	$8.1\cdot10^{9}$	1278	Ervens et al. (2003)
Succinate monoanion	OC(=O)CCC(=O)[O-]	CO(Om)CH2CH2CO(OH)	$2.6\cdot10^{8}$	$1.2\cdot10^{11}$	1808	TROPOS measurements
Succinate dianion	[O-]C(=O)CCC(=O)[O-]	CO(Om)CH2CH2CO(Om)	$5.0\cdot10^{8}$	$5.4\cdot10^{10}$	1413	Ervens et al. (2003)
Glutaric acid	OC(=O)CCCC(=O)O	CO(OH)CH2CH2CH2CO(OH)	$5.1\cdot10^{8}$	$2.5\cdot10^{10}$	1164	TROPOS measurements
Glutarate dianion	[O-]C(=O)CCCC(=O)[O-]	CO(Om)CH2CH2CH2CO(Om)	$8.2\cdot10^{8}$	$2.5\cdot10^{12}$	2355	TROPOS measurements
Adipic acid	OC(=O)CCCCC(=O)O	CO(OH)CH2CH2CH2CH2CO(OH)	$1.6\cdot10^{9}$	$3.2\cdot10^{11}$	1479	TROPOS measurements
Adipate monoanion	OC(=O)CCCCC(=O)[O-]	CO(Om)CH2CH2CH2CH2CO(OH)	$1.4\cdot10^{9}$	$9.7\cdot10^{12}$	2641	TROPOS measurements
Adipate dianion	[O-]C(=O)CCCCC(=O)[O-]	CO(Om)CH2CH2CH2CH2CO(Om)	$1.4\cdot10^{9}$	$1.2\cdot10^{12}$	1985	TROPOS measurements
Pimelic acid	OC(=O)CCCCCC(=O)O	CO(OH)CH2CH2CH2CH2CH2CO(OH)	$3.4\cdot10^{9}$	$3.0\cdot10^{11}$	1335	TROPOS measurements
Pimelate monoanion	OC(=O)CCCCCC(=O)[O-]	CO(Om)CH2CH2CH2CH2CH2CO(OH)	$1.8\cdot10^{9}$	$9.7\cdot10^{12}$	2641	TROPOS measurements
Pimelate dianion	[O-]C(=O)CCCCCC(=O)[O-]	CO(Om)CH2CH2CH2CH2CH2CO(Om)	$2.1\cdot10^{9}$	$1.7\cdot10^{13}$	2514	TROPOS measurements
Suberic acid	OC(=O)CCCCCCC(=O)O	CO(OH)CH2CH2CH2CH2CH2CH2CO(OH)	$5.0\cdot10^{9}$			Hesper (2003)
Suberate dianion	[O-]C(=O)CCCCCCC(=O)[O-]	CO(Om)CH2CH2CH2CH2CH2CH2CO(Om)	$5.8\cdot10^{9}$			Hesper (2003)
Azelaic acid	OC(=O)CCCCCCCC(=O)O	CO(OH)CH2CH2CH2CH2CH2CH2CH2CO(OH)	$5.4\cdot10^{9}$			Scholes and Willson (1967)[2]
Sebacic acid	OC(=O)CCCCCCCCC(=O)O	CO(OH)CH2CH2CH2CH2CH2CH2CH2CH2CO(OH)	$6.4\cdot10^{9}$			Scholes and Willson (1967)[2]
Fumaric acid	OC(=O)/C=C/C(=O)O	CO(OH)CdH=CdHCO(OH)	$6.0\cdot10^{9}$			Cabelli and Bielski (1985)[2]
Maleic acid	OC(=O)/C=C\C(=O)O	CO(OH)CdH=CdHCO(OH)	$6.0\cdot10^{9}$			Cabelli and Bielski (1985)[2]
3-hexene-1,6-dioate dianion	[O-]C(=O)CC=CCC(=O)[O-]		$5.9\cdot10^{9}$	$6.3\cdot10^{11}$	1395	Elliot and McCracken (1989)[1]
Crocetin	OC(=O)C(C)=CC=CC(C)=CC=C... ...C=C(C)C=CC=C(C)C(=O)O	CH3Cd(CO(OH))=CdHCdH=CdHCd(CH3)=CdH... ...CdH=CdHCdH=Cd(CH3)CdH=CdH... ...CdH=Cd(CH3)CO(OH)	$2.3\cdot10^{10}$			Bors et al. (1982)[2]
Acetylenedicarboxylate dianion	[O-]C(=O)C#CC(=O)[O-]		$2.6\cdot10^{9}$			Simhon et al. (1988)[1]
Organic peroxides						n = 3
Methyl hydrogen peroxide	COO	CH3(OOH)	$3.2\cdot10^{8}$			Average of Graedel and Weschler (1981) and Monod et al. (2007)
Ethyl hydrogen peroxide	CCOO	CH3CH2(OOH)	$5.8\cdot10^{8}$			Monod et al. (2007)
Tert-butyl hydrogen peroxide	CC(C)(C)OO	CH3C(OOH)(CH3)CH3	$8.0\cdot10^{7}$			Phulkar et al. (1990)[1]
Ethers						n = 17
Dimethyl ether	COC	CH3-O-CH3	$1.0\cdot10^{9}$			Eibenberger (1980)[2]

Reactant	SMILES	GECKO-A	k298 [$M^{-1}s^{-1}$]	A [$M^{-1}s^{-1}$]	E_a / R [K]	Reference/remarks n = 467 (282 aliphatic/185 aromatic)
Diethyl ether	CCOCC	CH3CH2-O-CH2CH3	$3.6 \cdot 10^{9}$			Buxton et al. (1988)
Methylal	COCOC	CH3-O-CH2-O-CH3	$1.2 \cdot 10^{9}$			Eibenberger (1980)[2]
Diethoxy methane	CCOCOCC	CH3CH2-O-CH2-O-CH2CH3	$1.6 \cdot 10^{9}$			Anbar et al. (1966a)
Ethylene glycol dimethyl ether	COCCOC	CH3-O-CH2CH2-O-CH3	$1.6 \cdot 10^{9}$			Anbar et al. (1966a)
Ethylene glycol diethyl ether	CCOCCOCC	CH3CH2-O-CH2CH2-O-CH2CH3	$2.3 \cdot 10^{9}$			Anbar et al. (1966a)
Diethylene glycol diethyl ether	CCOCCOCCOCC	CH3CH2-O-CH2CH2-O-CH2CH2-O-CH2CH3	$3.2 \cdot 10^{9}$			Anbar et al. (1966a)
Hydroxybutyl vinyl ether	OCCCCOC=C	CH2(OH)CH2CH2CH2-O-CdH=CdH2	$1.9 \cdot 10^{9}$			Moise et al. (2005)
di(ethylene glycol) divinyl ether	C=COCCOCCOC=C	CdH2=CdH-O-CH2CH2-O-CH2CH2-O-CdH=CdH2	$2.3 \cdot 10^{10}$			Moise et al. (2005)
tri(ethylene glycol) divinyl ether	C=COCCOCCOCCOC=C	CdH2=CdH-O-CH2CH2-O-CH2CH2-O-CH2... ...CH2-O-CdH=CdH2	$1.54 \cdot 10^{10}$	$2.3 \cdot 10^{13}$	2179	Gligorovski et al. (2009)
Dimethyl acetal	COC(C)OC	CH3-O-CH(CH3)-O-CH3	$2.2 \cdot 10^{9}$			Eibenberger (1980)[2]
Methyl tert-butyl ether	CC(C)(C)OC	CH3-O-C(CH3)(CH3)CH3	$2.1 \cdot 10^{9}$			Average of Eibenberger (1980)[2,5], Chang and Young (2000)[5], Adams et al. (1965a)[5], Mitani et al. (2002)[5], and Garoma and Gurol (2005)
Ethyl tert-butyl ether	CC(C)(C)OCC	CH3CH2-O-C(CH3)(CH3)CH3	$1.5 \cdot 10^{9}$	$1.2 \cdot 10^{10}$	580	Monod et al. (2005)
Di(iso-propyl) ether	CC(C)OC(C)C	CH3CH(CH3)-O-CH(CH3)CH3	$2.49 \cdot 10^{9}$			Mezyk et al. (2001)[3]
Di(tert-butyl) ether	CC(C)(C)OC(C)(C)C	CH3C(CH3)(CH3)-O-C(CH3)(CH3)CH3	$1.81 \cdot 10^{9}$			Mezyk et al. (2001)[3]
2-methyl-2-methoxy-butane	CCC(C)(C)OC	CH3CH2C(CH3)(CH3)-O-CH3	$2.37 \cdot 10^{9}$			Mezyk et al. (2001)[3]
2,4-dimethoxy pentane	COC(C)CC(C)OC	CH3-O-CH(CH3)CH2CH(CH3)-O-CH3	$3.7 \cdot 10^{9}$			Janik et al. (2000)[3]
Esters						n = 26
Ethyl formate	CCOC=O	CH3CH2-O-CHO	$7.9 \cdot 10^{8}$	$9.3 \cdot 10^{11}$	2106	Average of measurements within the MOST project[6]; 42.3% C_2H_5COCO and 57.7% $CH_3C(H)OCHO$[6]
Butyl formate	CCCCOC=O	CH3CH2CH2CH2-O-CHO	$2.8 \cdot 10^{9}$			Stemmler and von Gunten (2000)
Tert-butyl formate	CC(C)(C)OC=O	CH3C(CH3)(CH3)-O-CHO	$7.0 \cdot 10^{8}$			Acero et al. (2001)[5]
Methyl acetate	CC(=O)OC	CH3CO-O-CH3	$1.5 \cdot 10^{8}$			Average of Anbar et al. (1966a) and Adams et al. (1965a)[2]
Methyl propionate	CCC(=O)OC	CH3CH2CO-O-CH3	$4.5 \cdot 10^{8}$			Adams et al. (1965a)[2]
Ethyl acetate	CC(=O)OCC	CH3CH2-O-COCH3	$4.0 \cdot 10^{8}$			Adams et al. (1965a)[2]
Ethyl propionate	CCC(=O)OCC	CH3CH2CO-O-CH2CH3	$5.2 \cdot 10^{8}$			Average of Adams et al. (1965a)[8] and Bíró and Wojnárovits (1992)[1]
Propyl acetate	CCCOC(=O)C	CH3CH2CH2-O-COCH3	$1.4 \cdot 10^{9}$			Adams et al. (1965a)[2]
Methyl butyrate	CCCC(=O)OC	CH3CH2CH2CO-O-CH3	$1.7 \cdot 10^{9}$			Adams et al. (1965a)[1]
Butyl acetate	CCCCOC(=O)C	CH3CH2CH2CH2-O-COCH3	$1.8 \cdot 10^{9}$	$5.33 \cdot 10^{10}$	1000	Monod et al. (2005)
Ethyl butyrate	CCCC(=O)OCC	CH3CH2CH2CO-O-CH2CH3	$1.6 \cdot 10^{9}$			Adams et al. (1965a)[2]
Butyl propionate	CCCCOC(=O)CC	CH3CH2CH2CH2-O-COCH2CH3	$1.6 \cdot 10^{9}$			Adams et al. (1965a)[2]
Iso-propyl acetate	CC(C)OC(=O)C	CH3CO-O-CH(CH3)CH3	$5.3 \cdot 10^{8}$			Average of Hardison et al. (2002)[5,7] and Adams et al. (1965a)[1]
Methyl acrylate	C=CC(=O)OC	CH3-O-COCdH=CdH2	$5.3 \cdot 10^{9}$			Kumar et al. (1988)[1]
Ethyl acrylate	C=CC(=O)OCC	CH3CH2-O-COCdH=CdH2	$5.8 \cdot 10^{9}$			Kumar et al. (1988)[1]
Butyl acrylate	C=CC(=O)OCCCC	CH3CH2CH2CH2-O-COCdH=CdH2	$5.5 \cdot 10^{9}$			Kumar et al. (1988)[1]
Methyl methacrylate	C=C(C)C(=O)OC	CH3-O-COCd(CH3)=CdH2	$1.2 \cdot 10^{10}$			Average of Maruthamuthu (1980)[2] and Kumar et al. (1988)[1]
Butyl methacrylate	C=C(C)C(=O)OCCCC	CH3CH2CH2CH2-O-COCd(CH3)=CdH2	$1.2 \cdot 10^{10}$			Kumar et al. (1988)[1]
Dimethyl malonate	COC(=O)CC(=O)OC	CH3-O-COCH2CO-O-CH3	$2.7 \cdot 10^{8}$			George et al. (2003)
Diethyl malonate	CCOC(=O)CC(=O)OCC	CH3CH2-O-COCH2CO-O-CH2CH3	$6.5 \cdot 10^{8}$			Adams et al. (1965a)[1]
Dimethyl succinate	COC(=O)CCC(=O)OC	CH3-O-COCH2CH2CO-O-CH3	$5.3 \cdot 10^{8}$			George et al. (2003)
Diethyl succinate	CCOC(=O)CCC(=O)OCC	CH3CH2-O-COCH2CH2CO-O-CH2CH3	$7.8 \cdot 10^{8}$			Adams et al. (1965a)[2]
Diethyl meleate	CCOC(=O)/C=C\C(=O)OCC	CH3CH2-O-CHO	$5.9 \cdot 10^{9}$			Bíró and Wojnárovits (1996)
Diethyl fumarate	CCOC(=O)/C=C/C(=O)OCC	CH3CH2-O-CHO	$5.9 \cdot 10^{9}$			Bíró and Wojnárovits (1996)
Dimethyl carbonate	COC(=O)OC	CH3-O-CO-O-CH3	$5.1 \cdot 10^{7}$			George et al. (2003)
Diethyl carbonate	CCOC(=O)OCC	CH3CH2-O-CO-O-CH2CH3	$7.9 \cdot 10^{8}$			George et al. (2003)
Aliphatic polyfunctional compounds						n = 43
2-hydroxy-2-methyl propanal	CC(C)(O)C=O	CH3C(OH)(CH3)CHO	$3.0 \cdot 10^{9}$			Acero et al. (2001)[5]
2,3-dihydroxy-2-propenal	OC=C(O)C=O	CHOCd(OH)=CdH(OH)	$9.9 \cdot 10^{9}$			Horii et al. (1986)[2]
2,3-dihydroxy-2-propenal, conjugate base	[O-]C=C(O)C=O		$1.6 \cdot 10^{10}$			Horii et al. (1986)[2]
Hydroxy acetone	CC(=O)CO	CH3COCH2(OH)	$1.2 \cdot 10^{9}$	$4.0 \cdot 10^{10}$	1082	Gligorovski (2005)[7]
Acetoin	CC(O)C(=O)C	CH3CH(OH)COCH3	$2.9 \cdot 10^{9}$	$2.9 \cdot 10^{11}$	1323	Hesper (2003)
Glycolic acid	OCC(=O)O	CH2(OH)CO(OH)	$6.0 \cdot 10^{8}$			Buxton et al. (1988)
Glycolate	OCC(=O)[O-]	CH2(OH)CO(Om)	$1.2 \cdot 10^{9}$			Ross et al. (1998)
Hydrated glyoxylic acid	OC(O)C(=O)O	CH(OH)(OH)CO(OH)	$3.6 \cdot 10^{8}$	$8.1 \cdot 10^{9}$	1000	Ervens et al. (2003)
Hydrated glyoxylate	OC(O)C(=O)[O-]	CH(OH)(OH)CO(Om)	$2.6 \cdot 10^{9}$	$6.0 \cdot 10^{15}$	4330	Ervens et al. (2003)
Lactic acid	CC(O)C(=O)O	CH3CH(OH)CO(OH)	$5.24 \cdot 10^{8}$	$2.28 \cdot 10^{10}$	1120	Martin et al. (2009)
Lactate	CC(O)C(=O)[O-]	CH3CH(OH)CO(Om)	$7.77 \cdot 10^{8}$	$6.07 \cdot 10^{10}$	1295	Martin et al. (2009)
2-hydroxy-butyric acid	CCC(O)C(=O)O	CH3CH2CH(OH)CO(OH)	$1.3 \cdot 10^{9}$			Merz and Waters (1949)[1]

Reactant	SMILES	GECKO-A	k298 $[M^{-1}s^{-1}]$	A $[M^{-1}s^{-1}]$	E_a / R [K]	Reference/remarks	n = 467 (282 aliphatic/185 aromatic)
Pyruvic acid	CC(=O)C(=O)O	CH3COCO(OH)	$1.2\cdot10^{8}$	$1.0\cdot10^{12}$	2800	Ervens et al. (2003)	
Pyruvate	CC(=O)C(=O)[O-]	CH3COCO(Om)	$7.0\cdot10^{8}$	$1.3\cdot10^{12}$	2300	Ervens et al. (2003)	
Glucuronic acid	OCC(O)C(O)C(O)C(O)C(=O)O	CH2(OH)CH(OH)CH(OH)CH(OH)CH(OH)CO(OH)	$2.2\cdot10^{9}$			Average of different measurements of Phillips and Worthington (1970)[1]	
Tartronic acid	OC(=O)C(O)C(=O)O	CO(OH)CH(OH)CO(OH)	$3.4\cdot10^{8}$	$1.5\cdot10^{10}$	1112	TROPOS measurements	
Tartronate monoanion	OC(=O)C(O)C(=O)[O-]	CO(Om)CH(OH)CO(OH)	$3.6\cdot10^{8}$			Schuchmann et al. (1995)	
Tartronate dianion	[O-]C(=O)C(O)C(=O)[O-]	CO(Om)CH(OH)CO(Om)	$4.4\cdot10^{8}$			Schuchmann et al. (1995)	
Mesoxalic acid	OC(=O)C(=O)C(=O)O	CO(OH)COCO(OH)	$1.8\cdot10^{8}$	$3.8\cdot10^{10}$	1588	Gligorovski et al. (2009)	
Mesoxalate monoanion	OC(=O)C(=O)C(=O)[O-]	CO(Om)COCO(OH)	$5.7\cdot10^{7}$			Schuchmann et al. (1991)	
Mesoxalate dianion	[O-]C(=O)C(=O)C(=O)[O-]	CO(Om)COCO(Om)	$1.0\cdot10^{8}$			Schuchmann et al. (1991)	
Malic acid	OC(=O)CC(O)C(=O)O	CO(OH)CH2CH(OH)CO(OH)	$3.6\cdot10^{8}$	$7.9\cdot10^{10}$	1575	Gligorovski et al. (2009)	
Maleate monoanion	OC(=O)CC(O)C(=O)[O-]	CO(Om)CH2CH(OH)CO(OH)	$9.7\cdot10^{8}$	$9.7\cdot10^{8}$	1701	Gligorovski et al. (2009)	
Maleate dianion	[O-]C(=O)CC(O)C(=O)[O-]	CO(Om)CH2CH(OH)CO(Om)	$8.5\cdot10^{8}$	$1.2\cdot10^{11}$	1449	Gligorovski et al. (2009)	
Tartaric acid	OC(=O)C(O)C(O)C(=O)O	CO(OH)CH(OH)CH(OH)CO(OH)	$1.1\cdot10^{9}$			Average of Scholes and Willson (1967)[2] and Moore et al. (1979)[1]	
Tartrate dianion	[O-]C(=O)C(O)C(O)C(=O)[O-]	CO(Om)CH(OH)CH(OH)CO(Om)	$1.0\cdot10^{8}$			Average of Kraljic (1967)[1,2] and Logan (1989)	
Citric acid	OC(=O)CC(O)(C(=O)O)CC(=O)O	CO(OH)CH2C(OH)(CO(OH))CH2CO(OH)	$5.0\cdot10^{7}$			Adams et al. (1965a)[2]	
Citrate	[O-]C(=O)C... ...C(O)(C(=O)[O-])CC(=O)[O-]	CO(Om)CH2C(OH)(CO(Om))CH2CO(Om)	$1.5\cdot10^{8}$			Zepp et al. (1992)[1]	
Ethylene glycol methyl ether	COCCO	CH3-O-CH2CH2(OH)	$1.3\cdot10^{9}$			Anbar et al. (1966a)	
Ethylene glycol ethyl ether	CCOCCO	CH3CH2-O-CH2CH2(OH)	$1.7\cdot10^{9}$			Anbar et al. (1966a)	
Ethylene glycol butyl ether	CCCCOCCO	CH3CH2CH2CH2-O-CH2CH2(OH)	$5.1\cdot10^{9}$			Stemmler and von Gunten (2000)	
Diethylene glycol	OCCOCCO	CH2(OH)CH2-O-CH2CH2(OH)	$2.1\cdot10^{9}$			Anbar et al. (1966a)	
di(ethylene glycol) vinyl ether	C=COCCOCCO	CH2(OH)CH2-O-CH2CH2-O-CdH=CdH2	$4.2\cdot10^{10}$			Moise et al. (2005)	
Methoxyacetate	COCC(=O)[O-]	CH3-O-CH2CO(Om)	$6.1\cdot10^{8}$			Anbar et al. (1966a)	
2-methyl-2-methoxy propanol	OCC(C)(C)OC	CH3-O-C(CH3)(CH3)CH2(OH)	$8.02\cdot10^{8}$			Mezyk et al. (2009)	
2-methyl-2-methoxy propanal	O=CC(C)(C)OC	CH3-O-C(CH3)(CH3)CHO	$3.5\cdot10^{9}$			Mezyk et al. (2009)	
2-methyl-2-methoxy propanoic acid	O=C(O)C(C)(C)OC	CH3-O-C(CH3)(CH3)CO(OH)	$7.73\cdot10^{8}$			Mezyk et al. (2009)	
2-hydroxyethyl acetate	OCCOC(=O)C	CH3CO-O-CH2CH2(OH)	$9.1\cdot10^{8}$			Matsushige et al. (1975)[2]	
Butyl hydroxyacetate	CCCCOC(=O)CO	CH3CH2CH2CH2-O-COCH2(OH)	$3.2\cdot10^{9}$			Stemmler and von Gunten (2000)	
1-hydroxy ethyl butyrate	CCCC(=O)OCCO	CH3CH2CH2CO-O-CH2CH2(OH)	$2.1\cdot10^{9}$			Stemmler and von Gunten (2000)	
Methyl methoxy acetate	COCC(=O)OC	CH3-O-CH2CO-O-CH3	$1.8\cdot10^{9}$			Massaut et al. (1988)[2]	
Monoethyl adipate	CCOC(=O)CCCCC(=O)O	CH3CH2-O-COCH2CH2CH2CH2CO(OH)	$3.0\cdot10^{9}$			Haag and Yao (1992)[1]	
1-hydroxy ethyl acrylate	C=CC(=O)OCCO	CH2(OH)CH2-O-COCdH=CdH2	$5.8\cdot10^{9}$			Sáfrány and Wojnárovits (1993)[1]	
Polyols and Sugars							n = 14
Glycerol	OCC(O)CO	CH2(OH)CH(OH)CH2(OH)	$1.9\cdot10^{9}$	$2.8\cdot10^{11}$	1479	Hoffmann et al. (2009)	
Erythritol	OCC(O)C(O)CO	CH2(OH)CH(OH)CH(OH)CH2(OH)	$1.9\cdot10^{9}$	$1.3\cdot10^{12}$	1948	Hoffmann et al. (2009)	
Arabitol	OCC(O)C(O)C(O)CO	CH2(OH)CH(OH)CH(OH)CH(OH)CH2(OH)	$1.6\cdot10^{9}$	$2.5\cdot10^{10}$	794	Hoffmann et al. (2009)	
Mannitol	OCC(O)C(O)C(O)C(O)CO	CH2(OH)CH(OH)CH(OH)CH(OH)CH(OH)CH2(OH)	$1.6\cdot10^{9}$	$1.8\cdot10^{10}$	734	Hoffmann et al. (2009)	
Pentaerythritol	OCC(CO)(CO)CO	CH2(OH)C(CH2(OH))(CH2(OH))CH2(OH)	$3.3\cdot10^{9}$			Anbar et al. (1966a)	
Arabinose	OCC(O)C(O)C(O)C=O	CH2(OH)CH(OH)CH(OH)CH(OH)CHO	$1.8\cdot10^{9}$			Edwards et al. (1979)[2]	
D-fructose	OCC1C(O)C(O)C(CO)(O)O1/ OCC(O)C(O)C(O)C(=O)CO	C1H(OH)CH(OH)... ...C(OH)(CH2(OH))-O-C1HCH2(OH)/ CH2(OH)CH(OH)CH(OH)CH(OH)COCH2(OH	$1.6\cdot10^{9}$			Moore et al. (1979)[2]	
Ribose	O1C(O)C(O)C(O)C1CO/ OCC(O)C(O)C(O)C=O	C1H(OH)CH(OH)CH(OH)-O-C1HCH2(OH)/ CH2(OH)CH(OH)CH(OH)CH(OH)CHO	$1.5\cdot10^{9}$			Buxton et al. (1988)	
2-Deoxy-D-ribose	O1C(O)CC(O)C1CO/ OCC(O)C(O)CC=O	C1H(OH)CH2CH(OH)-O-C1HCH2(OH)/ CH2(OH)CH(OH)CH(OH)CH2CHO	$2.5\cdot10^{9}$			Baker et al. (1982)[2]	
Inositol	C1(O)C(O)C(O)C(O)C(O)C1(O)	C1H(OH)CH(OH)CH(OH)CH(OH)CH(OH)C1H(OH)	$1.7\cdot10^{9}$			Buxton et al. (1988)	
Levoglucosan	OC1C(O)C(O)C2OC1OC2	C1H2-O-CH(-O-C12H)CH(OH)CH(OH)C2H(OH)	$2.2\cdot10^{9}$	$1.0\cdot10^{11}$	1100	TROPOS measurements	
Glucose	O1C(O)C(O)C(O)C(O)C1CO/ OCC(O)C(O)C(O)C(O)C=O	C1H(OH)CH(OH)CH(OH)CH(OH)-O-C1HCH2(OH)/ CH2(OH)CH(OH)CH(OH)CH(OH)CH(OH)CHO	$1.5\cdot10^{9}$			Buxton et al. (1988)	
Galactose	O1C(O)C(O)C(O)C(O)C1CO/ OCC(O)C(O)C(O)C(O)C=O	C1H(OH)CH(OH)CH(OH)CH(OH)-O-C1HCH2(OH)/ CH2(OH)CH(OH)CH(OH)CH(OH)CH(OH)CHO	$2.0\cdot10^{9}$			Bucknall et al. (1978)[2]	
2-Deoxy-D-glucose	O1C(O)CC(O)C(O)C1CO/ OCC(O)C(O)C(O)CC=O	C1H(OH)CH(OH)CH2CH(OH)-O-C1HCH2(OH)/ CH2(OH)CH(OH)CH(OH)CH(OH)CH2CHO	$2.8\cdot10^{9}$			Baker et al. (1982)[2]	

Formatted Table

Reactant	SMILES	GECKO-A	k298 [$M^{-1}s^{-1}$]	A [$M^{-1}s^{-1}$]	E_a / R [K]	Reference/remarks	n = 467 (282 aliphatic/185 aromatic)
Cyclic aliphatic compounds							n = 27
Cyclobutane carboxylate	C1CCC1C(=O)[O-]	C1H2CH2CH2C1HCO(Om)	$3.0\cdot10^{9}$			Anbar et al. (1966a)	
Cyclopentane	C1CCCC1	C1H2CH2CH2CH2C1H2	$3.7\cdot10^{9}$			Buxton et al. (1988)	
Methyl cyclopentane	C1CCCC1C	C1H2CH2CH2CH2C1HCH3	$7.0\cdot10^{9}$			Rudakov et al. (1981)[2]	
Cyclopentane carboxylate	C1CCCC1C(=O)[O-]	C1H2CH2CH2CH2C1HCO(Om)	$4.2\cdot10^{9}$			Anbar et al. (1966a)	
Cyclohexane	C1CCCCC1	C1H2CH2CH2CH2CH2C1H2	$6.1\cdot10^{9}$			Rudakov et al. (1981)[2]	
Methyl cyclohexane	C1CCCCC1C	C1H2CH2CH2CH2CH2C1HCH3	$7.1\cdot10^{9}$			Rudakov et al. (1981)[2]	
Cyclohexane carboxylate	C1CCCCC1C(=O)[O-]	C1H2CH2CH2CH2CH2C1HCO(Om)	$5.5\cdot10^{9}$			Anbar et al. (1966a)	
Cycloheptane	C1CCCCCC1	C1H2CH2CH2CH2CH2CH2C1H2	$7.7\cdot10^{9}$			Rudakov et al. (1981)[2]	
Cyclopentene	C1CCC=C1	C1H2CH2CdH=CdHC1H2	$7.0\cdot10^{9}$			Soylemez and Schuler (1974)[2]	
Cyclohexene	C1CCCC=C1	C1H2CH2CdH=CdHCH2C1H2	$8.8\cdot10^{9}$			Michael and Hart (1970)[2]	
1,3-cyclohexadiene	C1CC=CC=C1	C1H2CdH=CdHCdH=CdHC1H2	$9.9\cdot10^{9}$			Michael and Hart (1970)[2]	
1,4-cyclohexadiene	C1C=CCC=C1	C1H2CdH=CdHCH2CdH=Cd1H	$7.7\cdot10^{9}$			Michael and Hart (1970)[2]	
cycloheptatriene	C1C=CC=CC=C1	C1H2CdH=CdHCdH=CdHCdH=Cd1H	$1.0\cdot10^{10}$			Schöneshöfer (1971)[2]	
Quinine	O=C1C=CC(=O)C=C1		$1.2\cdot10^{9}$			Adams and Michael (1967)[2]	
Oxirane	C1OC1	C1H2-O-C1H2	$6.8\cdot10^{7}$			Anbar et al. (1966a)	
Methyl oxirane	C1OC1C	C1H2-O-C1HCH3	$2.5\cdot10^{8}$			Anbar et al. (1966a)	
Ethyl oxirane	C1OC1CC	C1H2-O-C1HCH2CH3	$7.8\cdot10^{8}$			Anbar et al. (1966a)	
Glycidol	C1OC1CO	C1H2-O-C1HCH2(OH)	$4.7\cdot10^{8}$			Anbar et al. (1966a)	
Tetrahydrofuran	C1COCC1	C1H2CH2-O-CH2C1H2	$3.8\cdot10^{9}$			George et al. (2003)	
Dioxolane	C1OCOC1	C1H2-O-CH2-O-C1H2	$4.0\cdot10^{9}$			Eibenberger (1980)[2]	
2-methyl dioxolane	C1OC(C)OC1	C1H2-O-CH(CH3)-O-C1H2	$3.5\cdot10^{9}$			Eibenberger (1980)[2]	
2,2-dimethyl dioxolane	C1OC(C)(C)OC1	C1H2-O-C(CH3)(CH3)-O-C1H2	$2.1\cdot10^{9}$			Eibenberger (1980)[2]	
Tetrahydropyran	C1CCCCO1	C1H2CH2CH2-O-CH2C1H2	$1.5\cdot10^{9}$			Walling et al. (1974)	
1,3-dioxane	C1COCOC1	C1H2CH2-O-CH2-O-C1H2	$4.0\cdot10^{9}$			Eibenberger (1980)[2]	
1,4-dioxane	C1OCCOC1	C1H2-O-CH2CH2-O-C1H2	$2.8\cdot10^{9}$			Buxton et al. (1988)	
Trioxane	C1OCOCO1	C1H2-O-CH2-O-CH2-O1-	$1.0\cdot10^{9}$			Average of Anbar et al. (1966a) and Eibenberger (1980)[2]	
paraldehyde	CC1OC(C)OC(C)O1	-O1-CH(CH3)-O-CH(CH3)-O-C1HCH3	$1.6\cdot10^{9}$			Average of Anbar et al. (1966a) and Eibenberger (1980)[2]	
Terpenes and terpene oxidation products							n = 4
R(+)-limonene	CC1=CCC(CC1)C(C)=C	C1H2CH2Cd(CH3)=CdHCH2C1HCd(CH3)=CdH2	$2.9\cdot10^{9}$			TROPOS measurements	
α-pinene	CC2(C)C1CC=C(C)C2C1	C12HCH2CH(C1(CH3)CH3)CH2CdH=Cd2CH3	$1.4\cdot10^{9}$			Raabe (1996)	
Cis-verbenol	CC2(C)C1CC2C(O)C=C1C	C12HCH2CH(C1(CH3)CH3)CH(OH)CdH=Cd2CH3	$6.8\cdot10^{9}$			Buxton et al. (2000)[3]	
(-)-Myrtenal	CC2(C)C1CC=C(C=O)C2C1	CH3C1(CH3)CH(CH2C12H)CH2CdH=Cd2CHO	$1.7\cdot10^{9}$	$1.0\cdot10^{13}$	2600	TROPOS measurements	
Unclassified aliphatic compounds							n = 2
Disuccinyl peroxide	[O-]C(=O)CCC(=O)OO… …C(=O)CCC(=O)[O-]		$8.0\cdot10^{7}$			Graedel and Weschler (1981)[1]	
Diacetyl peroxide	CC(=O)OOC(=O)C		$6.0\cdot10^{7}$			Graedel and Weschler (1981)[1]	
Furans (including ascorbic acid)							n = 21
Furan	c1cocc1	-O1-CdH=CdHCdH=Cd1H	$3.9\cdot10^{9}$			Lilie (1971)[2]	
2-methylfuran	c1coc(C)c1	-O1-CdH=CdHCdH=Cd1CH3	$1.9\cdot10^{10}$			Vysotskaya et al. (1983)[2]	
Furfuryl alcohol	c1coc(CO)c1	-O1-CdH=CdHCdH=Cd1CH2(OH)	$1.5\cdot10^{10}$			Saveleva et al. (1973); Vysotskaya et al. (1983)[2]	
Furfural	c1coc(C=O)c1	-O1-CdH=CdHCdH=Cd1CHO	$6.3\cdot10^{9}$			Average of Vysotskaya et al. (1983)[2] and D'Angelantonio et al. (1999)	
5-methyl furfural	c1c(C)oc(C=O)c1	CH3Cd1=CdHCdH=Cd(-O1-)CHO	$7.2\cdot10^{9}$			Vysotskaya et al. (1983)[2]	
5-hydroxymethylfurfural	c1c(CO)oc(C=O)c1	CH2(OH)Cd1=CdHCdH=Cd(-O1-)CHO	$5.8\cdot10^{9}$			Vysotskaya et al. (1983)[2]	
5-nitro furfural	c1c(N(=O)=O)oc(C=O)c1	-O1-Cd(NO2)=CdHCdH=Cd1CHO	$5.5\cdot10^{9}$			Greenstock and Dunlop (1973); Chapman et al. (1973)[2]	
Acetylfuran	c1coc(C(=O)C)c1	-O1-CdH=CdHCdH=Cd1COCH3	$4.5\cdot10^{9}$			Vysotskaya et al. (1983)[1]	
Furan-2-carboxylate	c1coc(C(=O)[O-])c1	C1HcHcH-O-c1CO(Om)	$1.2\cdot10^{10}$			Saveleva et al. (1973)[2]	
5-carboxylate furfural	c1c(C=O)oc(C(=O)[O-])c1	CO(Om)c1-O-c(CHO)cHc1H	$3.8\cdot10^{9}$			Vysotskaya et al. (1983)[2]	
2-carboxylate-5-nitro-furan	c1c(N(=O)=O)oc(C(=O)[O-])c1	C1HcHc(NO2)-O-c1CO(Om)	$5.3\cdot10^{9}$			Greenstock and Dunlop (1973); Chapman et al. (1973)[2]	
Tetronate	O=C1C=C([O-])CO1		$9.2\cdot10^{9}$			Schuler et al. (1974)[1]	
α-Hydroxytetronate	O=C1C([O-])=C(O)CO1		$4.7\cdot10^{9}$			Schuler et al. (1974)[1]	
Ascorbic acid	O1C(=O)C(O)=C(O)C1C(O)CO	-O1-COCd(OH)=Cd(OH)C1HCH(OH)CH2(OH)	$1.0\cdot10^{10}$			Buxton et al. (1988)	
Ascorbate	O1C(=O)C([O-])=C(O)C1C(O)CO		$3.4\cdot10^{9}$			Average of Schuler (1977)[2], Redpath and Willson (1973)[2], Schöneshöfer (1972)[2], Bonifačić et al. (1994)[1], Bonifačić et al. (1994)[1], and Ye and Schuler (1990)[1]	
L-ascorbate-2-sulfate	O1C(=O)... ...C(OS(=O)(=O)[O-])=C(O)C1C(O)CO		$4.2\cdot10^{9}$			Cabelli et al. (1983)[2]	

Formatted Table

Reactant	SMILES	GECKO-A	k298 [M^{-1}s^{-1}]	A [M^{-1}s^{-1}]	E_a / R [K]	Reference/remarks	n = 467 (282 aliphatic/185 aromatic)
1-O-methyl ascorbic acid	O1C(=O)C(OC)=C(O)C1C(O)CO	-O1-COCd(-O-CH3)=Cd(OH)C1HCH(OH)CH2(OH)	$2.5\cdot10^{9}$			Cabelli et al. (1983)[2]	
2-O-methyl ascorbic acid	O1C(=O)C(O)=C(OC)C1C(O)CO	CH3-O-Cd1=Cd(OH)CO-O-C1HCH(OH)CH2(OH)	$2.7\cdot10^{9}$			Cabelli et al. (1983)[2]	
3-O-methyl ascorbic acid	O1C(=O)C(O)=C(O)C1C(OC)CO	-O1-COCd(OH)=Cd(OH)C1HCH(CH2(OH))-O-CH3	$3.0\cdot10^{9}$			Cabelli et al. (1983)[2]	
3-O-methyl ascorbate	O1C(=O)C([O-])=C(O)C1C(OC)CO		$4.8\cdot10^{9}$			Cabelli et al. (1983)[2]	
O-dimethyl ascorbic acid	O1C(=O)C(OC)=C(OC)C1C(O)CO	CH3-O-Cd1=Cd(-O-CH3)CO-O-C1HCH(OH)CH2(OH)	$4.2\cdot10^{9}$			Cabelli et al. (1983)[2]	
Benzols							n = 17
Benzol	c1ccccc1	c1HcHcHcHcHc1H	$7.8\cdot10^{9}$			Buxton et al. (1988)	
Toluol	c1ccccc1C	c1HcHcHcHcHc1CH3	$8.1\cdot10^{9}$			Albarran et al. (2003); branching rations o:m:p = 0.84:0.41:1 (i<0.2)	
Ethyl benzol	c1ccccc1CC	c1HcHcHcHcHc1CH2CH3	$7.5\cdot10^{9}$			Sehested and Holcman (1979)[2]	
o-xylene	Cc1ccccc1C	CH3c1cHcHcHcHc1CH3	$6.7\cdot10^{9}$			Sehested et al. (1975)[2]	
m-xylene	c1c(C)cccc1C	c1Hc(CH3)cHcHcHc1CH3	$7.5\cdot10^{9}$			Sehested et al. (1975)[2]	
p-xylene	c1cc(C)ccc1C	c1HcHc(CH3)cHcHc1CH3	$7.0\cdot10^{9}$			Sehested et al. (1975)[2]	
1,2,3-trimethyl benzol	Cc1cccc(C)c1C	CH3c1cHcHcHc(CH3)c1CH3	$7.0\cdot10^{9}$			Sehested et al. (1975)[2]	
1,2,4-trimethyl benzol	Cc1ccc(C)cc1C	CH3c1cHcHc(CH3)cHc1CH3	$6.2\cdot10^{9}$			Sehested et al. (1975)[2]	
Mesitylene	c1c(C)cc(C)cc1C	c1Hc(CH3)cHc(CH3)cHc1CH3	$6.4\cdot10^{9}$			Sehested et al. (1975)[2]	
1,2,3,4-tetramethyl benzol	Cc1ccc(C)c(C)c1C	CH3c1c(CH3)cHcHc(CH3)c1CH3	$7.2\cdot10^{9}$			Sehested et al. (1975)[1]	
1,2,3,5-tetramethyl benzol	Cc1cc(C)cc(C)c1C	CH3c1cHc(CH3)cHc(CH3)c1CH3	$7.1\cdot10^{9}$			Sehested et al. (1975)[1]	
1,2,4,5-tetramethyl benzol	Cc1cc(C)c(C)cc1C	CH3c1cHc(CH3)c(CH3)cHc1CH3	$7.0\cdot10^{9}$			Sehested et al. (1975)[1]	
Pentamethyl benzol	Cc1cc(C)c(C)c(C)c1C	CH3c1c(CH3)cHc(CH3)c(CH3)c1CH3	$7.5\cdot10^{9}$			Sehested et al. (1975)[2]	
Hexamethyl benzol	Cc1c(C)c(C)c(C)c(C)c1C	CH3c1c(CH3)c(CH3)c(CH3)c(CH3)c1CH3	$7.2\cdot10^{9}$			Sehested et al. (1975)[2]	
Cumene	c1ccccc1C(C)C	c1HcHcHcHcHc1CH(CH3)CH3	$7.5\cdot10^{9}$			Sehested and Holcman (1979)[2]	
Styrene	c1ccccc1C=C	c1HcHcHcHcHc1CdH=CdH2	$6.0\cdot10^{9}$			Brede et al. (1977)[2]	
α-methylstyrene	c1ccccc1C(C)=C	c1HcHcHcHcHc1Cd(CH3)=CdH2	$9.7\cdot10^{9}$			Brede et al. (1977)[2]	
N/S-substituted benzols							n = 7
Nitrosobenzol	c1ccccc1N=O	c1HcHcHc(NO)cHc1H	$1.8\cdot10^{10}$			Asmus et al. (1966)[2]	
Nitrobenzol	c1ccccc1N(=O)=O	c1HcHcHc(NO2)cHc1H	$3.9\cdot10^{9}$			Buxton et al. (1988)	
Benzolsulfonic acid	c1ccccc1S(=O)(=O)O		$1.6\cdot10^{9}$			Merz and Waters (1949)[2]	
Phenyl sulfonate	c1ccccc1S(=O)(=O)[O-]		$3.9\cdot10^{9}$			Average of Anbar et al. (1966b) and Neta and Dorfman (1968)[2]	
2,4-dinitro-toluol	c1c(N(=O)=O)cc(N(=O)=O)cc1C	c1Hc(NO2)cHc(NO2)cHc1CH3	$9.0\cdot10^{8}$			Makarov et al. (2008)	
2,4,6-trinitro-toluol	c1c(N(=O)=O)cc(N(=O)=O)cc1 ... ...(N(=O)=O)	c1Hc(NO2)cHc(NO2)cHc1(NO2)	$7.4\cdot10^{8}$			Makarov et al. (2008)	
1-methyl-3-nitro phenyl sulfonate	c1(C)cc(N(=O)=O)ccc1S(=O)(=O)[O-]		$1.6\cdot10^{9}$			Basinski and Lerke (1972)[2]	
Phenols and other aromatic alcohols							n = 25
Phenol	c1ccccc1O	c1HcHcHc(OH)cHc1H	$1.01\cdot10^{10}$			Chen and Schuler (1993); partial *k* @ o/m/p position: $2.37\cdot10^{9}/1.3\cdot10^{8}/3.56\cdot10^{9}$	
Phenolate	c1ccccc1[O-]		$9.6\cdot10^{9}$			Bonin et al. (2007)	
Catechol	c1cccc(O)c1O	c1HcHc(OH)c(OH)cHc1H	$1.1\cdot10^{10}$			Saveleva et al. (1972)[2]	
Resorcinol	c1ccc(O)cc1O	c1HcHc(OH)cHc(OH)c1H	$1.2\cdot10^{10}$			Saveleva et al. (1972)[2]	
Hydroquinone	c1cc(O)ccc1O	c1Hc(OH)cHcHc(OH)c1H	$1.2\cdot10^{10}$			Average of Adams et al. (1965a)[2]; *Al-Suhybani and Hughes,* 1986[2]; and *Heckel et al.,* 1966[2]	
phloroglucinol	c1c(O)cc(O)cc1O	c1Hc(OH)cHc(OH)cHc1(OH)	$1.0\cdot10^{10}$			*Wang et al.,* 1994[1]	
p-tert-butyl phenol	c1cc(O)ccc1C(C)(C)C	c1HcHc(OH)cHcHc1C(CH3)(CH3)CH3	$1.9\cdot10^{10}$			Saveleva et al. (1972)	
4-tert-butyl catechol	c1c(O)c(O)ccc1C(C)(C)C	c1HcHc(OH)c(OH)cHc1C(CH3)(CH3)CH3	$7.6\cdot10^{9}$			*Richter,* 1979[2]	
4-(1,2-dihydroxyethyl)-catechol	c1c(O)c(O)ccc1C(O)CO	c1HcHc(OH)c(OH)cHc1CH(OH)CH2(OH)	$1.6\cdot10^{10}$			Average of different measurements of *Ek et al.,* 1989 (8)	
Benzyl alcohol	c1ccccc1CO	c1HcHcHcHcHc1CH2(OH)	$8.4\cdot10^{9}$			Neta and Dorfman (1968)[2]	
Phenetyl alcohol	c1ccccc1CCO	c1HcHcHcHcHc1CH2CH2(OH)	$6.4\cdot10^{9}$			Buxton et al. (1988)	
o-cresol	c1(O)ccccc1C	c1HcHcHcHc(OH)c1CH3	$1.1\cdot10^{10}$			Saveleva et al. (1972)[1]	
p-cresol	c1cc(O)ccc1C	c1HcHc(OH)cHcHc1CH3	$1.2\cdot10^{10}$			Fisher and Hamill (1973)	
2,3-dihydroxy toluol	c1(O)c(O)cccc1C	c1HcHcHc(OH)c(OH)c1CH3	$1.6\cdot10^{10}$			Gohn and Getoff (1977)[1]	
3,4-dihydroxy toluol	c1c(O)c(O)ccc1C	c1HcHc(OH)c(OH)cHc1CH3	$1.6\cdot10^{10}$			Gohn and Getoff (1977)[2]	
1-phenylethanol	c1ccccc1C(O)C	c1HcHcHcHcHc1CH(OH)CH3	$1.1\cdot10^{10}$			Snook and Hamilton (1974)	
1-(p-ethylphenyl)ethanol	c1cc(CC)ccc1C(O)C	c1HcHc(CH(OH)CH3)cHcHc1CH2CH3	$1.3\cdot10^{10}$			Snook and Hamilton (1974)	
1-phenyl propanol	c1ccccc1C(O)CC	c1HcHcHcHcHc1CH(OH)CH2CH3	$1.0\cdot10^{10}$			Snook and Hamilton (1974)	
1-phenyl-2-methyl propanol	c1ccccc1C(O)C(C)C	c1HcHcHcHcHc1CH(OH)CH(CH3)CH3	$9.5\cdot10^{9}$			Snook and Hamilton (1974)	
1-phenyl-2,2-dimethyl propanol	c1ccccc1C(O)C(C)(C)C	c1HcHcHcHcHc1CH(OH)C(CH3)(CH3)CH3	$9.9\cdot10^{9}$			Snook and Hamilton (1974)	

Reactant	SMILES	GECKO-A	k298 [$M^{-1}s^{-1}$]	A [$M^{-1}s^{-1}$]	E_a / R [K]	Reference/remarks	n = 467 (282 aliphatic/185 aromatic)
1-phenyl-2-propanol	c1ccccc1CC(O)C	c1HcHcHcHcHc1CH2CH(OH)CH3	$2.1\cdot10^{10}$			Snook and Hamilton (1974)	
2-phenyl-2-propanol	c1ccccc1C(C)(O)C	c1HcHcHcHcHc1C(OH)(CH3)CH3	$4.6\cdot10^{9}$			Snook and Hamilton (1974)	
Phenyl tert-butyl alcohol	c1ccccc1CC(C)(O)C	c1HcHcHcHcHc1CH2C(OH)(CH3)CH3	$1.7\cdot10^{10}$			Snook and Hamilton (1974)	
4-phenyl-2-butanol	c1ccccc1CCC(O)C	c1HcHcHcHcHc1CH2CH2CH(OH)CH3	$2.0\cdot10^{10}$			Snook and Hamilton (1974)	
1,1-dimethyl-3-phenyl butanol	c1ccccc1CCC(C)(O)C	c1HcHcHcHcHc1CH2CH2C(OH)(CH3)CH3	$5.9\cdot10^{9}$			Snook and Hamilton (1974)	
Aromatic carbonyls, acids and diacids							n = 8
Benzaldehyde	c1ccccc1C=O	c1HcHcHcHcHc1CHO	$3.5\cdot10^{9}$			Average of Geeta et al. (2001) and Shevchuk et al. (1969)[2]	
Phenyl acetone	c1ccccc1C(=O)C	c1HcHcHcHcHc1COCH3	$5.3\cdot10^{9}$			Average of Geeta et al. (2001); Anbar et al. (1966b); Willson et al. (1971)[1]; and Neta and Dorfman (1968)[1]	
Benzoic acid	c1ccccc1C(=O)O	c1HcHcHcHcHc1CO(OH)	$3.1\cdot10^{9}$			Average of Wander et al. (1968)[2] and Ashton et al. (1995)[1]	
Benzoate	c1ccccc1C(=O)[O-]	c1HcHcHcHcHc1CO(Om)	$5.9\cdot10^{9}$			Buxton et al. (1988)	
o-phthalate	c1(C(=O)[O-])ccccc1C(=O)[O-]	CO(Om)c1cHcHcHcHc1CO(Om)	$5.9\cdot10^{9}$			Simic et al. (1973a)[2]	
p-phthalate	c1cc(C(=O)[O-])ccc1C(=O)[O-]	c1HcHc(CO(Om))cHcHc1CO(Om)	$3.3\cdot10^{9}$			Anbar et al. (1966b)	
Phenyl acetate	c1ccccc1CC(=O)[O-]	c1HcHcHcHcHc1CH2CO(Om)	$7.9\cdot10^{9}$			Neta and Dorfman (1968)[2]	
Cinnamate	c1ccccc1C=CC(=O)[O-]	c1HcHcHcHcHc1CdH=CdHCO(Om)	$8.1\cdot10^{9}$			Bobrowski and Raghavan (1982)[2]	
Anisoles, aromatic ethers and esters							n = 9
Anisole	c1ccccc1OC	c1HcHcHcHcHc1-O-CH3	$5.8\cdot10^{9}$			Average of Anbar et al. (1966b) and O'Neill et al. (1975)[2]	
o-dimethoxy benzol	COc1ccccc1OC	CH3-O-c1cHcHcHcHc1-O-CH3	$5.2\cdot10^{9}$			O'Neill et al. (1975)[2]	
m-dimethoxy benzol	c1c(OC)cccc1OC	CH3-O-c(c1H)cHcHcHc1-O-CH3	$7.2\cdot10^{9}$			O'Neill et al. (1975)[2]	
p-dimethoxy benzol	c1cc(OC)ccc1OC	c1HcHc(-O-CH3)cHcHc1-O-CH3	$7.0\cdot10^{9}$			O'Neill et al. (1975)[2]	
1,2,3-trimethoxy benzol	COc1cccc(OC)c1OC	CH3-O-c1cHcHcHc(-O-CH3)c1-O-CH3	$8.0\cdot10^{9}$			O'Neill et al. (1975)[2]	
1,2,4-trimethoxy benzol	COc1cc(OC)ccc1OC	CH3-O-c1cHcHc(-O-CH3)cHc1-O-CH3	$8.1\cdot10^{9}$			O'Neill et al. (1975)[2]	
benzyl methyl ether	c1ccccc1COC	c1HcHcHcHcHc1CH2-O-CH3	$1.0\cdot10^{10}$			Snook and Hamilton (1974)	
1-methoxy-2-methyl-1-phenylpropane	c1ccccc1C(OC)C(C)C	c1HcHcHcHcHc1CH(-O-CH3)CH(CH3)CH3	$7.4\cdot10^{9}$			Snook and Hamilton (1974)	
Phenyl acetate	c1ccccc1OC(=O)C	c1HcHcHcHcHc1-O-COCH3	$5.2\cdot10^{9}$			Anbar et al. (1966b)	
Polyfunctional aromatic compounds							n = 64
o-nitro phenol	Oc1ccccc1N(=O)=O	c1HcHc(OH)c(NO2)cHc1H	$9.2\cdot10^{9}$			Saveleva et al. (1972)[9]	
o-nitro phenolate	[O-]c1ccccc1N(=O)=O		$9.2\cdot10^{9}$			Saveleva et al. (1972)[2]	
m-nitro phenolate	c1c([O-])cccc1N(=O)=O		$7.1\cdot10^{9}$			Saveleva et al. (1972)[2]	
p-nitro phenol	c1cc(O)ccc1N(=O)=O	c1Hc(OH)cHcHc(NO2)c1H	$3.8\cdot10^{9}$			Cercek and Ebert (1968)[2]	
p-nitro phenolate	c1cc([O-])ccc1N(=O)=O		$7.6\cdot10^{9}$			Saveleva et al. (1972)[2]	
2-hydroxy benzaldehyde	c1(O)ccccc1C=O	c1HcHcHcHc(OH)c1CHO	$5.2\cdot10^{9}$			Geeta et al. (2001)	
2-hydroxy benzaldehyde, conjugate base	c1([O-])ccccc1C=O		$5.2\cdot10^{9}$			Saveleva et al. (1972)[2]	
3-hydroxy benzaldehyde	c1c(O)cccc1C=O	c1HcHcHc(OH)cHc1CHO	$7.7\cdot10^{9}$			Geeta et al. (2001)	
4-hydroxy benzaldehyde	c1cc(O)ccc1C=O	c1HcHc(OH)cHcHc1CHO	$1.21\cdot10^{10}$			Geeta et al. (2001)	
4-hydroxy benzaldehyde, conjugate base	c1cc([O-])ccc1C=O		$1.0\cdot10^{10}$			Saveleva et al. (1972)[2]	
3,4-dihydroxy benzaldehyde	c1c(O)c(O)ccc1C=O	c1HcHc(OH)c(OH)cHc1CHO	$8.3\cdot10^{9}$			Bors et al. (1982)	
2-hydroxyphenyl acetone	c1(O)ccccc1C(=O)C	c1HcHcHcHc(OH)c1COCH3	$2.7\cdot10^{9}$			Geeta et al. (2001)	
3-hydroxyphenyl acetone	c1c(O)cccc1C(=O)C	c1HcHcHc(OH)cHc1COCH3	$2.6\cdot10^{9}$			Geeta et al. (2001)	
4-hydroxyphenyl acetone	c1cc(O)ccc1C(=O)C	c1HcHc(OH)cHcHc1COCH3	$5.1\cdot10^{9}$			Geeta et al. (2001)	
3,4-dihydroxyphenyl acetone	c1c(O)c(O)ccc1C(=O)C	c1HcHc(OH)c(OH)cHc1COCH3	$1.0\cdot10^{10}$			Bors et al. (1982)[1]	
2,4-dihydroxyphenyl acetone	c1(O)cc(O)ccc1C(=O)C	c1HcHc(OH)cHc(OH)c1COCH3	$3.0\cdot10^{10}$			Bors et al. (1982)[1]	
2,5-dihydroxyphenyl acetone	c1(O)ccc(O)cc1C(=O)C	c1Hc(OH)cHcHc(OH)c1COCH3	$8.0\cdot10^{9}$			Bors et al. (1982)[1]	
2,6-dihydroxyphenyl acetone	c1(O)cccc(O)c1C(=O)C	c1HcHc(OH)c(c(OH)c1H)COCH3	$8.0\cdot10^{9}$			Bors et al. (1982)[2]	
2-hydroxy benzoic acid	c1(O)ccccc1C(=O)O	c1HcHcHcHc(OH)c1CO(OH)	$2.2\cdot10^{10}$			Buxton et al. (1988)	
2-hydroxy benzoate	c1(O)ccccc1C(=O)[O-]		$1.6\cdot10^{10}$			Buxton et al. (1988)	
4-hydroxy benzoic acid	c1cc(O)ccc1C(=O)O	c1HcHc(OH)cHcHc1CO(OH)	$7.7\cdot10^{9}$			Average of Neta and Dorfman (1968)[1]; Anderson et al. (1987)[1]; and Shetiya et al. (1976)[1]	
4-hydroxy benzoate	c1cc(O)ccc1C(=O)[O-]	c1HcHc(OH)cHcHc1CO(Om)	$8.5\cdot10^{9}$			Buxton et al. (1988)	
2,3-hydroxy benzoate	c1(O)c(O)cccc1C(=O)[O-]	c1HcHcHc(OH)c(OH)c1CO(Om)	$1.0\cdot10^{10}$			Oturan et al. (1992)[1]	
2,4-hydroxy benzoate	c1(O)cc(O)ccc1C(=O)[O-]	c1HcHc(OH)cHc(OH)c1CO(Om)	$1.6\cdot10^{10}$			Oturan et al. (1992)[1]	
2,5-hydroxy benzoate	c1(O)ccc(O)cc1C(=O)[O-]	c1Hc(OH)cHcHc(OH)c1CO(Om)	$1.7\cdot10^{10}$			Oturan et al. (1992)[1]	
2,6-hydroxy benzoate	c1(O)cccc(O)c1C(=O)[O-]	c1HcHc(OH)c(CO(Om))c(OH)c1H	$1.0\cdot10^{10}$			Oturan et al. (1992)[1]	
3,4,5-hydroxy benzoate	c1c(O)c(O)c(O)cc1C(=O)[O-]	c1Hc(OH)c(OH)c(OH)cHc1CO(Om)	$4.0\cdot10^{10}$			Oturan et al. (1992)[1]	

Reactant	SMILES	GECKO-A	k298 [$M^{-1}s^{-1}$]	A [$M^{-1}s^{-1}$]	E_a / R [K]	Reference/remarks n = 467 (282 aliphatic/185 aromatic)
2,3,4-hydroxy benzoate	c1(O)c(O)c(O)ccc1C(=O)[O-]	c1HcHc(OH)c(OH)c(OH)c1CO(Om)	$1.9\cdot10^{10}$			Oturan et al. (1992)[1]
2,4,6-hydroxy benzoate	c1(O)cc(O)cc(O)c1C(=O)[O-]	c1(OH)cHc(OH)cHc(OH)c1CO(Om)	$4.8\cdot10^{10}$			Oturan et al. (1992)[1]
4-methyl benzoate	c1cc(C)ccc1C(=O)[O-]	CH3c1cHcHc(CO(Om))cHc1H	$8.0\cdot10^{9}$			Neta et al. (1972)[1]
4-nitrobenzoate	c1cc(N(=O)=O)ccc1C(=O)[O-]	c1HcHc(NO2)cHcHc1CO(Om)	$2.6\cdot10^{9}$			Neta and Dorfman (1968)[2] Buxton et al. (1988)
(3-(4-hydroxyphenyl) propionate monoanion)	c1cc(O)ccc1CCC(=O)[O-]	c1HcHc(OH)cHcHc1CH2CH2CO(Om)	$1.2\cdot10^{10}$			Buxton et al. (1988)
(3-(4-hydroxyphenyl) propionate dianion)	c1cc([O-])ccc1CCC(=O)[O-]		$1.9\cdot10^{10}$			Buxton et al. (1988)
p-hydroxy cinnamate	c1cc(O)ccc1C=CC(=O)[O-]	c1HcHc(OH)cHcHc1CdH=CdHCO(Om)	$8.2\cdot10^{9}$			Bobrowski (1984)[2]
3,4-dihydroxy cinnamate	c1c(O)c(O)ccc1C=CC(=O)[O-]	c1HcHc(OH)c(OH)cHc1CdH=CdHCO(Om)	$2.8\cdot10^{10}$			Bors et al. (1982)[2]
o- methoxy phenol	Oc1ccccc1OC	c1HcHcHcHc(OH)c1-O-CH3	$2.0\cdot10^{10}$			O’Neill and Steenken (1977)[2]
m- methoxy phenol	c1c(O)cccc1OC	c1HcHcHc(OH)cHc1-O-CH3	$3.2\cdot10^{10}$			O’Neill and Steenken (1977)[2]
p- methoxy phenol	c1cc(O)ccc1OC	c1HcHc(OH)cHcHc1-O-CH3	$2.6\cdot10^{10}$			O’Neill and Steenken (1977)[9]
2,3-dimethoxy phenol	COc1c(OC)cccc1O	CH3-O-c1cHcHcHc(OH)c1-O-CH3	$2.0\cdot10^{10}$			O’Neill and Steenken (1977)[2]
2,6-dimethoxy phenol	c1(OC)cccc(OC)c1O	c1HcHcHc(-O-CH3)c(OH)c1-O-CH3	$2.6\cdot10^{10}$			O’Neill and Steenken (1977)[2]
3,5-dimethoxy phenol	c1c(OC)cc(OC)cc1O	CH3-O-c(c1H)cHc(OH)cHc1-O-CH3	$2.0\cdot10^{10}$			O’Neill and Steenken (1977)[2]
2-methoxy benzoate	c1(OC)ccccc1C(=O)[O-]	CH3-O-c1cHcHcHcHc1CO(Om)	$5.4\cdot10^{9}$			O’Neill et al. (1977)[2]
3-methoxy benzoate	c1c(OC)cccc1C(=O)[O-]	CH3-O-c1cHcHcHc(c1H)CO(Om)	$6.6\cdot10^{9}$			O’Neill et al. (1977)[2]
4-methoxy benzoate	c1cc(OC)ccc1C(=O)[O-]	CH3-O-c1cHcHc(CO(Om))cHc1H	$7.2\cdot10^{9}$			O’Neill et al. (1977)[2]
2-hydroxy-5-methoxy benzoate	c1(O)ccc(OC)cc1C(=O)[O-]	CH3-O-c1cHcHc(OH)c(c1H)CO(Om)	$1.8\cdot10^{10}$	$9.0\cdot10^{10}$	1323	O’Neill et al. (1977)[2]
3-methoxy-4-hydroxy benzoate	c1c(OC)c(O)ccc1C(=O)[O-]	CH3-O-c1c(OH)cHcHc(c1H)CO(Om)	$1.4\cdot10^{10}$			O’Neill et al. (1977)[2]
2,3-dimethoxy benzoate	c1(OC)c(OC)cccc1C(=O)[O-]	CH3-O-c1cHcHcHc(CO(Om))c1-O-CH3	$1.0\cdot10^{10}$			O’Neill et al. (1977)[2]
2,4-dimethoxy benzoate	c1(OC)cc(OC)ccc1C(=O)[O-]	CH3-O-c1cHc(-O-CH3)cHcHc1CO(Om)	$1.0\cdot10^{10}$			O’Neill et al. (1977)[2]
3,4-dimethoxy benzoate	c1c(OC)c(OC)ccc1C(=O)[O-]	CH3-O-c1cHcHc(CO(Om))cHc1-O-CH3	$1.2\cdot10^{10}$			O’Neill et al. (1977)[2]
2,6-dimethoxy benzoate	c1(OC)cccc(OC)c1C(=O)[O-]	CH3-O-c1cHcHcHc(-O-CH3)c1CO(Om)	$6.6\cdot10^{9}$			O’Neill et al. (1977)[2]
3,5-dimethoxy benzoate	c1c(OC)cc(OC)cc1C(=O)[O-]	CH3-O-c(c1H)cHc(CO(Om))cHc1-O-CH3	$7.0\cdot10^{9}$			O’Neill et al. (1977)[2]
3,5-dimethoxy-4-hydroxy benzoate	c1c(OC)c(O)c(OC)cc1C(=O)[O-]	CH3-O-c1c(OH)c(-O-CH3)cHc(c1H)CO(Om)	$1.6\cdot10^{10}$			O’Neill et al. (1977)[2]
2,3,4-trimethoxy benzoate	c1(OC)c(OC)c(OC)ccc1C(=O)[O-]	CH3-O-c1c(-O-CH3)cHcHc(CO(Om))c1-O-CH3	$1.0\cdot10^{10}$			O’Neill et al. (1977)[2]
2,3,5-trimethoxy benzoate	c1(OC)c(OC)cc(OC)cc1C(=O)[O-]	CH3-O-c1cHc(-O-CH3)cHc(CO(Om))c1-O-CH3	$7.0\cdot10^{9}$			O’Neill et al. (1977)[2]
2,4,6-trimethoxy benzoate	c1(OC)cc(OC)cc(OC)c1C(=O)[O-]	CH3-O-c1cHc(-O-CH3)cHc(-O-CH3)c1CO(Om)	$1.2\cdot10^{10}$			O’Neill et al. (1977)[2]
3,4,5-trimethoxy benzoate	c1c(OC)c(OC)c(OC)cc1C(=O)[O-]	CH3-O-c1c(-O-CH3)cHc(CO(Om))cHc1-O-CH3	$1.3\cdot10^{10}$			O’Neill et al. (1977)[2]
3-methoxy-4-hydroxy cinnamate	c1c(OC)c(O)ccc1C=CC(=O)[O-]	CH3-O-c1c(OH)cHcHc(c1H)CdH=CdHCO(Om)	$1.0\cdot10^{10}$			Bors et al. (1982)[2]
3,5-dimethoxy-4-hydroxy cinnamate	c1c(OC)c(O)c(OC)cc1C=CC(=O)[O-]	CH3-O-c1c(OH)c(-O-CH3)cHc(c1H)CdH=CdHCO(Om)	$2.2\cdot10^{10}$			Buxton et al. (1988)
phenoxy acetic acid	c1ccccc1OCC(=O)O	c1HcHcHcHcHc1-O-CH2CO(OH)	$1.0\cdot10^{10}$			Zona et al. (2002)[3]
1-(p-ethoxyphenyl)ethanol	c1cc(OCC)ccc1C(O)C	CH3CH(OH)c1cHcHc(cHc1H)-O-CH2CH3	$2.7\cdot10^{9}$			Snook and Hamilton (1974)
1-(p-methoxyphenyl)-2,2-dimethyl propanol	c1cc(OC)ccc1C(O)C(C)(C)C	c1HcHc(-O-CH3)cHcHc1CH(OH)C(CH3)(CH3)CH3	$7.6\cdot10^{9}$			Snook and Hamilton (1974)
3,5-dinitro anisole	c1c(N(=O)=O)cc(N(=O)=O)cc1OC	c1Hc(NO2)cHc(NO2)cHc1-O-CH3	$4.0\cdot10^{9}$			Tamminga et al. (1979)[2]
Isoeugenol	c1c(OC)c(O)ccc1C=CC	CH3-O-c1c(OH)cHcHc(c1H)CdH=CdHCH3	$3.9\cdot10^{10}$			Buxton et al. (1988)
Propyl 3,4,5-trihydroxybenzoate	c1c(O)c(O)c(O)cc1C(=O)OCCC	c1Hc(OH)c(OH)c(OH)cHc1CO-O-CH2CH2CH3	$1.1\cdot10^{10}$			Buxton et al. (1988)
Polycyclic aromatic compounds (including sugars)						n = 34
Endothall	OC(=O)C2C(C1CCC2O1)C(=O)O	CO(OH)C1HCH(CO(OH))C2H-O-C1HCH2C2H2	$1.5\cdot10^{9}$			Haag and Yao (1992)[8]
Camphor	CC2(C)C1CC(=O)C2(C)CC1	C2H2CH2CH(C1(CH3)CH3)CH2COC12CH3	$4.1\cdot10^{9}$			Land and Swallow (1979)
2-phenyl furan	c1ccccc1c2ccco2	-O2-CdH=CdHCdH=Cd2c1cHcHcHcHc1H	$1.6\cdot10^{10}$			Vysotskaya et al. (1983)[2]
5-phenyl furfural	c1ccccc1c2ccc(C=O)o2	-O2-Cd(CHO)=CdHCdH=Cd2c1cHcHcHcHc1H	$5.9\cdot10^{9}$			Vysotskaya et al. (1983)[2]
Biphenyl	c1ccccc1c2ccccc2	c1HcHcHcHcHc1c2cHcHcHcHc2H	$1.04\cdot10^{10}$			Chen and Schuler (1993); partial *k* @ o/m/p position: $1.07\cdot10^{9}/5.5\cdot10^{8}/1.52\cdot10^{9}$
Biphenyl-4-carboxylate	c1ccccc1c2ccc(C(=O)[O-])cc2	c1HcHc(CO(Om))cHcHc1c2cHcHcHcHc2H	$6.8\cdot10^{9}$			Simic et al. (1973a)[2]
Biphenyl-2,2’-dicarboxylate	[O-]C(=O)c1ccccc1c2ccccc2C(=O)[O-]	CO(Om)c1cHcHcHcHc1c2cHcHcHcHc2CO(Om)	$7.0\cdot10^{9}$			Simic et al. (1973a)[2]
Biphenyl-4,4’-dicarboxylate	c1cc(C(=O)[O-])ccc1c2ccc(C(=O)[O-])cc2	c1HcHc(CO(Om))cHcHc1c2cHcHc(CO(Om))cHc2H	$8.3\cdot10^{9}$			Simic et al. (1973a)[2]
Benzophenone	c1ccccc1C(=O)c2ccccc2	c1HcHcHcHcHc1COc2cHcHcHcHc2H	$8.8\cdot10^{9}$			Buxton et al. (1988)
Diphenyl acetate	c1ccccc1C(C(=O)[O-])c2ccccc2		$4.0\cdot10^{9}$			Neta et al. (1972)[2]
4-Phenoxybenzoate	c1ccccc1Oc2ccc(C(=O)[O-])cc2		$7.0\cdot10^{9}$			Neta and Schuler (1975)[2]
1,4-(3,4-dihydroxyphenyl)-2,3-dimethyl butane	c1cc(O)c(O)cc1CC(C)C(C)Cc2cc(O)c(O)cc2	c1HcHc(OH)c(OH)cHc1CH2CH(CH3)CH(CH3)CH2c2cHc(OH)c(OH)cHc2H	$1.5\cdot10^{10}$			Bors et al. (1982)[2]
1,2,3,4-tetrahydro-1-naphthol/ α-tetralol	OC2CCCc1ccccc12	c2HcHcHcHc1CH(OH)CH2CH2CH2c12	$7.0\cdot10^{9}$			Snook and Hamilton (1974)[2]

Reactant	SMILES	GECKO-A	k298 [$M^{-1}s^{-1}$]	A [$M^{-1}s^{-1}$]	E_a / R [K]	Reference/remarks n = 467 (282 aliphatic/185 aromatic)
Coumarin	O=C1C=Cc2ccccc2O1		$2.0\cdot10^{9}$			Gopakumar et al. (1977)
β-Benzylglucoside	c1ccccc1COC2C(O)C(O)C(O)C(CO)O2	C2H(OH)CH(OH)CH(OH)CH(CH2(OH))-O-C2H-O-CH2c1cHcHcHcHc1H	$4.2\cdot10^{10}$			Mittal and Mittal (1986)[2]
2,4dimethylphenyl-β-D-glucopyranoside	Cc1cc(C)ccc1COC2C(O)C(O)C(O)C(CO)O2	C2H(OH)CH(OH)CH(OH)CH(CH2(OH))-O-C2H-O-CH2c1cHcHc(CH3)cHc1CH3	$3.9\cdot10^{9}$			Phillips et al. (1971)[2]
3,4dimethylphenyl-β-D-glucopyranoside	c1c(C)c(C)ccc1COC2C(O)C(O)C(O)C(CO)O2	C2H(OH)CH(OH)CH(OH)CH(CH2(OH))-O-C2H-O-CH2c(cHc1CH3)cHcHc1CH3	$4.2\cdot10^{9}$			Phillips et al. (1971)[2]
Naphthalene	c1cccc2ccccc12	c12cHcHcHcHc1cHcHcHc2H	$9.6\cdot10^{9}$			Average of Evers et al. (1980)[2]; Zevos and Sehested (1978)[2]; Roder et al. (1990)[1]; and Kanodia et al. (1988)[1]
1-naphthol	Oc2cccc1ccccc12	c2HcHcHcHc1c(OH)cHcHcHc12	$1.2\cdot10^{10}$			Average of Doherty et al. (1986)[8] and Kanodia et al. (1988)[8]
2-naphthol	Oc1ccc2ccccc2c1	c2HcHcHcHc1cHc(OH)cHcHc12	$1.2\cdot10^{10}$			Kanodia et al. (1988)[1]
1-naphthoate	[O-]C(=O)c2cccc1ccccc12	CO(Om)c2cHcHcHc1cHcHcHcHc12	$7.9\cdot10^{9}$			Simic et al. (1973a)[2]
2-naphthoate	[O-]C(=O)c1ccc2ccccc2c1	CO(Om)c(c2H)cHcHc1cHcHcHcHc12	$7.6\cdot10^{9}$			Simic et al. (1973a)[2]
1-naphthylacetate	[O-]C(=O)Cc2cccc1ccccc12	CO(Om)CH2c2cHcHcHc1cHcHcHcHc12	$8.7\cdot10^{9}$			Shetiya et al. (1972)[2]
Di-tert-butylnaphtalenesulfonate	CC(C)(C)c1ccc2c(c1)cc(cc2S([O-])(=O)=O)C(C)(C)C		$1.1\cdot10^{10}$			Barber and Thomas (1978)[2]
chromotropic acid	O=S(=O)(O)c2cc1cc(cc(O)c1c(O)c2)S(=O)(=O)O		$1.2\cdot10^{8}$			Ahrens (1967)[2]
9,10-Anthraquinone-1-sulfonate	[O-]S(=O)(=O)c3cccc2C(=O)c1ccccc1C(=O)c23		$7.2\cdot10^{9}$			Hulme et al. (1972)[2]
9,10-Anthraquinone-2-sulfonate	[O-]S(=O)(=O)c2ccc3C(=O)c1ccccc1C(=O)c3c2		$5.6\cdot10^{9}$			Hulme et al. (1972)[2]
8-Methoxypsoralen	COc1c3occc3cc2C=CC(=O)Oc12		$1.1\cdot10^{10}$			Redpath et al. (1978)[2]
Flourescein	[O-]C(=O)c4ccccc4C=1c3ccc([O-])cc3OC2=CC(=O)C=CC=12		$1.2\cdot10^{10}$			Prütz (1973)[2]
Pyrene butyrate	[O-]C(=O)CCCc1cc2ccc3cccc4ccc(c1)c2c34		$1.3\cdot10^{10}$			Barber and Thomas (1978)[2]
D-cellobiose	OCC1OC(O)C(O)C(O)C1OC2C(O)C(O)C(O)C(CO)O2	C2H(OH)CH(OH)CH(OH)CH(CH2(OH))-O-C2H-O-C1HCH(OH)CH(OH)CH(OH)-O-C1HCH2(OH)	$3.6\cdot10^{9}$			Zakatova et al. (1969)[2]
crocin	O1C(CO)C(O)C(O)C(O)C1OCC2C(O)C(O)C(O)C(O2)OC(=O)C(C)=CC=CC(C)=CC=CC=C(C)C=CC=C(C)C(=O)OC3C(O)C(O)C(O)C(O3)COC4C(O)C(O)C(O)C(O4)CO		$3.1\cdot10^{9}$			Buxton et al. (1988)
carmine	OC1C(O)C(O)C(OC1CO)c4c(O)c3C(=O)c2c(C)c(C(=O)O)c(O)cc2C(=O)c3c(O)c4O		$1.3\cdot10^{10}$			Sychev et al. (1979)[2]
9-anthroate ion			$8.0\cdot10^{9}$			Simic et al. (1973b)[2]
Remarks: References taken from:	[1]NIST database: Ross et al. (1998); [2]Buxton et al. (1988); [3]Herrmann (2003); [4] Gligorovski et al. (2009); [5](Cooper et al. (2009); [6]CAPRAM database available at http://projects.tropos.de/capram/; [7] de Sémainville et al. (2007); [8]Warneck (2005); [9]Barzaghi and Herrmann (2004)					

Table S2 Recommend kinetic data for NO_3 reactions with organic compounds.

Reactant	SMILES	GECKO-A	k298 [$M^{-1}s^{-1}$]	A [$M^{-1}s^{-1}$]	E_a / R [K]	Reference/remarks	n = 130 (81 aliphatic/49 aromatic)
Alkenes							n = 1
Isoprene	C=C(C)C=C	CdH2=CdHCd(CH3)=CdH2	$1.0\cdot10^{9}$			TROPOS measurements	
Monoalcohols							n = 14
Methanol	CO	CH3OH	$5.1\cdot10^{5}$	$9.4\cdot10^{11}$	4300	Average of Exner et al. (1993) and Rousse and George (2004)	
Ethanol	CCO	CH3CH2OH	$2.2\cdot10^{6}$	$1.4\cdot10^{11}$	3300	Herrmann and Zellner (1998)	
Propanol	CCCO	CH3CH2CH2OH	$3.2\cdot10^{6}$			Herrmann et al. (1994)	
Butanol	CCCCO	CH3CH2CH2CH2OH	$1.9\cdot10^{6}$			Shastri and Huie (1990)	
Pentanol	CCCCCO	CH3CH2CH2CH2CH2OH	$2.4\cdot10^{6}$			Shastri and Huie (1990)	
Hexanol	CCCCCCO	CH3CH2CH2CH2CH2CH2OH	$3.3\cdot10^{6}$			Shastri and Huie (1990)	
Heptanol	CCCCCCCO	CH3CH2CH2CH2CH2CH2CH2OH	$3.6\cdot10^{6}$			Shastri and Huie (1990)	
octanol	CCCCCCCCO	CH3CH2CH2CH2CH2CH2CH2CH2OH	$5.8\cdot10^{6}$			Shastri and Huie (1990)	
Iso-propanol	CC(O)C	CH3CH(OH)CH3	$3.7\cdot10^{6}$	$3.1\cdot10^{8}$	1323	Herrmann et al. (1994) with E_a/R of Ito et al. (1989b)	
Iso-butanol	CC(C)CO	CH3CH(CH3)CH2(OH)	$1.6\cdot10^{6}$			Shastri and Huie (1990)	
Tert-butanol	CC(C)(C)O	CH3C(OH)(CH3)CH3	$6.6\cdot10^{4}$			Herrmann et al. (1994)	
Allyl alcohol	C=CCO	CH2(OH)CdH=CdH2	$2.2\cdot10^{8}$			Average of Alfassi et al. (1993) and Ito et al. (1989b)	
2-butenol	CC=CCO	CH3CdH=CdHCH2(OH)	$2.1\cdot10^{9}$			Alfassi et al. (1993)	
3-methyl 3-buten-1-ol	C=C(C)CCO	CH2(OH)CH2Cd(CH3)=CdH2	$2.4\cdot10^{9}$			Alfassi et al. (1993)	
Diols and Polyols							n = 2
ethylene glycol	OCCO	CH2(OH)CH2(OH)	$6.6\cdot10^{6}$	$7.1\cdot10^{9}$	2117	Hoffmann et al. (2009)	
1,2-propanediol	CC(O)CO	CH3CH(OH)CH2(OH)	$9.9\cdot10^{6}$	$6.8\cdot10^{10}$	2622	Hoffmann et al. (2009)	
Aldehydes and gem-diols							n = 11
Formaldehyde	C=O	CH2O	$3.5\cdot10^{6}$	$3.36\cdot10^{6}$	674	Average of (Ito et al. (1989a)[6] and Wayne et al. (1991) with E_a/R of Wayne et al. (1991)	
Hydrated formaldehyde	OCO	CH2(OH)(OH)	$1.0\cdot10^{6}$	$3.6\cdot10^{12}$	4500	Exner et al. (1993)[1]	
Acetaldehyde	CC=O	CH3CHO	$1.9\cdot10^{6}$			Zellner et al. (1996)	
Hydrated acetaldehyde	CC(O)O	CH3CH(OH)(OH)	$2.0\cdot10^{6}$			Average of Zellner et al. (1996)[2] and Rousse and George (2004)	
Propionaldehyde	CCC=O	CH3CH2CHO	$5.8\cdot10^{7}$	$3.2\cdot10^{11}$	2646	de Sémainville et al. (2007)	
Butyraldehyde	CCCC=O	CH3CH2CH2CHO	$5.6\cdot10^{7}$	$4.9\cdot10^{10}$	2045	de Sémainville et al. (2007)	
Iso-butyraldehyde	CC(C)C=O	CH3CH(CH3) CHO	$6.3\cdot10^{7}$	$3.7\cdot10^{8}$	529	Wayne et al. (1991)	
2,2-dimethyl propanal	CC(C)(C)C=O	CH3C(CH3)(CH3)CHO	$7.0\cdot10^{7}$	$3.8\cdot10^{8}$	505	Wayne et al. (1991)	
Methacrolein	C=C(C)C=O	CH3Cd(CHO)=CdH2	$4.0\cdot10^{7}$	$5.8\cdot10^{8}$	842	Schöne et al. (2014)	
Glyoxal	O=CC=O	CHOCHO	$1.1\cdot10^{6}$	$9.9\cdot10^{10}$	3400	TROPOS measurement	
Hydrated glyoxal	OC(O)C(O)O	CH(OH)(OH)CH(OH)(OH)	$1.1\cdot10^{6}$	$8.9\cdot10^{10}$	3368	Herrmann et al. (1995b)[2]	
Ketones							n = 3
Acetone	CC(=O)C	CH3COCH3	$3.7\cdot10^{3}$	$7.6\cdot10^{9}$	4330	Herrmann and Zellner (1998)	
Methyl ethyl ketone	CC(=O)CC	CH3CH2COCH3	$2.2\cdot10^{7}$	$3.9\cdot10^{11}$	2887	de Sémainville et al. (2007)	
Methyl vinyl ketone	CC(=O)C=C	CH3COCdH=CdH2	$9.7\cdot10^{6}$	$6.2\cdot10^{8}$	1200	Schöne et al. (2014)	
Monocarboxylic acids (undissociated and dissociated)							n = 10
Formic acid	C(=O)O	CHO(OH)	$3.8\cdot10^{5}$	$3.4\cdot10^{10}$	3400	Exner et al. (1994)	
Formate	C(=O)[O-]	CHO(Om)	$5.1\cdot10^{7}$	$8.2\cdot10^{10}$	2200	Exner et al. (1994)[3]	
Acetic acid	CC(=O)O	CH3CO(OH)	$1.3\cdot10^{4}$	$4.9\cdot10^{9}$	3800	Exner et al. (1994)[4]	
Acetate	CC(=O)[O-]	CH3CO(Om)	$2.9\cdot10^{6}$	$1.0\cdot10^{12}$	3800	Exner et al. (1994)[4]	
Propionic acid	CCC(=O)O	CH3CH2CO(OH)	$7.7\cdot10^{4}$			Rousse and George (2004)	
Acrylic acid	C=CC(=O)O	CO(OH)CdH=CdH2	$6.9\cdot10^{6}$	$2.2\cdot10^{13}$	4450	Schöne et al. (2014)	
Acrylate	C=CC(=O)[O-]	CO(Om)CdH=CdH2	$4.4\cdot10^{7}$	$2.2\cdot10^{9}$	1200	Schöne et al. (2014)	
Crotonic acid	CC=CC(=O)O	CH3CdH=CdHCO(OH)	$5.1\cdot10^{7}$			Neta and Huie (1986)	
Methacrylic acid	C=C(C)C(=O)O	CH3Cd(CO(OH))=CdH2	$9.2\cdot10^{7}$			Schöne et al. (2014)	
Methacrylate	C=C(C)C(=O)[O-]	CH3Cd(CO(Om))=CdH2	$1.7\cdot10^{8}$			Schöne et al. (2014)	
Dicarboxylic acids (undissociated and dissociated)							n = 9
Oxalic acid	OC(=O)C(=O)O	CO(OH)CO(OH)	$2.4\cdot10^{4}$			Yang et al. (2004)	
Oxalate monoanion	OC(=O)C(=O)[O-]	CO(OH)CO(Om)	$6.1\cdot10^{7}$	$8.4\cdot10^{9}$	-2180	Average of Yang et al. (2004) and de Sémainville et al. (2010) with E_a/R of Raabe (1996)	

Formatted Table

Reactant	SMILES	GECKO-A	k298 [$M^{-1}s^{-1}$]	A [$M^{-1}s^{-1}$]	E_a / R [K]	Reference/remarks n = 130 (81 aliphatic/49 aromatic)
Oxalate dianion	[O-]C(=O)C(=O)[O-]	CO(Om)CO(Om)	$2.2\cdot10^{8}$	$2.2\cdot10^{12}$	2766	Average of Yang et al. (2004) and de Sémainville et al. (2010) with E_a/R of de Sémainville et al. (2010)
Malonic acid	OC(=O)CC(=O)O	CO(OH)CH2CO(OH)	$5.1\cdot10^{4}$			de Sémainville et al. (2010)
Malonate monoanion	OC(=O)CC(=O)[O-]	CO(OH)CH2CO(Om)	$5.6\cdot10^{6}$	$5.0\cdot10^{11}$	3368	de Sémainville et al. (2010)
Malonate dianion	[O-]C(=O)CC(=O)[O-]	CO(Om)CH2CO(Om)	$2.3\cdot10^{7}$	$6.3\cdot10^{11}$	3007	de Sémainville et al. (2010)
Succinic acid	OC(=O)CCC(=O)O	CO(OH)CH2CH2CO(OH)	$5.0\cdot10^{3}$			de Sémainville et al. (2010)
Succinate monoanion	OC(=O)CCC(=O)[O-]	CO(OH)CH2CH2CO(Om)	$1.1\cdot10^{7}$			de Sémainville et al. (2010)
Succinate dianion	[O-]C(=O)CCC(=O)[O-]	CO(Om)CH2CH2CO(Om)	$1.8\cdot10^{7}$	$6.2\cdot10^{11}$	3127	de Sémainville et al. (2010)
Ethers and Esters						n = 9
Methyl tert-butyl ether	CC(C)(C)OC	CH3-O-C(CH3)(CH3)CH3	$3.9\cdot10^{5}$			Rousse and George (2004)
Methyl formate	COC=O	CH3-O-CHO	$3.5\cdot10^{6}$			Buxton et al. (2001)[5]
Ethyl formate	CCOC=O	CH3CH2-O-CHO	$4.7\cdot10^{6}$			Buxton et al. (2001)
Methyl acetate	CC(=O)OC	CH3CO-O-CH3	$<10^{4}$			Buxton et al. (2001)
Ethyl acetate	CC(=O)OCC	CH3CH2-O-COCH3	$<10^{4}$			Buxton et al. (2001)
Dimethyl malonate	COC(=O)CC(=O)OC	CH3-O-COCH2CO-O-CH3	$2.6\cdot10^{4}$			Rousse and George (2004)
Dimethyl succinate	COC(=O)CCC(=O)OC	CH3-O-COCH2CH2CO-O-CH3	$3.4\cdot10^{4}$			Rousse and George (2004)
Dimethyl carbonate	COC(=O)OC	CH3-O-CO-O-CH3	$8.4\cdot10^{4}$			Rousse and George (2004)
Diethyl carbonate	CCOC(=O)OCC	CH3CH2-O-CO-O-CH2CH3	$1.5\cdot10^{4}$			Rousse and George (2004)
Aliphatic polyfunctional compounds						n = 11
Hydroxy acetone	CC(=O)CO	CH3COCH2(OH)	$1.8\cdot10^{7}$	$4.0\cdot10^{9}$	1564	de Sémainville et al. (2007)
Glycolic acid	OCC(=O)O	CH2(OH)CO(OH)	$9.1\cdot10^{5}$	$4.5\cdot10^{11}$	3969	de Sémainville et al. (2007)
Glycolate	OCC(=O)[O-]	CH2(OH)CO(Om)	$1.0\cdot10^{7}$	$1.8\cdot10^{11}$	3007	de Sémainville et al. (2007)
Lactic acid	CC(O)C(=O)O	CH3CH(OH)CO(OH)	$2.1\cdot10^{6}$	$1.0\cdot10^{11}$	3248	de Sémainville et al. (2007)
Lactate	CC(O)C(=O)[O-]	CH3CH(OH)CO(Om)	$1.0\cdot10^{7}$	$8.3\cdot10^{10}$	2646	de Sémainville et al. (2007)
Pyruvic acid	CC(=O)C(=O)O	CH3COCO(OH)	$2.4\cdot10^{6}$	$8.8\cdot10^{8}$	1804	de Sémainville et al. (2007)
Pyruvate	CC(=O)C(=O)[O-]	CH3COCO(Om)	$1.9\cdot10^{7}$	$3.7\cdot10^{11}$	2887	de Sémainville et al. (2007)
Mesoxalic acid	OC(=O)C(=O)C(=O)O	CO(OH)COCO(OH)	$1.7\cdot10^{6}$	$5.1\cdot10^{8}$	1564	de Sémainville et al. (2010)
Mesoxalate monoanion	OC(=O)C(=O)C(=O)[O-]		$2.3\cdot10^{7}$			de Sémainville et al. (2010)
Mesoxalate dianion	[O-]C(=O)C(=O)C(=O)[O-]		$4.9\cdot10^{7}$	$1.4\cdot10^{12}$	3127	de Sémainville et al. (2010)
Fumaric acid	OC(=O)/C=C/C(=O)O	CO(OH)CdH=CdHCO(OH)	$<1.0\cdot10^{6}$			Neta and Huie (1986)[3]
Polyols and sugars						n = 5
Glycerol	OCC(O)CO	CH2(OH)CH(OH)CH2(OH)	$1.3\cdot10^{7}$	$1.4\cdot10^{12}$	3452	Hoffmann et al. (2009)
Erythritol	OCC(O)C(O)CO	CH2(OH)CH(OH)CH(OH)CH2(OH)	$1.4\cdot10^{7}$	$3.4\cdot10^{10}$	2321	Hoffmann et al. (2009)
Arabitol	OCC(O)C(O)C(O)CO	CH2(OH)CH(OH)CH(OH)CH(OH)CH2(OH)	$1.5\cdot10^{7}$	$1.1\cdot10^{10}$	1997	Hoffmann et al. (2009)
Mannitol	OCC(O)C(O)C(O)C(O)CO	CH2(OH)CH(OH)CH(OH)CH(OH)CH(OH)CH(OH)	$1.4\cdot10^{7}$	$5.1\cdot10^{10}$	2466	Hoffmann et al. (2009)
Levoglucosan	OC1C(O)C(O)C2OC1OC2	C1H2-O-CH(-O-C12H)CH(OH)CH(OH)C2H(OH)	$1.6\cdot10^{7}$	$2.5\cdot10^{10}$	2150	TROPOS measurements
Cyclic aliphatic compounds						n = 6
Cyclopentanol	C1CCCC1O	C1H2CH2CH(OH)CH2C1H2	$3.2\cdot10^{6}$			Shastri and Huie (1990)[6]
Oxetane	C1COC1	C1H2CH2-O-C1H2	$1.5\cdot10^{6}$			Shastri and Huie (1990)[6]
Tetrahydrofuran	C1COCC1	C1H2CH2-O-CH2C1H2	$1.5\cdot10^{7}$			Herrmann and Zellner (1998)[4]
Tetrahydropyran	C1CCCCO1	C1H2CH2CH2-O-CH2C1H2	$4.9\cdot10^{6}$			Shastri and Huie (1990)
1,3-dioxane	C1COCOC1	C1H2CH2-O-CH2-O-C1H2	$7.7\cdot10^{5}$			Shastri and Huie (1990)
1,4-dioxane	C1OCCOC1	C1H2-O-CH2CH2-O-C1H2	$1.3\cdot10^{6}$			Shastri and Huie (1990)
Benzols						n = 6
Benzol	c1ccccc1	c1HcHcHcHcHc1H	$4.0\cdot10^{8}$			Herrmann et al. (1996)
Toluol	c1ccccc1C	c1HcHcHcHcHc1CH3	$1.2\cdot10^{9}$	$5.7\cdot10^{11}$	1800	Herrmann and Zellner (1998)
Ethyl benzol	c1ccccc1CC	c1HcHcHcHcHc1CH2CH3	$1.3\cdot10^{9}$			Herrmann et al. (1996)
Tert-butyl benzol	c1ccccc1C(C)(C)C	c1HcHcHcHcHc1C(CH3)(CH3)CH3	$1.1\cdot10^{9}$			TROPOS measurements
p-xylene	c1cc(C)ccc1C	c1HcHc(CH3)cHcHc1CH3	$1.6\cdot10^{9}$			Herrmann et al. (1996)
Mesitylene	c1c(C)cc(C)cc1C	c1Hc(CH3)cHc(CH3)cHc1CH3	$1.3\cdot10^{9}$			Herrmann et al. (1996)
Phenols and other aromatic alcohols						n = 10
Phenol	c1ccccc1O	c1HcHcHc(OH)cHc1H	$1.9\cdot10^{9}$	$1.4\cdot10^{12}$	2100	Umschlag et al. (2002)
Catechol	c1cccc(O)c1O	c1HcHc(OH)c(OH)cHc1H	$5.6\cdot10^{8}$	$3.7\cdot10^{15}$	4691	Barzaghi and Herrmann (2004)
Hydroquinone	c1cc(O)ccc1O	c1Hc(OH)cHcHc(OH)c1H	$1.1\cdot10^{9}$			TROPOS measurements
pyrogallol	Oc1c(O)cccc1O	c1HcHc(OH)c(OH)c(OH)c1H	$1.7\cdot10^{9}$	$6.9\cdot10^{10}$	1100	TROPOS measurements

Reactant	SMILES	GECKO-A	k298 [M^{-1}s^{-1}]	A [M^{-1}s^{-1}]	E_a / R [K]	Reference/remarks	n = 130 (81 aliphatic/49 aromatic)
o-ethyl phenol	CCc1ccccc1O	c1HcHcHcHc(OH)c1CH2CH3	$6.7\cdot10^{8}$		2165	Barzaghi and Herrmann (2004)	
p-ethyl phenol	c1cc(CC)ccc1O	c1HcHc(OH)cHcHc1CH2CH3	$1.6\cdot10^{9}$	$4.6\cdot10^{11}$	1672	TROPOS measurements	
p-tert-butyl phenol	c1cc(O)ccc1C(C)(C)C	c1HcHc(OH)cHcHc1C(CH3)(CH3)CH3	$1.1\cdot10^{9}$			TROPOS measurements	
Benzyl alcohol	c1ccccc1CO	c1HcHcHcHcHc1CH2(OH)	$4.5\cdot10^{8}$			Ito et al. (1989b)[3]	
o-cresol	c1(O)ccccc1C	c1HcHcHcHc(OH)c1CH3	$8.5\cdot10^{8}$	$6.1\cdot10^{12}$	2646	Barzaghi and Herrmann (2004)	
p-cresol	c1cc(O)ccc1C	c1HcHc(OH)cHcHc1CH3	$1.7\cdot10^{9}$	$9.0\cdot10^{11}$	1756	TROPOS measurements	
Aromatic carbonyls and acids							n = 5
Phenyl acetone	c1ccccc1C(=O)C	c1HcHcHcHcHc1COCH3	$1.4\cdot10^{7}$			Neta and Huie (1986)[3]	
Benzoic acid	c1ccccc1C(=O)O	c1HcHcHcHcHc1CO(OH)	$6.5\cdot10^{7}$	$4.9\cdot10^{9}$	1300	Umschlag et al. (2002)	
4-methyl benzoic acid	c1cc(C)ccc1C(=O)O	CH3c1cHcHc(CO(OH))cHc1H	$6.0\cdot10^{8}$	$1.6\cdot10^{12}$	2400	Umschlag et al. (2002)	
Phenyl acetic acid	c1ccccc1CC(=O)O	c1HcHcHcHcHc1CH2CO(OH)	$1.8\cdot10^{9}$			Neta and Huie (1986)	
Phenyl acetate	c1ccccc1CC(=O)[O-]	c1HcHcHcHcHc1CH2CO(Om)	$1.4\cdot10^{8}$			TROPOS measurements	
Anisoles							n = 4
Anisole	c1ccccc1OC	c1HcHcHcHcHc1-O-CH3	$1.0\cdot10^{9}$			Herrmann et al. (1995a)	
m-methyl anisole	c1c(C)cccc1OC	c1Hc(CH3)cHcHcHc1-O-CH3	$2.0\cdot10^{9}$			TROPOS measurements	
p-methyl anisole	c1cc(C)ccc1OC	c1HcHc(CH3)cHcHc1-O-CH3	$3.2\cdot10^{9}$			TROPOS measurements	
p-dimethoxy benzol	c1cc(OC)ccc1OC	c1HcHc(-O-CH3)cHcHc1-O-CH3	$1.2\cdot10^{9}$	$7.8\cdot10^{9}$	500	TROPOS measurements	
Polyfunctional aromatic compounds							n = 22
o-nitro phenol	Oc1ccccc1N(=O)=O	c1HcHc(OH)c(NO2)cHc1H	$2.3\cdot10^{7}$			Barzaghi and Herrmann (2004)	
p-nitro phenol	c1cc(O)ccc1N(=O)=O	c1Hc(OH)cHcHc(NO2)c1H	$1.4\cdot10^{9}$	$4.0\cdot10^{11}$	1684	TROPOS measurements	
2,4-dinitro phenol	Oc1ccc(N(=O)=O)cc1N(=O)=O	c1Hc(OH)c(NO2)cHc(NO2)c1H	$5.3\cdot10^{7}$			Umschlag et al. (2002)[5]	
2,6-dinitro phenol	Oc1c(N(=O)=O)cccc1N(=O)=O	c1HcHc(NO2)c(OH)c(NO2)c1H	$2.8\cdot10^{8}$	$3.2\cdot10^{11}$	2165	TROPOS measurements	
2-nitro-4-methyl phenol	Oc1ccc(C)cc1N(=O)=O	c1HcHc(OH)c(NO2)cHc1CH3	$1.0\cdot10^{8}$			Umschlag et al. (2002)	
2,6-dinitro p-cresol	Oc1c(N(=O)=O)cc(C)cc1N(=O)=O	c1Hc(NO2)c(OH)c(NO2)cHc1CH3	$1.4\cdot10^{8}$			Umschlag et al. (2002)	
4-hydroxy benzoic acid	c1cc(O)ccc1C(=O)O	c1HcHc(OH)cHcHc1CO(OH)	$1.6\cdot10^{9}$	$3.2\cdot10^{11}$	1588	TROPOS measurements	
4-hydroxy benzoate	c1cc(O)ccc1C(=O)[O-]		$6.0\cdot10^{9}$			Anderson et al. (1987)[7]	
3-nitro benzoic acid	c1c(N(=O)=O)cccc1C(=O)O	c1HcHcHc(NO2)cHc1CO(OH)	$2.0\cdot10^{7}$			Umschlag et al. (2002)	
4-nitro benzoic acid	c1cc(N(=O)=O)ccc1C(=O)O	c1HcHc(NO2)cHcHc1CO(OH)	$2.0\cdot10^{7}$			Umschlag et al. (2002)	
3-nitro-4-methyl benzoate	c1cc(C)c(N(=O)=O)cc1C(=O)[O-]	CH3c1c(NO2)cHc(CO(OH))cHc1H	$3.3\cdot10^{7}$			Umschlag et al. (2002)	
o- methoxy phenol	Oc1ccccc1OC	c1HcHcHcHc(OH)c1-O-CH3	$1.1\cdot10^{8}$	$2.7\cdot10^{12}$	3007	Barzaghi and Herrmann (2004)	
p- methoxy phenol	c1cc(O)ccc1OC	c1HcHc(OH)cHcHc1-O-CH3	$2.8\cdot10^{9}$	$1.8\cdot10^{10}$	698	TROPOS measurements	
2,6-dimethoxy phenol	c1(OC)cccc(OC)c1O	c1HcHcHc(-O-CH3)c(OH)c1-O-CH3	$1.6\cdot10^{9}$	$1.0\cdot10^{12}$	1924	TROPOS measurements	
3-methoxy-4-hydroxy benzaldehyde	c1c(OC)c(O)ccc1C=O	CH3-O-c1c(OH)cHcHc(c1H)CHO	$1.1\cdot10^{9}$	$7.8\cdot10^{11}$	1924	TROPOS measurements	
2,4-dimethoxy-3-hydroxy benzaldehyde	c1c(OC)c(O)c(OC)cc1C=O	CH3-O-c1c(OH)c(-O-CH3)cHc(c1H)CHO	$1.7\cdot10^{9}$	$2.8\cdot10^{12}$	2165	TROPOS measurements	
4-methoxy benzoic acid	c1cc(OC)ccc1C(=O)O	CH3-O-c1cHcHc(CO(OH))cHc1H	$6.9\cdot10^{8}$			Umschlag et al. (2002)	
4-methoxy benzoate	c1cc(OC)ccc1C(=O)[O-]		$8.0\cdot10^{9}$			O’Neill et al. (1977)[7]	
3-hydroxy-4-methoxy benzoic acid	c1c(O)c(OC)ccc1C(=O)O	CH3-O-c1c(OH)cHc(CO(OH))cHc1H	$1.0\cdot10^{9}$			TROPOS measurements	
3-methoxy-4-hydroxy benzoic acid	c1c(OC)c(O)ccc1C(=O)O	CH3-O-c1c(OH)cHcHc(c1H)CO(OH)	$1.0\cdot10^{9}$	$3.8\cdot10^{11}$	1804	TROPOS measurements	
3,5-dimethoxy-4-hydroxy benzoic acid	c1c(OC)c(O)c(OC)cc1C(=O)O	CH3-O-c1c(OH)c(-O-CH3)cHc(c1H)CO(OH)	$1.4\cdot10^{9}$	$2.8\cdot10^{12}$	2285	TROPOS measurements	
4-hydroxyphenyl ethyl ether	c1cc(O)ccc1OCC	c1HcHc(OH)cHcHc1-O-CH2CH3	$8.0\cdot10^{8}$			Barzaghi and Herrmann (2004)	
Polycyclic aromatic compounds							n = 2
2-phenylphenol	c1ccccc1c2ccccc2O	c2HcHcHcHc(OH)c2c1cHcHcHcHc1H	$2.4\cdot10^{8}$			Barzaghi and Herrmann (2004)	
naphthalene	c1cccc2ccccc12	c12cHcHcHcHc1cHcHcHc2H	$1.7\cdot10^{9}$			TROPOS measurements	

Remarks: References taken from: [1]Toyota et al. (2004); [2]CAPRAM database available at http://projects.tropos.de/capram/; [3]NIST database: Ross et al. (1998); [4] de Sémainville et al. (2007); [5]Herrmann (2003); [6] Wayne et al. (1991); [7]Barzaghi and Herrmann (2004)

S2 Additional information about the evaluation of prediction methods for radical reactions with organic compounds

This section mainly presents additional tabulated statistical data and graphics to validate the different methods to predict aqueous phase kinetic data of organic compounds with the radicals OH and NO_3. Simple correlations are discussed in sections S2.1 to S2.3, while Evans-Polanyi-type correlations and structure activity relationships are discussed in the main article with additional information on Evans-Polanyi-type correlations in section S2.4.

S2.1 Gas–aqueous phase correlations

S2.1.1 OH rate constant prediction

In a first and very simple attempt, the reactivity of the hydroxyl radical in the gas phase and the aqueous phase have been compared. This method is very easy to use and can be readily implemented in computer assisted rate prediction tools. Although gas phase rate constants are usually quite well known and several recommendations with large sets of experimental values already exist (Atkinson, 2003; Atkinson et al., 2006; Burkholder et al., 2015), the method relies on gas phase kinetic data. If no experimental data is present, the method fails or has to be extended by estimated gas phase kinetic data from a different prediction method, which then increases errors.

For completeness, correlations between the experimental aqueous phase rate constants and the experimental gas phase rate constants are shown in Figure S1 for the different compound classes. In this and all other plots, data points from the various compound classes are colour-coded with the same colours. Regression lines are shown in the same colour as the corresponding data points and the 1:1 line is given as a dashed-dotted grey line. Regression lines of overall data are shown as black solid lines. The corresponding equations for the regression lines in Figure S1 and the statistical data can be found in Table S1. The aqueous phase data used for the correlations is given in Table S1. Gas phase rate constants are taken from Atkinson et al. (2006) and Atkinson (2003) or from the GECKO-A gas phase kinetics database and are listed in Table S2.

Even if this approach is simple, coefficients of determination of up to 0.9 are reached for the simplest compound class of alkanes. For the other compound classes, the coefficients of determination lie between 0.4 and 0.6. The only exception is found for unsaturated hydrocarbons, which do not correlate indicated by an R^2 of only 0.04. The poor correlation might result from a different reaction mechanism of this compound class. While all other compound classes investigated react by H-atom abstraction, unsaturated organic compounds prefer radical addition to the double bond – apparently, this step is being influenced by the solvent. Overall, it can be expected to obtain at least the correct order of magnitude of the predicted kinetic data with this prediction method when restricted to H-abstraction reactions.

Table S1 Parameters for the regression lines k_{aq} / M^{-1} s^{-1} = $A \cdot k_g$ / cm^3 s^{-1} + B, coefficients of determination R^2, standard deviations σ, and number N of the correlation of the OH rate constants in the gas and the aqueous phase as given in Figure S1.

Compound class	A / M^{-1} cm^{-3}	B / 10^9 M^{-1} s^{-1}	R^2	σ / 10^9 M^{-1} s^{-1}	N
all data	0.13±0.02	0.19±0.04	0.280	2.38	79
alkanes	1.08±0.11	0.10±0.05	0.911	0.87	11
unsat. HCs	0.04±0.05	0.52±0.18	0.085	2.91	10
alcohols	0.37±0.09	0.04±0.09	0.557	1.54	15
carbonyls	0.14±0.06	0.10±0.09	0.251	2.30	17
acids	0.29±0.28	0.01±0.02	0.514	0.11	3
ethers	0.10±0.04	0.10±0.06	0.396	0.95	11
esters	0.30±0.12	0.03±0.03	0.388	0.61	12

Formatted Table ... [3]
Deleted: Table S1 Recommended kinetic data for OH ... [1]
Formatted Table ... [2]
Deleted: paper
Formatted ... [4]
Formatted ... [5]
Deleted: Figure S1… for the different compound classes. In this ... [6]
Formatted ... [7]
Deleted: Table S3…. The aqueous phase data used for the ... [8]
Deleted: correlation …oefficients of determination of up to 0.9 are ... [9]
Deleted: , correlation
Formatted ... [10]
Deleted: 3
Formatted ... [11]
Deleted: Equations of
Formatted ... [12]
Formatted ... [13]
Field Code Changed ... [14]
Formatted ... [15]
Deleted: Regression
Formatted ... [16]
Inserted Cells ... [17]
Deleted: $k_{(aq)}$ = (0.22±0.04) · $k_{(g)}$ + (1.73±0.34)·10^9
Formatted ... [18]
Deleted: 305
Inserted Cells ... [19]
Deleted: 3·10^9
Deleted: 77
Deleted: $k_{(aq)}$ = (1.80±0.18) · $k_{(g)}$ + (9.49±4.61)·10^8
Formatted ... [20]
Deleted: 914
Deleted: 9.1·10^8
Inserted Cells ... [21]
Deleted: $k_{(aq)}$ = (0.05±0.09) · $k_{(g)}$ + (5.96±1.76)·10^9
Formatted ... [22]
Deleted: 042
Deleted: 3.…·10^9 ... [23]
Deleted: $k_{(aq)}$ = (0.62±0.16) · $k_{(g)}$ + (2.92±9.20)·10^8
Formatted ... [24]
Deleted: 570
Inserted Cells ... [25]
Deleted: 6·10^9
Deleted: 14
Deleted: $k_{(aq)}$ = (
Formatted ... [26]
Deleted: 20…4±0.06) · $k_{(g)}$ + (5.66±3.97)·10^8 ... [27]
Deleted: 508
Deleted: 9.5·10^8
Deleted: 15
Inserted Cells ... [28]
Deleted: $k_{(aq)}$ = (0.48±0.47) · $k_{(g)}$ - (7.54±24.1)·10^7
Formatted ... [29]
Inserted Cells ... [30]
Deleted: 1.5·10^8
Deleted: $k_{(aq)}$ = (0.18±0.07) · $k_{(g)}$ + (8.43±5.89)·10^8
Formatted ... [31]
Deleted: 415
Deleted: 9.8·10^8
Inserted Cells ... [32]
Deleted: $k_{(aq)}$ = (0.49±0.19) · $k_{(g)}$ + (3.13±3.21)·10^8
Formatted ... [33]
Deleted: 391
Deleted: 6.3·10^8
Deleted: 13
Inserted Cells ... [34]

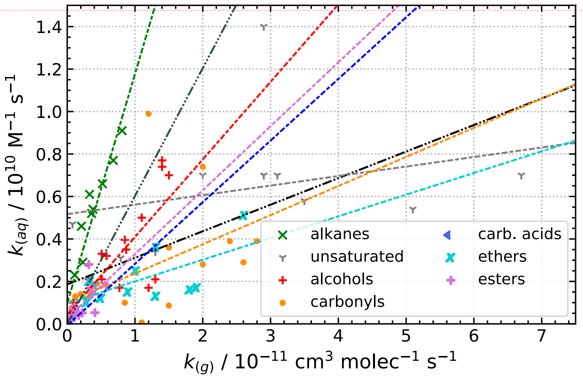

Figure S1 Correlation of aqueous phase rate constants of the hydroxyl radicals with aliphatic organic compounds with the corresponding gas phase rate constants distinguished by compound class. The equations for the regression lines as well as the corresponding R^2-, σ-, and N-values are given in Table S1.

Table S2 Compilation of gas phase kinetic data of hydroxyl radical reactions with organic compounds used for the correlation with the respective aqueous phase reactions.

Compound	Chemical formula	k_{2nd} / cm^3 $molec^{-1}$ s^{-1}	Reference
Methane	CH_4	$6.4\cdot10^{-15}$	Atkinson et al. (2006)
Ethane	CH_3CH_3	$2.4\cdot10^{-13}$	Atkinson et al. (2006)
Propane	$CH_3CH_2CH_3$	$1.1\cdot10^{-12}$	Atkinson et al. (2006)
Butane	$CH_3[CH_2]_2CH_3$	$2.3\cdot10^{-12}$	Atkinson et al. (2006)
Pentane	$CH_3[CH_2]_3CH_3$	$3.8\cdot10^{-12}$	Atkinson and Arey (2003)
Hexane	$CH_3[CH_2]_4CH_3$	$5.2\cdot10^{-12}$	Atkinson and Arey (2003)
Heptane	$CH_3[CH_2]_5CH_3$	$6.8\cdot10^{-12}$	Atkinson and Arey (2003)
Octane	$CH_3[CH_2]_6CH_3$	$8.1\cdot10^{-12}$	Atkinson and Arey (2003)
Iso-butane	$CH(CH_3)_3$	$2.1\cdot10^{-12}$	Atkinson and Arey (2003)
2-methyl butane	$CH_3CH_2CH(CH_3)_2$	$3.6\cdot10^{-12}$	Atkinson and Arey (2003)
2,2,4-trimethyl pentane	$(CH_3)_3CCH_2CH(CH_3)_2$	$3.3\cdot10^{-12}$	Atkinson and Arey (2003)
Ethylene	$CH_2{=}CH_2$	$7.9\cdot10^{-12}$	Atkinson et al. (2006)
Propylene	$CH_3CH{=}CH_2$	$2.9\cdot10^{-11}$	Atkinson et al. (2006)
1-butylene	$CH_3CH_2CH{=}CH_2$	$3.1\cdot10^{-11}$	Atkinson and Arey (2003)
butadiene	$CH_2{=}CHCH{=}CH_2$	$6.7\cdot10^{-11}$	Atkinson and Arey (2003)
Isobutylene	$CH_2{=}C(CH_3)_2$	$5.1\cdot10^{-11}$	Atkinson and Arey (2003)
Acetylene	$CH{\equiv}CH$	$7.8\cdot10^{-13}$	Atkinson et al. (2006)
Methanol	$CH_3(OH)$	$9.0\cdot10^{-13}$	Atkinson et al. (2006)
Ethanol	$CH_3CH_2(OH)$	$3.2\cdot10^{-12}$	Atkinson et al. (2006)
Propanol	$CH_3CH_2CH_2(OH)$	$5.8\cdot10^{-12}$	Atkinson et al. (2006)
Butanol	$CH_3[CH_2]_2CH_2(OH)$	$8.5\cdot10^{-12}$	Atkinson et al. (2006)
Pentanol	$CH_3[CH_2]_3CH_2(OH)$	$1.1\cdot10^{-11}$	Atkinson and Arey (2003)
Hexanol	$CH_3[CH_2]_4CH_2(OH)$	$1.5\cdot10^{-11}$	Atkinson and Arey (2003)

Deleted:

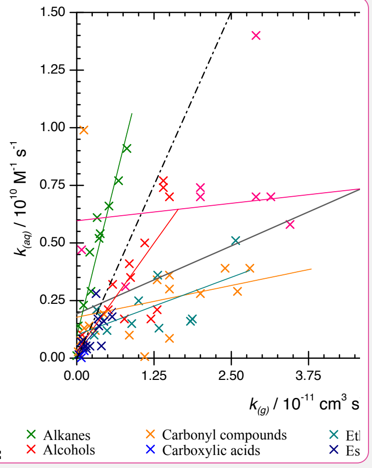

Formatted: Highlight

Deleted: Table S3

Deleted: 4

Heptanol	$CH_3[CH_2]_5CH_2(OH)$	$1.4\cdot10^{-11}$	Atkinson and Arey (2003)
Octanol	$CH_3[CH_2]_6CH_2(OH)$	$1.4\cdot10^{-11}$	Atkinson and Arey (2003)
Isobutanol	$(CH_3)_2CH(OH)$	$5.1\cdot10^{-12}$	Atkinson et al. (2006)
2-butanol	$CH_3CH_2CH(OH)CH_3$	$8.7\cdot10^{-12}$	Atkinson et al. (2006)
Tert-butanol	$(CH_3)_3C(OH)$	$1.1\cdot10^{-12}$	Atkinson and Arey (2003)
3-pentanol	$CH_3CH_2CH(OH)CH_2CH_3$	$1.3\cdot10^{-11}$	Atkinson and Arey (2003)
Ethylene glycol	$CH_2(OH)CH_2(OH)$	$7.7\cdot10^{-12}$	Atkinson (1989)
1,2-propanediol	$CH_3CH(OH)CH_2(OH)$	$1.2\cdot10^{-11}$	Atkinson (1989)
Formaldehyde	$HCHO$	$8.5\cdot10^{-12}$	Atkinson et al. (2006)
Acetaldehyde	CH_3CHO	$1.5\cdot10^{-11}$	Atkinson et al. (2006)
Propionaldehyde	CH_3CH_2CHO	$2.0\cdot10^{-11}$	Atkinson et al. (2006)
Butyraldehyde	$CH_3[CH_2]_2CHO$	$2.4\cdot10^{-11}$	Atkinson et al. (2006)
Valeraldehyde	$CH_3[CH_2]_3CHO$	$2.8\cdot10^{-11}$	Atkinson and Arey (2003)
Isobutyraldehyde	$(CH_3)_2CHCHO$	$2.6\cdot10^{-11}$	Atkinson and Arey (2003)
Acrolein	$CH_2{=}CHCHO$	$2.0\cdot10^{-11}$	Magneron et al. (2002)
Methacrolein	$CH_2{=}CH(CH_3)CHO$	$2.9\cdot10^{-11}$	Atkinson et al. (2006)
Crotonaldehyde	$CH_3CH{=}CHCHO$	$3.5\cdot10^{-11}$	Magneron et al. (2002)
Acetone	CH_3COCH_3	$1.8\cdot10^{-13}$	Atkinson et al. (2006)
Hydroxyacetone	$CH_3COCH_2(OH)$	$3.0\cdot10^{-12}$	Atkinson et al. (2006)
Methyl ethyl ketone	$CH_3CH_2COCH_3$	$1.2\cdot10^{-12}$	Atkinson et al. (2006)
Methyl propyl ketone	$CH_3CH_2CH_2COCH_3$	$4.4\cdot10^{-12}$	Atkinson and Arey (2003)
Diethyl ketone	$CH_3CH_2COCH_2CH_3$	$2.0\cdot10^{-12}$	Atkinson and Arey (2003)
Methyl vinyl ketone	$CH_2{=}CHCOCH_3$	$2.0\cdot10^{-11}$	Atkinson et al. (2006)
Methyl isobutyl ketone	$CH_3COCH_2CH(CH_3)_2$	$1.3\cdot10^{-11}$	Atkinson and Arey (2003)
Glyoxal	$CHOCHO$	$1.1\cdot10^{-11}$	Atkinson et al. (2006)
Methylglyoxal	$CH_3COCOCH_3$	$1.5\cdot10^{-11}$	Atkinson et al. (2006)
Diacetyl	$CH_3COCOCH_3$	$2.4\cdot10^{-13}$	Atkinson (1989)
Acetylacetone	$CH_3COCH_2COCH_3$	$1.2\cdot10^{-11}$	Atkinson (1989)
Acetonyl acetone	$CH_3COCH_2CH_2COCH_3$	$6.8\cdot10^{-13}$	Atkinson (1989)
Formic acid	$HC(O)OH$	$4.5\cdot10^{-13}$	Atkinson et al. (2006)
Acetic acid	$CH_3C(O)OH$	$7.4\cdot10^{-13}$	Atkinson et al. (2006)
Propionic acid	$CH_3CH_2C(O)OH$	$1.2\cdot10^{-12}$	Atkinson et al. (2006)
Dimethyl ether	$CH_3–O–CH_3$	$2.8\cdot10^{-12}$	Atkinson et al. (2006)
Diethyl ether	$CH_3CH_2–O–CH_2CH_3$	$1.3\cdot10^{-11}$	Atkinson and Arey (2003)
Methylal	$CH_3–O–CH_2–O–CH_3$	$4.9\cdot10^{-12}$	Carter (2010)
Diethoxy methane	$CH_3CH_2–O–CH_2–O–CH_2CH_3$	$1.8\cdot10^{-11}$	Thüner et al. (1999)
Ethylene glycol methyl ether	$CH_3–O–CH_2CH_2(OH)$	$1.3\cdot10^{-11}$	Carter (2010)
Ethylene glycol ethyl ether	$CH_3CH_2–O–CH_2CH_2(OH)$	$1.9\cdot10^{-11}$	Carter (2010)
Ethylene glycol butyl ether	$CH_3[CH_2]_3–O–CH_2CH_2(OH)$	$2.6\cdot10^{-11}$	Carter (2010)
Methyl tert-butyl ether	$CH_3–O–C(CH_3)_3$	$3.2\cdot10^{-12}$	Teton et al. (1996)
Ethyl tert-butyl ether	$CH_3CH_2–O–C(CH_3)_3$	$8.9\cdot10^{-12}$	Teton et al. (1996)
Di-isopropyl ether	$(CH_3)_2CH–O–CH(CH_3)_2$	$1.0\cdot10^{-11}$	Mellouki et al. (1995)

Deleted: 2,2,4-trimethyl pentane

Di-tert-butyl ether	$(CH_3)_3C–O–C(CH_3)_3$	$3.9\cdot10^{-12}$	Average of Nielsen et al. (1995) and Langer et al. (1996)
Ethyl formate	$CH_3CH_2–O–CHO$	$1.0\cdot10^{-12}$	Carter (2010)
Butyl formate	$CH_3[CH_2]_3–O–CHO$	$3.1\cdot10^{-12}$	Carter (2010)
Tert-butyl formate	$(CH_3)_3C–O–CHO$	$7.5\cdot10^{-13}$	Le Calvé et al. (1997c)
Methyl acetate	$CH_3CO–O–CH_3$	$3.4\cdot10^{-13}$	El Boudali et al. (1996)
Methyl propionate	$CH_3CH_2CO–O–CH_3$	$1.0\cdot10^{-12}$	Carter (2010)
Ethyl acetate	$CH_3CH_2–O–COCH_3$	$1.6\cdot10^{-12}$	Carter (2010)
Ethyl propionate	$CH_3CH_2CO–O–CH_2CH_3$	$2.14\cdot10^{-12}$	Wallington et al. (1988)
Propyl acetate	$CH_3[CH_2]_2–O–COCH_3$	$3.6\cdot10^{-12}$	El Boudali et al. (1996)
Methyl butyrate	$CH_3[CH_2]_2CO–O–CH_3$	$3.4\cdot10^{-12}$	Le Calvé et al. (1997a)
Butyl acetate	$CH_3[CH_2]_3–O–COCH_3$	$5.7\cdot10^{-12}$	El Boudali et al. (1996)
Ethyl butyrate	$CH_3[CH_2]_2CO–O–CH_2CH_3$	0	Ferrari et al. (1996)
Isopropyl acetate	$(CH_3)_2CH–O–COCH_3$	$4.0\cdot10^{-12}$	Le Calvé et al. (1997b)
Dimethyl succinate	$CH_3–O–CO[CH_2]_2CO–O–CH_3$	$1.5\cdot10^{-12}$	Carter (2010)

S2.1.2 NO_3 rate constant prediction

This method is not suitable for NO_3 rate constant prediction. There are only few species for which NO_3 rate constants exist in both the gas and the aqueous phase. Correlations can only be derived for limited compound classes with a distinct structure and the method is not suitable to predict the whole range of organic compounds relevant for tropospheric chemistry as needed by mechanism auto-generation.

S2.2 Homologous series of compound classes

S2.2.1 OH rate constant prediction

Linear extrapolations or other suitable regression methods can be used to extrapolate the abundant measurements of small molecules in a homologous series to larger carbon numbers. However, the method is restricted to very defined structures such as alkanes or alkanes with a terminal functionality.

For proof of concept, the method was first tested for alkanes despite their irrelevance for aqueous phase chemistry. Even for pure hydrocarbons, the restrictions of the method can be seen. Figure S2a shows the regression of the homologous series of alkanes. The dataset demonstrates the necessity for a distinction by chemical structure and two regression lines can be found: one for linear (with 8 data points) and one for branched alkanes (with 4 data points). The regression lines, however, show a high accuracy with coefficients of determination R^2 of 0.98 and 0.97, respectively.

Figure S2b shows the data for mono-alcohols, which underlines the importance of the structure of the molecules. The rate constants of unsaturated alcohols have a very poor correlation with the carbon number and mono-alcohols with internal hydroxyl groups seem to be totally uncorrelated. Only the regression of linear mono-alcohols with terminal hydroxyl groups shows satisfactory results, which is, therefore, the only regression line for mono-alcoholic compounds shown in Figure S2b. The data of linear alcohols points at another general problem in the data analysis – data selection. In Figure S2b, the last three data points show a different slope in the regression than the first five data points. Data for the C_5 to C_8 alcohols were measured by Scholes and Willson (1967) while the other data are from different sources. It is hard to evaluate whether the different trends derive from different experimental setups or are the consequence of other effects like the approach of the reaction limit. Using separate correlations for the n-alcohol series split between C_5 and C_6 (dashed lines in Figure S2b) instead of the overall trend

Deleted: relevant organics compounds

Deleted: for automatic

Deleted: self

Deleted: prove

Deleted: Figure S2

Deleted: correlation

Deleted: Figure S2

Deleted: again,

Deleted: Figure S2

Deleted: From this regression, another crucial parameter becomes obvious, which is valid for all estimation methods; that is the large compounds. For example, a predicted rate constant for a C_{12} alcohol would be only 74% of the rate constant, which uses the overall data, compared to the prediction with separate correlations.

Moved (insertion) [1]

Formatted: Font: Times New Roman

Deleted: ¶

(solid line) would result in predicted rate constant of a C_{12} alcohol that is only 74% of that predicted by the overall trend. This demonstrates that careful evaluation is necessary as well as a revision how far extrapolations can be extended to not violate other rules like the limits of reaction.

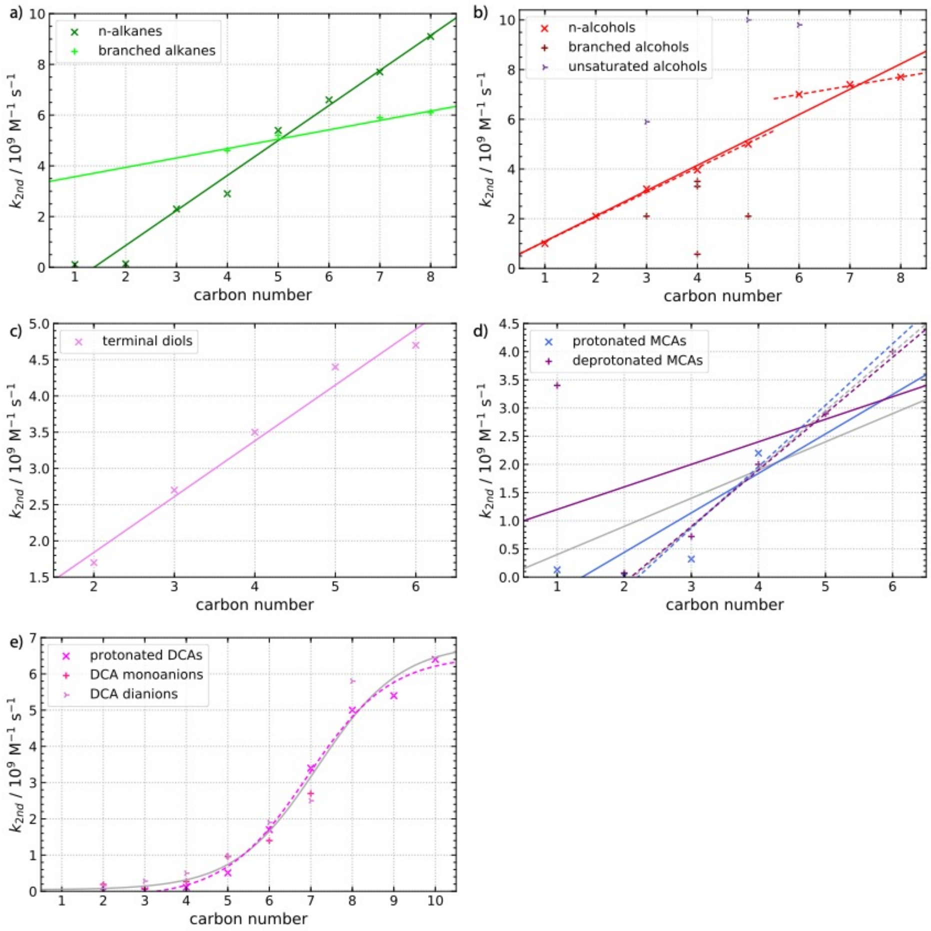

Figure S2 Homologous series of OH reaction rate constants for various compound classes. Correlation lines are shown in the same colour as the data points. The dashed lines in subfigure b are separate correlations for C_1 to C_5 and C_6 to C_8 compounds. Dashed lines in subfigure d refer to correlations without formic acid/formate. In subfigure e, the pink line represents the best fit of the Markov distribution of the fully protonated acids and the grey line is the fit of all protonation states. The respective equations for the regression lines (including the Markov distributions) can be found in in Table S3.

Deleted: c

Deleted: d

Deleted: Table S5

Field Code Changed

Table S3 Equations of the regression lines, coefficients of determination R^2, standard deviations σ (or χ^2 for DCAs), and number N for the correlation of the OH reactivity over the carbon number.

Deleted: 5

Deleted: correlation

Compound class	Regression	R^2	σ / M^{-1} s^{-1} $\chi^{2\ a}$	N

Linear alkanes	$k_{2nd} = (1.38\pm0.08)\cdot10^9 \cdot CN - (1.9\pm0.4)\cdot10^9$	0.980	$5.2\cdot10^8$	8
Branched alkanes	$k_{2nd} = (3.7\pm0.4)\cdot10^8 \cdot CN + (3.2\pm0.3)\cdot10^9$	0.971	$1.4\cdot10^8$	4
Terminal alcohols	$k_{2nd} = (1.02\pm0.06)\cdot10^9 \cdot CN + (7\pm33)\cdot10^7$	0.977	$4.2\cdot10^8$	8
Terminal C_1 - C_5 alcohols	$k_{2nd} = (9.9\pm0.3)\cdot10^8 \cdot CN + (9\pm12)\cdot10^7$	0.996	$1.1\cdot10^8$	5
Terminal C_6 - C_8 alcohols	$k_{2nd} = (3.5\pm0.3)\cdot10^8 \cdot CN + (4.9\pm0.2)\cdot10^9$	0.993	$4.1\cdot10^7$	3
Diols	$k_{2nd} = (7.7\pm0.7)\cdot10^8 \cdot CN + (3\pm3)\cdot10^8$	0.975	$2.2\cdot10^8$	5
Monoacids	$k_{2nd} = (5\pm2)\cdot10^8 \cdot CN - (1\pm9)\cdot10^8$	0.378	$1.2\cdot10^9$	10
Undissociated monoacids	$k_{2nd} = (7\pm3)\cdot10^8 \cdot CN - (9.6\pm9)\cdot10^8$	0.667	$7.3\cdot10^8$	4
Dissociated monoacids	$k_{2nd} = (4\pm4)\cdot10^8 \cdot CN + (8\pm13)\cdot10^8$	0.236	$1.5\cdot10^9$	6
Monoacids (woC$_1$)	$k_{2nd} = (1.03\pm0.08)\cdot10^9 \cdot CN - (2.2\pm0.3)\cdot10^9$	0.966	$2.9\cdot10^8$	8
Undissociated monoacids (woC$_1$)	$k_{2nd} = (1.09\pm0.5)\cdot10^9 \cdot CN - (2.4\pm1)\cdot10^9$	0.852	$6.4\cdot10^8$	3
Dissociated monoacids (woC$_1$)	$k_{2nd} = (1.00\pm0.05)\cdot10^9 \cdot CN - (2.1\pm0.2)\cdot10^9$	0.993	$1.6\cdot10^8$	5
DCAs	$k_{2nd} = \frac{(4\pm15)\cdot10^7-(6.8\pm0.3)\cdot10^9}{1+\exp\{CN-(6.0\pm0.1)/(0.8\pm0.1)\}} + (6.8\pm0.3)\cdot10^9$	0.958	$2.2\cdot10^{17}$	21
Undissociated DCAs	$k_{2nd} = \frac{(2\pm2)\cdot10^8-(6.5\pm0.5)\cdot10^9}{1+\exp\{CN-(5.9\pm0.2)/(0.8\pm0.1)\}} + (6.5\pm0.5)\cdot10^9$	0.995	$4.9\cdot10^{16}$	9

[a]for DCAs a Boltzmann distribution is used. For these compound classes χ^2 is given instead of σ.

Another group of alcohols for which the extrapolation of a homologous series works well are terminal diols with an alcohol function at each end of the molecule. Only minimal absolute errors are observed as can be seen from Figure 1 in the main article.

Furthermore, the method was tested for linear carboxylic acids. Results are given in Figure S2d and Table S3. These data show no big differences for the rate constants for protonated and deprotonated acids, respectively. Furthermore, for both forms the C_1 acid forms an exception with higher rate constants than the ones expected from a linear regression. This effect is much stronger for the deprotonated forms. When omitting formic acid, however, the good performance of the prediction method can be confirmed with a coefficient of determination R^2 of 0.97 for the regression line using both, the dissociated and undissociated forms. When investigating both forms separately, the deprotonated form correlates better with a R^2 of 0.99 compared to R^2 = 0.85 of the protonated form.

Interesting effects are observed for the correlation of linear dicarboxylic acids (DCAs). The dataset for all three forms, the protonated forms, the mono-anions, and the di-anions, is shown in Figure S2e. From this Figure it can be seen that no linear regression is valid for DCAs. There is only a moderate, non-linear increase in the rate constants for DCAs with less than 7 carbon atoms. Rate constants stay below $2\cdot10^9$ M^{-1} s^{-1}. Then the rate constants jump to values above $5\cdot10^9$ M^{-1} s^{-1} for DCAs with more than 7 carbon atoms and do, again, only moderately increase. For such a distribution, a sigmoidal function can be used and the Markov distribution has been applied. There is again a good correlation with a R^2 of 0.96 for the overall data.

It can only be speculated on the reason why a linear correlation does not apply to dicarboxylic acids. A likely explanation is the special structure of this compound class. The polarity and the large diffusion volume of the carboxyl group may shield the inner methylene groups in the carbon skeleton and hinder any radical attack for small DCAs. If a certain size of the carbon skeleton is reached (i.e. C_7), an unproportional increase of the reaction rate constant is seen to values without the shielding effect. These rate constants of large DCAs are close to the diffusion limits of hydroxyl radical reactions (see Schöne et al., 2014), thus, only a moderate increase is observed afterwards. This effect was seen for all dissociation states of carboxylic acids, therefore, different reaction mechanisms such as electron transfer reactions (ETRs) are an unlikely explanation for this effect.

Deleted: 10^8

Deleted: 1

Deleted: $$k_{2nd} = \frac{-(9\pm15)\cdot10^7-(6.3\pm0.3)\cdot10^9}{1+\exp\{CN-(6.9\pm0.1)/(0.9\pm0.1)\}} + (6.3\pm0.3)\cdot10^9$$

Deleted: $$k_{2nd} = \frac{-(2\pm2)\cdot10^8-(6.5\pm0.5)\cdot10^9}{1+\exp\{CN-(7.2\pm0.2)/(0.7\pm0.1)\}} + (6.5\pm0.5)\cdot10^9$$

Moved (insertion) [2]

Deleted: dependence on the experimental dataset. From Figure S2b can be seen that C_6 to C_8 compounds show a different behaviour than the lower weight compounds up to C_5. The data of the C_6 to C_8 compounds is taken from the study of

Moved up [1]: Scholes and Willson (1967)

Formatted: Font: Times New Roman

Deleted: [2] while the rate data of the other compounds is from different sources. Without confirming measurements, it cannot be clarified whether this effect is due to the experimental determination of the data or a real effect of the carbon number of larger compounds. While the correlation of the overall data is still very good with an R^2 of 0.98, considering a different correlation for C_6 and higher compounds would have a significant effect due to the different slopes of the regression lines. This is the case especially for large compounds. For example, using the regression line from the C_6 to C_8 data to predict the rate constant of a C_{12} alcohol yields a k_{2nd} value only 74% of the prediction from the overall correlation using all data points. …

Moved up [2]: Another group of alcohols for which the extrapolation of a homologous series works well are terminal diols with an alcohol function at each end of the molecule. Only minimal absolute errors are observed as can be seen from Figure 1 in the main

Deleted: paper.¶

Deleted: Figure S2

Deleted: Table S5

Deleted: correlation

Deleted: Figure S2

Deleted: d

S2.2.2 NO_3 rate constant prediction

Homologous series are, again, impractical to predict NO_3 rate constants due to the limited experimental dataset. The dataset allowed the determination of regression lines only for several alcohols and for aldehydes. However, for the regressions no more than 8 data points could be used (see Table S4). An exception is the correlation of all alcohols including linear, branched and substituted saturated mono-alcohols and gem-diols. However, the correlation is weak with a coefficient of determination R^2 of 0.5. All correlation data can be found in Table S4. Moreover, Figure S3a gives the dataset and regression lines of the NO_3 reaction rate constants of various alcohols plotted against the carbon number. Further compound classes show a bad correlation with the exception of aldehydes with a coefficient of determination R^2 of 0.85 as shown in Figure S3b and Table S4.

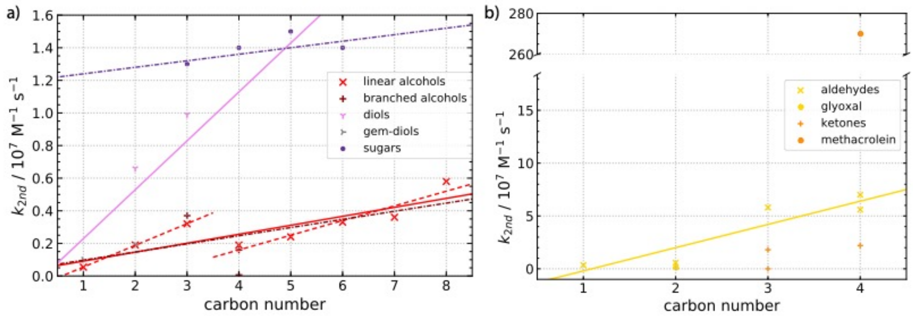

Figure S3 Homologous series of NO_3 reaction rate constants of various compound classes as indicated in the figure legend. The respective equations for the regression lines can be found in Table S4.

Table S4 Equations of the regression lines, coefficients of determination R^2, standard deviations σ, and number N for the correlation of the NO_3 reactivities over the carbon number.

Compound class	Regression	R^2	σ / M^{-1} s^{-1}	N
Linear monoalcohols	$k_{2nd} = (5.5\pm1.3)\cdot10^5 \cdot CN + (3.6\pm6.6)\cdot10^5$	0.748	$8.4\cdot10^5$	8
- C1 – C3	$k_{2nd} = (1.33\pm0.02)\cdot10^6 \cdot CN - (7.8\pm0.4)\cdot10^5$	1.000	$2.4\cdot10^4$	3
- C4 – C8	$k_{2nd} = (9.0\pm1.8)\cdot10^5 \cdot CN - (2.0\pm1.1)\cdot10^6$	0.894	$5.7\cdot10^5$	5
- with substitutions/ gem-diols	$k_{2nd} = (5.0\pm1.5)\cdot10^5 \cdot CN + (4.7\pm6.6)\cdot10^5$	0.501	$1.1\cdot10^6$	13
Polyols	$k_{2nd} = (3.0\pm0.9)\cdot10^6 \cdot CN - (7.1\pm34.2)\cdot10^5$	0.746	$3.7\cdot10^6$	6
- sugars	$k_{2nd} = (4.0\pm3.5)\cdot10^5 \cdot CN + (1.2\pm0.2)\cdot10^7$	0.400	$7.7\cdot10^5$	4
Aldehydes	$k_{2nd} = (2.2\pm0.5)\cdot10^7 \cdot CN - (2.4\pm1.6)\cdot10^7$	0.853	$1.4\cdot10^7$	5

The regression lines from Table S6 have been used to predict the rate constants of the nitrate radical with organic compounds. The absolute errors have been determined and plotted as box plots in Figure 1 of the main article. Although the errors are relatively small, it is not recommended to use this method. The dataset to derive the regression lines is small, and possible

Deleted: Table S6

Deleted: correlation

Deleted: Table S6

Deleted: Figure S3

Deleted: correlation

Deleted: Figure S3

Deleted: Table S6

Deleted: ¶

¶

(a) Alcohol compounds

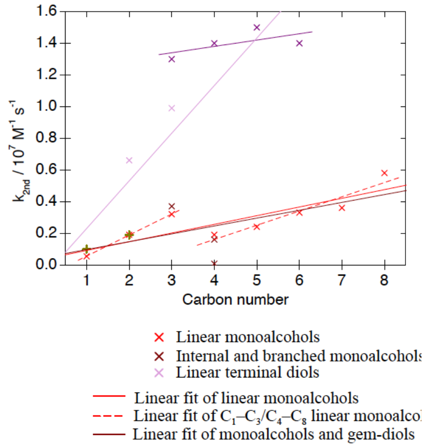

Deleted: **Table S6**

Deleted: **6**

Deleted: **correlation**

Deleted: S4.

changes in only a few experimental values could lead to substantial changes in the predicted rate data. With no use of separate training and validation sets, correlations are too uncertain for any computer-based mechanism auto-generation protocols.

S2.3 Reactivity comparison between OH and NO_3

The kinetics database (presented in and) has been used to compare the reactivities of the hydroxyl and nitrate radicals. Results from the evaluation are shown in Figure S4. In general, the reactivity of NO_3 is smaller than that of OH. On average, the decrease in the reactivity is about 2 orders of magnitude as can be seen from the data points as well as the correlation line of all data (dashed violet line) in Figure S4. The only exception is oxalic acid, where the electron transfer of oxalate with the nitrate radical is so fast that the reactivity of the mono-anion is close to the reactivity of the corresponding OH reaction and that of the di-anion is even higher than the corresponding OH reaction.

The regression lines (see also Table S5) can be used to predict the reaction rates of the nitrate radical when the aqueous OH reactivities are known. However, with coefficients of determination R^2 between 0.21 and 0.89 and 0.06 for the overall data, the quality of the prediction is weak. Moreover, the method is restricted to the dataset of the hydroxyl reactions in the aqueous phase and therefore unsuitable for automated rate prediction.

Table S5 Equations of the regression lines $\log(k_{NO3}$ / M^{-1} $s^{-1}) = A \cdot \log(k_{OH}$ / M^{-1} $s^{-1}) + B$, coefficients of determination R^2, standard deviations σ, and number N for the correlation of the OH and NO_3 reactivities.

compound class	A / M^{-1} s^{-1}	B / M^{-1} s^{-1}	R^2	σ	N
Alcohols	1.26±0.24	5.74±2.26	0.757	0.27	11
Di- and polyols	4.58±0.66	35.28±6.05	0.873	0.18	9
Carbonyls	1.43±0.49	6.33±4.44	0.521	0.89	10
Mono-carboxylic acids	1.05±0.22	2.77±2.00	0.598	0.71	17
Di-carboxylic acids	1.39±0.61	4.62±4.85	0.425	1.26	9
All data	0.77±0.15	0.33±1.39	0.316	0.89	56

Deleted: …based mechanism self ... [35]
Formatted ... [36]
Field Code Changed ... [37]
Deleted: Figure S4…. In general, the reactivity of NO_3 is smaller ... [38]
Deleted: Table S7…) can be used to predict the reaction rates of ... [39]
Deleted: 7… **Equations of the regression lines, correlation** ... [40]
Deleted: regression
Formatted ... [41]
Formatted ... [42]
Deleted: R^2
Deleted Cells ... [43]
Deleted: σ
Formatted ... [44]
Inserted Cells ... [45]
Inserted Cells ... [46]
Deleted: k_{NO3} = (
Formatted ... [47]
Deleted: 3…6±0.3) · k_{OH} - (5.9±2.4) ... [48]
Inserted Cells ... [49]
Deleted: 741
Deleted: 29
Deleted: k_{NO3} = (
Formatted ... [50]
Deleted: 5…8±0.6) · k_{OH} - (34.5±5.5) ... [51]
Deleted: 889
Deleted: k_{NO3} = (
Formatted ... [52]
Deleted: 6…3±0.6) · k_{OH} - (7.8±5.0) ... [53]
Deleted: 549
Deleted: 97
Deleted: 9
Deleted: k_{NO3} = (
Formatted ... [54]
Deleted: 3…5±0.3) · k_{OH} - (5.0±2.6) ... [55]
Deleted: 654
Deleted: 68
Deleted: 12
Deleted: k_{NO3} = (0.6±0.8) · k_{OH} + (2.1±6.3)
Formatted ... [56]
Deleted: 212
Deleted: 97
Deleted: 4
Formatted Table ... [57]
Deleted: k_{NO3} = (
Formatted ... [58]
Deleted: 4…7±0.2) · k_{OH} + (2.8±2.0) ... [59]
Deleted: 0.059
Deleted Cells ... [60]
Deleted: 16
Deleted: 54
Inserted Cells ... [61]
Inserted Cells ... [62]

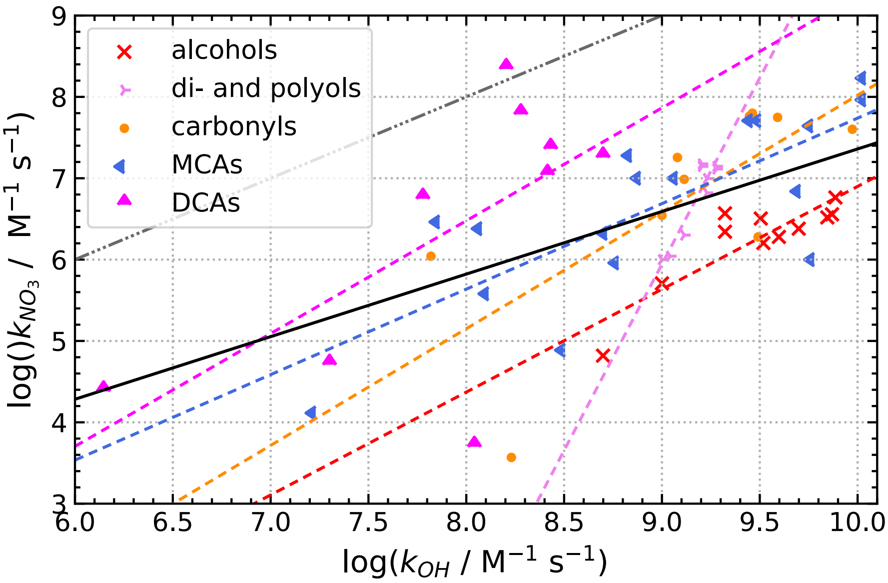

Figure S4 Correlation of the reactivities of the hydroxyl and the nitrate radical with aliphatic organic compounds as listed in the figure legend. The equations for the regression lines as well as the corresponding R^2-, σ-, and N-values are given in Table S5.

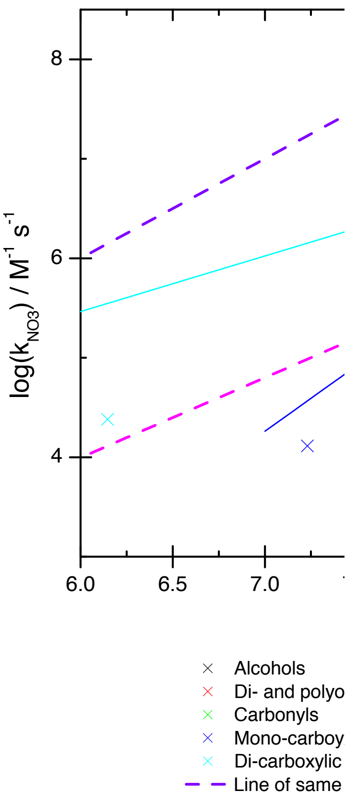

Deleted:

Deleted: Table S7

S2.4 Evans-Polanyi-type correlations

S2.4.1 OH radical reactions

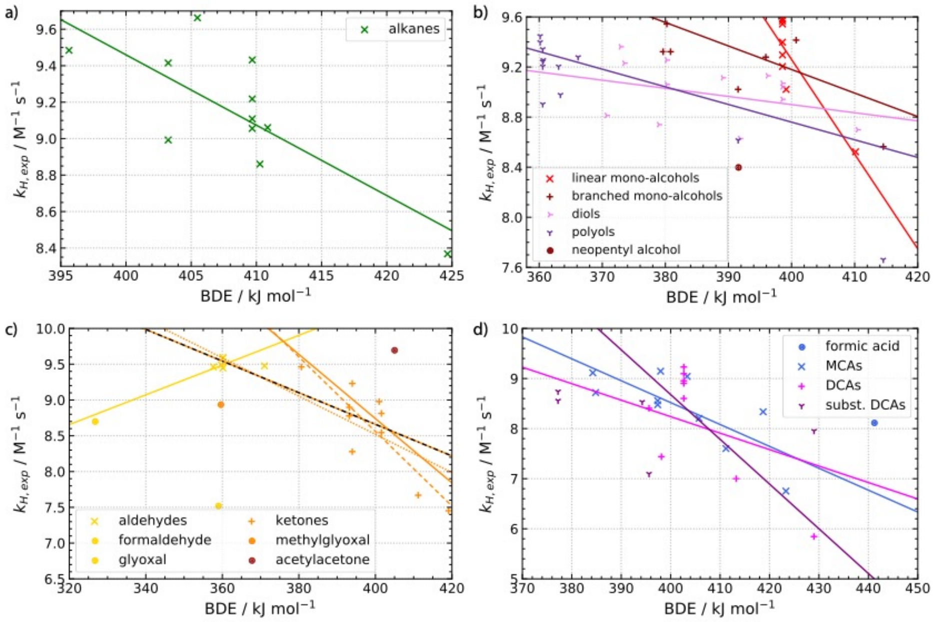

Figure S5 Evans-Polanyi-type correlations of hydroxyl radicals with the respective compound classes. In subfigure c, the dotted line represents the linear fit of ketones excluding methylglyoxal, the dashed line represents the correlation of ketones without acetylacetone. For the dashed-dotted line, both compounds have been omitted. The black dashed-dotted line in subfigure c is the overall correlation of all carbonyl compounds except glyoxal and formaldehyde. The respective equations for the regression lines can be found in Table S6.

Deleted:

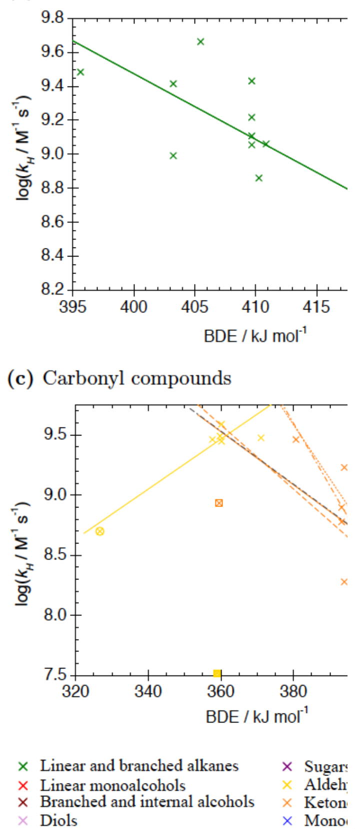

Deleted: grey

Deleted: Table S8

Table S6 Parameters for the regression equations log(k_H/M^{-1} s^{-1}) = A·(BDE/kJ mol^{-1}) + B and statistical data derived from the Evans-Polanyi-type correlations of aqueous phase hydroxyl radical reactions with organic compounds for the various compound classes.

Deleted: 8

Compound class	$10^2 \cdot A^{(a)}$	$10^{-1} \cdot B^{(b)}$	R^2	σ / M^{-1} s^{-1}	N
Alkanes	-(3.86±1.1)	2.49±0.4	0.595	0.24	11
Linear terminal monoalcohols	-(7.56±1.9)	3.95±0.7	0.732	0.20	8
All monoalcohols	-(1.88±0.8)	1.67±0.3	0.315	0.28	15
Diols	-(0.65±0.5)	1.15±0.2	0.126	0.22	13
Diols and sugars	-(1.41±0.3)	1.44±0.1	0.439	0.28	25
Monoaldehydes	2.08±0.4	0.20±0.1	0.852	0.13	7
Ketones and diketones	-(2.21±1.2)	1.75±0.5	0.254	0.60	12
- without methylglyoxal	-(4.49±1.7)	2.67±0.7	0.444	0.54	11
- without acetylacetone	-(2.67±1.0)	1.92±0.4	0.453	0.48	11
- without both	-(5.21±1.1)	2.94±0.4	0.745	0.35	10
Carbonyl compounds (without glyoxal and formaldehyde)	-(2.21±0.6)	1.75±0.2	0.497	0.48	18
Monocarboxylic acids (without formic acid)	-(4.37±1.3)	2.60±0.5	0.573	0.52	10
All dicarboxylic acids	-(3.29±1.6)	2.14±0.6	0.257	0.88	14
Unsubstituted carboxylic acids	-(8.93±2.8)	4.44±1.1	0.601	0.78	5

$^{(a)}$ in l kJ^{-1} s^{-1}, $^{(b)}$ in M^{-1} s^{-1}

Deleted: -(.065

Deleted: 9

Deleted: mol

Deleted: $^{-1}$ M

2.4.2 NO$_3$ radical reactions

Table S7 Parameters for the regression equations log(k_H/M^{-1} s^{-1}) = A·(BDE/kJ mol^{-1}) + B and statistical data derived from the Evans-Polanyi-type correlations of aqueous phase nitrate radical reactions with organic compounds for the various compound classes.

Deleted: 9

Compound class	$10^2 \cdot A^{(a)}$	$10^{-1} \cdot B^{(b)}$	R^2	σ / M^{-1} s^{-1}	N
Monoalcohols	-(6.91±1.8)	3.35±0.7	0.628	0.49	11
Diols	-(2.76±0.7)	1.70±0.3	0.680	0.35	9
All alcohols	-(3.45±0.6)	1.96±0.3	0.616	0.47	20
Carbonyl compounds	-(2.89±1.7)	1.73±0.6	0.256	1.41	10
Carboxylic acids (without formic and mesoxalic acid)	-(5.65±1.7)	2.80±0.7	0.698	0.61	7

$^{(a)}$ in l kJ^{-1} s^{-1}, $^{(b)}$ in M^{-1} s^{-1}

S2.4.3 Improved Evans-Polanyi-type correlations

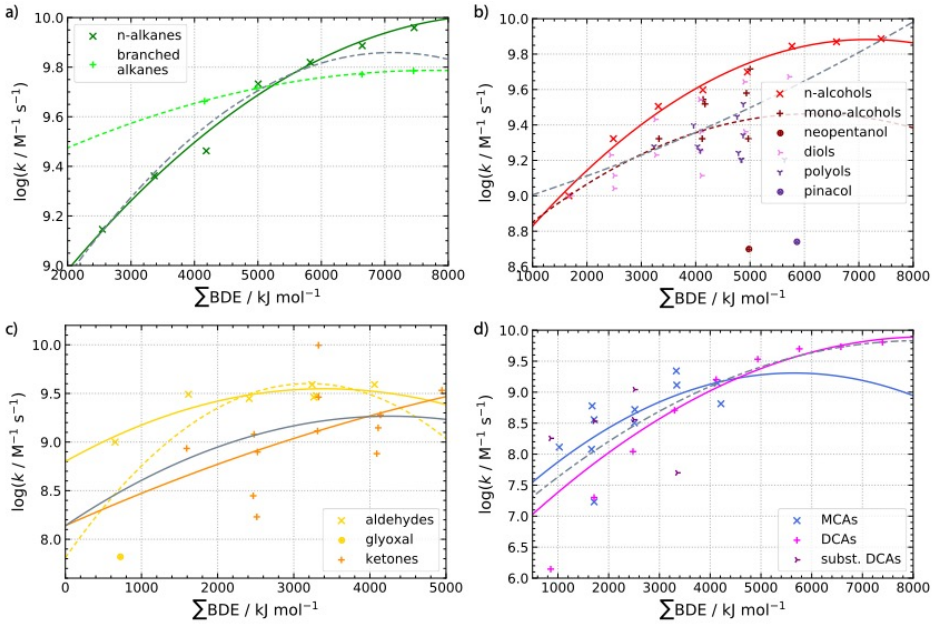

Figure S6 Improved Evans-Polanyi-type correlations of hydroxyl radical reactions with organic compounds for the respective compound classes. The grey line in subfigure b represents the quadratic regression of all alcohol compounds except linear mono-alcohols and the dashed orange line in subfigure c is the regression line of all aldehydes (including glyoxal as only dialdehyde). The respective equations for the regression lines can be found in Table S8.

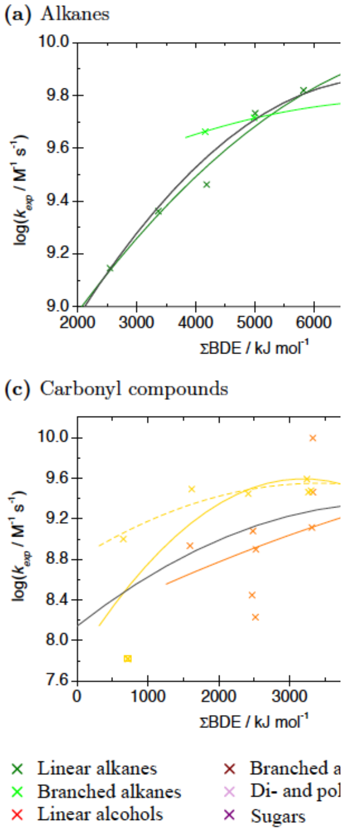

Deleted:

Deleted: monoalcohols

Deleted: respecitive

Deleted: Table S10

Table S8 Parameters for the regression equations log(k/M^{-1} s^{-1}) = A·(∑BDE/kJ mol^{-1})^2 + B·(∑BDE/kJ mol^{-1}) + C and statistical data derived from the improved Evans-Polanyi-type correlations of aqueous phase hydroxyl radical reactions with organic compounds for the various compound classes.

Compound class	$10^8 \cdot A^{(a)}$	$10^4 \cdot B^{(b)}$	$C^{(c)}$	R^2	σ / M^{-1} s^{-1}	N
Linear alkanes	-(2.21±0.7)	3.90±0.7	8.29±0.17	0.986	0.04	7
Branched alkanes	-(0.94±0.2)	1.46±0.5	9.22±0.07	0.998	0.04	4
All alkanes	-(3.46±1.0)	4.92±1.1	8.11±0.26	0.923	0.08	11
Linear terminal mono-alcohols	-(2.77±0.5)	3.97±0.4	8.46±0.09	0.987	0.04	8
All other alcohols*	-(2.31±2.5)	2.84±2.0	8.59±0.36	0.346	0.15	32
All alcohols	0.55±1.2	0.90±1.0	8.91±0.22	0.523	0.17	40
Monoaldehydes	-(6.44±3.8)	4.39±1.8	8.80±1.09	0.810	0.11	7
All aldehydes	-(17.5±14.5)	11.2±6.6	7.81±0.61	0.630	0.43	8
Ketones	-(1.67±14.3)	3.49±9.5	8.14±1.50	0.238	0.46	10
All carbonyl compounds	-(6.19±5.2)	5.48±3.1	8.14±0.43	0.288	0.41	23
Monocarboxylic acids	-(6.62±11.1)	7.49±6.6	7.19±0.86	0.548	0.46	12
Di- and polycarboxylic acids	-(4.70±4.7)	7.81±3.9	6.65±0.66	0.665	0.66	14
All carboxylic acids	-(4.33±3.3)	7.04±2.6	6.97±0.44	0.602	0.57	26

(a) in mol l kJ^{-2} s^{-1}, (b) in l kJ^{-1} s^{-1}, (c) in M^{-1} s^{-1}

*except outliers neopentanol and pinacol

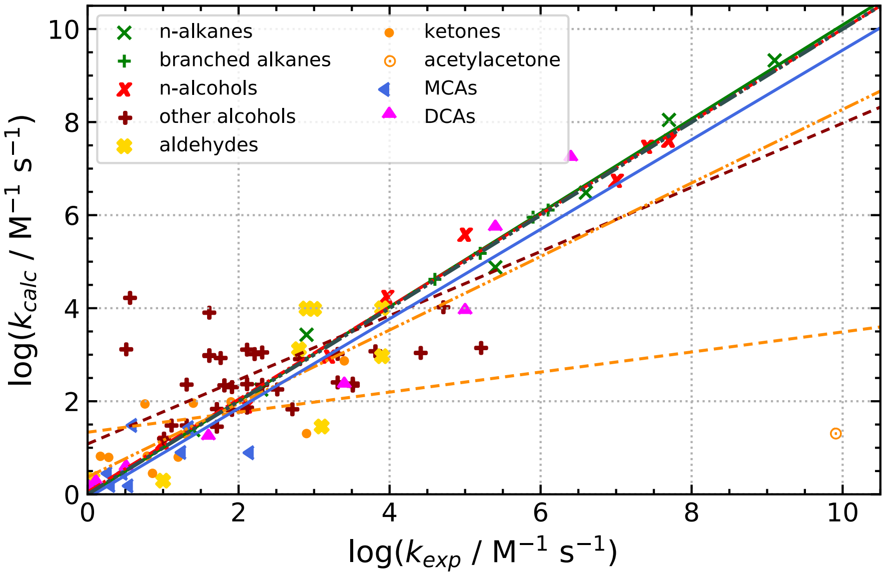

Figure S7 Plot of predicted versus experimental data for hydroxyl radical reactions separated by compound class together with the linear regression lines. For the calculation of the predicted values, the regression lines of Table S8 together with the kinetic data from have been used. For ketones, the dashed line includes the outlier acetylacetone while the solid line does not. The black dashed-dotted line is the line of same reactivity.

Deleted: 10

Deleted: monoalcohols

Deleted: l^2

Deleted:

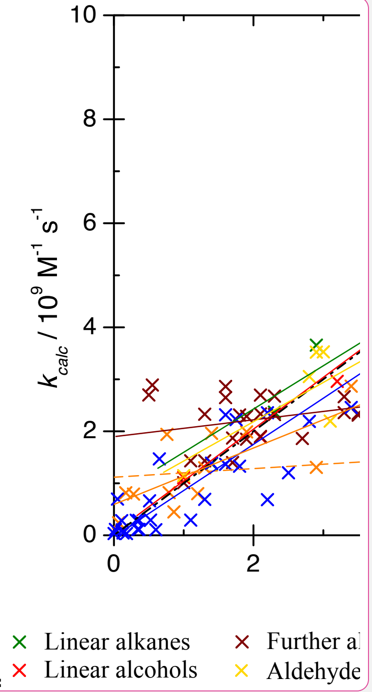

Deleted: Table S10

Field Code Changed

Table S9 Parameters for the linear regression equations log(k_H/M^{-1} s^{-1}) = A·(BDE/kJ mol^{-1}) + B and statistical data derived from the improved Evans-Polanyi-type correlations of aqueous phase nitrate radical reactions with organic compounds for the various compound classes.

Deleted: 11

Compound class	$10^4 \cdot A^{(a)}$	$B^{(b)}$	R^2	σ / M^{-1} s^{-1}	N
Monoalcohols and gem-diols	1.18±0.27	5.87±0.11	0.601	0.18	15
Di- and polyols	0.91±0.36	6.71±0.15	0.611	0.10	6
Carbonyl compounds	5.44±0.91	5.82±0.23	0.799	0.34	10
Carboxylic acids	-(3.92±4.3)	5.23±0.78	0.173	0.67	6

$^{(a)}$ in l kJ^{-1} s^{-1}, $^{(b)}$ in M^{-1} s^{-1}

Table S10 Parameters for the quadratic regression equations log(k_{exp}/M^{-1} s^{-1}) = A·(∑BDE/kJ mol^{-1})^2 + B·(∑BDE/kJ mol^{-1}) + C and statistical data derived from the improved Evans-Polanyi-type correlations of aqueous phase nitrate radical reactions with organic compounds for the various compound classes.

Deleted: 12

Compound class	$10^8 \cdot A^{(a)}$	$10^4 \cdot B^{(b)}$	$C^{(c)}$	R^2	σ / M^{-1} s^{-1}	N
Monoalcohols and gem-diols	-(1.85±1.6)	2.77±1.4	5.59±0.27	0.639	0.18	15
Di- and polyols	-(6.71±2.2)	6.37±1.8	5.68±0.35	0.905	0.05	6
Carbonyl compounds	-(3.84±10.0)	7.16±4.6	5.67±0.44	0.803	0.36	10
Carboxylic acids	8.15±106.3	-(6.71±36.7)	5.44±2.83	0.175	0.77	6

$^{(a)}$ in mol kJ^{-2} s^{-1}, $^{(b)}$ in l kJ^{-1} s^{-1}, $^{(c)}$ in M^{-1} s^{-1}

Deleted: l^2

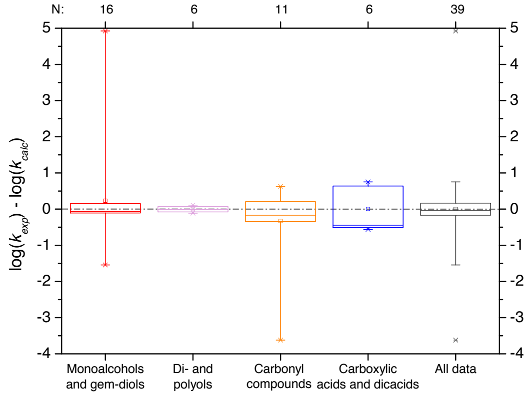

Figure S8 Box plots for the absolute errors of the improved Evans-Polanyi-type correlations of nitrate radical reactions with the respective compound classes.

S2.5 Evaluation of structure-activity relationships

Table S11. Parameters for the regression equations (k_{calc} / M^{-1} s^{-1}) = A· (k_{exp} / M^{-1} s^{-1}) + B and statistical data derived from the evaluation process of the structure-activity relationship by Doussin and Monod (2013).

Deleted: 13

Compound class	*A*	10^{-8}·*B*	R^2	σ / 10^8 M^{-1} s^{-1}	N
Alkanes	0.80±0.08	4.28±4.8	0.908	6.81	11
Monoalcohols	0.97±0.09	1.52±4.0	0.886	7.73	16
Di- and polyols	1.40±0.21	0.10±5.3	0.701	10.75	21
Carbonyl compounds$^{(a)}$	1.14±0.15	-0.65±3.6	0.828	7.78	14
Monocarboxylic acids	0.96±0.10	1.48±1.8	0.869	4.38	16
Dicarboxylic acids	0.90±0.07	3.20±2.1	0.902	6.49	19
Polyfunctional compounds	0.44±0.29	-0.004±1.7	0.333	5.22	24

(a) including dicarbonyl compounds except acetylacetone

Table S12. Parameters for the regression equations (k_{calc} / M^{-1} s^{-1}) = A· (k_{exp} / M^{-1} s^{-1}) + B and statistical data derived from the evaluation process of the structure-activity relationship by Minakata et al (2009).

Deleted: 14

Compound class	*A*	10^{-8}·*B*	R^2	σ / 10^8 M^{-1} s^{-1}	N
Alkanes	0.98±0.11	4.04±6.4	0.891	9.11	11
Monoalcohols	0.99±0.17	4.04±7.5	0.697	1.49	16
Di- and polyols	0.78±0.36	21.4±9.0	0.201	18.39	21
Carbonyl compounds$^{(a)}$	0.89±0.17	-0.43±4.1	0.695	8.87	14
Monocarboxylic acids	1.09±0.18	-1.89±3.2	0.726	7.86	16
Dicarboxylic acids	1.22±0.07	2.65±2.1	0.934	6.75	20
Polyfunctional compounds	0.58±0.29	-0.11±3.7	0.160	11.48	23

(a) including dicarbonyl compounds except acetylacetone

S3. Sensitivity runs of crucial parameters

S3.1 Influence of the chosen SAR

(a) Acetic acid (b) Oxalic acid

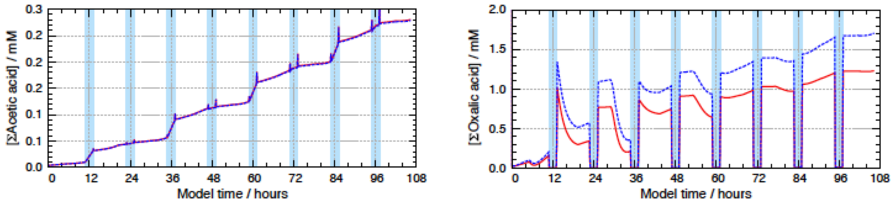

(c) Propionaldehyde (d) Lactic acid

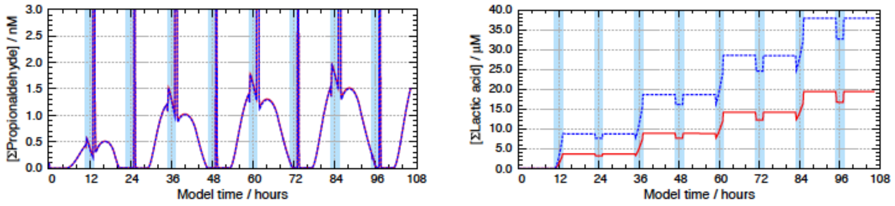

(e) n-Butanol (f) 2,3-Dioxo butyric acid

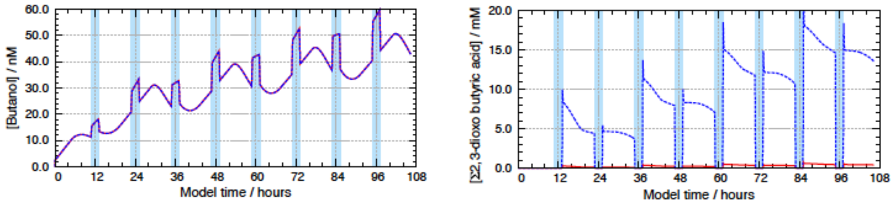

(g) pH value (h) Dry and organic mass

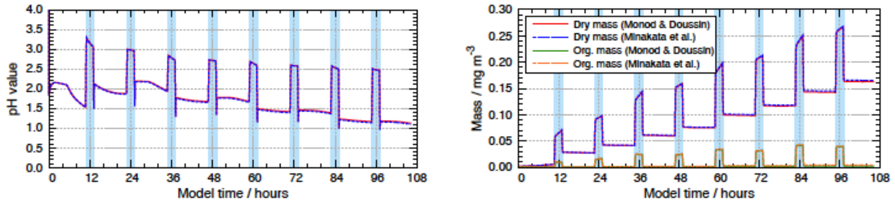

Figure S9 Concentration-time profiles for selected organic compounds (a – f) as well as pH value (g) and dry and organic mass (h) in the sensitivity runs investigating the influence of the chosen SAR. Model runs with the standard set of SARs (Doussin and Monod, 2013 complimented by Minakata et al., 2009, see Table 2 in the main article) are represented by red solid lines. Blue dashed lines represent model runs, where the SAR by Minakata et al. (2009) was given sole preference.

Deleted: give

S3.2 Processing of the organic mass fraction

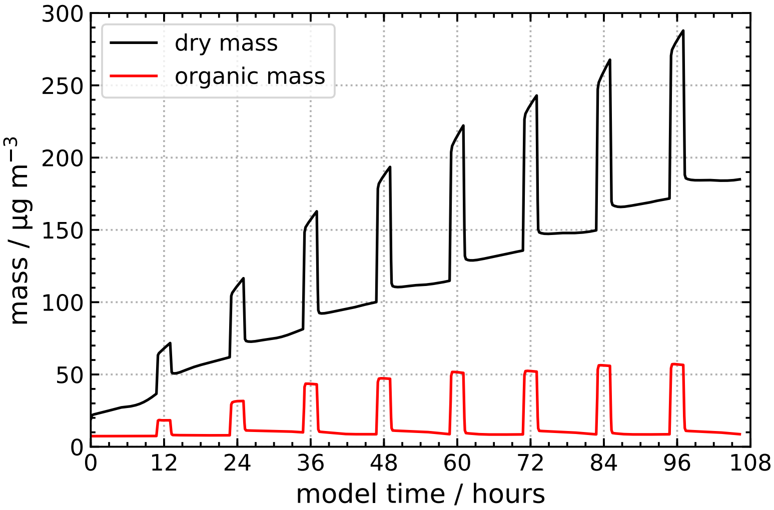

Figure S10 Concentration-time profile of the total particulate dry mass and the organic particulate dry mass in the base scenario 'orig'.

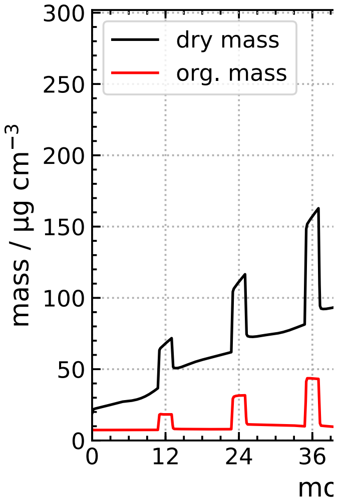

Deleted:

Deleted: sensitivity run orig investigating the effects of nitrate radical chemistry

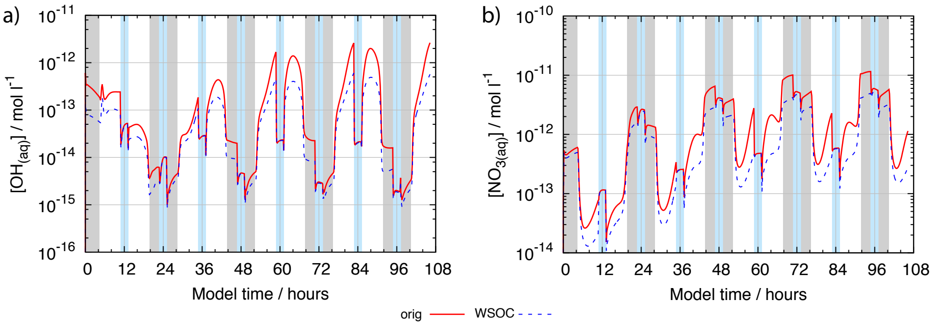

Figure S11 Aqueous phase concentration-time profiles of OH and NO_3 radicals in runs introducing parameterisations for radical reactions of WSOC/HULIS in comparison to the original mechanism.

S3.3 Influence of nitrate radical chemistry under remote conditions

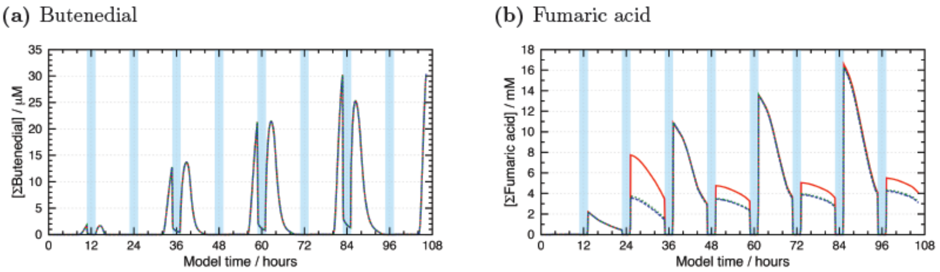
(a) Butenedial

(b) Fumaric acid

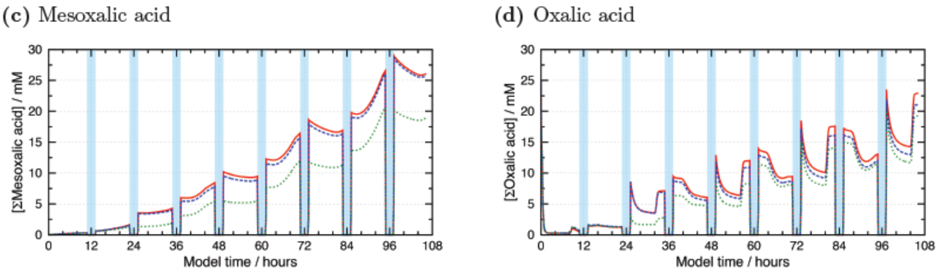
(c) Mesoxalic acid

(d) Oxalic acid

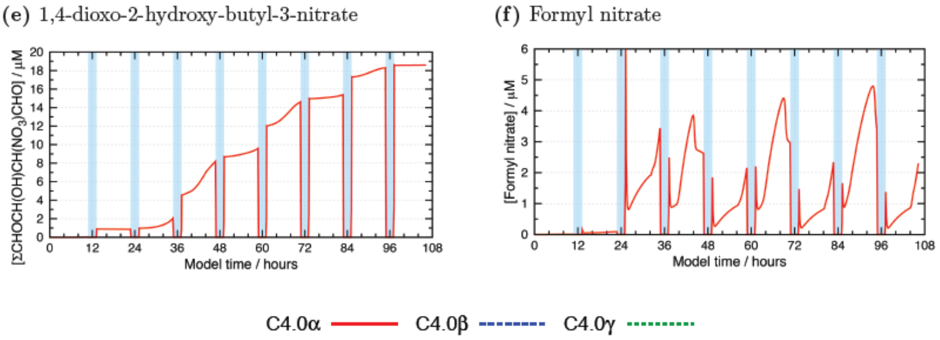
(e) 1,4-dioxo-2-hydroxy-butyl-3-nitrate

(f) Formyl nitrate

Figure S12 Concentration-time profiles of selected organic compounds calculated with different subsets of a CAPRAM test scenario under urban conditions, where the alpha version is with the full chemical scheme, the beta version without nitrate radical chemistry of unsaturated organic compounds, and the gamma version with only the nitrate radical chemistry already present in CAPRAM 3.0n (see also explanations in subsection 3.4 of the main article).

Deleted: . Explanations for

Deleted: ,

Deleted: scenarios are given

Deleted: .

S3.4 Investigation of the sensitivity of cut-off parameters for minor branches

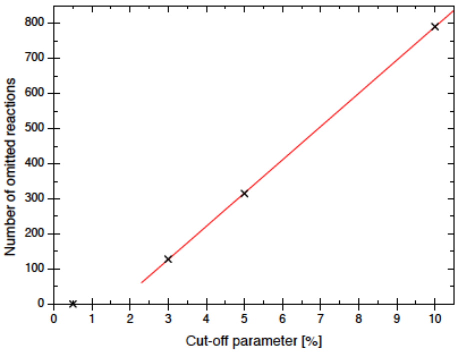

Figure S13 Overview of the reduction potential for mechanisms with different cut-off parameters for minor branches.

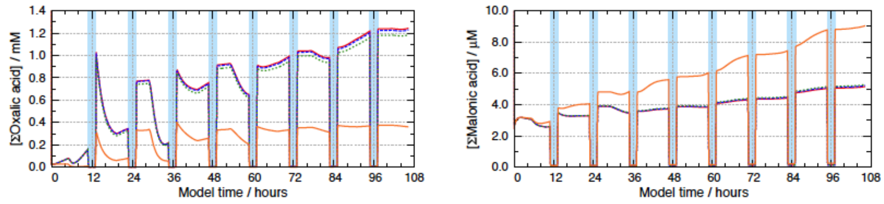
(a) Oxalic acid

(b) Malonic acid

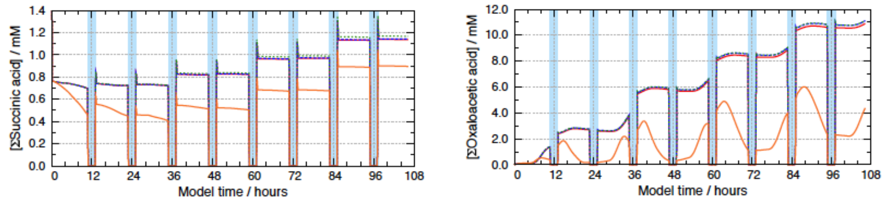
(c) Succinic acid

(d) Oxaloacetic acid

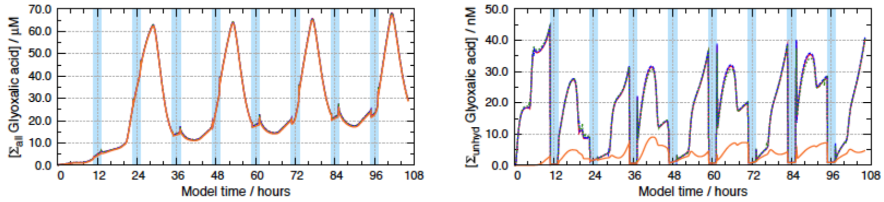
(e) Glyoxalic acid (sum of all forms)

(f) Glyoxalic acid (unhydrated form)

Figure S14 Concentration-time profiles for selected organic compounds in sensitivity runs investigating the influence of the cut-off parameter for minor product channels. Model runs have been performed under urban summer conditions with 8 non-permanent cloud periods (blue shades). Red solid lines represent concentrations of the runs with a 0.5% threshold, blue dashed lines with a 3% threshold, green dotted lines with a 5% threshold and orange solid lines with a 10% threshold.

Deleted: inverstigating

S3.5 Investigations on peroxy radical chemistry

To demonstrate the validity to neglect the recombination channels of α-hydroxy peroxy radicals, a simple simulation has been performed, where these types of peroxy radicals are oxidised with the recombination and HO_2 elimination rate constants as given in the main article. The simulation was initialised with typical radical concentrations and no sources of peroxy radicals were defined. Only two sink reactions were implemented in the run, the HO_2 elimination channel leading to a carboxyl acid with a rate constant of 1000 s^{-1} and the peroxy radical recombination, where all products were combined ($k_{2nd} = 7.3\cdot10^{8}$ M^{-1} s^{-1}). With typical radical concentrations of 10^{-13} M and the ubiquitous availability of water (c = 55.5 M), the difference in the rate constants of more than 5 orders of magnitude is still not enough to produce visible amounts of recombination products as can be seen from Figure S15. Therefore, it is safe to consider HO_2 as the only reaction pathway and reduce the size of the chemical mechanism.

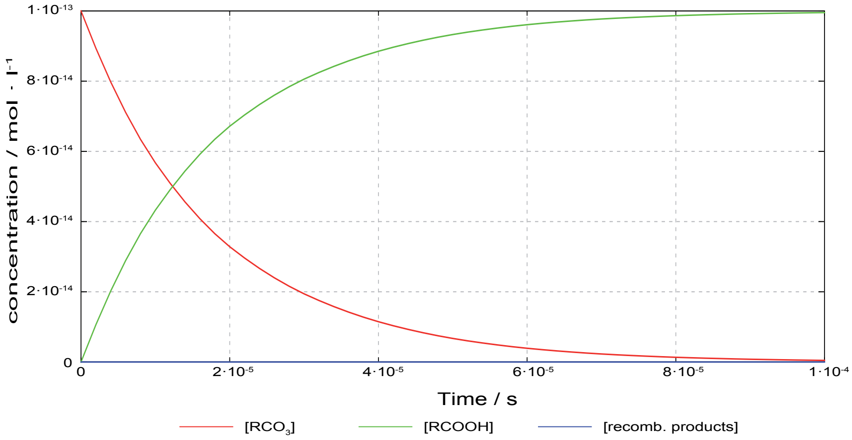

Figure S15 Concentration-time profiles for the aqueous phase decay of α-hydroxy peroxy radicals and the build-up of their oxidation products.

S4 Additional information about the LEAK chamber runs

Table S13 Additional uptake processes and initial aqueous phase reactions used in the scenarios UPT and RXN. Scenario $RXN_{0.4}$ is the same as RXN, but with reduced WSCO yields by a factor of 0.4.

Process[(a)]	UPT[(b)]	RXN/$RXN_{0.4}$ [(c)]
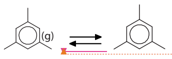	$9.6\cdot10^{-2}$	$9.6\cdot10^{-2}$
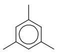 + OH ⟶ 0.4 WSOC		$6.4\cdot10^{9}$ (d)
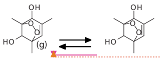	$2.34\cdot10^{5}$	$2.34\cdot10^{-5}$ (e)
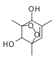 + OH ⟶ 0.4 WSOC		$6.89\cdot10^{9}$ (f)

Deleted: type

Deleted: initilised

Deleted: Figure S15

Deleted: 15

Deleted: ⇄

Field Code Changed

Deleted: ⇄

Field Code Changed

Process[(a)]	**UPT**[(b)]	**RXN/RXN$_{0.4}$** [(c)]
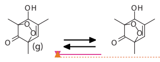	5.92·10^6	5.92·10^6 [(e)]
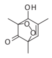 + OH $\longrightarrow$ 0.4 WSOC		1.19·10^{10} [(f)]
	3.81·10^1	3.81·10^1 [(e)]
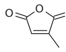 + OH $\longrightarrow$ 0.4 WSOC		2.00·10^9
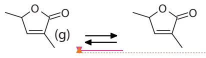	1.02·10^1	1.02·10^1 [(e)]
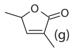 + OH $\longrightarrow$ 0.4 WSOC		1.30·10^9
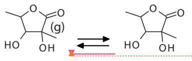	6.92·10^4	6.92·10^4
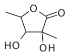 + OH $\longrightarrow$ 0.4 WSOC		2.29·10^9
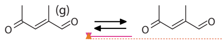	2.23·10^4	3.10·10^3
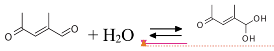 + H_2O		6.2
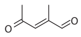 + OH $\longrightarrow$ 0.4 WSOC		6.33·10^{10}
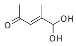 + OH $\longrightarrow$ 0.4 WSOC		1.06·10^{11}
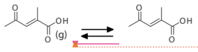	9.89·10^5 [(g)]	9.89·10^5
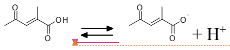 + H^+		2.32·10^{-4}
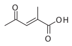 + OH $\longrightarrow$ 0.4 WSOC		2.47·10^{10}
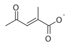 + OH $\longrightarrow$ 0.4 WSOC		1.06·10^{11}
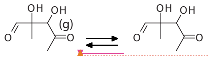	6.76·10^5	1.70·10-4
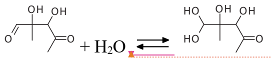 + H_2O		3.39·10^1
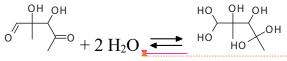 + 2 H_2O		3.15
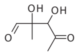 + OH $\longrightarrow$ 0.4 WSOC		1.5·10^9

Deleted: ⇌
Field Code Changed
Deleted: ⇌
Field Code Changed
Deleted: ⇌
Field Code Changed
Deleted: ⇌
Field Code Changed
Deleted: ⇌
Field Code Changed
Deleted: ⇌
Field Code Changed
Deleted: ⇌
Field Code Changed
Deleted: ⇌
Field Code Changed
Deleted: ⇌
Field Code Changed
Deleted: ⇌
Field Code Changed
Deleted: ⇌
Field Code Changed
Deleted: ⇌
Field Code Changed

Process[(a)]	UPT[(b)]	RXN/RXN$_{0.4}$ [(c)]
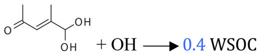 + OH → 0.4 WSOC		$1.26\cdot10^9$
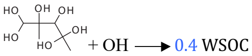 + OH → 0.4 WSOC		$1.64\cdot10^9$
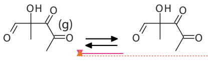 (g) ⇌	$7.07\cdot10^7$	$1.21\cdot10^4$
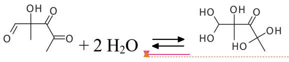 + 2 H_2O ⇌		7.69
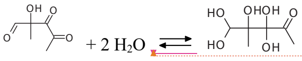 + 2 H_2O ⇌		$5.42\cdot10^1$
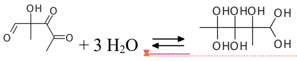 + 3 H_2O ⇌		$3.07\cdot10^1$
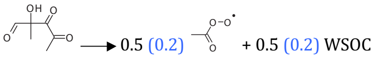 → 0.5 (0.2) + 0.5 (0.2) WSOC		$1.00\cdot10^{-1}$
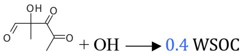 + OH → 0.4 WSOC		$1.12\cdot10^9$
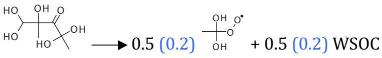 → 0.5 (0.2) + 0.5 (0.2) WSOC		$1.00\cdot10^{-1}$
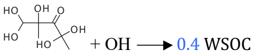 + OH → 0.4 WSOC		$1.29\cdot10^9$
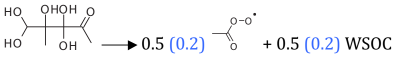 → 0.5 (0.2) + 0.5 (0.2) WSOC		$1.00\cdot10^{-1}$
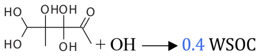 + OH → 0.4 WSOC		$1.31\cdot10^9$
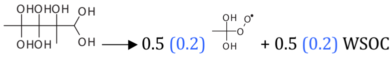 → 0.5 (0.2) + 0.5 (0.2) WSOC		$1.00\cdot10^{-1}$
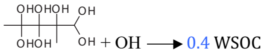 + OH → 0.4 WSOC		$1.72\cdot10^9$
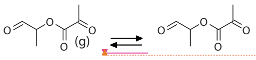 (g) ⇌	$4.99\cdot10^6$	$6.31\cdot10^2$
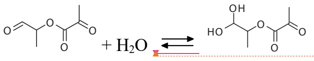 + H_2O ⇌		$1.80\cdot10^3$
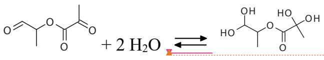 + 2 H_2O ⇌		$3.02\cdot10^3$
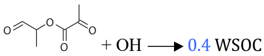 + OH → 0.4 WSOC		$1.31\cdot10^9$
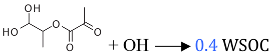 + OH → 0.4 WSOC		$1.41\cdot10^9$

Deleted: ⇌

Field Code Changed

Deleted: ⇌

Field Code Changed

Deleted: ⇌

Field Code Changed

Deleted: ⇌

Field Code Changed

Deleted: ⇌

Field Code Changed

Deleted: ⇌

Field Code Changed

Deleted: ⇌

Field Code Changed

Process(a)	UPT(b)	RXN/RXN$_{0.4}$ (c)
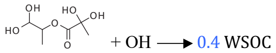 + OH ⟶ 0.4 WSOC		$1.97\cdot10^{9}$
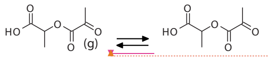	$9.01\cdot10^{5}$ (g)	$2.05\cdot10^{5}$
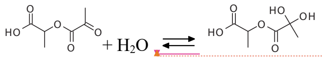 + H_2O		1.90
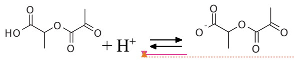 + H^+		$1.5\cdot10^{-3}$
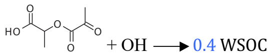 + OH ⟶ 0.4 WSOC		$4.68\cdot10^{8}$
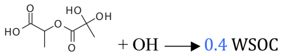 + OH ⟶ 0.4 WSOC		$5.50\cdot10^{8}$
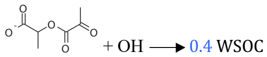 + OH ⟶ 0.4 WSOC		$2.13\cdot10^{8}$
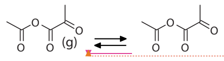	$2.14\cdot10^{4}$	$1.84\cdot10^{3}$
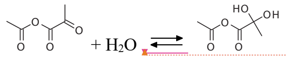 + H_2O		3.00
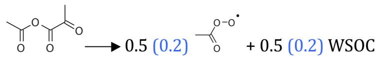 ⟶ 0.5 (0.2) + 0.5 (0.2) WSOC		$1.00\cdot10^{-1}$
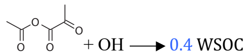 + OH ⟶ 0.4 WSOC		$1.09\cdot10^{8}$
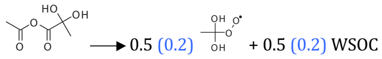 ⟶ 0.5 (0.2) + 0.5 (0.2) WSOC		$1.00\cdot10^{-1}$
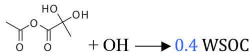 + OH ⟶ 0.4 WSOC		$4.24\cdot10^{9}$
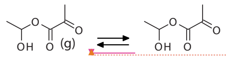	$7.75\cdot10^{3}$	$2.85\cdot10^{3}$
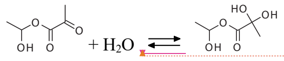 + H_2O		1.72
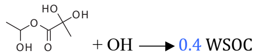 + OH ⟶ 0.4 WSOC		$5.68\cdot10^{8}$
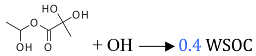 + OH ⟶ 0.4 WSOC		$1.35\cdot10^{9}$
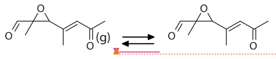	$1.70\cdot10^{6}$	$8.69\cdot10^{2}$
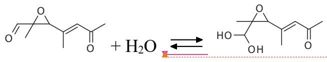 + H_2O		$1.95\cdot10^{3}$

Deleted: ⇄
Field Code Changed

Deleted: ⇄
Field Code Changed

Deleted: ⇄
Field Code Changed

Deleted: ⇄
Field Code Changed

Deleted: ⇄
Field Code Changed

Deleted: ⇄
Field Code Changed

Deleted: ⇄
Field Code Changed

Deleted: ⇄
Field Code Changed

Deleted: ⇄
Field Code Changed

Process[a]	**UPT**[b]	**RXN/RXN$_{0.4}$** [c]
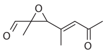 + OH → 0.4 WSOC		$1.08\cdot10^{10}$
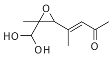 + OH → 0.4 WSOC		$1.09\cdot10^{10}$
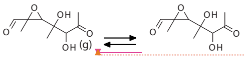	$2.54\cdot10^{9}$	$6.96\cdot10^{5}$
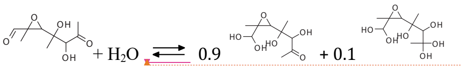		$3.65\cdot10^{3}$
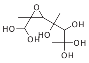 + OH → 0.4 WSOC		$1.43\cdot10^{9}$
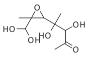 + OH → 0.4 WSOC		$1.91\cdot10^{9}$
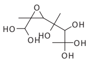 + OH → 0.4 WSOC		$2.29\cdot10^{9}$
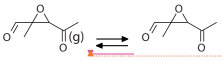	$7.39\cdot10^{4}$	$7.09\cdot10^{-1}$
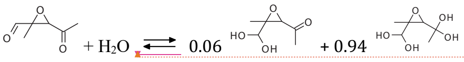		$1.04\cdot10^{5}$
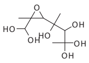 + OH → 0.4 WSOC		$1.07\cdot10^{9}$
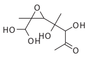 + OH → 0.4 WSOC		$1.37\cdot10^{9}$
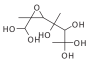 + OH → 0.4 WSOC		$1.83\cdot10^{9}$
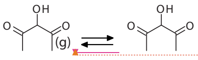	$2.84\cdot10^{3}$	$2.00\cdot10^{3}$
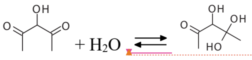		$3.92\cdot10^{-1}$
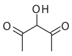 + OH → 0.4 WSOC		$2.89\cdot10^{8}$
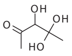 + OH → 0.4 WSOC		$6.80\cdot10^{8}$
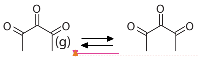	$2.66\cdot10^{7}$	$3.61\cdot10^{4}$
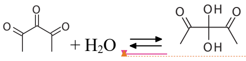		$4.28\cdot10^{1}$

Deleted: ⇌

Field Code Changed

Deleted: ⇌

Field Code Changed

Deleted: ⇌

Field Code Changed

Deleted: ⇌

Field Code Changed

Deleted: ⇌

Field Code Changed

Deleted: ⇌

Field Code Changed

Deleted: ⇌

Field Code Changed

Deleted: ⇌

Field Code Changed

Process[(a)]	UPT[(b)]	RXN/RXN$_{0.4}$ [(c)]
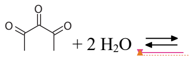 + 2 H_2O		$9.85\cdot10^{1}$
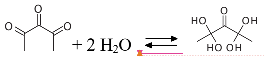 + 2 H_2O		$5.91\cdot10^{1}$
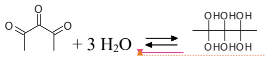 + 3 H_2O		$1.00\cdot10^{-1}$
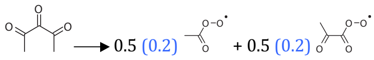 0.5 (0.2) + 0.5 (0.2)		$1.39\cdot10^{8}$
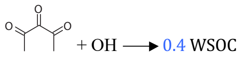 + OH → 0.4 WSOC		$1.00\cdot10^{-1}$
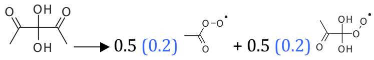 0.5 (0.2) + 0.5 (0.2)		$4.19\cdot10^{8}$
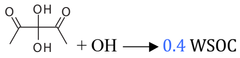 + OH → 0.4 WSOC		$1.00\cdot10^{-1}$
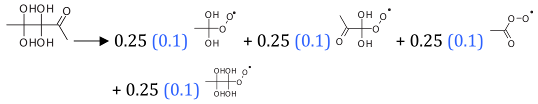 0.25 (0.1) + 0.25 (0.1) + 0.25 (0.1) + 0.25 (0.1)		$8.22\cdot10^{8}$
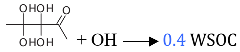 + OH → 0.4 WSOC		$1.00\cdot10^{-1}$
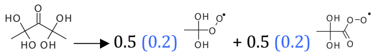 0.5 (0.2) + 0.5 (0.2)		$8.11\cdot10^{8}$
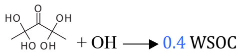 + OH → 0.4 WSOC		$1.00\cdot10^{-1}$
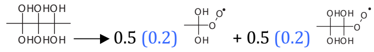 0.5 (0.2) + 0.5 (0.2)		$1.23\cdot10^{9}$
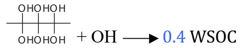 + OH → 0.4 WSOC		$1.00\cdot10^{-1}$
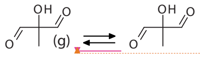 (g)	$8.16\cdot10^{5}$	$1.40\cdot10^{2}$
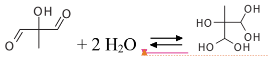 + 2 H_2O		$6.28\cdot10^{1}$
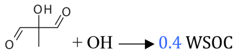 + OH → 0.4 WSOC		$1.91\cdot10^{9}$
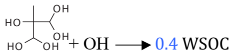 + OH → 0.4 WSOC		$1.68\cdot10^{9}$

(a) Branching ratios from the scenario RXN$_{0.4}$ are given in blue, from all other scenarios in black.

(b) Column shows $K_{H,eff}$ in M^n atm^{-1} (n = order of reaction) for the scenario UPT. Data according to the new CAPRAM/GECKO-A protocol unless reference is indicated by further footnotes.

(c) Column shows K_H in M atm^{-1}, K_{hyd} in M^{m-n}, K_{diss} in M, k_n in $M^{-(n-1)}$ s^{-1} for scenarios RXN and RXN$_{0.4}$. Data according to the new CAPRAM/GECKO-A protocol unless reference is indicated by further footnotes.

(d) Sehested et al. (1975)

Deleted: ⇄

Field Code Changed

Deleted: ⇄

Field Code Changed

Deleted: ⇄

Field Code Changed

Deleted: ⇄

Field Code Changed

Deleted: ⇄

Field Code Changed

(e) Estimated with EPI Suite 4.1 (http://www.epa.gov/opptintr/exposure/pubs/episuite.htm)

(f) Rate constant calculated with the SAR by Minakata et al. (2009) ignoring the oxygen atoms in the –O–O– group as this group is bound solely to quaternary carbon atoms and thus in β-position of any reactive group. As the group itself contains no H-atoms and is, therefore, unreactive and no β-parameters are used in the SAR βυ Minakata et al. (2009), it was possible to derive a rate constant with the SAR without further assumptions.

(g) Contributions of dissociation to the effective Henry's Law constant calculated manually as GROMHE does not consider dissociations of carboxylic acids.

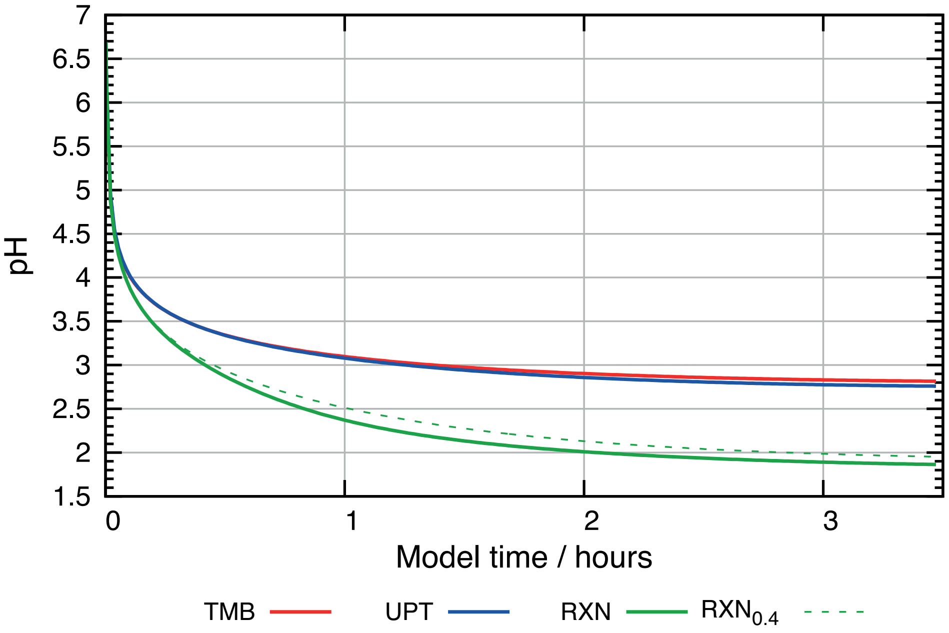

Figure S16 Modelled particle pH in the different sensitivity runs for the mesitylene oxidation experiment.

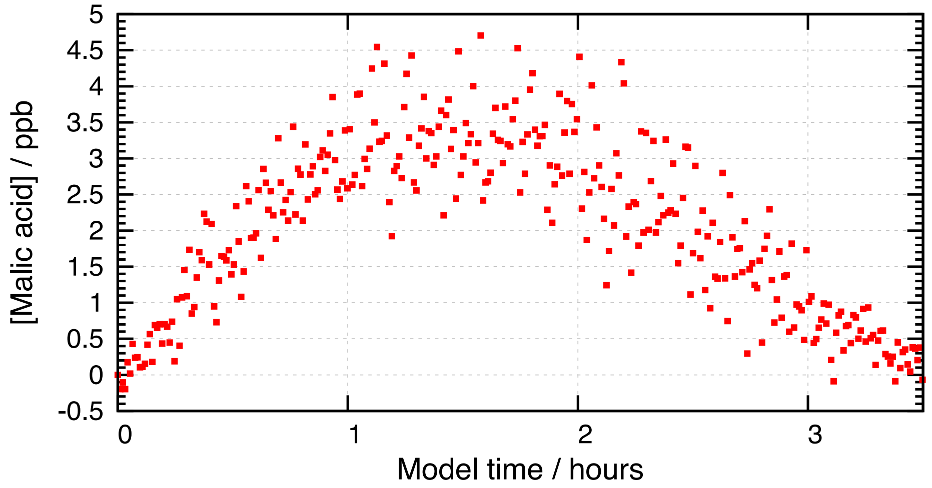

Figure S17 Malic acid concentrations as monitored by PTR-MS in the LEAK chamber during the mesitylene oxidation experiment.

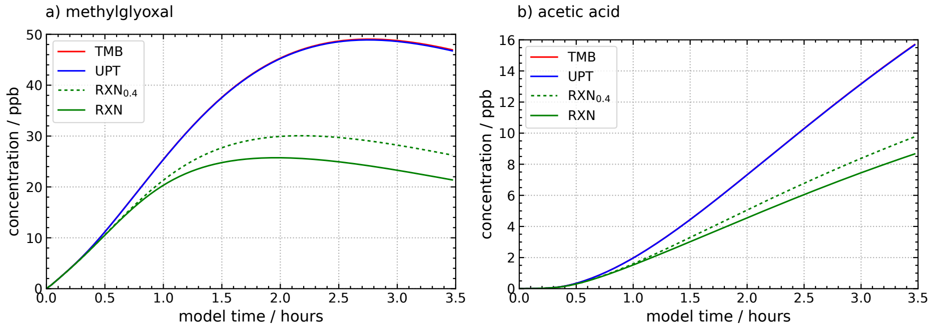

Figure S18 Concentrations-time profiles of the major gas phase oxidation products methylglyoxal (a) and acetic acid (b) in the sensitivity runs TMB, UPT, RXN$_{0.4}$, and RXN.

References

Acero, J. L., Haderlein, S. B., Schmidt, T. C., Suter, M. J.-F. and von Gunten, U.: MTBE Oxidation by Conventional Ozonation and the Combination Ozone/Hydrogen Peroxide: Efficiency of the Processes and Bromate Formation, Environ. Sci. Technol., 35(21), 4252–4259, doi:10.1021/es010044n, 2001.

Adams, G. E. and Michael, B. D.: Pulse radiolysis of benzoquinone and hydroquinone. Semiquinone formation by water elimination from trihydroxy-cyclohexadienyl radicals, Trans. Faraday Soc., 63, 1171–1180, doi:10.1039/TF9676301171, 1967.

Adams, G. E., Boag, J. W., Currant, J. and Michael, B. D.: Absolute rate constants for the reaction of the hydroxyl radical with organic compounds, in Pulse Radiolysis, edited by M. Ebert, J. P. Keen, A. J. Swallow, and J. H. Baxendale, pp. 131–143, Academic Press, New York., 1965a.

Adams, G. E., Boag, J. W. and Michael, B. D.: Reactions of the hydroxyl radical. Part 2.—Determination of absolute rate constants, Trans. Faraday Soc., 61, 1417–1424, doi:10.1039/TF9656101417, 1965b.

Ahrens, R. W.: Gamma Radiolysis of Aqueous Solutions Containing Fe (II) and Selected Substituted Phenols, Radiat. Res., 30(3), 611–619, doi:10.2307/3572125, 1967.

Al-Sheikhly, M., Silverman, J., Simic, M. and Michael, B.: Formation and Reactions of Alkyl, Allyl, Biallylic, and Peroxyl Radicals from Unsaturated Fatty Acids in Micellar and Monomeric Aqueous Solutions, J. Phys. Chem. B, 108(45), 17618–17627, doi:10.1021/jp047738d, 2004.

Alam, M. ., Rao, B. S. . and Janata, E.: OH reactions with aliphatic alcohols: evaluation of kinetics by direct optical absorption measurement. A pulse radiolysis study, Radiat. Phys. Chem., 67(6), 723–728, doi:10.1016/S0969-806X(03)00310-4, 2003.

Albarran, G., Bentley, J. and Schuler, R. H.: Substituent Effects in the Reaction of OH Radicals with Aromatics: Toluene, J. Phys. Chem. A, 107(39), 7770–7774, doi:10.1021/jp030550u, 2003.

Alfassi, Z. B., Padmaja, S., Neta, P. and Huie, R. E.: Rate constants for reactions of nitrate (NO3·) radicals with organic compounds in water and acetonitrile, J. Phys. Chem., 97(15), 3780–3782, doi:10.1021/j100117a025, 1993.

Almgren, M., Grieser, F. and Thomas, J. K.: Rate of exchange of surfactant monomer radicals and long chain alcohols between micelles and aqueous solutions. A pulse radiolysis study, J. Chem. Soc. Faraday Trans. 1 Phys. Chem. Condens. Phases, 75, 1674–1687, doi:10.1039/F19797501674, 1979.

Anbar, M., Meyerstein, D. and Neta, P.: Reactivity of aliphatic compounds towards hydroxyl radicals, J. Chem. Soc. B Phys. Org., 742–747, doi:10.1039/J29660000742, 1966a.

Anbar, M., Meyerstein, D. and Neta, P.: The Reactivity of Aromatic Compounds toward Hydroxyl Radicals, J. Phys. Chem., 70(8), 2660–2662, doi:10.1021/j100880a034, 1966b.

Anderson, R. F. and Schulte-Frohlinde, D.: Reactions induced by hydroxyl radical attack on acetylene in aqueous solution. A pulse radiolysis study, J. Phys. Chem., 82(1), 22–26, doi:10.1021/j100490a006, 1978.

Anderson, R. F., Patel, K. B. and Stratford, M. R. L.: Radical spectra and product distribution following electrophilic attack by the $OH^{\cdot}$ radical on 4-hydroxybenzoic acid and subsequent oxidation, J. Chem. Soc. Faraday Trans. 1 Phys. Chem. Condens. Phases, 83(10), 3177–3187, doi:10.1039/F19878303177, 1987.

Ashton, L., Buxton, G. V and Stuart, C. R.: Temperature dependence of the rate of reaction of OH with some aromatic compounds in aqueous solution. Evidence for the formation of a π-complex intermediate?, J. Chem. Soc. Faraday Trans., 91(11), 1631–1633, doi:10.1039/FT9959101631, 1995.

Asmus, K.-D., Beck, G., Henglein, A. and Wigger, A.: Pulsradiolytische Untersuchung der Oxydation und Reduktion des Nitrobenzols in wässriger Lösung, Berichte der Bunsen-Gesellschaft für Phys. Chemie, 70(8), 869, 1966.

Asmus, K. D. and Taub, I. A.: Spectrum and kinetics of the hydroxynitromethane anion radical in pulse-irradiated alkaline nitromethane solutions, J. Phys. Chem., 72(10), 3382–3387, doi:10.1021/j100856a005, 1968.

Atkinson, R.: Kinetics and mechanisms of the gas-phase reactions of the hydroxyl radical with organic compounds, J. Phys. Chem. Ref. Data, Monograph No. 1, 1989.

Atkinson, R.: Kinetics of the gas-phase reactions of OH radicals with alkanes and cycloalkanes, Atmos. Chem. Phys., 3, 2233–2307, 2003.

Atkinson, R. and Arey, J.: Atmospheric degradation of volatile organic compounds, Chem. Rev., 103(12), 4605–4638, doi:10.1021/cr0206420, 2003.

Atkinson, R., Baulch, D. L., Cox, R. A., Crowley, J. N., Hampson, R. F., Hynes, R. G., Jenkin, M. E., Rossi, M. J., Troe, J. and Subcommittee, I.: Evaluated kinetic and photochemical data for atmospheric chemistry: Volume II – Gas phase reactions of organic species, Atmos. Chem. Phys., 6(11), 3625–4055, 2006.

Bakalik, D. P. and Thomas, J. K.: Micellar catalysis of radical reactions. A spin trapping study, J. Phys. Chem., 81(20), 1905–

1908, doi:10.1021/j100535a004, 1977.

Baker, M. Z., Badiello, R., Tamba, M., Quintiliani, M. and Gorin, G.: Pulse Radiolytic Study of Hydrogen Transfer from Glutathione to Organic Radicals, Int. J. Radiat. Biol. Relat. Stud. Physics, Chem. Med., 41(6), 595–602, doi:10.1080/09553008214550691, 1982.

Balazs, E. A., Davies, J. V, Phillips, G. O. and Scheufele, D. S.: Polyanions and their complexes. Part III. Reactions of heparin, hyaluronic acid, sodium poly(ethylenesulphonate), sodium poly(styrenesulphonate), and sodium carboxymethylcellulose with hydroxyl radicals and hydrated electrons, J. Chem. Soc. C Org., 1420–1423, doi:10.1039/J39680001420, 1968.

Barber, D. J. W. and Thomas, J. K.: Reactions of Radicals with Lecithin Bilayers, Radiat. Res., 74(1), 51–65, doi:10.2307/3574756, 1978.

Barlow, S., Buxton, G. V, Murray, S. A. and Salmon, G. A.: Free-radical-induced oxidation of hydroxymethanesulfonate in aqueous solution Part 2A pulse and steady-state radiolysis study of oxygenated solutions, J. Chem. Soc. Faraday Trans., 93(20), 3641–3645, doi:10.1039/A703266H, 1997.

Barzaghi, P. and Herrmann, H.: Kinetics and mechanisms of reactions of the nitrate radical (NO3) with substituted phenols in aqueous solution, Phys. Chem. Chem. Phys., 6(23), 5379–5388, doi:10.1039/B412933D, 2004.

Basinski, A. and Lerke, G.: Reactivity of certain aromatic compounds with respect to OH radical, Bull. l Acad. Pol. des Sci. – Ser. des Sci. Chim., 20(4), 319, 1972.

Behar, D., Fessenden, R. W. and Hornak, J. P.: ESR and pulse radiolysis investigation of the radiolysis of sodium vinyl sulfonate, Radiat. Phys. Chem., 20(4), 267–273, doi:10.1016/0146-5724(82)90036-X, 1982.

Bíró, Á. and Wojnárovits, L.: Pulse radiolysis of ethyl propionate in aqueous solution, J. Radioanal. Nucl. Chem., 166(1), 7–14, doi:10.1007/BF02167993, 1992.

Bíró, Á. and Wojnárovits, L.: Reaction of diethyl maleate and diethyl fumarate with hydrated electrons and hydroxyl radicals, Radiat. Phys. Chem., 47(3), 389–392, doi:10.1016/0969-806X(95)00122-E, 1996.

Bobrowski, K.: Pulse radiolysis of p-hydroxycinnamic acid in aqueous solution, J. Chem. Soc. Faraday Trans. 1 Phys. Chem. Condens. Phases, 80(6), 1377–1389, doi:10.1039/F19848001377, 1984.

Bobrowski, K. and Raghavan, N. V.: Pulse radiolytic and product analysis studies of the reaction of hydroxyl radicals with cinnamic acid. The relative extent of addition to the ring and side chain, J. Phys. Chem., 86(22), 4432–4435, doi:10.1021/j100219a033, 1982.

Bonifačić, M., Ljubenkov, I. and Eckert-Maksić, M.: One-electron Oxidation and Reduction Reactions of Vitamin C Derivatives: 6-bromo- and 6-chloro-6-deoxy-ascorbic Acid, Int. J. Radiat. Biol., 66(2), 123–131, doi:10.1080/09553009414551021, 1994.

Bonin, J., Janik, I., Janik, D. and Bartels, D. M.: Reaction of the Hydroxyl Radical with Phenol in Water Up to Supercritical Conditions, J. Phys. Chem. A, 111(10), 1869–1878, doi:10.1021/jp0665325, 2007.

Bors, W., Saran, M. and Michel, C.: Radical Intermediates Involved in the Bleaching of the Carotenoid Crocin. Hydroxyl Radicals, Superoxide Anions and Hydrated Electrons, Int. J. Radiat. Biol. Relat. Stud. Physics, Chem. Med., 41(5), 493–501, doi:10.1080/09553008214550571, 1982.

El Boudali, A., Le Calvé, S., Le Bras, G. and Mellouki, A.: Kinetic studies of OH reactions with a series of acetates, J. Phys. Chem., 100(30), 12364–12368, doi:10.1021/jp9606218, 1996.

Brede, O., Bos, J., Helmstreit, W. and Mehnert, R.: Nanosecond pulse-radiolysis of 1-methylstyrene and 1,1'-diphenylethylene in aqueous solution, Zeitschrift für Chemie, 17(12), 447–448, 1977.

Broszkiewicz, R. K., Söylemez, T. and Schulte-Frohlinde, D.: Reactions of OH Radicals with Acetylacetone in Aqueous Solution. A Pulse Radiolysis and Electron Spin Resonance Study, Zeitschrift für Naturforsch. B, 37, 368, doi:10.1515/znb-1982-0318, 1982.

Bucknall, T., Edwards, H. E., Kemsley, K. G., Moore, J. S. and Phillips, G. O.: The formation of malonaldehyde in irradiated carbohydrates, Carbohydr. Res., 62(1), 49–59, doi:10.1016/S0008-6215(00)83377-7, 1978.

Burkholder, J. B., Sander, S. P., Abbatt, J., Barker, J. R., Huie, R. E., Kolb, C. E., Kurylo, M. J., Orkin, V. L., Wilmouth, D. L. and Wine, P. H.: Chemical Kinetics and Photochemical Data for Use in Atmospheric Studies, Evaluation No. 18, Pasadena, CA, USA. [online] Available from: http://jpldataeval.jpl.nasa.gov, 2015.

Buxton, G. V., Greenstock, C. L., Helman, W. P. and Ross, A. B.: Critical review of rate constants for reactions of hydrated electrons, hydrogen atoms and hydroxyl radicals (OH/O-) in aqueous solution, J. Phys. Chem. Ref. Data, 17(2), 513–886, 1988.

Buxton, G. V., Malone, T. N. and Salmon, G. A.: Oxidation of glyoxal initiated by OH in oxygenated aqueous solution, J. Chem. Soc. Faraday Trans., 93(16), 2889–2891, doi:10.1039/A701468F, 1997.

Buxton, G. V, Salmon, G. A. and Williams, J. E.: The Reactivity of Biogenic Monoterpenes towards OH· and SO4-· Radicals in De-Oxygenated Acidic Solution, J. Atmos. Chem., 36(2), 111–134, doi:10.1023/A:1006340727148, 2000.

Buxton, G. V, Wang, J. and Salmon, G. A.: Rate constants for the reactions of NO3•, SO4•− and Cl• radicals with formate and acetate esters in aqueous solution, Phys. Chem. Chem. Phys., 3(13), 2618–2621, doi:10.1039/B101932P, 2001.

Cabelli, D. E. and Bielski, B. H. J.: A Pulse Radiolysis Study of Some Dicarboxylic Acids of the Citric Acid Cycle. The Kinetics and Spectral Properties of the Free Radicals Formed by Reaction with the OH Radical, Zeitschrift für Naturforsch. B, 40, 1731–1737, doi:10.1515/znb-1985-1223, 1985.

Cabelli, D. E., Comstock, D. A. and Bielski, B. H. J.: Free Radical Mechanisms for the Oxidation of Substituted Ascorbates. A Pulse Radiolysis Study of L-Ascorbic Acid-2-Sulfate, Radiat. Res., 95(3), 530–540, doi:10.2307/3576098, 1983.

Le Calvé, S., Le Bras, G. and Mellouki, A.: Kinetic Studies of OH Reactions with a Series of Methyl Esters, J. Phys. Chem. A, 101(48), 9137–9141, doi:10.1021/jp972369p, 1997a.

Le Calvé, S., Le Bras, G. and Mellouki, A.: Kinetic studies of OH reactions with Iso-propyl, Iso-butyl, Sec-butyl, and Tert-butyl acetate, Int. J. Chem. Kinet., 29(9), 683–688, doi:10.1002/(SICI)1097-4601(1997)29:9<683::AID-KIN5>3.0.CO;2-Q, 1997b.

Le Calvé, S., Le Bras, G. and Mellouki, A.: Temperature Dependence for the Rate Coefficients of the Reactions of the OH Radical with a Series of Formates, J. Phys. Chem. A, 101(30), 5489–5493, doi:10.1021/jp970554x, 1997c.

Carter, W. P. L.: Development of the SAPRC-07 chemical mechanism, Atmos. Environ., 44(40), 5324–5335, doi:10.1016/j.atmosenv.2010.01.026, 2010.

Cercek, B. and Ebert, M.: Radiolytic transients from p-nitrophenol and their inter- and intramolecular reactions, Adv. Chem. Ser., 81, 210, 1968.

Chang, P. B. L. and Young, T. M.: Kinetics of methyl tert-butyl ether degradation and by-product formation during UV/hydrogen peroxide water treatment, Water Res., 34(8), 2233–2240, doi:10.1016/S0043-1354(99)00392-9, 2000.

Chapman, J. D., Greenstock, C. L., Reuvers, A. P., McDonald, E. and Dunlop, I.: Radiation Chemical Studies with Nitrofurazone as Related to Its Mechanism of Radiosensitization, Radiat. Res., 53(2), 190–203, doi:10.2307/3573524, 1973.

Chen, X. and Schuler, R. H.: Directing effects of phenyl substitution in the reaction of hydroxyl radical with aromatics: the radiolytic hydroxylation of biphenyl, J. Phys. Chem., 97(2), 421–425, doi:10.1021/j100104a025, 1993.

Chin, M. and Wine, P. H.: A temperature-dependent competitive kinetics study of the aqueous-phase reactions of OH radicals with formate, formic acid, acetate, acetic acid and hydrated formaldehyde, in Aquatic Surface Photochemistry, edited by G. R. Helz, R. G. Zepp, and D. G. Crosby, pp. 85–96, Lewis Publishers, Boca Raton, FL., 1992.

Cooper, W. J., Cramer, C. J., Martin, N. H., Mezyk, S. P., O'Shea, K. E. and Sonntag, C. von: Free Radical Mechanisms for the Treatment of Methyl tert-Butyl Ether (MTBE) via Advanced Oxidation/Reductive Processes in Aqueous Solutions, Chem. Rev., 109(3), 1302–1345, doi:10.1021/cr078024c, 2009.

D'Angelantonio, M., Emmi, S. S., Poggi, G. and Beggiato, G.: Reaction of the OH Radical with Furfural. Spectral and Kinetic Investigation by Pulse Radiolysis and by ab Initio and Semiempirical Methods, J. Phys. Chem. A, 103(7), 858–864, doi:10.1021/jp983883d, 1999.

Doherty, M. d'Arcy, Wilson, I., Wardman, P., Basra, J., Patterson, L. H. and Cohen, G. M.: Peroxidase activation of 1-naphthol to naphthoxy or naphthoxy-derived radicals and their reaction with glutathione, Chem. Biol. Interact., 58, 199–215, doi:10.1016/S0009-2797(86)80098-9, 1986.

Doussin, J.-F. and Monod, A.: Structure–activity relationship for the estimation of OH-oxidation rate constants of carbonyl compounds in the aqueous phase, Atmos. Chem. Phys., 13(23), 11625–11641, doi:10.5194/acp-13-11625-2013, 2013.

Eibenberger, J.: Pulse radiolytic investigations concerning the formation and oxidation of organic radicals in aqueous solutions, University of Vienna., 1980.

Elliot, A. J. and McCracken, D. R.: Effect of temperature on O- reactions and equilibria – A pulse radiolysis study, Radiat. Phys. Chem., 33(1), 69–74, 1989.

Elliot, A. J. and Simsons, A. S.: Rate constants for reactions of hydroxyl radicals as a function of temperature, Radiat. Phys. Chem., 24(2), 229–231, doi:10.1016/0146-5724(84)90056-6, 1984.

Ervens, B., Gligorovski, S. and Herrmann, H.: Temperature-dependent rate constants for hydroxyl radical reactions with organic compounds in aqueous solutions, Phys. Chem. Chem. Phys., 5(9), 1811–1824, doi:10.1039/B300072A, 2003.

Evers, E. L., Jayson, G. G., Robb, I. D. and Swallow, A. J.: Determination by pulse radiolysis of the distribution of solubilizates between micellar and nonmicellar phases. Naphthalene and its reduced free radical in aqueous sodium dodecyl sulphate solutions, J. Chem. Soc. Faraday Trans. 1 Phys. Chem. Condens. Phases, 76, 528–536, doi:10.1039/F19807600528, 1980.

Exner, M., Herrmann, H., Michel, J. W. and Zellner, R.: Laser pulse initiated measurements of NO3 reactions with S(IV) and organic compounds in aqueous solutions, in Proceedings of EUROTRAC Symposiium '92: Photo-oxidants: Precursors and Products, edited by T. Cvitaš and W. Seiler, pp. 615–618, SPB Academic Publishing, The Hague, Netherlands., 1993.

Exner, M., Herrmann, H. and Zellner, R.: Rate constants for the reactions of the NO3 radical with HCOOH/HCOO− and CH3COOH/CH3COO− in aqueous solution between 278 and 328 K., 1994.

Ferrari, C., Roche, A., Jacob, V., Foster, P. and Baussand, P.: Kinetics of the reaction of OH radicals with a series of esters under simulated conditions at 295K, Int. J. Chem. Kinet., 28(8), 609–614, doi:10.1002/(SICI)1097-4601(1996)28:8<609::AID-KIN6>3.0.CO;2-Z, 1996.

Fisher, M. M. and Hamill, W. H.: Electronic processes in pulse-irradiated aqueous and alcoholic systems, J. Phys. Chem., 77(2), 171–177, doi:10.1021/j100621a006, 1973.

Flyunt, R., Makogon, O., Schuchmann, M. N., Asmus, {K.-D.} and von Sonntag, C.: OH-radical-induced oxidation of methanesulfinic acid. The reactions of the methanesulfonyl radical in the absence and presence of dioxygen, J. Chem. Soc. – Perkin Trans. 2, 5, 787–792, doi:10.1039/B009631H, 2001.

Garoma, T. and Gurol, M. D.: Modeling Aqueous Ozone/UV Process Using Oxalic Acid as Probe Chemical, Environ. Sci. Technol., 39(20), 7964–7969, doi:10.1021/es050878w, 2005.

Geeta, S., Sharma, S. B., Rao, B. S. M., Mohan, H., Dhanya, S. and Mittal, J. P.: Study of kinetics and absorption spectra of OH adducts of hydroxy derivatives of benzaldehyde and acetophenone, J. Photochem. Photobiol. A Chem., 140(2), 99–107, doi:10.1016/S1010-6030(01)00402-6, 2001.

George, C., Rousse, D., Perraudin, E. and Strekowski, R.: A new approach for studying aqueous phase OH kinetics: Application of Teflon waveguides, Phys. Chem. Chem. Phys., 5(8), 1562–1569, doi:10.1039/B301145N, 2003.

Getoff, N.: Advancements of radiation-induced degradation of pollutants in drinking and waste-water, Appl. Radiat. Isot., 40(7), 585–594, doi:10.1016/0883-2889(89)90114-7, 1989.

Getoff, N., Schwörer, F., Markovic, V. M., Sehested, K. and Nielsen, S. O.: Pulse radiolysis of oxalic acid and oxalates, J. Phys. Chem., 75(6), 749–755, doi:10.1021/j100676a004, 1971.

Gilbert, B. C. and Whitwood, A. C.: Vinyl-radical rearrangements. E.s.r. evidence for the formation of enol radical cations by the protonation at carbon of β-hydroxyvinyl radicals and for a 1,4-hydrogen shift in some β-sulphur-substituted analogues, J.

Chem. Soc. Perkin Trans. 2, (11), 1921–1927, doi:10.1039/P29890001921, 1989.

Gligorovski, S.: Laser based studies of OH radical reactions in aqueous solution, University of Leipzig., 2005.

Gligorovski, S. and Herrmann, H.: Kinetics of reactions of OH with organic carbonyl compounds in aqueous solution, Phys. Chem. Chem. Phys., 6(16), 4118–4126, doi:10.1039/B403070B, 2004.

Gligorovski, S., Rousse, D., George, C. H. and Herrmann, H.: Rate constants for the OH reactions with oxygenated organic compounds in aqueous solution, Int. J. Chem. Kinet., 41(5), 309–326, doi:10.1002/kin.20405, 2009.

Gohn, M. and Getoff, N.: Pulse radiolysis of 3,4-dihydroxytoluene, J. Chem. Soc. Faraday Trans. 1 Phys. Chem. Condens. Phases, 73, 1207–1215, doi:10.1039/F19777301207, 1977.

Gopakumar, K., Kini, U. R., Ashawa, S. C., Bhandari, N. S., Krishnan, G. U. and Krishnan, D.: Gamma irradiation of coumarin in aqueous solution, Radiat. Eff., 32(3–4), 199–203, doi:10.1080/00337577708233075, 1977.

Graedel, T. E. and Weschler, C. J.: Chemistry within aqueous atmospheric aerosols and raindrops, Rev. Geophys., 19(4), 505–539, doi:10.1029/RG019i004p00505, 1981.

Greenstock, C. and Dunlop, I.: Pulse Radiolysis Studies of Nitrofurans. Radiation Chemistry of Nifuroxime, J. Phys. Chem., 77(15), 1834–1838, doi:10.1021/j100634a600, 1973.

Haag, W. R. and Yao, C. C. D.: Rate constants for reaction of hydroxyl radicals with several drinking water contaminants, Environ. Sci. Technol., 26(5), 1005–1013, doi:10.1021/es00029a021, 1992.

Hardison, D. R., Cooper, W. J., Mezyk, S. P. and Bartels, D. M.: The free radical chemistry of tert-butyl formate: rate constants for hydroxyl radical, hydrated electron and hydrogen atom reaction in aqueous solution, Radiat. Phys. Chem., 65(4–5), 309–315, doi:10.1016/S0969-806X(02)00333-X, 2002.

Hart, E. J., Thomas, J. K. and Gordon, S.: A review of the radiation chemistry of single-carbon compounds and some reactions of the hydrated electron in aqueous solution, Radiat. Res. Suppl., 4, 74–88, 1964.

Herrmann, H.: Kinetics of Aqueous Phase Reactions Relevant for Atmospheric Chemistry, Chem. Rev., 103(12), 4691–4716, doi:10.1021/cr020658q, 2003.

Herrmann, H. and Zellner, R.: Reactions of NO3·-radicals in aqueous solution, in N-Centered Radicals, edited by Z. B. Alfassi, pp. 291–343, Wiley, New York., 1998.

Herrmann, H., Exner, M. and Zellner, R.: Reactivity trends in reactions of the nitrate radical (NO3) with inorganic and organic cloudwater constituents, Geochim. Cosmochim. Acta, 58(15), 3239–3244, doi:10.1016/0016-7037(94)90051-5, 1994.

Herrmann, H., Exner, M., Jacobi, H.-W., Raabe, G., Reese, A. and Zellner, R.: Laboratory studies of atmospheric aqueous-phase free-radical chemistry: kinetic and spectroscopic studies of reactions of NO3 and SO4– radicals with aromatic compounds, Faraday Discuss., 100, 129–153, doi:10.1039/FD9950000129, 1995a.

Herrmann, H., Reese, A. and Zellner, R.: Time-resolved UV/VIS diode array absorption spectroscopy of SOx−(x=3, 4, 5) radical anions in aqueous solution, J. Mol. Struct., 348, 183–186, doi:10.1016/0022-2860(95)08619-7, 1995b.

Herrmann, H., Jacobi, H.-W., Raabe, G., Reese, A., Umschlag, T. and Zellner, R.: Free radical reactions in the tropospheric aqueous phase, in The oxidizing capacity of the troposphere, pp. 503–512, Proceedings of the seventh European symposium on physico-chemical behaviour of atmospheric pollutants, Venice, Italy., 1996.

Hesper, J.: Spektroskopische und kinetische Untersuchungen von Reaktionen der Radikale O2- und OH in wässriger Phase, University of Leipzig., 2003.

Hoffmann, D., Weigert, B., Barzaghi, P. and Herrmann, H.: Reactivity of poly-alcohols towards OH, NO3 and SO4− in aqueous solution, Phys. Chem. Chem. Phys., 11(41), 9351, doi:10.1039/b908459b, 2009.

Horii, H., Abe, Y. and Taniguchi, S.: Pulse Radiolysis Study of Reaction of OH Radicals with Triose Reductone, Bull. Chem. Soc. Jpn., 59(3), 721–724, doi:10.1246/bcsj.59.721, 1986.

Hulme, B. E., Land, E. J. and Phillips, G. O.: Pulse radiolysis of 9,10-anthraquinones. Part 1.—Radicals, J. Chem. Soc. Faraday Trans. 1 Phys. Chem. Condens. Phases, 68, 1992–2002, doi:10.1039/F19726801992, 1972.

Ito, O., Akiho, S. and Iino, M.: Kinetic Study for Reactions of Nitrate Radical (NO3·) with Alcohols in Solutions, Bull. Chem. Soc. Jpn., 62(5), 1606–1611, doi:10.1246/bcsj.62.1606, 1989a.

Ito, O., Akiho, S. and Iino, M.: Kinetics for reactions of the nitrate radical (NO3.cntdot.) with aldehydes in acetonitrile, J. Phys. Chem., 93(10), 4079–4083, doi:10.1021/j100347a041, 1989b.

Janata, E.: Direct optical observation of the formation of some aliphatic alcohol radicals. A pulse radiolysis study, Proc. Indian Acad. Sci., 114(6), 731–737, 2002.

Janik, I., Ulanski, P., Rosiak, J. M. and von Sonntag, C.: Hydroxyl-radical-induced reactions of the poly(vinyl methyl ether) model 2,4-dimethoxypentane in the absence and presence of dioxygen: a pulse radiolysis and product study, J. Chem. Soc. Perkin Trans. 2, (10), 2034–2040, doi:10.1039/B004776G, 2000.

Kanodia, S., Madhaven, V. and Schuler, R. H.: Oxidation of naphthalene by radiolytically produced OH radicals, Int. J. Radiat. Appl. Instrumentation. Part C. Radiat. Phys. Chem., 32(5), 661–664, doi:10.1016/1359-0197(88)90083-5, 1988.

Kraljic, I.: Kinetics of OH radical reactions in radiolysis, photolysis, and the Fenton system, in The Chemistry of Ionization and Excitation, edited by G. R. A. Johnsons and G. Scholes, pp. 167–173, Taylor and Francis Ltd., 1967.

Kumar, M. and Rao, M. H.: Pulse Radiolysis Study of Initiation, Dimerization, and Propagation Steps of 3,3-Dimethylacrylic Acid in Aqueous Medium, J. Macromol. Sci. Part A - Chem., 28(5–6), 531–544, doi:10.1080/00222339108052105, 1991.

Kumar, M., Rao, M. H., Moorthy, P. N. and Rao, K. N.: Structural influences on the reactivity of vinyl monomers with OH radicals and hydrated electrons studied by pulse radiolysis, Radiat. Eff. Express, 1(4), 167–173, 1988.

Land, E. J. and Swallow, A. J.: Some free radical reactions of camphor in relation to the action of cytochrome P450, J. Chem. Soc. Faraday Trans. 1 Phys. Chem. Condens. Phases, 75(0), 1849–1856, doi:10.1039/F19797501849, 1979.

Langer, S., Ljungström, E., Wängberg, I., Wallington, T. J., Hurley, M. D. and Nielsen, O. J.: Atmospheric chemistry of di-tert-butyl ether: Rates and products of the reactions with chlorine atoms, hydroxyl radicals, and nitrate radicals, Int. J. Chem. Kinet., 28(4), 299–306, doi:10.1002/(SICI)1097-4601(1996)28:4<299::AID-KIN8>3.0.CO;2-Q, 1996.

Lilie, J.: Pulse radiolytic investigations of oxydative ring scission of furan, thiophen and pyrrol, Zeitschrift für Naturforsch. Part B, 26(3), 197, 1971.

Lilie, J. and Henglein, A.: Pulse radiolytic studies of oxidation of unsaturated carbonyl compounds in aqueous solution, Berichte der Bunsen-Gesellschaft für Phys. Chemie, 74(4), 388, 1970.

Lind, J. and Eriksen, T. E.: The reactions of hydroxyl radicals with alkyl disulphonic acids in aqueous solution studied by pulse radiolysis, Radiat. Phys. Chem., 10(5–6), 349–352, doi:10.1016/0146-5724(77)90043-7, 1977.

Logan, S. R.: Redox reactions of organic radicals with ferrocene/ferricenium species in aqueous solution. Part 1. Radicals derived from carboxylic acids, J. Chem. Soc. - Perkin Trans. 2, 7, 751–754, doi:10.1039/P29890000751, 1989.

Magneron, I., Thévenet, R., Mellouki, A., Le Bras, G., Moortgat, G. K. and Wirtz, K.: A Study of the Photolysis and OH-initiated Oxidation of Acrolein and trans-Crotonaldehyde, J. Phys. Chem. A, 106(11), 2526–2537, doi:10.1021/jp013413a, 2002.

Makarov, I. E., Protasova, E. L. and Khaikin, G. I.: The kinetics of radical reactions in the radiolysis of aqueous solutions of organic nitro compounds, Russ. J. Phys. Chem. A, Focus Chem., 82(11), 1833–1837, doi:10.1134/S0036024408110083, 2008.

Martin, L. R., Mezyk, S. P. and Mincher, B. J.: Determination of Arrhenius and Thermodynamic Parameters for the Aqueous Reaction of the Hydroxyl Radical with Lactic Acid, J. Phys. Chem. A, 113(1), 141–145, doi:10.1021/jp806290s, 2009.

Maruthamuthu, P.: Absolute rate constants for the reactions of sulfate, phosphate and hydroxyl radicals with monomers, Die Makromol. Chemie, Rapid Commun., 1(1), 23–25, doi:10.1002/marc.1980.030010105, 1980.

Maruthamuthu, P. and Dhandavel, R.: Binding of bromocresol green onto poly(n-vinyl-2-pyrrolidone), Makromol. Chemie – Rapid Commun., 1(10), 633–636, 1980.

Massaut, B., Tilquin, B. and Hickel, B.: Reactivity of the capto-dative methylmethoxyacetate (mma) toward radicals, studied by electron pulse-radiolysis in neutral aqueous medium, Bull. Des Soc. Chim. Belges, 97(11–12), 1031–1036, 1988.

Matsushige, T., Koltzenburg, G. and Schulte-Frohlinde, D.: Pulse-radiolysis of aqueous solutions of acetic acid 2-hydroxyethyl ester – Fast elimination of acetic-acid from a primary radical, Berichte der Bunsen-Gesellschaft für Phys. Chemie, 79(8), 657–661, 1975.

Mellouki, A., Teton, S. and Le Bras, G.: Kinetics of OH radical reactions with a series of ethers, Int. J. Chem. Kinet., 27(8), 791–805, doi:10.1002/kin.550270806, 1995.

Merz, J. H. and Waters, W. A.: 511. The oxidation of aromatic compounds by means of the free hydroxyl radical, J. Chem. Soc., 2427–2433, doi:10.1039/JR9490002427, 1949.

Mezyk, S. P., Cooper, W. J., Bartels, D. M., O'She, K. E. and Wu, T.: Radiation Chemistry of Alternative Fuel Oxygenates: Substituted Ethers, J. Phys. Chem. A, 105(14), 3521–3526, doi:10.1021/jp003892y, 2001.

Mezyk, S. P., Rance Hardison, D., Song, W., O'Shea, K. E., Bartels, D. M. and Cooper, W. J.: Advanced oxidation and reduction process chemistry of methyl tert-butyl ether (MTBE) reaction intermediates in aqueous solution: 2-Methoxy-2-methyl-propanal, 2-methoxy-2-methyl-propanol, and 2-methoxy-2-methyl-propanoic acid, Chemosphere, 77(10), 1352–1357, doi:10.1016/J.CHEMOSPHERE.2009.09.029, 2009.

Michael, B. D. and Hart, E. J.: Rate constants of hydrated electron, hydrogen atom, and hydroxyl radical reactions with benzene, 1,3-cyclohexadiene, 1,4-cyclohexadiene, and cyclohexene, J. Phys. Chem., 74(15), 2878–2884, doi:10.1021/j100709a005, 1970.

Minakata, D., Li, K., Westerhoff, P. and Crittenden, J.: Development of a group contribution method to predict aqueous phase hydroxyl radical (HO) reaction rate constants, Environ. Sci. Technol., 43(16), 6220–6227, doi:10.1021/es900956c, 2009.

Mitani, M. M., Keller, A. A., Bunton, C. A., Rinker, R. G. and Sandall, O. C.: Kinetics and products of reactions of MTBE with ozone and ozone/hydrogen peroxide in water, J. Hazard. Mater., 89(2–3), 197–212, doi:10.1016/S0304-3894(01)00309-0, 2002.

Mittal, L. J. and Mittal, J. P.: Site of attack in the interaction of hydrated electrons and hydroxy radicals in the pulse radiolysis of arylalkylamines in aqueous solutions, Int. J. Radiat. Appl. Instrumentation. Part C. Radiat. Phys. Chem., 28(4), 363–371, doi:10.1016/1359-0197(86)90019-6, 1986.

Moise, T., Rudich, Y., Rousse, D. and George, C.: Multiphase Decomposition of Novel Oxygenated Organics in Aqueous and Organic Media, Environ. Sci. Technol., 39(14), 5203–5208, doi:10.1021/es048488h, 2005.

Monod, A., Poulain, L., Grubert, S., Voisin, D. and Wortham, H.: Kinetics of OH-initiated oxidation of oxygenated organic compounds in the aqueous phase: new rate constants, structure-activity relationships and atmospheric implications, Atmos. Environ., 39(40), 7667–7688, 2005.

Monod, A., Chevallier, E., Durand Jolibois, R., Doussin, J. F., Picquet-Varrault, B. and Carlier, P.: Photooxidation of methylhydroperoxide and ethylhydroperoxide in the aqueous phase under simulated cloud droplet conditions, Atmos. Environ., 41(11), 2412–2426, doi:10.1016/J.ATMOSENV.2006.10.006, 2007.

Moore, J. S., Kemsley, K. G., Davies, J. V. and Phillips, G. O.: Pulse radiolysis of carbohydrates, in Radiation Biology and Chemistry, edited by H. E. Edwards, pp. 99–113, Elsevier., 1979.

Nauser, T. and Bühler, R. E.: Pivalic acid as combined buffer and scavenger for studies of cloud water chemistry with pulse radiolysis, J. Chem. Soc. Faraday Trans., 90(24), 3651–3656, doi:10.1039/FT9949003651, 1994.

Neta, P. and Dorfman, L. M.: Pulse Radiolysis Studies. XIII. Rate Constants for the Reaction of Hydroxyl Radicals with Aromatic Compounds in Aqueous Solutions, in Radiation Chemistry, vol. 81, pp. 15–222, American Chemical Society., 1968.

Neta, P. and Huie, R. E.: Rate constants for reactions of nitrogen oxide (NO3) radicals in aqueous solutions, J. Phys. Chem., 90(19), 4644–4648, doi:10.1021/j100410a035, 1986.

Neta, P. and Schuler, R. H.: Oxidation of phenol to phenoxyl radical by oxygen (1-) ions, J. Am. Chem. Soc., 97(4), 912–913, doi:10.1021/ja00837a049, 1975.

Neta, P., Hoffman, M. Z. and Simic, M.: Electron spin resonance and pulse radiolysis studies of the reactions of OH and O-radicals with aromatic and olefinic compounds, J. Phys. Chem., 76(6), 847–853, doi:10.1021/j100650a009, 1972.

Nielsen, O. J., Sehested, J., Langer, S., Ljungström, E. and Wängberg, I.: UV absorption spectra and kinetics for alkyl and alkyl peroxy radicals originating from di-tert-butyl ether, Chem. Phys. Lett., 238(4–6), 359–364, doi:10.1016/0009-2614(95)00401-O, 1995.

O'Neill, P. and Steenken, S.: Pulse-radiolytic and electron-spin resonance studies on formation of phenoxyl radicals by reaction of OH radicals with methoxylated phoenols and hydroxybenzoic acids, Berichte der Bunsen-Gesellschaft für Phys. Chemie, 81(6), 550–556, 1977.

O'Neill, P., Steenken, S. and Schulte-Frohlinde, D.: Formation of radical cations of methoxylated benzenes by reaction with hydroxyl radicals, thallium(2+), silver(2+), and peroxysulfate (SO4.-) in aqueous solution. Optical and conductometric pulse radiolysis and in situ radiolysis electron spin resonance s, J. Phys. Chem., 79(25), 2773–2779, doi:10.1021/j100592a013, 1975.

O'Neill, P., Steenken, S. and Schulte-Frohlinde, D.: Formation of radical zwitterions from methoxylated benzoic acids. 2. Hydroxyl adducts as precursors, J. Phys. Chem., 81(1), 31–34, doi:10.1021/j100516a008, 1977.

Oturan, M. A., Pinson, J., Deprez, D. and Terlain, B.: Polyhydroxylation of salicyclic acid by electrochemically generated OH radicals, New J. Chem., 16(6), 705–710, 1992.

Park, S. E., Joo, H. and Kang, J.-W.: Photodegradation of methyl tertiary butyl ether (MTBE) vapor with immobilized titanium dioxide., 2003.

Patterson, L. K. and Hasegawa, K.: Pulse-radiolysis studies in model lipid systems – Influence of aggregation on kinetic behavior of OH induced radicals in aqueous sodium linleate, Berichte der Bunsen-Gesellschaft für Phys. Chemie, 82(9), 951–956, 1978.

Phillips, G. O. and Worthington, N. W.: Effects of Ionizing Radiations on Glucuronic Acid, Radiat. Res., 43(1), 34–44, doi:10.2307/3572856, 1970.

Phillips, G. O., Filby, W. G., Moore, J. S. and Davies, J. V.: Radiation studies of aryl glycosides : Part III. The reactivity of aryl glucosides towards hydroxyl radicals and hydrated electrons, Carbohydr. Res., 16(1), 105–111, doi:10.1016/S0008-6215(00)86103-0, 1971.

Phulkar, S., Rao, B. S. M., Schuchmann, H.-P. and von Sonntag, C.: Radiolysis of tertiary butyl hydroperoxide in aqueous solution – Reductive cleavage by the solvated electron, the hydrogen atom, and, in particluar, the superoxide radical anion, Zeitschrift für Naturforsch. Part B, 45(10), 1425 – 1432, 1990.

Prütz, W. A.: Chemiluminescence of aqueous fluorescein solutions under x-irradiation – effect of pH, Zeitschrift für Phys. Chemie – Frankfurt, 83(5–6), 309–321, 1973.

Raabe, G.: Eine laserphotolytische Studie zur Kinetik von Reaktionen des NO3-Radikals in wäßriger Lösung, University of Essen., 1996.

Redpath, J. L. and Willson, R. L.: Reducing Compounds in Radioprotection and Radio-sensitization: Model Experiments Using Ascorbic Acid, Int. J. Radiat. Biol. Relat. Stud. Physics, Chem. Med., 23(1), 51–65, doi:10.1080/09553007314550051, 1973.

Redpath, J. L., Ihara, J. and Patterson, L. K.: Pulse-radiolysis Studies of 8-methoxypsoralen, Int. J. Radiat. Biol. Relat. Stud. Physics, Chem. Med., 33(4), 309–315, doi:10.1080/09553007814550221, 1978.

Roder, M., Wojnárovits, L. and Földiák, G.: Pulse radiolysis of aqueous solutions of aromatic hydrocarbons in the presence of oxygen, Int. J. Radiat. Appl. Instrumentation. Part C. Radiat. Phys. Chem., 36(2), 175–176, doi:10.1016/1359-0197(90)90236-B, 1990.

Ross, A. B., Bielski, B. H. J., Buxton, G. V., Cabelli, D. E., Helman, W. P., Huie, R. E., Grodkovski, J., Neta, P., Mulazzani, Q. G. and Wilkinson, F.: NIST standard reference database 40: NDRL/NIST solution kinetics database vers. 3.0, Gaithersburg, MD, USA., 1998.

Rousse, D. and George, C.: A novel long path photolysis cell--application to the reactivity of selected organic compounds toward the nitrate radical (NO3), Phys. Chem. Chem. Phys., 6(13), 3408–3414, doi:10.1039/B400175C, 2004.

Rudakov, E. S., Volkova, L. K. and Tretyakov, V. P.: Low selectivity reactions of OH radicals with alkanes in aqueous solutions, React. Kinet. Catal. Lett., 16(4), 333–337, 1981.

Sáfrány, A. and Wojnárovits, L.: Radiolysis of hydroxy ethylacrylate in dilute aqueous solutions, Radiat. Phys. Chem., 41(3), 531–537, doi:10.1016/0969-806X(93)90016-N, 1993.

Saveleva, O. S., Vysotskaya, N. A. and Shevchuk, L. G.: Reactions of substituted phenols with hydroxyl radicals and their dissociated form O-, Zhurnal Org. Khimii, 8(2), 283, 1972.

Saveleva, O. S., Shevchuk, L. G. and Vysotskaya, N. A.: Reactivity of substituted benzene, furan and pyridine in relation to hydroxyl radicals, Zhurnal Org. Khimii, 9(4), 737–739, 1973.

Scholes, G. and Willson, R. L.: γ-Radiolysis of aqueous thymine solutions. Determination of relative reaction rates of OH radicals, Trans. Faraday Soc., 63(540P), 2983, doi:10.1039/tf9676302983, 1967.

Schöne, L., Schindelka, J., Szeremeta, E., Schaefer, T., Hoffmann, D., Rudzinski, K. J., Szmigielski, R. and Herrmann, H.: Atmospheric aqueous phase radical chemistry of the isoprene oxidation products methacrolein, methyl vinyl ketone, methacrylic acid and acrylic acid – kinetics and product studies, Phys. Chem. Chem. Phys., 16(13), 6257, doi:10.1039/c3cp54859g, 2014.

Schöneshöfer, M.: Pulse radiolysis of tropylium-ion, tropylcarbinol and tropilidene in aqeous solution, Zeitschrift für Naturforsch. Part B, 26(11), 1120, 1971.

Schöneshöfer, M.: Pulse radiolysis studies of oxidation of ascorbic acid by OH radicals and halide radical anion complexes in aqueous solution, Zeitschrift für Naturforsch. Part B, 27(6), 649, 1972.

Schuchmann, M. N. and von Sonntag, C.: The rapid hydration of the acetyl radical. A pulse radiolysis study of acetaldehyde in aqueous solution, J. Am. Chem. Soc., 110(17), 5698–5701, doi:10.1021/ja00225a019, 1988.

Schuchmann, M. N., Schuchmann, H. P., Hess, M. and Von Sonntag, C.: O2.cntdot.- Addition to ketomalonate leads to decarboxylation: a chain reaction in oxygenated aqueous solution, J. Am. Chem. Soc., 113(18), 6934–6937, doi:10.1021/ja00018a033, 1991.

Schuchmann, M. N., Schuchmann, H.-P. and von Sonntag, C.: Oxidation of Hydroxymalonic Acid by OH Radicals in the Presence and in the Absence of Molecular Oxygen. A Pulse-Radiolysis and Product Study, J. Phys. Chem., 99(22), 9122–9129, doi:10.1021/j100022a026, 1995.

Schuler, M. H., Bhatia, K. and Schuler, R. H.: Radiation chemical studies on systems related to ascorbic acid. Radiolysis of aqueous solutions of alpha-bromotetronic acid, Abstr. Pap. Am. Chem. Soc., 15, 1974.

Schuler, R. H.: Oxidation of Ascorbate Anion by Electron Transfer to Phenoxyl Radicals, Radiat. Res., 69(3), 417–433, doi:10.2307/3574655, 1977.

Sehested, K. and Holcman, J.: Radical Cations of Ethyl-, Isopropyl-, and Tert-Butylbenzene in Aqueous Solution, Nukleonika, 24(9), 941–950, 1979.

Sehested, K., Christensen, H. C., Hart, E. J. and Corfitzen, H.: Rates of reaction of O-, OH, and H with methylated benzenes in aqueous solution – optical spectra of radicals, J. Phys. Chem., 79(4), 310–315, doi:10.1021/j100571a005, 1975.

de Sémainville, P. G., Hoffmann, D., George, C. and Herrmann, H.: Study of nitrate radical (NO3) reactions with carbonyls and acids in aqueous solution as a function of temperature, Phys. Chem. Chem. Phys., 9(8), 958–968, doi:10.1039/B613956F, 2007.

de Sémainville, P. G., D'Anna, B. and George, C.: Aqueous Phase Reactivity of Nitrate Radicals (NO3) Toward Dicarboxylic Acids, Zeitschrift für Phys. Chemie, 224, 1247, doi:10.1524/zpch.2010.6150, 2010.

Shastri, L. V and Huie, R. E.: Rate constants for Hydrogen abstraction reactions of NO3 in aqueous solution, Int. J. Chem. Kinet., 22(5), 505–512, doi:10.1002/kin.550220507, 1990.

Shetiya, R. S., Rao, K. N. and Shankar, J.: Determination of rate constants for the reactions of H, OH and e aq with indole-3-

acetic acid and other plant hormones, Radiat. Eff., 14(3–4), 185–189, doi:10.1080/00337577208231199, 1972.

Shetiya, R. S., Roa, K. N. and Shankar, J.: OH radical rate constants of phenols using para-nitrosodimethylaniline, Indian J. Chem. Sect. A, 14(8), 575–578, 1976.

Shevchuk, L. G., Zhikharev, V. S. and Vysotskaya, N. A.: Kinetics of the reactions of hydroxyl radicals with benzene and pyridine derivates, Zhurnal Org. Khimii, 5, 1606–1608, 1969.

Simhon, E., Cohen, H. and Meyerstein, D.: Enhancement of the rate of addition of free radicals to dicarboxylacetylene by π acid complexation to ruthenium(II)-pentaamine. A pulse radiolysis study, Inorganica Chim. Acta, 142(1), 5–6, doi:10.1016/S0020-1693(00)80645-3, 1988.

Simic, M., Hoffman, M. Z. and Ebert, M.: Reaction of OH and O- radicals with aromatic carboxylate anions in aqueous solutions, J. Phys. Chem., 77(9), 1117–1120, doi:10.1021/j100628a007, 1973a.

Simic, M., Neta, P. and Hayon, E.: Reactions of hydroxyl radicals with unsaturated aliphatic alcohols in aqueous solution. Spectroscopic and electron spin resonance radiolysis study, J. Phys. Chem., 77(22), 2662–2667, doi:10.1021/j100640a018, 1973b.

Snook, M. E. and Hamilton, G. A.: Oxidation and fragmentation of some phenyl-substituted alcohols and ethers by peroxydisulfate and Fenton's reagent, J. Am. Chem. Soc., 96(3), 860–869, doi:10.1021/ja00810a035, 1974.

Soylemez, T. and Schuler, R. H.: Radiolysis of aqueous solutions of cyclopentane and cyclopentene, J. Phys. Chem., 78(11), 1052–1062, doi:10.1021/j100604a003, 1974.

Stefan, M. I. and Bolton, J. R.: Reinvestigation of the acetone degradation mechanism in dilute aqueous solution by the UV/H2O2 process, Environ. Sci. Technol., 33(6), 870–873, doi:10.1021/es9808548, 1999.

Stemmler, K. and von Gunten, U.: OH radical-initiated oxidation of organic compounds in atmospheric water phases: part 1. Reactions of peroxyl radicals derived from 2-butoxyethanol in water, Atmos. Environ., 34(25), 4241–4252, doi:10.1016/S1352-2310(00)00218-1, 2000.

Sychev, A. Y., Isak, V. G. and Pfannmeller, U.: Determination of the rate constants of hydroxyl radicals with organic and inorgnic substances under the conditions of H2O2 catalytic decomposition, Zhurnal Fiz. Khimii, 53(11), 2790–2793, 1979.

Tamminga, J. J., Vandenende, C. A. M., Warman, J. M. and Hummel, A.: Absorption spectra and reaction kinetics of the radical anion, radical cation and OH adduct(s) of 3,5-dinitroanisole studied by pulse radiolysis, Recl. Des Trav. Chim. Des Pays-Bas – J. R. Netherlands Chem. Soc., 98(5), 305–315, 1979.

Teton, S., Mellouki, A., Le Bras, G. and Sidebottom, H.: Rate constants for reactions of OH radicals with a series of asymmetrical ethers and tert-Butyl alcohol, Int. J. Chem. Kinet., 28(4), 291–297, doi:10.1002/(SICI)1097-4601(1996)28:4<291::AID-KIN7>3.0.CO;2-Q, 1996.

Thomas, J. K.: Pulse radiolysis of aqueous solutions of methyl iodide and methyl bromide. The reactions of iodine atoms and methyl radicals in water, J. Phys. Chem., 71(6), 1919–1925, doi:10.1021/j100865a060, 1967.

Thüner, L. P., Barnes, I., Maurer, T., Sauer, C. G. and Becker, K. H.: Kinetic study of the reaction of OH with a series of acetals at 298 ± 4 K, Int. J. Chem. Kinet., 31(11), 797–803, doi:10.1002/(SICI)1097-4601(1999)31:11<797::AID-JCK6>3.0.CO;2-C, 1999.

Toyota, K., Kanaya, Y., Takahashi, M. and Akimoto, H.: A box model study on photochemical interactions between VOCs and reactive halogen species in the marine boundary layer, Atmos. Chem. Phys., 4(7), 1961–1987, doi:10.5194/acp-4-1961-2004, 2004.

Ulanski, P., Bothe, E., Rosiak, J. M. and von Sonntag, C.: OH-radical-induced crosslinking and strand breakage of poly(vinyl alcohol) in aqueous solution in the absence and presence of oxygen. A pulse radiolysis and product study, Macromol. Chem. Phys., 195(4), 1443–1461, doi:10.1002/macp.1994.021950427, 1994.

Umschlag, T., Zellner, R. and Herrmann, H.: Laser-based studies of NO3 radical reactions with selected aromatic compounds in aqueous solution, Phys. Chem. Chem. Phys., 4(13), 2975–2982, doi:10.1039/B110263J, 2002.

Vysotskaya, N. A., Shevchuk, L. G., Gavrilova, S. P., Badovskaya, L. A. and Kulnevich, V. G.: Reactivity of substitued furans with hydroxyl radicals, Zhurnal Org. Khimii, 19(7), 1502–1505, 1983.

Walling, C.: Fenton's reagent revisited, Acc. Chem. Res., 8(4), 125–131, doi:10.1021/ar50088a003, 1975.

Walling, C. and El-Taliawi, G.: Fenton's reagent. III. Addition of hydroxyl radicals to acetylenes and redox reactions of vinyl radicals, J. Am. Chem. Soc., 95(3), 848–850, doi:10.1021/ja00784a036, 1973a.

Walling, C. and El-Taliawi, G. M.: Fenton's reagent. II. Reactions of carbonyl compounds and .alpha.,.beta.-unsaturated acids, J. Am. Chem. Soc., 95(3), 844–847, doi:10.1021/ja00784a035, 1973b.

Walling, C., El-Taliawi, G. M. and Johnson, R. A.: Fenton's reagent. IV. Structure and reactivity relations in the reactions of hydroxyl radicals and the redox reactions of radicals, J. Am. Chem. Soc., 96(1), 133–139, doi:10.1021/ja00808a022, 1974.

Wallington, T. J., Dagaut, P., Liu, R. and Kurylo, M. J.: The gas phase reactions of hydroxyl radicals with a series of esters over the temperature range 240 – 440K, Int. J. Chem. Kinet., 20(2), 177–186, doi:10.1002/kin.550200210, 1988.

Wander, R., Neta, P. and Dorfman, L. M.: Pulse radiolysis studies. XII. Kinetics and spectra of the cyclohexadienyl radicals in aqueous benzoic acid solution, J. Phys. Chem., 72(8), 2946–2949, doi:10.1021/j100854a044, 1968.

Warneck, P.: Multi-Phase Chemistry of C2 and C3 Organic Compounds in the Marine Atmosphere, J. Atmos. Chem., 51(2), 119–159, doi:10.1007/s10874-005-5984-7, 2005.

Wayne, R. ., Barnes, I., Biggs, P., Burrows, J. ., Canosa-Mas, C. ., Hjorth, J., Le Bras, G., Moortgat, G. ., Perner, D., Poulet, G., Restelli, G. and Sidebottom, H.: The nitrate radical: Physics, chemistry, and the atmosphere, Atmos. Environ. Part A. Gen. Top., 25(1), 1–203, doi:10.1016/0960-1686(91)90192-A, 1991.

Willson, R. L., Greenstock, C. L., Adams, G. E., Wageman, R. and Dorfman, L. M.: The standardization of hydroxyl radical rate data from radiation chemistry, Int. J. Radiat. Phys. Chem., 3(3), 211–220, doi:10.1016/0020-7055(71)90023-4, 1971.

Witter, R. A. and Neta, P.: Mode of reaction of hydrogen atoms with organic compounds in aqueous solutions, J. Org. Chem., 38(3), 484–487, doi:10.1021/jo00943a016, 1973.

Yang, X., Wang, J. and Wang, T.: Rate constants for the reaction of NO3· and SO4- radicals with oxalic acid and oxalate anions in aqueous solution, Chinese Chem. Lett., 15(5), 583–586, 2004.

Ye, M. and Schuler, R. H.: Determination of Oxidation Products in Radiolysis of Halophenols with Pulse Radiolysis, HPLC, And Ion Chromatography, J. Liq. Chromatogr., 13(17), 3369–3387, doi:10.1080/01483919008049108, 1990.

Zakatova, N. V, Minkhadzhiddinova, D. P. and Sharpatyi, V. A.: Role of oh-radicals in the radiolytic decomposition of carbohydrates and polysaccharides, Bull. Acad. Sci. USSR, Div. Chem. Sci., 18(7), 1520, doi:10.1007/BF00908773, 1969.

Zellner, R., Herrmann, H., Exner, M., Jacobi, H.-W., Raabe, G. and Reese, A.: Formation and reactions of oxidants in the aqueous phase, in Heterogeneous and Liquid Phase Processes, edited by P. Warneck, pp. 146–152, Springer., 1996.

Zepp, R. G., Faust, B. C. and Hoigné, J.: Hydroxyl radical formation in aqueous reactions (pH 3-8) of iron(II) with hydrogen peroxide: the photo-Fenton reaction, Environ. Sci. Technol., 26(2), 313–319, doi:10.1021/es00026a011, 1992.

Zevos, N. and Sehested, K.: Pulse radiolysis of aqueous naphthalene solutions, J. Phys. Chem., 82(2), 138–141, doi:10.1021/j100491a004, 1978.

Zona, R., Solar, S., Sehested, K., Holcman, J. and Mezyk, S. P.: OH-Radical Induced Oxidation of Phenoxyacetic Acid and 2,4-Dichlorophenoxyacetic Acid. Primary Radical Steps and Products, J. Phys. Chem. A, 106(29), 6743–6749, doi:10.1021/jp020125l, 2002.